Advances
in Clinical and Experimental Medicine

Wroclaw
MEDICAL UNIVERSITY

Advances
in Clinical and Experimental
Medicine

Editorial Office
ul. Marcinkowskiego 2–6
50-368 Wrocław, Poland
Tel.: +48 71 784 12 05
E-mail: redakcja@umed.wroc.pl

Publisher
Wroclaw Medical University
Wybrzeże L. Pasteura 1
50-367 Wrocław, Poland

Editorial Policy

Advances in Clinical and Experimental Medicine (Adv Clin Exp Med) is an independent multidisciplinary forum for exchange of scientific and clinical information, publishing original research and news encompassing all aspects of medicine, including molecular biology, biochemistry, genetics, biotechnology and other areas. During the review process, the Editorial Board conforms to the "Uniform Requirements for Manuscripts Submitted to Biomedical Journals: Writing and Editing for Biomedical Publication" approved by the International Committee of Medical Journal Editors (www.ICMJE.org/). The journal publishes (in English only) original papers and reviews. Short works considered original, novel and significant are given priority. Experimental studies must include a statement that the experimental protocol and informed consent procedure were in compliance with the Helsinki Convention and were approved by an ethics committee.

For all subscription-related queries please contact our Editorial Office:
redakcja@umed.wroc.pl

For more information visit the journal's website:
www.advances.umed.wroc.pl

**Ministry of Science
and Higher Education**
Republic of Poland

Indexed in: MEDLINE, Science Citation Index Expanded, Journal Citation Reports/Science Edition, Scopus, EMBASE/Excerpta Medica, Ulrich's™ International Periodicals Directory, Index Copernicus

Contents

Original papers

Reviews

Does the transplantation of keratinocytes really reduce the risk of death? Survival analysis of patients hospitalized at the Dr Stanisław Sakiel Centre for Burns Treatment in 2008–2015

Diana Kitala[1,2,A–D], Agnieszka Klama-Baryła[1,C], Małgorzata Kraut[1,D], Dariusz Łowicki[1,B], Wojciech Łabuś[1,D], Justyna Glik[1,3,E,F], Marcelina Misiuga[1,4,B,D], Mariusz Nowak[1,E,F], Grażyna Lisowska[5,F], Raphael Olszewski[6,E], Marek Kawecki[1,7,A,E,F]

[1] Dr Stanisław Sakiel Centre for Burns Treatment, Siemianowice Śląskie, Poland

[2] Silesian Higher Medical School, Katowice, Poland

[3] Department of Chronic Wounds Management Organization, School of Health Sciences, Medical University of Silesia, Katowice, Poland

[4] Silesian Analytical Laboratories, Katowice, Poland

[5] Department and Clinical Ward of Otolaryngology and Laryngological Oncology, School of Medicine with the Division of Dentistry, Medical University of Silesia, Zabrze, Poland

[6] Department of Oral and Maxillofacial Surgery, University Hospital St. Luc, Catholic University of Leuven, Brussels, Belgium

[7] Department of Emergency Medicine, School of Health Sciences, University of Bielsko-Biala, Poland

A – research concept and design; B – collection and/or assembly of data; C – data analysis and interpretation;
D – writing the article; E – critical revision of the article; F – final approval of the article

Abstract

Background. Keratinocyte transplantation is an adjuvant procedure in the extensive burn therapy method. However, it must be taken into consideration that clinical results of keratinocyte transplantation are ambiguous and progress achieved in this method is still being verified, especially due to the high cost of cultured epithelial autograft (CEA) transplants.

Objectives. The aim of this study was to verify the impact of cultured keratinocyte application on patients' survival. This study included a group of patients with the highest chance for a successful outcome of the therapy and excluded patients with no compelling reason to apply for such an expensive therapy.

Material and methods. This study included all the patients with burns diagnosed between January 1, 2008 and January 1, 2016, who were treated with cultured skin cells. Patients' age and gender, percentage of total body surface area (TBSA) affected, percentage of burn depth of the $3^{rd}/4^{th}$ degree, number of days between admission and surgery, and need for rehabilitation were analyzed.

Results. The cultured cell application did not significantly affect the risk of death ($p > 0.05$).

Conclusions. Keratinocytes should be applied as an adjunctive method for the treatment of burns with at least 40% TBSA affected, but with a maximal burn depth of the 2nd degree. In the group of patients below 50 years of age, a higher number of transplants with a cell population above 20 million/mL and a significantly lower mortality rate were observed, which means that in the mentioned age group, this graft was more effective. It has been suggested that patients older than 50 years of age with burns deeper than of the 2nd degree should be treated with more advanced methods like, e.g., the application of stem cells.

Key words: burn, keratinocytes, advanced therapy medicinal product, cell graft

Introduction

During the last decades, the methods of managing burns have changed.[1–3] The early excision of necrotic tissue and wound closure with autologous, split-thickness skin graft (STSG) are now the basis of treatment.[4–6] In the case of extensive burns, donor site access is limited. Keratinocyte transplantation is an adjuvant procedure in the extensive burn therapy method.[1] Using cellular epithelial autografts (CEA) in burns treatment has recently also become more popular.[7] This technique provides the ability to obtain a high volume of cultured epithelial cells from a skin punch biopsy within 3–4 weeks.[8] Cell transplantation increases wound healing by providing 1-stage coverage of extensive skin loss, thereby reducing the number of necessary surgeries.[7] However, it must be taken into consideration that clinical results of keratinocyte transplantation are ambiguous and progress achieved since Rheinwald and Green's era, when they described keratinocyte culture technique for the first time, is still being verified, especially due to the high cost of CEA transplants.[1,9] It has been proven, for instance, that a positive result of this therapy is related to the cell donor's age.[10] Among other limitations of this method, there is the long waiting time for cultured skin components, as well as the susceptibility of the cell culture to infections.[11] The discrepancy between the observed therapeutic effects is puzzling. Still et al. suggested that keratinocyte application gave a disappointing clinical effect.[12] Desai et al. observed hyperkeratosis and formation of scar contractures as an after-effect of the cellular therapy.[13]

The aim of this study was to verify the impact of cultured keratinocyte application on patients' survival, based on an analysis of a group of burn patients with cell transplants, in relation to the mean number of deaths among all patients and to the selection of predictive factors related to the risk of death in patients treated with CEA. This study would then allow us to select a group of patients with the highest chance for a successful outcome of the therapy and to exclude patients who do not have a compelling reason to apply for such an expensive therapy.

Material and methods

Cell culture

Keratinocytes and fibroblasts were collected from living donors who signed informed consent forms for autologous skin transplantation. A small skin fragment was collected under operating theater conditions. Then, in aseptic rooms with laminar flow cabinets, cells were isolated in accordance with Good Manufacturing Practice (GMP) standards (our laboratory has the manufacturing approval issued by GMP). Firstly, the epidermis was separated from the dermal layer by using the 2.4 U/mL disphase enzyme (Corning,

Tewksbury, USA). The incubation in the enzyme lasted about 60 min (at 37°C). Later, singular keratinocytes were digested from the dermis by incubation in an enzymatic solution at 37°C for 5 min, using TrypLE (Gibco; Thermo Fisher Scientific, Waltham, USA). The culture medium was used for enzyme inactivation. Then, cell suspension was centrifuged for 10 min at 1500 rpm. A cell pellet was suspended in the keratinocyte growth medium Keratinocyte Serum-Free Growth Medium (KSFM) (Gibco; Thermo Fisher Scientific) and seeded into 75 cm^2 culture bottles (Sarstedt AG & CO, Nümbrecht, Germany). The dermis was placed on a Petri dish (Thermo Fisher Scientific), filled with the TrypLE solution, and then incubated for 10 min. After incubation, the enzyme was inactivated and added to Dulbecco's Modified Eagle Medium (DMEM) (Cytogen, Princeton, USA). Established cultures of skin cells were placed in an incubator at a constant temperature of 37°C, 5% concentration of CO_2 and 95% humidity. The cell culture was immersed in the medium, which was changed approx. every 48 h, and the growth of the colony was monitored. After reaching 80% confluence, the cells were passed using TrypLE. Before the transplantation procedure, the cells were counted and their viability was tested using the Tali® Dead Cell Red Kit on Tali® Image-Based Cytometer (Life Technologies, Carlsbad, USA). The analysis was performed in accordance with the manufacturer's protocol.

Population analysis and data collection

This study included all the patients with burns diagnosed between January 1, 2008 and January 1, 2016, who were treated with cultured skin cells. The study was carried out at the Dr Stanisław Sakiel Centre for Burns Treatment in Siemianowice Śląskie (Poland). The data of burn patients had been collected until the end of their hospitalization period and stored using the Solmed computer software (SPIN Sp. z o.o., Katowice, Poland), as well as in the Laboratory of in vitro Cell and Tissue Culturing with Tissue Bank, localized at the Dr Stanisław Sakiel Centre for Burns Treatment in Siemianowice Śląskie, Poland. To create and encode the database, we used Microsoft Excel 2007 (Microsoft, Redmond, USA).

Analyzed parameters

Patients' age and gender, percentage of TBSA affected, percentage of burn depth of the 3rd/4th degree, number of days between admission and surgery, and need for rehabilitation were analyzed.

The analysis included 81 patients diagnosed with thermal burns (Table 1) who were treated with autologous skin components. Within this group, 86% patients were male. The control group included 3,919 patients with thermal burns, hospitalized at the Dr Stanisław Sakiel Centre for Burns Treatment in Siemianowice Śląskie, in the same period. The age of the patients admitted to hospital

and the patients who underwent cell transplantation was not significantly different; however, there was a difference in their burn surfaces (p < 0.01). Most of the patients with cultured cells had burns covering 40–79% TBSA (59% of the patients), whereas among the admitted patients, burns with up to 39% TBSA dominated (75% of the patients). Patients with cultured cells later underwent a necrotic tissue demarcation procedure, mainly due to the larger size of the burn surface, which required a longer hemodynamic stabilization of those patients.

Statistical analysis

The STATISTICA v. 12 (StatSoft Inc., Tulsa, USA) program was used. For the analysis of variances, Cox's proportional hazard models were constructed. The model assumptions were checked by the Schoenfeld residuals analysis. If the assumption of proportional hazard was not fulfilled, the variance proved to be linearly time-dependent. The goodness of fit was evaluated by Akaike's Information Criterion (AIC). The model with the best statistical fit was selected (AIC = 65.48). To compare the group of patients who underwent autologous keratinocyte transplantation with the total number of hospitalized patients, the Mann-Whitney U test was used for both groups. The assumption of normal distribution was analyzed by the Shapiro-Wilk normality test. The χ^2 test was used to compare frequency distribution. The statistical significance obtained was $\alpha = 0.05$. Furthermore, the relative risk reduction (RRR) for number of deaths was compared:

$$RRR = \frac{z_c}{n_c} - \frac{n_k}{z_k}$$

where:
n_c – total number of patients in the CEA group;
n_k – total number of patients in the control (non-CEA) group;
z_e – event rate in the CEA group (number of deaths);
z_k – event rate in the control group (number of deaths).

Results

The analysis showed that the only significant prognostic factor was the burn surface of the 3rd degree at least (p = 0.029). Every 10% increase in the burn surface resulted in increasing the risk of death by 75.2% (hazard ratio confidence interval (HR CI): 1.06–2.9). In the case of burns of the 3rd/4th degree, covering more than 40% TBSA, the probability of a 3-month survival

Table 1. Description of 81 burn patients treated with autologous cell transplants compared to all patients hospitalized due to thermal injury between 2008 and 2015

Grouping descriptive parameters	CEA-graft group	Non-CEA graft group	Difference between the 2 groups
Age [years], mean ±SD	41.1 ±14.7	45.3 ±16.9	p > 0.05
TBSA affected [%] 0–19 20–39 40–59 60–79 >80	12 26 31 28 2	60 25 9 4 2	p < 0.01
Burn depth of the 3rd/4th degree [%] 0–9 10–19 20–29 30–39 >40	41 23 14 16 6	37 26 12 12 13	p > 0.05
Number of days since admission to the ward for the 1st necrotic tissue demarcation, mean ±SD	37.0 ±20.7	8.0 ±8.1	p < 0.01
Gender, n [%] female male	11 (14) 70 (86)	999 (25) 2,919 (75)	p = 0.015
Death, n [%] yes no	10 (12) 71 (88)	556 (14) 3,362 (86)	p > 0.05
Need for rehabilitation, n [%] yes no	22 (27) 59 (73)	542 (14) 3,376 (86)	p = 0.014
Total number of days of hospitalization, mean ±SD	79.9 ±44.8	26.5 ±25.3	p < 0.01

SD – standard deviation; TBSA – total body surface area; CEA – cellular epithelial autografts.

was 60% (Fig. 1). The cultured cell application did not significantly affect the risk of death (p > 0.05); however, when a selected group of patients was taken into consideration (40–79% TBSA affected), the relative reduction of death was 69.6% in the group of patients with CEA transplantation in comparison to the pair-matched group without CEA graft (Table 2).

Table 2. Differences between pair-matched groups with 40–79% TBSA affected

Grouping descriptive parameters	CEA group	Non-CEA group
Patients with TBSA affected, n [%] 40–59% 60–79% total	25 (52.08) 23 (47.92) 48	25 (52.08) 23 (47.92) 48
Age [years]	38 ±13	41 ±18
Number of days from admission to main operation, mean ±SD	38 ±21	11 ±11
Hospitalization length [days], mean ±SD	82 ±44	38 ±36
Number of rehabilitated patients	13	6
Death, n [%]	7 (14.6)	23 (48.0)

TBSA – total body surface area; SD – standard deviation; CEA – cellular epithelial autografts.

The application of keratinocyte cells was not a procedure which could eliminate the need for rehabilitation; 73% of patients who underwent skin cell transplantation needed rehabilitation due to contracture scars. It has to be pointed out, however, that in the group of patients without cell transplantation, rehabilitation was necessary in 86% of the cases, which represents a significantly higher percentage of patients than in the previous group.

Burn patients were divided into 2 age groups: ≤50 years and >50 years, and then they were compared using the following criteria: burn surface, burn depth, number of days between the admission to hospital, time length of the cell culture, and deaths (Table 3). The comparison was performed to verify if the patient's age over 50 years could affect the proliferation of cultured keratinocytes.

The average number of transplanted cells in the ≤50 years group was 7.7 million/mL (Fig. 2), and in the >50 years group, it was 6.2 million/mL ($p > 0.05$). The percentage of persons with a cell transplant higher than 20 million cells/mL in the ≤50 years group was 11%; however, in the >50 years group, no patients were reported to reach such a high volume of culture (above 20 milion/mL). Additionally, in patients over 50 years of age, the average time

length of the cell culture was 10 days longer. In the group of patients aged ≤50 years, the cultured cells were applied to persons with a higher median of burn surface (42% TBSA affected) and, despite that, the mortality rate was significantly lower (4%).

Discussion

The application of cultured keratinocytes is considered a step forward in the treatment of massive burns.[14] The transplantation of skin cells is regarded as a procedure which minimizes the number of autologous donor sites and reduces hypertrophic scarring.[9] Keratinocyte engraftment at the level of 50–90% is believed to be possible in the case of partial thickness burns.[11,15] It has to be remembered, however, that in the case of large burn surfaces, a singular transplantation of skin cells is not sufficient, and that single-place multiple harvesting of a skin section for the culturing purpose requires a large surface.[16] Using allogeneic cell transplants or an autologous cell culture, supported with an allogeneic human skin matrix, can be the solution here.[15] The latter solution prevents the 'alligator skin effect', which occurs as a result of a meshed autologous skin graft.[16] It also helps with performing an earlier closure of the burn wound.[14]

The average survival of patients who underwent CEA transplantation, as presented by Sood et al., is 91%.[17] Such a result is in line with those presented in our study (88%). Postoperative complications are divided into both early and late. Early complications include the presence of blisters (31%) and pruritus (4.7%). Late complications include cell transplant loss (2.3%) and the presence of scar contractures

Table 3. Age, burn surface, time length of the cell culture, and deaths in 2 age groups of patients: ≤50 years and >50 years

Parameter	Age ≤50 years	Age >50 years	Difference between the 2 groups
Age [years], median ±SD	35.2 ±9.4	60.6 ±8	–
TBSA affected [%], median ±SD	41.8 ±21.6	32.3 ±19.1	$p = 0.01^*$
Percentage of burn of the 3rd/4th degree, median ±SD	8 ±3.5	7.6 ±1.9	$p > 0.05$
Time length of cell culture [days], median ±SD	35.5 ±16.2	44.8 ±27.1	$p > 0.05$
Deaths [%]	4	9	$p = 0.038^*$

SD – standard deviation; TBSA – total body surface area; * burned body surface area.
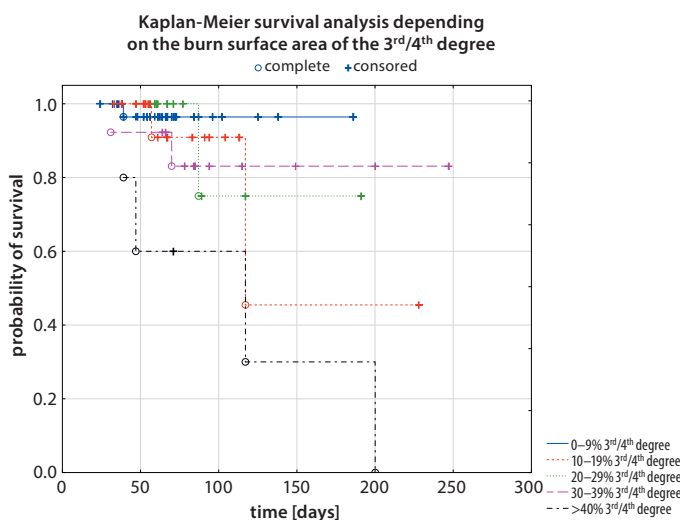
Fig. 1. Probability of survival depending on the burn surface, burns of the 3rd/4th degree
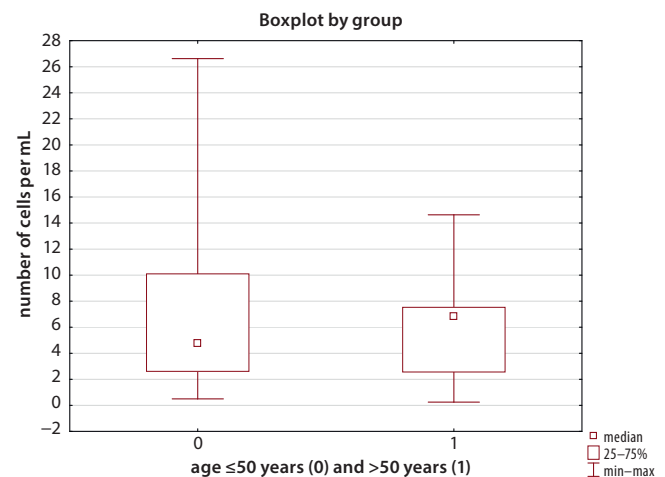
Fig. 2. Number of cells per mL transplanted in groups of patients aged ≤50 years and >50 years

(66%). Therefore, it is important that the group of cell transplant recipients should be clearly and precisely defined. The desirability of performing an expensive, time-consuming and esthetically uncertain procedure is morally and clinically unjustified for groups of patients with spontaneously healed burn wounds (2nd degree burns) or in groups of patients with deep 3rd/4th degree burns of more than 40% TBSA affected, in which the probability of 200-day survival is equal to 0. Carrying out cell cultures for patients with a high risk of death is particularly difficult, because initially, the cell culture is a reflection of the patient's overall condition, which impinges on the epidermal cell viability and population doubling.[18]

The patient's dressing prior to cell collection can also affect the therapeutic success. It has been proven that cultured cells do not reveal the adhesive abilities in the presence of wound dressings such as Adaptic®, Xeroform®, EZ Derm®, and Mepilex®. Using wound dressings like Mepitel®, N-Terface®, Polyskin®, and Biobrane® has no negative impact on keratinocytes.[19] From our own experience, we can say that particular attention has to be paid to the applied antiseptic substance and to proper preparation of the donor site. Proper wound preparation for grafting is crucial – the high sensitivity of cultured cells to bacterial proteases and cytotoxins present in wound can impair the healing process and may result in a total loss of a cell transplant. This is another critical moment.[20–23] That said, however, proper wound preparation is not sufficient – integrin profiles, as a result of a carried out culture, influence keratinocyte engraftment as well. When keratinocytes reach a high confluence, they evolve from a high proliferative state into stunted growth and differentiation. This is linked with integrin expression disturbances, such as the loss of expression of integrin alpha 1 and alpha 5.[24] In the group of patients over 50 years of age, a moderately lower number of cells and a longer time necessary to obtain a clinically significant number of cells was reported.

All the above-mentioned obstacles lead to an increased cost of treatment and a prolonged hospital stay. This results in a lowered number of performed CEA transplantation procedures, even in reference centers.[25] Pellegrini et al. suggested using stem cell transplants; however, in order to obtain a satisfying clinical result and to reduce the cost, a more careful selection of patients for a transplantation procedure is absolutely necessary.[26] There is no doubt that the traditional predictive factors of mortality, like the burn surface and the patient's age, should be examined in detail.[4] The results of the present study show that age has no influence on the survival rate of patients with a CEA transplant. This result is not surprising and is derived clearly from the evaluated data – the median age of a patient qualified for a cell culture was 41 years. Moreover, it has to be taken into consideration that the median age of all hospitalized patients was 45 years and a significant group of admissions included patients below 30 years

of age (victims of communication accidents and flammable substance explosions). It is believed that the patient's age >50 years is a negative prognostic factor.[27] The qualification of patients below 50 years of age for a cell culture is dictated not only by the median age of the admitted patients, but also by the skin aging process and the influence of this process on the normal morphology of cells, i.e., their ability to multiply.[28,29] Patients with burns with <20% TBSA affected are those most frequently admitted to burn centers; however, patients qualified for cell cultures are diagnosed with average burns of 40% TBSA. Nevertheless, TBSA in the group of patients who underwent the epidermal cells therapy is not a predictive factor, but a larger surface area of 3rd/4th degree burns increases the risk of death. In the group of patients with a cell transplant, this situation is clinically justified. Epidermal cells promote the healing process of burn wounds with a maximal depth of the 2nd degree. Therefore, in the case of large-scale burns, they can effectively support the wound healing process. Epidermal cells are unable to effectively stimulate the healing of deep (3rd degree) wounds; thus, their application does not influence the survival in this group, and with a 20% increase of the 3rd degree burn surface, the risk of death increases by 1.72 times. However, the mortality in the group of patients who underwent keratinocyte cell transplantation with a diagnosed burn of <60% TBSA is 1%, but in the case of >60% TBSA affected, the reported mortality rate is at the level of 16%. Tang et al. reported a zero mortality in the group of patients with burns of <51% TBSA. It has been suggested that a unified system for surgical treatment procedures would cause the mortality rate decline in the group of burn patients.[30] The influence of cell transplants on increased patient survival was not reported despite the fact that in the group of patients aged <50 years with keratinocytes applied, the mortality rate was only 4%. Auxenfans et al. postulated using keratinocytes as a clinically effective method in managing donor sites and 2nd degree burns with a large burn surface; in this case, together with a free split-thickness skin graft.[31]

In the case of extensive, deep burns (3rd degree), the use of stem cells is recommended.[32,33] At present, we can agree that the CEA transplant is a life-saving, but expensive procedure, unsuitable for the permanent coverage of burn wounds deeper than the 2nd degree.[34] Matters related to the optimal donor site selection for cell culture purposes, wound dressing applied to the wound before harvesting the donor skin for the culture and post-cell transplantation, and, most importantly, an informed choice of the group of patients for whom applying keratinocytes will give a maximum clinical effect, should have all been systematized many years ago. The lack of studies giving clear guidelines for using cultured skin components is to blame. The aim of this study was to establish preliminary standards for patient enrollment for keratinocyte cultures. It should be the basis for further discussion on this topic.

In conclusion, keratinocytes and fibroblasts should be applied as an adjunctive method for the treatment of burns of at least 40% TBSA, but with a maximal depth of the 2nd degree. In the group of patients below 50 years of age, a higher number of transplants with a cell population above 20 million/mL and a significantly lower mortality rate were observed, which means that in the mentioned age group, this graft is more effective. It has been suggested that patients older than 50 years of age with burns deeper than of the 2nd degree should be treated with more advanced methods like, for example, the application of stem cells.

References

1. Atiyeh BS, Costagliola M. Cultured epithelial autograft (CEA) in burn treatment: Three decades later. *Burns*. 2007;33(4):405–413. doi: 10.1016/j.burns.2006.11.002
2. Sorg H, Betzler C, Rennekampff HO, Vogt PM. Burns [in German]. *Unfallchirurg*. 2012;115(7):635–648.
3. Atiyeh B, Masellis A, Conte C. Optimizing burn treatment in developing low- and middle-income countries with limited health care resources (Part 1). *Ann Burns Fire Disasters*. 2009;22(3):121–125.
4. Macedo JL, Santos JB. Predictive factors of mortality in burn patients. *Rev Inst Med Trop Sao Paulo*. 2007;49(6):365–370. doi: http://dx.doi.org/10.1590/S0036-46652007000600006
5. Shen YM, Hu XH, Mi HR, et al. Early treatment of high-voltage electric burn wound in the limbs [in Chinese]. *Zhonghua Shao Shang Za Zhi*. 2011;27(3):173–177. doi: 10.3760/cma.j.issn.1009-2587.2011.03.003
6. Kawecki M, Hoff-Lenczewska D, Klama-Baryła A, et al. *Przegląd piśmiennictwa chirurgicznego*. Warszawa, Poland: Fundacja Polski Przegląd Chirurgiczny; 2012:185–196.
7. Sood R, Balledux J, Koumanis DJ, et al. Coverage of large pediatric wounds with cultured epithelial autografts in congenital nevi and burns: Results and technique. *J Burn Care Res*. 2009;30(4):576–586. doi: 10.1097/BCR.0b013e3181ac02de
8. Bargues L, Prat M, Leclerc T, et al. Present and future of cell therapy in burns. *Pathol Biol (Paris)*. 2011;59(3):e49–56. doi: 10.1016/j.patbio.2009.12.006
9. Rab M, Koller R, Ruzicka M, et al. Should dermal scald burns in children be covered with autologous skin grafts or with allogeneic cultivated keratinocytes? – "The Viennese concept". *Burns*. 2005;31(5):578–586. doi: 10.1016/j.burns.2005.01.001
10. Carsin H, Ainaud P, Le Bever H, et al. Cultured epithelial autografts in extensive burn coverage of severely traumatized patients: A five-year single-center experience with 30 patients. *Burns*. 2000;26(4):379–387. doi: http://dx.doi.org/10.1016/S0305-4179(99)00143-6
11. Paddle-Ledinek JE, Cruickshank DG, Masterton JP. Skin replacement by cultured keratinocyte grafts: An Australian experience. *Burns*. 1997;23(3):204–211. doi: http://dx.doi.org/10.1016/S0305-4179(96)00123-4
12. Still JM, Orlet HK, Law EJ. Use of cultured epidermal autografts in the treatment of large burns. *Burns*. 1994;20(6):539–541. doi: http://dx.doi.org/10.1016/0305-4179(94)90017-5
13. Desai MH, Mlakar JM, McCauley RL, et al. Lack of long-term durability of cultured keratinocyte burn-wound coverage: A case report. *J Burn Care Rehabil*. 1991;12(6):540–545. doi: 10.1097/00004630-199111000-00009
14. Lataillade JJ, Bey E, Thepenier C, et al. Skin engineering for burns treatment [in French]. *Bull Acad Natl Med*. 2010;194(7):1339–1351.
15. Mühlbauer W, Henckel von Donnersmarck G, Hoefter E, Hartinger A. Keratinocyte culture and transplantation in burns [in German]. *Chirurg*. 1995;66(4):271–276.
16. Braye F, Pascal P, Bertin-Maghit M, et al. Advantages of using a bank of allogenic keratinocytes for the rapid coverage of extensive and deep second-degree burns. *Med Biol Eng Comput*. 2000;38(2):248–252.
17. Sood R, Roggy D, Zieger M, et al. Cultured epithelial autografts for coverage of large burn wounds in eighty-eight patients: The Indiana University experience. *J Burn Care Res*. 2010;31(4):559–568. doi: 10.1097/BCR.0b013e3181e4ca29
18. Klama-Baryła A, Kraut M, Łabuś W, et al. Application of platelet leukocyte gel in in vitro cultured autologous keratinocite grafts. *Pol Przegl Chir*. 2011;2(22):77–86.
19. Esteban-Vives R, Young MT, Ziembicki J, et al. Effects of wound dressings on cultured primary keratinocytes. *Burns*. 2016;42(1):81–90. doi: 10.1016/j.burns.2015.06.016
20. Chester DL, Balderson DS, Papini RPG. A review of keratinocyte delivery to the wound bed. *J Burn Care Rehabil*. 2004;25(3):266–275.
21. Guilbaud J. Problems created by the use of cultured epithelia. *Annals of the Mediterranean Burn Club*. 1993;4(2):176–178.
22. Munster AM. Editorial: Whither skin replacement? *Burns*. 1997;23(2):195. doi: http://dx.doi.org/10.1016/S0305-4179(97)86850-7
23. Ronfard V, Rives JM, Neveux Y, et al. Long-term regeneration of human epidermis on third degree burns transplanted with autologous cultured epithelium grown on a fibrin matrix. *Transplantation*. 2000;70(11):1588–1598. doi: 10.1097/00007890-200012150-00009
24. Poumay Y, Pittelkow MR. Cell density and culture factors regulate keratinocyte commitment to differentiation and expression of suprabasal K1/K10 keratins. *J Invest Dermatol*. 1995;104(2):271–276. doi: http://dx.doi.org/10.1111/1523-1747.ep12612810
25. Barret JP, Wolf SE, Desai MH, Herndon DN. Cost-efficacy of cultured epidermal autografts in massive pediatric burns. *Ann Surg*. 2000;231(6):869–876.
26. Pellegrini G, Ranno R, Stracuzzi G, et al. The control of epidermal stem cells (holoclones) in the treatment of massive full-thickness burns with autologous keratinocytes cultured on fibrin. *Transplantation*. 1999;68(6):868–879. doi: 10.1097/00007890-199909270-00021
27. Wolf SE, Rose JK, Desai MH. Mortality determinants in massive pediatric burns: An analysis of 103 children with > or = 80% TBSA burns (> or = 70% full-thickness). *Ann Surg*. 1997;225(5):554–565.
28. Gilchrest BA. In vitro assessment of keratinocyte aging. *J Invest Dermatol*. 1983;81(Suppl 1):184–189. doi: http://dx.doi.org/10.1111/1523-1747.ep12541084
29. Ito M, Liu Y, Yang Z, et al. Stem cells in the hair follicle bulge contribute to wound repair but not to homeostasis of the epidermis. *Nat Med*. 2005;11(12):1351–1354. doi: 10.1038/nm1328
30. Tang W, Li X, Deng Z, et al. Effects of unified surgical scheme for wounds on the treatment outcome of patients with extensive deep burn [in Chinese]. *Zhonghua Shao Shang Za Zhi*. 2015;31(4):254–258. doi: 10.3760/cma.j.issn.1009-2587.2015.04.004
31. Auxenfans C, Menet V, Catherine Z, et al. Cultured autologous keratinocytes in the treatment of large and deep burns: A retrospective study over 15 years. *Burns*. 2015;41(1):71–79. doi: 10.1016/j.burns.2014.05.019
32. Mansilla E, Marín GH, Berges M, et al. Cadaveric bone marrow mesenchymal stem cells: First experience treating a patient with large severe burns. *Burns Trauma*. 2015;3(17):1–9. doi: 10.1186/s41038-015-0018-4
33. Rasulov MF, Vasilchenkov AV, Onishchenko NA, et al. First experience of the use bone marrow mesenchymal stem cells for the treatment of a patient with deep skin burns. *Bull Exp Biol Med*. 2005;139(1):141–144. doi: 10.1007/s10517-005-0232-3
34. Mcheik JN, Barrault C, Levard G, et al. Epidermal healing in burns. Autologous keratinocyte transplantation as a standard procedure: Update and perspective. *Plast Reconstr Surg Glob Open*. 2014;2(9):e218. doi: 10.1097/GOX.0000000000000176

Expression rate of myogenic regulatory factors and muscle growth factor after botulinum toxin A injection in the right masseter muscle of dystrophin deficient (mdx) mice

Ute U. Botzenhart[1,C–F], Ricarda Gerlach[1,B], Tomasz Gredes[1,C–F], Ines Rentzsch[2,B], Tomasz Gedrange[1,F], Christiane Kunert-Keil[1,A–F]

[1] Department of Orthodontics, Carl Gustav Carus Campus, Technische Universität Dresden, Germany

[2] Department of Anesthesiology and Intensive Care Medicine, University Hospital Carl Gustav Carus, Technische Universität Dresden, Germany

A – research concept and design; B – collection and/or assembly of data; C – data analysis and interpretation;
D – writing the article; E – critical revision of the article; F – final approval of the article

Abstract

Background. The mdx mouse, the most approved animal model for basic research in Duchenne muscular dystrophy (DMD), has the ability to compensate muscle degeneration by regeneration process, which is obvious at approx. 3 months of age. Hence, this mouse model is only temporarily suitable to proof craniofacial changes which are usually evident in humans with the progression of the disease.

Objectives. The purpose of our study was to examine the impact of botulinum toxin A (BTX-A) in influencing muscle regeneration in the masticatory muscles of healthy and mdx mice.

Material and methods. Chemo-denervation of the right masseter muscle was induced in 100-day-old, healthy and dystrophic mice by a specific intramuscular BTX-A injection. Gene expression and protein content of myogenic regulatory factors and muscle growth factor (MyoD1, myogenin and myostatin) in the right and left masseter, temporal and the tongue muscle were determined 4 and 21 days after injection, respectively, using quantitative reverse transcription polymerase chain reaction (qRT-PCR) and western blot technique.

Results. The 4 day and 21 day interval proved significant but varying changes of mRNA expression in both control and mdx mice. At the protein level, myogenin expression was increased in the temporal and masseter muscle on the injection side in controls, whereas dystrophic mice showed the same effect for MyoD1 expression. Additionally, increased protein expression of all studied genes could be found in dystrophic mice compared to controls, except the left temporal and the tongue muscle.

Conclusions. Muscle regeneration is not constant in BTX-A injected mdx masticatory muscles, presumably due to the already exhausted capacity or functional loss of satellite cells caused by dystrophin deficiency, and, therefore, disturbed regeneration potential of myofibrils. Botulinum toxin A injection cannot fully break down regulatory processes at molecular level in 100-day-old mdx mice. Further investigations are necessary to fully understand the regeneration process following BTX-A injection into dystrophic muscles.

Key words: myostatin, BTX-A, MyoD1, myogenin, mdx mice

Introduction

Skeletal muscles, the most abundant tissue of the body, are composed of myofibers and grow in size by fusing postnatal muscle stem cells, called satellite cells. These mononucleated cells are located between the plasma membrane and the basal lamina that surrounds each muscle fiber. They play a key role in the regeneration of adult skeletal muscles by compensating for daily muscle stress and strain and can be activated after muscle injury.[1] Satellite cells are affected by several growth factors as well as transcription factors, such as members of the myogenic regulatory factor (MRF) family. Among them, myogenic transcriptional regulators, such as MyoD and myogenin, are essential for the proliferation of satellite cells and for the development of early regenerating fibers, even in dystrophic muscles. MyoD is considered as one of the key regulatory factor of muscle regeneration.[2] Based on numerous studies, it could be demonstrated that MyoD is required for the determination of skeletal myoblasts, whereas myogenin plays a decisive role in the expression of the terminal muscle phenotype, regulating skeletal muscle metabolism and exercise capacity during adult life.[3] Increased myopathy was observed by a lack of MyoD, which had a negative effect on the embryonic formation, postnatal survival and function of satellite cells, and thus an adverse influence on muscle formation. In contrast, the growth factor myostatin has a negative impact on the postnatal muscle growth, due to its suppressive effect on satellite cell activation, proliferation and self-renewal, as well as myoblast proliferation and differentiation.[4,5] The proliferation and differentiation of satellite cells during muscle repair is largely influenced by vascularization, innervation, hormones, nutrition, and the extent of muscle damage, which takes place either under physiological or pathological conditions, for example in muscular dystrophies.[6]

Muscular dystrophy is a general term that covers a diverse group of inherited myogenic disorders characterized by progressive muscle wasting and degeneration among them Duchenne muscular dystrophy (DMD) is the most common one. It results from mutations in the dystrophin gene and lack of its functional protein. The absence or enormous reduction of functional dystrophin protein results in muscle fiber necrosis without further regenerative processes. At the beginning of the disease, new muscle fibers are formed by satellite cells or by fusion of resistant myoblasts. In more advanced stages of DMD, inadequate muscle regeneration, probably due to loss of satellite cells, which after many rounds of muscle degeneration and regeneration processes become "exhausted", leads to the degeneration of skeletal muscles, which are then replaced by fatty and connective tissue.[7] Additionally, loss of muscle tissue is not homogenous, but involves specific muscle groups.[1] Proximal muscles of the extremities are affected first, followed by upper arms and upper legs. Interestingly, approx. 2 years after the patient had become wheelchair-bound, the orofacial muscles are affected, which results

in muscle imbalance and severe craniofacial and dental abnormalities.[8] This affirms the assumption that a relationship between muscle dysfunction and craniofacial morphology may exist.

In contrast to DMD patients, skeletal muscles of the mdx mouse, the most commonly used animal model for DMD, can regenerate throughout life. Ongoing muscle degeneration can be found in mdx mouse muscles, which usually peaks at 3 weeks of age, and is characterized by a decrease of myofibers and pathological features becoming more severe with age.[9] Due to a spontaneous and effective recovery of muscle cells, compared to humans, the mdx mouse has a modest dystrophic phenotype, exhibits a more benign progression of the dystrophy, and can, therefore, not accurately be compared with human DMD disease pattern.[10] Nevertheless, it will be assumed that the myogenic activity of satellite cells in mdx muscles also appears to be depleted with age.[11]

Botulinum toxin is a purified form of the neurotoxin derived from the bacterium *Clostridium botulinum* responsible for botulism. Following local injection into the muscle, the toxin inhibits the vesicular release of acetylcholine (Ach) neurotransmitter at the neuromuscular junction producing chemical denervation and paralysis of the striated muscles in humans and animals.[12] Resulting muscle paralysis and safety of botulinum toxins have permitted their widespread use in a variety of therapeutic applications, such as unloading the jaws, alleviation of facial pain involving the temporomandibular join, masticatory myalgia, sialorrhoea, bruxism, and hemifacial spasm.[13] Hence, with botulinum toxin A (BTX-A) injection just a temporary paralysis is possible, because in healthy muscle tissue after a certain time, reinnervation occurs. At the neuromuscular junctions of humans, functional recovery of the nerve terminal takes 2–4 months, whereas in rats and mice functional muscle recovery is reported to be much faster.[14] The onset of toxin action in rodents is 24 h after injection, usually peaks at 2 weeks and paralysis lasts 4–6 weeks.[15]

Research in the field of orthodontics as well as in yet unpublished data of our own research group in the mdx mouse during maximal dystrophic muscle degeneration could already show a relationship between muscle weakness and craniofacial deformities, which had originally been described by Melvin L. Moss as the so called "functional matrix theory".[8] Due to recovery, in the mdx mouse these effects disappear, so that this mouse model cannot adequately be used to scientifically prove this correlation. Thus, to analyze muscle-function influence on craniofacial bone growth and development in a sufficient way, a specific and durable muscle dysfunction should be induced. As it is known that BTX-A causes muscle paralysis as well as muscle degeneration in healthy muscle tissue, this toxin might also be able to trigger dystrophic features in mdx mice, making this mouse model comparable to the human disease of DMD and accessible for research in the craniofacial region. Hence, we wanted to examine whether BTX-A is suited to generate a sustained dystrophy in the mdx mouse masticatory

muscles by verifying these effects on the basis of regeneration processes. In a recently published paper about MyHC expression in the masticatory muscles of 100-day-old mice following the same protocol, a single specific intramuscular BTX-A injection in the right masseter muscle induced changes of MyHC expression in healthy mice, indicating a shift to type I fibers and simulating dystrophic features in these mice, whereas dystrophic muscles did not react to BTX-A injection.[16] In contrast to the abovementioned results, on the one hand our research group could find changes in caveolin 1, caveolin 3 and VEGF protein expression in dystrophic mice after a single injection of that toxin in the right masseter muscle with raised expression of all studied proteins, whereas in the right masseter muscle of controls a decrease of caveolin 3 expression, due to BTX-A injection, could be found. On the other hand, mRNA expression was unchanged in both mouse strains.[17]

The aim of the present study was to examine BTX-A influence on the regenerative capacity in mdx masticatory muscles by identifying MRFs and a muscle growth factor as markers for muscle regeneration and repair after a single specific intramuscular BTX-A injection in the right masseter muscle of healthy and dystrophic mice, and to evaluate if this drug was able to induce or prologue dystrophic features in the masticatory muscles of these mouse strains.

Material and methods

Animals and experimental protocol

Male and female mice of the inbred strain C57BL-10ScSn (control group, n = 20) and C57BL/-Dmdy (mdx) (test group, n = 25), originally obtained from Jackson Laboratory (Bar Harbor, USA) and borne in the Laboratory Animal Experimental Bioassay Centre Dresden (experimental centre of the medical faculty, TU Dresden, Germany), were used in this study. At the beginning of the experiments, mice of both strains were aged 100 days and had a body mass of approx. 30 g. All procedures performed in this study were approved by the Laboratory Animal Research Committee of Saxony (Germany) with the No.: 24–9168.11–1/2013–46. An intraperitoneal injection consisting of a mixture of 10% ketamine (Ceva Tiergesundheit GmbH, Düsseldorf, Germany) and 2% Rompun® (Bayer, HealthCare AG, Leverkusen, Germany) at a ratio of 3:2 (0.1 mL per 100 g body mass) was used for temporal anesthesia. Chemodenervation was induced by a single specific intramuscular injection of 0.025 mL BTX-A (Botox®; Allergan, Irvine, USA; 1.25 IU/0.1 mL in physiologic NaCl solution) in the superficial and deep venter of the right masseter muscle as described recently by Botzenhart et al.[16,17] After injection both healthy and mdx mice were randomized into 2 groups according to the postinjection periods of 4 days (T1; control group: n = 7; test group: n = 9) and 21 days (T2; control group: n = 13; test group: n = 16), respectively.

Due to the fact that paralysis of masseter muscle is usually evident 3 days after injection by teeth chattering and the refusal of solid food, during the first 7 postinjection days soft food was offered additionally.[16] After 4 days (T1) and 21 days (T2), the mice were painlessly killed using an overdose of isoflurane. Immediately, the head was separated from the body and samples of the following muscles were carefully dissected by the same trained observer: right and left masseter muscle, right and left temporal muscle and tongue muscle. Samples were immediately frozen in liquid nitrogen (–173°C) and stored at –80°C until further processing. Muscles harvested, corresponded to the superficial and (in parts) the deep masseter muscle, the medial temporal muscle and the flexible part of the tongue, including the internal tongue muscles.[18] For both investigation periods, mRNA expression and protein content of MRFs, MyoD1 and myogenin, and muscle growth factor, myostatin, were analyzed. Some of the samples examined in this study had already been used for quantification of MyHC isoforms as well as caveolin 1, caveolin 3 and VEGF expression.[16,17]

Quantitative reverse transcription polymerase chain reaction

The isolation of total RNA and its reverse transcription in cDNA was carried out exactly as described by Botzenhart et al.[16,17]

Gene expression analysis of the myogenic differentiation factors *MyoD1* and myogenin (*Myf4*) as well as muscle growth factor myostatin (*MSTN/GDF8*) in the extracted muscle samples was performed by quantitative reverse transcription polymerase chain reaction (qRT-PCR) using specific TaqMan PCR probes and primers (Taq-Man® Assays: *MyoD1*: Mm00440387_m1; *Myf4*: Mm00446194_m1; *MSTN*: Mm03024050_m1; PE Applied Biosystems, Weiterstadt, Germany) and the TOptical cycler (Analytik Jena AG, Jena, Germany) as described previously.[16,17]

The 2-ΔΔCt method was used in order to quantify the studied genes in mdx mice relative to controls in relation to those of 18s rRNA (Eukaryotic 18S rRNA Endogenous control: 4310893E; PE Applied Biosystems).[19]

Western blot

Muscle protein which had been isolated from each murine tissue sample, following the protocol described earlier, was loaded onto Citerion™ TGX Stain-free™ Precast Gels (Bio-RAD Laboratories GmbH, Munich, Germany) for 60 min under constant voltage of 100 V, and after separation, transferred to PVDF membranes (Trans-Blot® Semi-Dry transfer system, Trans-Blot® Turbo™ Midi PVDF Transfer Packs; Trans-Blot® Turbo™ blotting apparatus; Bio-RAD Laboratories GmbH).[16] Dry milk (5%) in phosphate-buffered saline (PBS) buffer with 0.05% tween at 4°C was used overnight to block the western blot membranes.

Specific antibodies against myogenin (EPR4789; Abcam, Cambridge, UK), MyoD1 (C20; Santa Cruz, Heidelberg, Germany) and myostatin (AB 71808; Abcam) were used for incubation, followed by horseradish peroxidase (HRP)-conjugate goat anti-mouse or anti-rabbit immunoglobulins (1:5,000; Dako, Hamburg, Germany).

Bound antibodies were detected and visualized with an enhanced chemiluminescence system (WesternBright Chemiluminescence Substrate Quantum; Advansta Inc., Menlo Park, USA). In order to calculate the protein content on each gel, monoclonal anti-glyceraldehyde-phosphate dehydrogenase (GAPDH) antibody (clone 6C5; 1:1000; Millipore, Billerica, USA; incubation for 2 h at room temperature) severed as loading control. GelScan 5.2 software (Serva, Heidelberg, Germany) was used to quantify protein bands (mean optical density ± standard error of the mean [SEM]), in each case of n = 3 different muscle samples (different animals) and 2 independent western blot analysis.

Statistical analysis

Statistical analysis for evaluation of differences in mRNA expression and protein content of the investigated MRFs and muscle growth factor in the extracted muscle samples after BTX-A treatment was performed using SigmaStat v. 3.5 (Systat Software Inc., San Jose, USA). In the case of normal distribution unpaired t-test and otherwise, the Mann-Whitney U test was used (significance level: $p \leq 0.05$).

Results

As no gender differences could be observed, in all examinations no distinction between male and female mice was made.

mRNA expression
4 days after BTX-A injection

When considering the gene expression of *Myf4*, no differences in mRNA amount were found between BTX-A-treated and untreated masseter muscle for both, control and mdx mice. In contrast, compared to the left side, in the right temporal muscle a 4.6-fold as well as a 2-fold increase in *Myf4* gene expression could be detected in control and mdx mice, respectively (Fig. 1A).

Four days after BTX-A injection in the right masseter muscle of control mice the mRNA expression of *MyoD1* was significantly increased in the treated masseter muscle compared to the untreated muscle tissue (p = 0.021), whereas no significant differences in mRNA amount were detected in dystrophic mice. At the same time, a 3.6-fold increase in *MyoD1* mRNA expression could be observed in the right temporal muscle of controls compared to the left side (Fig. 1B).

For *MSTN* decreased levels of the mRNA expression could be detected in the right masseter muscle of dystrophic mice, whereas the expression counted only 35.8% of that found in the left untreated masseter muscle.

In contrast, in healthy mice no differences in mRNA amount of *MSTN* were found between treated and untreated masseter muscle. In those animals, however, significant decreased *MSTN* expression by 50% was detected in the right temporal muscle compared to the left side, which was not found in mdx mice (Fig. 1C).

Furthermore, significant differences were detected between healthy and dystrophic mice, e.g., in the left masseter muscle for *Myf4* and *MSTN*, and in the right temporal muscle for *MyoD1* and *MSTN* (Fig. 1).

mRNA expression 21 days after BTX-A injection

Twenty-one days after BTX-A injection, significant differences could be detected in both healthy and dystrophic mice, including a 6.2- and 6.0-fold increase in mRNA
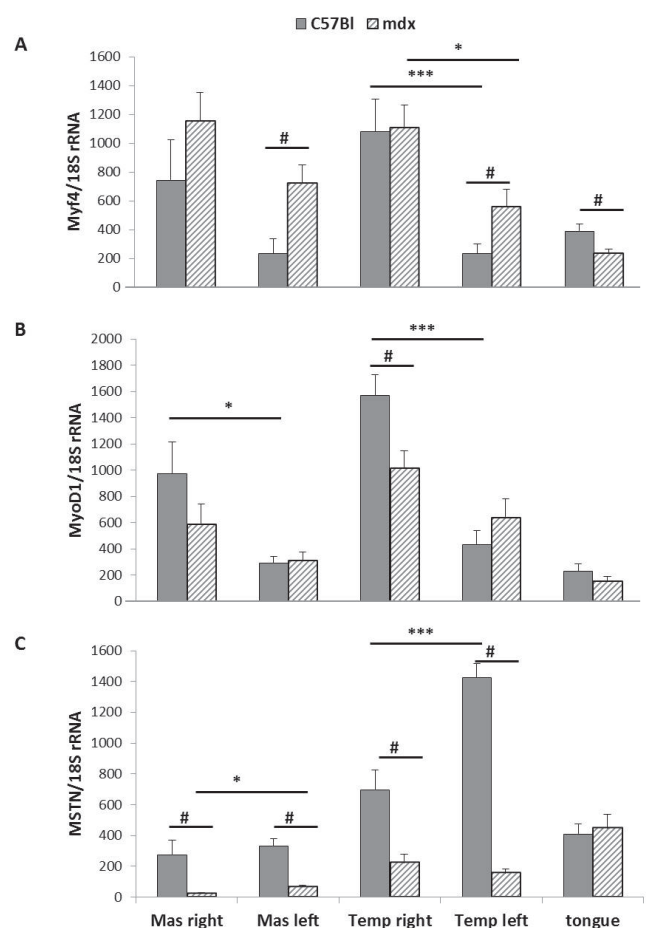
Fig. 1. Myostatin, myogenin and MyoD1-mRNA expression in treated and untreated muscle tissue 4 days post-toxin injection in the right masseter muscle of healthy and mdx mice

Means ± standard deviations (SD) for controls (n = 7) and mdx mice (n = 9); Mann-Whitney U test; * p ≤ 0.05 treated vs untreated masseter muscle; # p ≤ 0.05 control vs mdx.; * right vs left.

expression for *Myf4* in the BTX-A-treated masseter muscle compared to the left side, respectively (Fig. 2A) and a 3.7-fold increase in *MyoD1* mRNA amount in the BTX-A-treated masseter muscle of control and mdx mice, respectively (Fig. 2B).

Only 22% as well as 53% of the *MSTN* mRNA amount of the left side could be found in the right masseter and right temporal muscle of control mice (Fig. 2C), and reduced *MSTN* mRNA levels in dystrophic mice could be detected compared to healthy animals in the left masseter and left temporal muscle (Fig. 2C).

Protein content 21 days post-injection

Quantitative analysis of specific protein bands for myogenin, MyoD1 and myostatin, respectively (Fig. 3), revealed the following results: a 1.7-fold and 1.9-fold increase of myogenin expression on the right side compared to the contralateral side for both, masseter and temporal muscle in control mice (Fig. 4A). In dystrophic mice, significantly
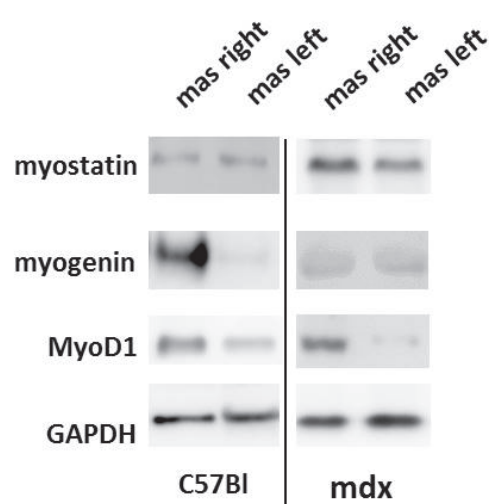
Fig. 3. Detection of myostatin, myogenin and MyoD1 in masseter muscle. Representative western blots of the right (injected) and left (non-injected) masseter muscle of control (C57Bl) and mdx mice. A monoclonal antibody was used to detect glyceraldehyde 3-phosphate dehydrogenase (GAPDH) serving as an internal control
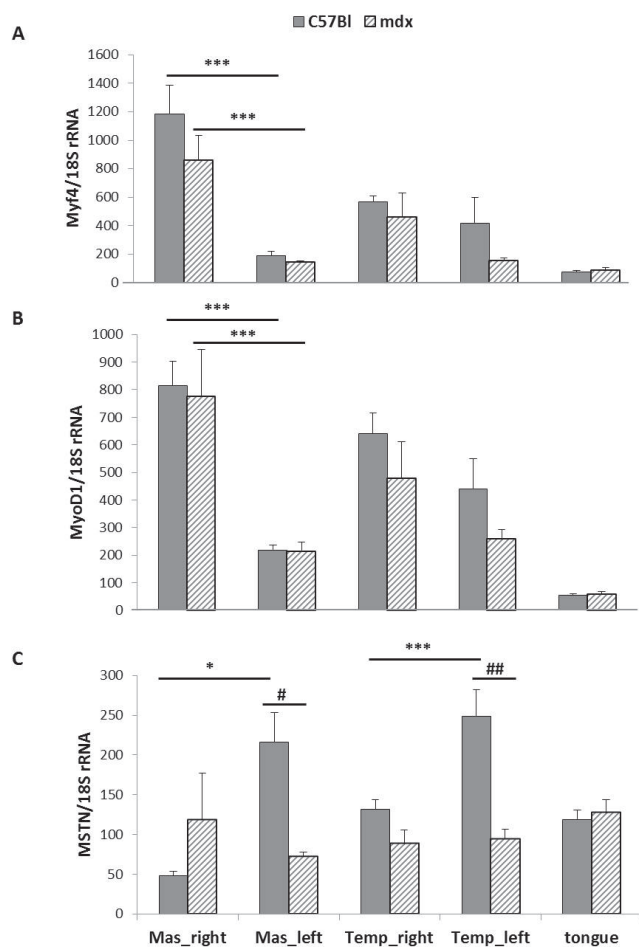
Fig. 2. Myostatin, myogenin and MyoD1-mRNA expression in treated and untreated muscle tissue 21 days post-toxin injection in the right masseter muscle of healthy and mdx mice

Means ± standard deviations (SD) for controls (n = 10) and mdx mice (n = 13); Mann-Whitney U test; * p ≤ 0.05 treated versus untreated masseter muscle; # p ≤ 0.05 control vs mdx; * right vs left.
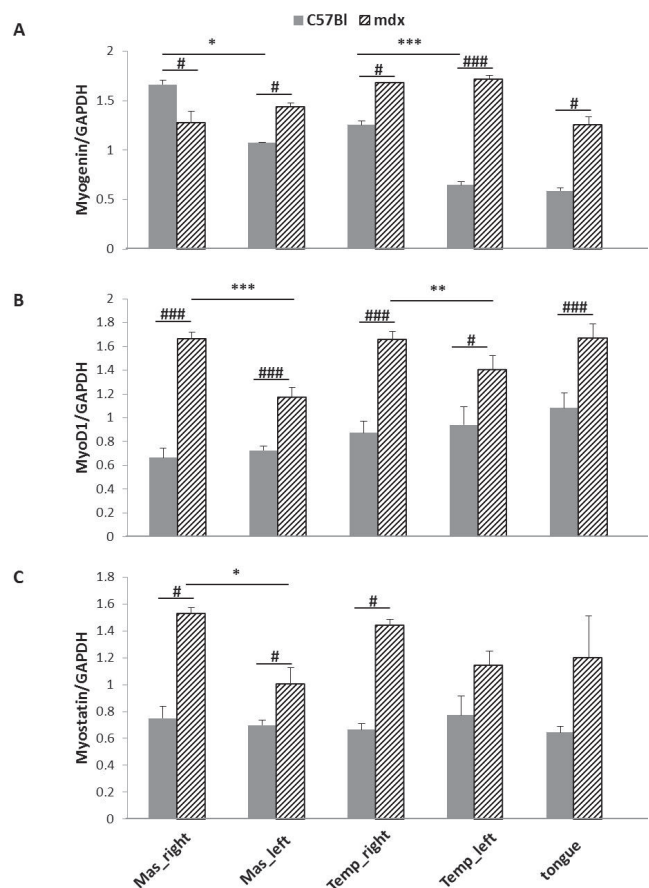
Fig. 4. Quantitative analysis of myostatin, myogenin and MyoD1 western blots in masseter, temporal and tongue muscle of mdx and control mice 21 days after BTX-A injection in the right masseter muscle of healthy and mdx mice

Protein bands attributed to myostatin, myogenin and MyoD1 were evaluated using GelScan 5.2 software (Serva, Heidelberg, Germany); mean optical densities (MOD) ± standard error of the mean (SEM) of control and mdx mice are given in all cases for n = 3 muscle samples (different animals) and 2 independent experiments (* p ≤ 0.05 right vs left; # p ≤ 0.05 control vs mdx).

increased protein levels of MyoD1 as well as myostatin were found in the BTX-A-treated masseter compared to the untreated muscle. The same changes were also found in temporal muscle in the case of MyoD1 (Fig. 4).

Furthermore, significantly increased protein amounts for myogenin, MyoD1 and myostatin could be detected in almost all dystrophic muscle samples compared to controls, with the exception of the left temporal and the tongue muscle in case of myostatin (Fig. 4).

Discussion

In this study 2 postinjection time points were analyzed to examine the time course of muscle recovery and regeneration in BTX-A-injected masseter and noninjected masticatory muscles; a 4-day interval reflecting the full characteristics of toxin effect and a 21-day interval illustrating changes after full paralysis and induction of myogenesis. The expression analysis of the genes and proteins, which are known to play a key role in skeletal muscle development and regeneration, demonstrated that the repair of healthy and dystrophic muscles occurred at staggered intervals. Furthermore, the gene analysis of *Myf4*, *MyoD1* and *MSTN* after 4 and 21 days allowed for better insight into the molecular mechanisms involved in muscle regeneration after muscle paralysis induced by BTX-A. Earlier studies have shown that MyoD protein expression in diaphragm, quadriceps and intrinsic laryngeal muscles do not show any significant differences between control and mdx mice at the age of 1, 4 and 9 months.[20] The same could be demonstrated for the expression of myogenin and MyoD1 protein in the masticatory muscles of 100-day-old dystrophic mice compared to the controls.[21] For this reason, the present study was performed using 100-day-old control and mdx mice. On the 4th day after BTX-A injection, by means of gene expression in the right masseter muscle, it could be concluded that the full effect of muscle paralysis was obtained. A significantly increased expression of *MyoD1* suggests that regenerative processes in the right masseter muscle of controls had already begun. This is in accordance with previous findings of Hatade et al.[22] Recently, it has been shown that 3 days after BTX-A injection, full paresis of the muscle was present and electrical stimulation failed to elicit any visible muscle contraction.[23] Between 3–7 days, initial sprouting occurred and at 4 days remodeling of these poisoned terminals became apparent. SNAP-25, a synaptic membrane protein that is involved in the vesicle exocytosis process, was present 9 days postinjection; however, only a minor reorganization of Ach receptors could be found.[23] In our study, gene analysis after 4 days revealed that healthy mice responded faster to muscle paralysis indicated by initiation of muscle regenerative and adaptive processes, while in mdx mice these processes could not be determined at that time. Furthermore, due to the enhanced expression of *MyoD1*

and *Myf4* and the decreased gene expression of *myostatin* in healthy mice, it can be assumed that the right temporal muscle supported masticatory function after the paralysis of the right masseter.

Three weeks after BTX-A injection, an increase of both *MyoD1* and *Myf4* genes could be detected in the right masseter muscle of healthy and mdx mice. At a molecular level, control animals as well as dystrophic mice showed a similar development of regenerative processes. However, BTX-A-induced paralysis of the right masseter muscle was diminished after 3 weeks, indicating that a reinnervation of the treated muscle had already begun by sprouting new nerve branches. It has previously been reported that the injection of animal neurotoxins in mice muscles accelerated the recovery of neurotransmission, and BTX-A treatment is known to result in rapid initiation of neurite sprouting from the paralyzed nerves.[23] The process of axon sprouting plays a key role in the subsequent recovery of paralyzed motor endplates and is a striking example of synaptic plasticity, which allows survival and, eventually, complete recovery from BTX-A-induced neuroparalysis.[23] Recovery from BTX-A-induced paralysis can be divided into different sections, at the neuromuscular junction (NMJ) as well as in the muscle fibres, which do not run synchronically. Thus, functional recovery of muscles is not concomitant with recovery of the NMJ. Furthermore, it should be mentioned that short-term denervation stimulates satellite cells to proliferate, whereas long-term denervation exhausts the satellite cell pool.[24] It is known that nerve terminal regeneration and functional reinnervation after BTX-A injection saw progress within 28–30 days and the first functional resumption of muscle activity appeared.[25] Usually, between 3–7 days, initial sprouting occurs and remodeling of these poisoned terminals becomes apparent at 4 days.[23] Furthermore, recovery of the NMJ was accompanied by an upregulation of Ach receptor subunits. Hence, after BTX-A injection most Ach subunit mRNAs are upregulated early and return to normal levels by approx, 2 weeks, so that 18–28 days after intoxication reorganization and clustering of Ach receptors facilitates reinnervation, and by 28 days, the first muscle twitch is possible.[26] Thus, it is apparent that neurotransmission is mediated by functional synapses formed between the terminal sprouts and the muscle fibers and these branches can at least temporarily adopt the function of the parent terminals in muscles paralyzed by BTX-A. Within 42–63 days after BTX-A-induced paralysis, sprouts receded, and the original nerve terminals immediately returned to functionality, and up to 3 months endplates regained morphologies and patterns indistinguishable from those visualized before poisoning.[23] *MRF4* and *myogenin* are significantly elevated compared to control levels at 3 days following BTX-A injection and return to control levels by 30 to 90 days after injection, while mRNA levels of *Myf5* and *MyoD* do not significantly change.[27] Recently, it has been demonstrated that BTX-A treatment significantly increased MyoD

expression in functionally denervated extraocular muscles, while a population of activated satellite cells became stably integrated into existing myofibers.[28] It is well-known that MyoD and myogenin are expressed in activated mononuclear muscle precursor cells and that they are the nodal point during the specification of the myogenetic lineage. The enhanced expression of these genes is associated with the growth of skeletal muscles in embryonic development, followed by a neonatal decrease. MyoD knock-out mice have no macroscopic degenerative phenotype under normal conditions but show significant deficiencies in regeneration.[29] It was postulated that, in the absence of MyoD, some essential steps in the myogenic progression were blocked, leading to a population of activated satellite cells, which returns to a quiescent stage. These satellite cells also exhibited major differences in myogenic gene expression, e.g., failure in up-regulation of MRF4 and myogenin.[29] However, in the mdx mouse, elevated MyoD and myogenin expression was detected at about 21 days of age, at the postnatal onset, at which regenerative activity is first observed in dystrophic muscles.[30] The postnatal levels of these genes were not reduced to those observed in the control mice and these maintained expression of MyoD and myogenin confirmed the regenerative processes in the skeletal muscles of adult mdx mice.[30] However, it has been proven that the deletion of myogenin in mdx mice neither reversed the pathologic effects of dystrophy nor aggravated their DMD, indicating that myogenin is dispensable for muscle regeneration in adult mice.[31] The expression of both, MyoD1 and myogenin genes, is necessary in the regenerative process, for the proliferation of myoblasts and for the development of early regenerating myotubes, even in dystrophic muscles. Within the active regenerating process these 2 genes were expressed at reasonably high levels in mdx mice after a single administration of bupivacaine hydrochloride, which is in accordance with our study. In the case of BTX-A administration, in comparison to untreated mice, in mdx mice a strongly increased MyoD expression could be detected at protein level.

The loss of myogenin during adult life confers a resistance to denervation-induced muscle atrophy.[32] After BTX-A injection myogenin upregulation usually persists for a longer period, which is also in accordance with our results. At protein level the right masseter muscle of controls showed a significant increase in myogenin expression. Entering myogenic differentiation a dysfunction of satellite cells has recently been discussed in dystrophic muscles due to the loss of polarity, abnormal division patterns including centrosome amplifications, impaired mitotic spindle orientation, and prolonged cell divisions based on the lack of dystrophin in mdx muscle stem cells.[33] This may explain the results found at protein level with a lack of myogenin expression in BTX-A-treated masseter muscle compared to healthy controls, whereas MyoD1 expression in the right masseter muscle of mdx mice was upregulated, indicating a delay in differentiation.

It has been proven that myostatin activity determines skeletal muscle mass. The inhibition of myostatin gene promotes muscle regeneration in humans and in animals in the postnatal period by increasing muscle mass and strength, and it has been shown that the inhibition of myostatin could be effective for increasing muscle mass and preventing muscle degeneration even in adults.[34] In contrast, skeletal muscle atrophy is associated with increased expression of this growth and differentiation factor. The significantly reduced gene expression of MSTN in the right masseter and temporal muscle of control animals might therefore be explained by an advanced regenerative process of the paralyzed muscle and/or a continuing compensatory effect of its neighboring muscle. However, in dystrophic muscles no significant changes regarding MSTN expression could be found at that time point. Several studies could demonstrate a significant effect of myostatin postnatally in muscle misuse and wasting.[35] Mice lacking myostatin induced a widespread increased muscle mass resulting from both hyperplasia and hypertrophy.[36] In mdx mice in which myostatin was knocked out or postnatally inhibited a less severe phenotype with greater absolute force and less fibrosis of individual muscles could be found.[37] Both antibody-mediated or myostatin propeptide-mediated myostatin blockade in mdx mice increased muscle strength and reduced the dystrophic pathophysiology.[38] The genetic inactivation of myostatin in muscle-derived stem cells (MDSC) was associated with the silencing of critical genes for early myogenesis. Skeletal myogenesis-related genes, e.g., MyoD1 and Myf5 are downregulated in MDSCs from myostatin knock-out mice compared to controls. For this reason, MDSCs from myostatin knock-out mice showed multipotent non-myogenic differentiation but no myogenic differentiation.[39] An increase in myostatin in necrotic muscle tissue and its significant reduction in regenerating myogenic cells could also be proven.[40] Compared to controls, a significantly reduced MSTN expression could have recently been observed in the masticatory muscles of 100-day-old dystrophic mice.[21] In the complete regenerated muscle in the mdx mouse after 9 weeks of birth, there was no evidence of myostatin.[40] Based on our findings, one can act on the assumption that regenerative processes in the masticatory muscles of the mdx mouse after BTX-A injection in the right masseter muscle were highly activated in these mice, which usually cannot be found at this age. In this regard, our study will contribute to a better understanding of regenerative processes at a molecular level in healthy and dystrophic mice muscles.

Conclusions

This study for the first time demonstrated that an intramuscular BTX-A injection into the masseter muscle induced changes in the gene and protein expression of myogenin, myostatin and MyoD1 in the masticatory muscles

of both healthy and mdx mice. In comparison to mdx mice, healthy mice showed a faster regeneration process of the paralyzed skeletal muscle; at the same time, however, compensatory effects could be found in the other masticatory muscles in both mice strains. Due to the increase of protein expression of the investigated genes in mdx mice, it can be assumed that the regeneration processes had been evolved much more slowly, which could be associated with the muscle dystrophy. Further investigations are necessary to better understand the time course of regeneration processes in the mdx mouse after BTX-A injection.

References

1. Ciciliot S, Rossi AC, Dyar KA, Blaauw B, Schiaffino S. Muscle type and fiber type specificity in muscle wasting. *Int J Biochem Cell Biol*. 2013;45(10):2191–2199.
2. Zanou N, Gailly P. Skeletal muscle hypertrophy and regeneration: Interplay between the myogenic regulatory factors (MRFs) and insulin-like growth factors (IGFs) pathways. *Cell Mol Life Sci*. 2013;70(21):4117–4130.
3. Flynn JM, Meadows E, Fiorotto M, Klein WH. Myogenin regulates exercise capacity and skeletal muscle metabolism in the adult mouse. *PloS One*. 2010;5(10):e13535.
4. Megeney LA, Kablar B, Garrett K, Anderson JE, Rudnicki MA. MyoD is required for myogenic stem cell function in adult skeletal muscle. *Genes Dev*. 1996;10(10):1173–1183.
5. McCroskery S, Thomas M, Platt L, et al. Improved muscle healing through enhanced regeneration and reduced fibrosis in myostatin-null mice. *J Cell Sci*. 2005;118(Pt 15):3531–3541.
6. Lepper C, Partridge TA, Fan CM. An absolute requirement for Pax7-positive satellite cells in acute injury-induced skeletal muscle regeneration. *Development*. 2011;138(17):3639–3646.
7. Morgan JE, Zammit PS. Direct effects of the pathogenic mutation on satellite cell function in muscular dystrophy. *Exp Cell Res*. 2010;316(18):3100–3108.
8. Eckardt L, Harzer W. Facial structure and functional findings in patients with progressive muscular dystrophy (Duchenne). *Am J Orthod Dentofacial Orthop*. 1996;110(2):185–190.
9. Pichavant C, Pavlath GK. Incidence and severity of myofiber branching with regeneration and aging. *Skelet Muscle*. 2014;4:9.
10. Bulfield G, Siller WG, Wight PA, Moore KJ. X chromosome-linked muscular dystrophy (mdx) in the mouse. *Proc Natl Acad Sci U S A*. 1984;81(4):1189–1192.
11. Heslop L, Morgan JE, Partridge TA. Evidence for a myogenic stem cell that is exhausted in dystrophic muscle. *J Cell Sci*. 2000;113(Pt 12):2299–2308.
12. Hirai Y. *Clostridium botulinum* and botulinum neurotoxin [in Japanese]. *Brain Nerve*. 2011;63(7):755–761.
13. Awan KH. The therapeutic usage of botulinum toxin (Botox) in non-cosmetic head and neck conditions: An evidence based review. *Saudi Pharm J*. 2017;25(1):18–24.
14. Pantano S, Montecucco C. The blockade of the neurotransmitter release apparatus by botulinum neurotoxins. *Cell Mol Life Sci*. 2014;71(5):793–811.
15. Tarabal O, Caldero J, Ribera J, et al. Regulation of motoneuronal calcitonin gene-related peptide (CGRP) during axonal growth and neuromuscular synaptic plasticity induced by botulinum toxin in rats. *Eur J Neurosci*. 1996;8(4):829–836.
16. Botzenhart UU, Wegenstein C, Todorov T, Kunert-Keil C. Influence of botulinum toxin A on the expression of adult myhc isoforms in the masticatory muscles in dystrophin-deficient mice (mdx-mice). *Biomed Res Int*. 2016;2016:7063093.
17. Botzenhart UU, Vaal V, Rentzsch I, Gredes T, Gedrange T, Kunert-Keil C. Changes in caveolin-1, caveolin-3 and vascular endothelial growth factor (VEGF) expression and protein content after botulinum toxin A (BTX-A) injection in the right masseter muscle of dystrophin deficient (mdx-) mice. *J Physiol Pharmacol*. 2017;68(1):181–189.
18. Baverstock H, Jeffery NS, Cobb SN. The morphology of the mouse masticatory musculature. *J Anat*. 2013;223(1):46–60.
19. Livak KJ, Schmittgen TD. Analysis of relative gene expression data using real-time quantitative PCR and the 2(-Delta Delta C(T)) Method. *Methods*. 2001;25(4):402–408.
20. Barros Maranhao J, de Oliveira Moreira D, Mauricio AF, et al. Changes in calsequestrin, TNF-alpha, TGF-beta and MyoD levels during the progression of skeletal muscle dystrophy in mdx mice: A comparative analysis of the quadriceps, diaphragm and intrinsic laryngeal muscles. *Int J Clin Exp Pathol*. 2015;96(5):285–293.
21. Spassov A, Gredes T, Lehmann C, et al. Myogenic differentiation factor 1 and myogenin expression not elevated in regenerated masticatory muscles of dystrophic (mdx) mice. *J Orofac Orthop*. 2011;72(6):469–475.
22. Hatade T, Takeuchi K, Fujita N, Arakawa T, Miki A. Effect of heat stress soon after muscle injury on the expression of MyoD and myogenin during regeneration process. *J Musculoskelet Neuronal Interact*. 2014;14(3):325–333.
23. de Paiva A, Meunier FA, Molgo J, Aoki KR, Dolly JO. Functional repair of motor endplates after botulinum neurotoxin type A poisoning: Biphasic switch of synaptic activity between nerve sprouts and their parent terminals. *Proc Natl Acad Sci U S A*. 1999;96(6):3200–3205.
24. Bornemann A, Maier F, Kuschel R. Satellite cells as players and targets in normal and diseased muscle. *Neuropediatrics*. 1999;30(4):167–175.
25. Duregotti E, Zanetti G, Scorzeto M, et al. Snake and spider toxins induce a rapid recovery of function of botulinum neurotoxin paralysed neuromuscular junction. *Toxins*. 2015;7(12):5322–5336.
26. Ma J, Shen J, Lee CA, et al. Gene expression of nAChR, SNAP-25 and GAP-43 in skeletal muscles following botulinum toxin A injection: A study in rats. *J Orthop Res*. 2005;23(2):302–309.
27. Shen J, Ma J, Elsaidi GA, et al. Gene expression of myogenic regulatory factors following intramuscular injection of botulinum A toxin in juvenile rats. *Neurosci Lett*. 2005;381(3):207–210.
28. Ugalde I, Christiansen SP, McLoon LK. Botulinum toxin treatment of extraocular muscles in rabbits results in increased myofiber remodeling. *Invest Ophthalmol Vis Sci*. 2005;46(11):4114–4120.
29. Cornelison DD, Olwin BB, Rudnicki MA, Wold BJ. MyoD$^{-/-}$ satellite cells in single-fiber culture are differentiation defective and MRF4 deficient. *Dev Biol*. 2000;224(2):122–137.
30. Beilharz MW, Lareu RR, Garrett KL, Grounds MD, Fletcher S. Quantitation of muscle precursor cell activity in skeletal muscle by Northern analysis of MyoD and myogenin expression: Application to dystrophic (mdx) mouse muscle. *Mol Cell Neurosci*. 1992;3(4):326–331.
31. Meadows E, Flynn JM, Klein WH. Myogenin regulates exercise capacity but is dispensable for skeletal muscle regeneration in adult mdx mice. *PloS One*. 2011;6(1):e16184.
32. Moresi V, Williams AH, Meadows E, et al. Myogenin and class II HDACs control neurogenic muscle atrophy by inducing E3 ubiquitin ligases. *Cell*. 2010;143(1):35–45.
33. Dumont NA, Wang YX, von Maltzahn J, et al. Dystrophin expression in muscle stem cells regulates their polarity and asymmetric division. *Nat Med*. 2015;21(12):1455–1463.
34. Tsuchida K. The role of myostatin and bone morphogenetic proteins in muscular disorders. *Expert Opin Biol Ther*. 2006;6(2):147–154.
35. Wehling M, Cai B, Tidball JG. Modulation of myostatin expression during modified muscle use. *FASEB J*. 2000;14(1):103–110.
36. McPherron AC, Lawler AM, Lee SJ. Regulation of skeletal muscle mass in mice by a new TGF-beta superfamily member. *Nature*. 1997;387(6628):83–90.
37. Wagner KR, Liu X, Chang X, Allen RE. Muscle regeneration in the prolonged absence of myostatin. *Proc Natl Acad Sci U S A*. 2005;102(7):2519–2524.
38. Tsuchida K. Myostatin inhibition by a follistatin-derived peptide ameliorates the pathophysiology of muscular dystrophy model mice. *Acta Myol*. 2008;27:14–18.
39. Tsao J, Vernet DA, Gelfand R, et al. Myostatin genetic inactivation inhibits myogenesis by muscle-derived stem cells in vitro but not when implanted in the mdx mouse muscle. *Stem Cell Res Ther*. 2013;4(1):4.
40. Abe S, Soejima M, Iwanuma O, et al. Expression of myostatin and follistatin in Mdx mice, an animal model for muscular dystrophy. *Zoolog Sci*. 2009;26(5):315–320.

Vitamin C may exert variable effects on viability and proliferation of HeLa cells exhibiting high and low chromosomal instability

Aastha Sindhwani[B,C], Sasikala Muthusammy[B,C], Alka Bhatia[A,C–F]

Department of Experimental Medicine & Biotechnology, Postgraduate Institute of Medical Education & Research, Chandigarh, India

A – research concept and design; B – collection and/or assembly of data; C – data analysis and interpretation;
D – writing the article; E – critical revision of the article; F – final approval of the article

Address for correspondence
Alka Bhatia
E-mail: alkabhatia@ymail.com

Conflict of interest
None declared

Abstract

Background. Chromosomal instability (CIN), defined as abnormality in chromosome structure or number, is the hallmark of malignancies. The role of vitamin C in cancer treatment is controversial and its effect on CIN is still an open field of research. In this work, we tried to study the effect of high-dose L-ascorbic acid (L-AA) on CIN-induced (CIN_{hi} = CIN high) and non-CIN-induced (CIN_{lo} = CIN low) cervical cancer cells.

Objectives. The aim of this study was to explore the effect of high-dose L-AA on CIN in the cervical cancer cell line (HeLa) cells.

Material and methods. The HeLa cells (CIN_{hi} and CIN_{lo}) were treated with 2 doses (5 mM and 8 mM) of L-AA for 24 h and 48 h. They were then analyzed by micronucleus (MN) scoring, cell ploidy and flow cytometry, the latter regarding γH2AX expression. Cell viability was assessed by the methylthiazol tetrazolium (MTT) and Annexin V assays.

Results. Treatment of CIN_{hi} cells with L-AA led to a decrease in MN score (colchicine – 71.5 ±4.95, 67.5 ±0.71; L-AA (5 mM) – 49 ±7.07, 46.5 ±4.95; L-AA (8 mM) – 42 ±9.89, 41 ±1.41, at 24 h and 48 h, respectively; $p < 0.05$). Treatment of CIN_{lo} cells with L-AA resulted in increased MN score (5 mM – 45 ±7.07, 36 ±4.24; 8 mM – 34.5 ±4.95, 31 ±1.41, at 24 h and 48 h, respectively; control – 15.5 ±0.71, 12.5 ±0.71; $p < 0.05$) and reduction in cancer cell viability (control – 100%; L-AA (5 mM) – 76.32% ±28.73, 72.74% ±20.30; L-AA (8 mM) – 66.14% ±19.13, 66.99% ±19.99, at 24 h and 48 h, respectively; $p < 0.05$). The expression of γH2AX was high in both groups at 48 h (mean CIN_{hi} = 19.42%, CIN_{lo} = 21.14%; control = 1.19% and 1.58%, respectively) with the 8 mM dose of L-AA.

Conclusions. L-ascorbic acid was found to have a differential effect on CIN_{hi} and CIN_{lo} HeLa cells, which may be due to differences in oxidation status of these 2 categories.

Key words: cancer, vitamin C, chromosomal instability

Introduction

Chromosomal instability (CIN) is the defining feature of most malignancies. Many environmental factors, including dietary influences, may contribute to CIN.[1] L-ascorbic acid (L-AA), commonly known as vitamin C, is a water-soluble vitamin with pro- and antioxidant roles. The role of L-AA in cancer is controversial, with studies variably reporting its anti- and pro-cancer effects.[2–4] Although various mechanisms have been proposed for its anti-cancer effects, the exact mode of action of L-AA on cancer cells is not well understood. Yun et al. in their work on the effect of a high dose of vitamin C in colorectal cancer demonstrated its cytotoxicity to KRAS and BRAF mutated cancer cells, owing to the uptake and reduction of its oxidized form, dehydroascorbate.[5] Doskey et al. in their work on pancreatic cancer cell lines, demonstrated that cytotoxicity of ascorbate to cancer cells was due to the generation of H_2O_2, which cancer cells fail to clear because of low catalase activity.[4] More recently, vitamin C has been found to be effective in targeting cancer stem cells.[6] Although it has been suggested that it may selectively inflict

DNA damage in cancer cells, there is no conclusive data on the effect of L-AA on DNA damage and CIN in cancer. We carried out this study with the aim of evaluating the effect of high-dose L-AA on CIN in the cervical cancer cell line (HeLa) cells.

Material and methods

The HeLa was used in the study to evaluate the effect of high-dose L-AA on cancer cells. The HeLa cells were obtained from a commercial source (National Centre for Cell Science, Pune, India) and maintained in the RPMI (Roswell Park Memorial Institute) 1640 formulation with 10% fetal calf serum (FCS) at 37°C in an atmosphere of 5% carbon dioxide (CO_2). The cells were plated in 6-well culture plates for incubation with drugs and all the experiments were carried out thrice. For the induction of CIN, the cells were treated with metaphase-arresting drug colchicine (0.2–200 μg/mL) for 24 h and 48 h, respectively. Chromosomal instability in the cells was assessed by staining them with Giemsa stain and counting the number of micronuclei
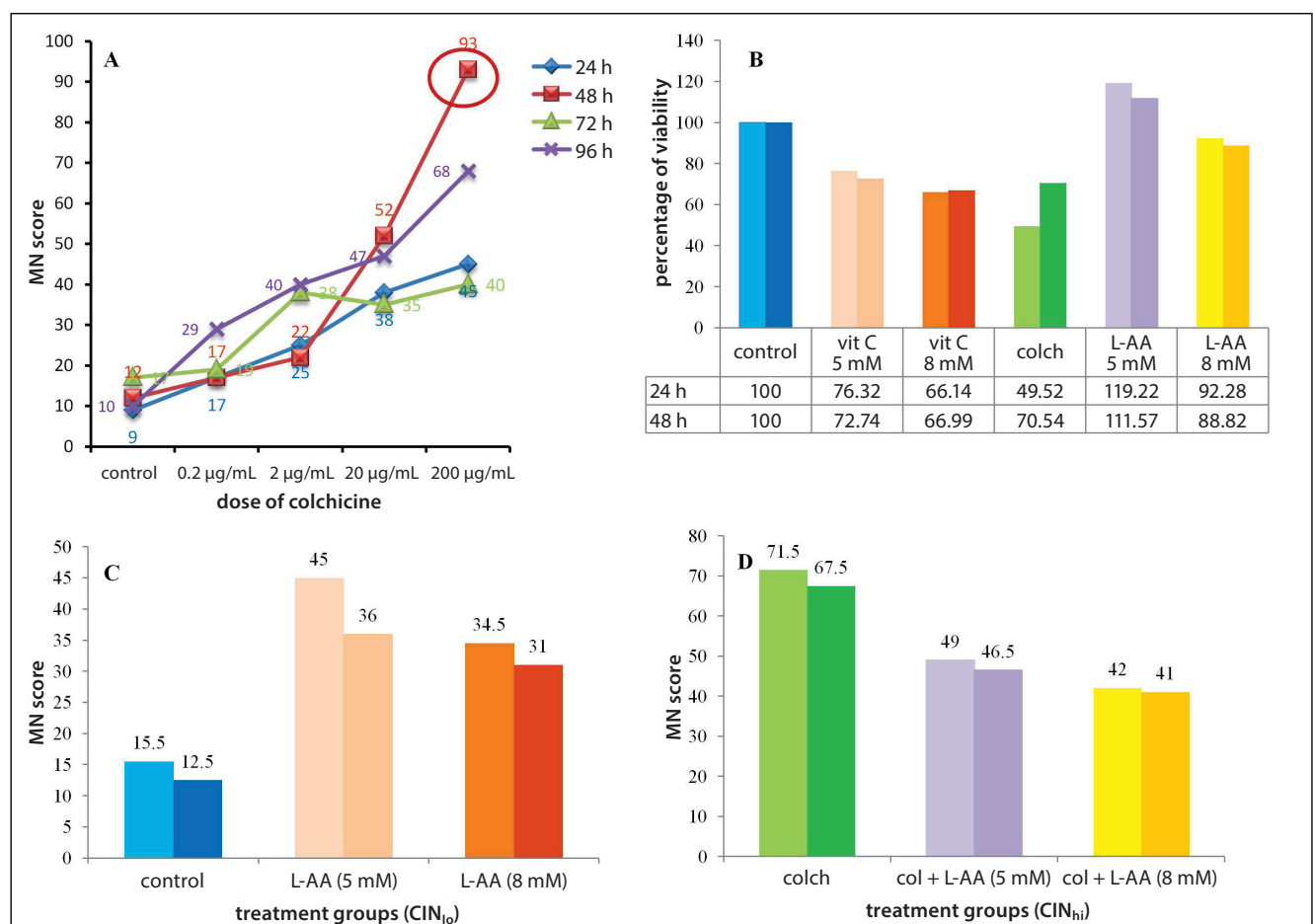
Fig. 1. A – micronucleus (MN) score at different concentrations of colchicine. Note that the highest score was found with 200 μg/mL at 48 h (encircled). This concentration was therefore chosen to induce chromosomal instability (CIN) in our study; B – percentage of viability of the HeLa cells in different treatment groups at 24 h and 48 h (double bars). Note the decreased viability in non-CIN-induced (CIN$_{lo}$) cells upon treatment with L-ascorbic acid (L-AA). However, in CIN-induced (CIN$_{hi}$) cells, no decrease was observed; C, D – MN score in CIN$_{lo}$ and CIN$_{hi}$ cells, respectively. Note that there was a higher score in the former group as compared to the control, whereas in the latter group, the score was found to be lower when compared to colchicine treatment alone

(MN) present per 1,000 cells under a light microscope. The dose of colchicine causing maximum CIN was chosen for the induction of CIN in further experiments. Both CIN-induced (CIN_{hi} = CIN high) and non-CIN-induced (CIN_{lo} = CIN low) cells were then treated with 2 doses of L-AA (5 mM and 8 mM) for 2 time periods of 24 h and 48 h, respectively. At the end of the incubation period, the effect on parameters, like cell viability (methylthiazol tetrazolium (MTT) assay), apoptosis (Annexin V assay) and CIN MN counting, and the expression of DNA double-strand breaks (DSB) marker (γH2AX), was assessed.

Results

Micronucleus score after treatment with colchicine

Upon treatment with colchicine, the HeLa cells showed a variable number of MN (9–93/1,000 cells). However,

the maximum number of MN (93/1,000 cells) was noted with 200 µg/mL at 48 h. Therefore, the latter dose and duration was used for the induction of CIN in HeLa cells (Fig. 1A).

Effect of L-ascorbic acid on proliferation and viability of CIN_{hi} and CIN_{lo} HeLa cells

A reduction in proliferation and viability of CIN_{lo} cells was noted upon treatment with L-AA at both doses (5 mM – 76.32% ±28.73%, 72.74% ±20.30%; 8 mM – 66.14% ±19.13%, 66.99% ±19.99%, at 24 h and 48 h, respectively; $p < 0.05$, paired t-test). However, the reduction in viability was totally absent or only minimal in CIN_{hi} cells (Fig. 1B).

Effect of different doses of L-ascorbic acid on micronucleus scoring in CIN_{hi} and CIN_{lo} HeLa cells

Treatment of CIN_{hi} HeLa cells with L-AA led to a significant decrease in MN score at both durations (colchicine alone – 71.5 ±4.95, 67.5 ±0.71; CIN_{hi} (5 mM) – 49.00 ±7.07, 46.5 ±4.95; CIN_{hi} (8 mM) – 42 ±9.89, 41 ±1.41, at 24 h and 48 h, respectively; $p < 0.055$, paired t-test) (Fig. 1C). However, in CIN_{lo} cells, the MN score upon treatment with vitamin C (5 mM = 45 ±7.07, 36 ±4.24; 8 mM = 34.5 ±4.95, 31 ±1.41 at 24 h and 48 h, respectively) was found to be significantly higher than in the untreated control (15.5 ±0.71, 12.5 ±0.71, p-value <0.05, paired t-test) at both durations of treatment (Fig. 1D).

	control	col	col + L-AA 5 mM	col + L-AA 8 mM	L-AA 5 mM	L-AA 8 mM
24 h	0.42	6.06	0.42	0.34	4.8	0.99
48 h	0.17	2.42	5.73	6.08	5.46	5.4

	S phase	G1 phase	G2 phase
i) Control	50.41	39.27	10.21
ii) L-AA (5 mM)	61.16	23.75	15.10
iii) L-AA (8 mM)	63.59	23.87	12.54
iv) Colchicine	1.60	10.90	87.50
v) Colch + L-AA (5 mM)	41.16	14.33	44.51
vi) Colch + L-AA (8 mM)	31.32	18.19	50.49

	S phase	G1 phase	G2 phase
i) Control	30.03	65.76	4.21
ii) L-AA (5 mM)	22.66	9.63	67.71
iii) L-AA (8 mM)	40.02	10.93	49.05
iv) Colchicine	16.83	17.70	65.47
v) Colch + L-AA (5 mM)	42.58	18.26	39.17
vi) Colch + L-AA (8 mM)	44.55	25.26	30.20

Fig. 2. A – percentage of apoptosis in HeLa cells upon treatment with various drugs. No significant increase was observed; B, C – distribution of cells in different phases of the cell cycle in different treatment groups: i) control; ii) L-ascorbic acid (L-AA) 5 mM; iii) L-AA 8 mM; iv) colchicine; v) colchicine + LAA 5 mM; vi) colchicine + L-AA 8 mM, at 24 h and 48 h, respectively. Note the G2/M arrest caused by colchicine at both durations, and the presence of the majority of cells in the S and G2/M phases in L-AA-treated groups with or without colchicine

Effect of L-ascorbic acid on apoptogenicity of CIN$_{hi}$ and CIN$_{lo}$ cells

Annexin V assay showed no significant increase in the percentage of apoptotic cells with any of the drugs used in our experiments (Fig. 2A).

Effect of L-ascorbic acid on the cell cycle of CIN$_{hi}$ and CIN$_{lo}$ HeLa cells

Treatment with colchicine resulted in cell cycle arrest at the G2/M phase (87.50% and 65.47% at 24 h and 48 h, respectively). When the cells CIN$_{hi}$ were treated with both doses of L-AA, the majority of cells were found to be distributed in the S and G2/M phases of the cell cycle at both treatment durations. The cells CIN$_{lo}$ were found to be mainly distributed in the S phase at 24 and the G2/M phase at 48 h, respectively (Fig. 2B,C).

Effect of L-ascorbic acid on the expression of DNA damage response marker γH2AX in HeLa cells

An increase in the percentage of γH2AX-positive cells was noted in both CIN$_{hi}$ and CIN$_{lo}$ cells, particularly after treatment with 8 mM L-AA (mean γH2AX expression – 19.42%, 21.14%; control – 1.19%, 1.58%, respectively) after

48 h of treatment (Fig. 3). However, there was no significant change in the expression of γH2AX in colchicine-treated cells.

Discussion

Cancers are heterogeneous in nature. Some degree of numerical and structural defect in chromosomes, termed as CIN, is present in most tumors. The current literature has emphasized the presence of populations of more differentiated and more aggressive cells in cancers, the latter harboring more genetic defects and being less susceptible to therapy. Therefore, the agents being tested for targeting cancer should be investigated in the light of their effects on different populations of cells present in cancer.[1]

Many past studies have stressed the beneficial effect of high-dose vitamin C intake in cancer. Many papers have described the inhibitory effect of millimolar concentrations of L-AA in vitro. However, many other studies have reported contrary results.[2–4,7] In view of the controversial literature on the effect of L-AA on cancer cells, we undertook the present work to investigate its effect on HeLa cells harboring CIN.

To induce a higher degree of CIN, we treated the HeLa cells with a high dose of colchicine.[8] The 2 types of cells, when treated with vitamin C, showed paradoxical results.

	control	L-AA 5 mM	L-AA 8 mM	col	col + L-AA 5 mM	col + L-AA 8 mM
24 h	1.89	1.05	4.25	1.33	2.51	4.3
48 h	1.58	6.36	21.14	1.19	7.06	19.42
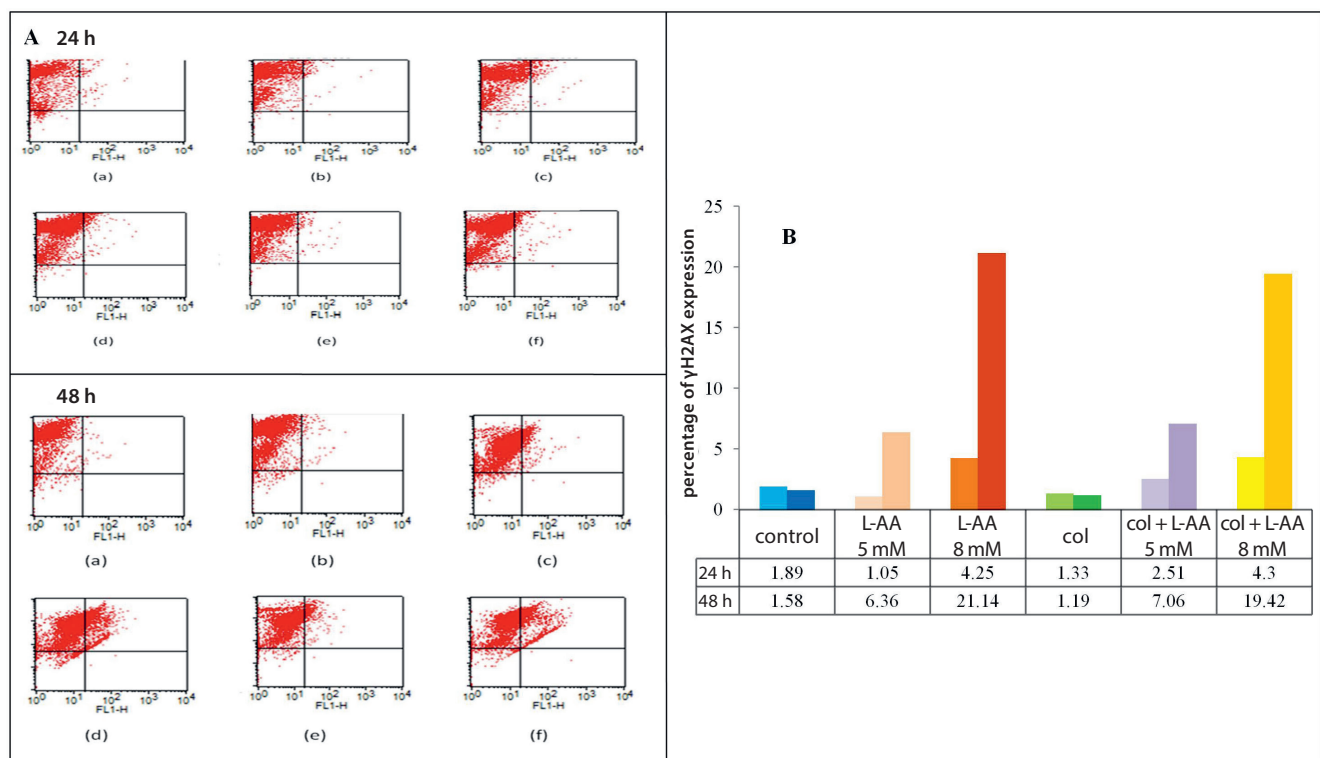
Fig. 3. A – the expression of γH2AX in HeLa cells in different treatment groups: (a) control; (b) L-ascorbic acid (L-AA) 5 mM; (c) L-AA 8 mM; (d) colchicine; (e) colchicine + L-AA 5 mM; (f) colchicine + L-AA 8 mM, at 24 h and 48 h, respectively; B – bar diagram comparing the γH2AX expression in different groups. Note a significant increase in expression at the 8 mM dose of L-AA, particularly at 48 h, in both low chromosomal instability (CIN$_{lo}$) and high CIN (CIN$_{hi}$) groups, indicating the induction of DNA damage repair response with vitamin C
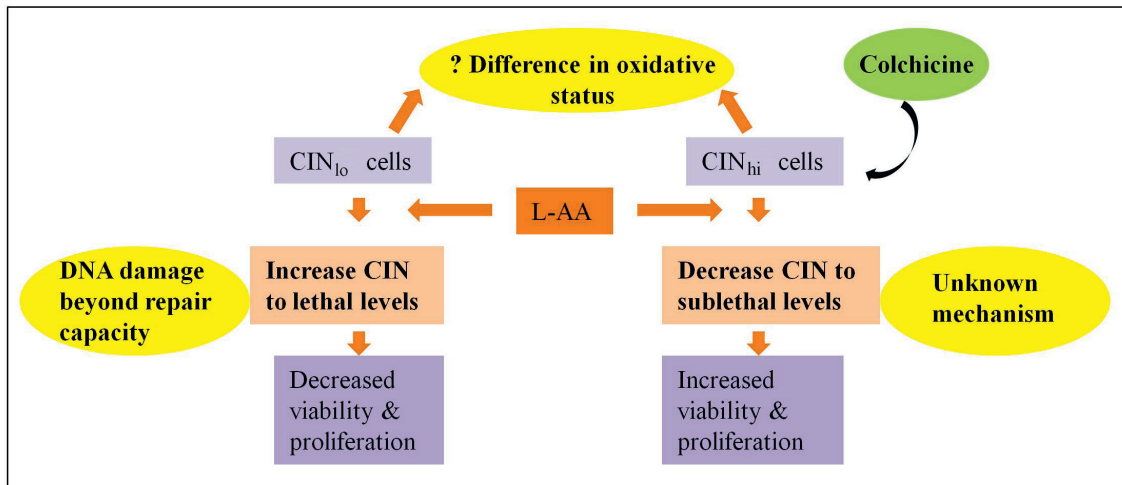
Fig. 4. Possible explanation for the differential effect of vitamin C in high chromosomal instability (CIN$_{hi}$) and low CIN (CIN$_{lo}$) HeLa cells: a hypothesis

L-AA – L-ascorbic acid.

Vitamin C was found to enhance CIN in CIN$_{lo}$ cells, at the same time decreasing their viability and proliferation. However, in CIN$_{hi}$ cells, vitamin C was observed to reduce CIN, at the same time increasing their viability and proliferation. We hypothesize that this may be due to cell death being triggered by L-AA via the induction of DNA damage beyond the repair capacity of the cancer cells in the former case. In the latter case (CIN$_{hi}$ cells), treatment with L-AA was probably decreasing CIN to sublethal levels by unknown mechanisms, allowing the more aggressive population of cells to proliferate (Fig. 4). Some of the previous studies carried out on lymphocytes have also demonstrated the genotoxic potential of L-AA, especially in the presence of oxidizing agents like H$_2$O$_2$ or heavy metals like iron. The induction of single-strand breaks in the presence of oxidative stress was suggested as the mechanism behind the toxicity described above. Other studies have shown the protective effect of vitamin C on cisplatin-induced chromosome aberrations in lymphocytes in cancer patients.[9,10] Interestingly, a study carried out on the HeLa cells by Azqueta et al. did not show any effect of L-AA on DNA strand break or base excision repair; however, the concentration used in their study was much lower (up to 200 μM) than that used by us.[11] High-dose vitamin C has also been proposed to cause increased DNA damage via the generation of reactive oxygen species (ROS) in gene-mutated cancer cells.[5]

Chromosomal instability is a double-edged sword. Up to a certain threshold, it is believed to increase cell proliferation; however, beyond that threshold, it is known to cause cell death.[12] The results of our study, together with an increase in the expression of DNA damage response marker γH2AX in both categories of cells, demonstrate the clastogenic potential of L-AA on the HeLa cells, especially during longer exposure (48 h). However, whereas the clastogenicity of L-AA was able to cause killing in CIN$_{lo}$ cells, it was not found to reduce the viability of CIN$_{hi}$ cells. The differential effect on 2 categories of cells may help to explain the contradictory results of the studies trying to investigate the effect of vitamin C on cancer cells.

A complex effect was observed on the cell cycle upon treatment with L-AA. Colchicine, being a mitotic spindle inhibitor, resulted in cell cycle arrest in the G2/M phase. Treatment of these cells with L-AA resulted in the distribution of the cells to the S and G2/M phases. Also, in these CIN$_{hi}$ cells, the S-phase fraction (SPF) was seen to increase. Treatment with L-AA alone showed complex effects with a mild increase in SPF. Previous studies have also highlighted that the irregular cell cycle kinetics observed with L-AA, with cell cycle arrest in the S, G2M and G0/G1 phases, is dependent on the cell line being studied, and that this inhibition of cell division promoted necrosis of the malignant cells. In those studies, L-AA was found to act by regulating the activity of various molecules related to cell cycles, such as Cdc25C, Chk2-p53-p21$^{waf1/cip1}$, etc.[13–16]

The apoptosis assay carried out in our study did not demonstrate much increase in the population of the apoptotic cells, thereby indicating that L-AA may be causing cell death by mechanisms other than apoptosis. Previous studies have also reported different mechanisms of cell death caused by vitamin C like autoschizis (cell splitting), apoptosis progressing to pyknosis/necrosis on prolonged treatment, etc.[15–18] The exact modes of cell death involved in vitamin C induced cytotoxicity, therefore, remain to be investigated.

Thus, our study suggests that treatment with L-AA may have different effects on CIN$_{hi}$ and CIN$_{lo}$ cancer cells. The genotoxic and cytotoxic effect of high-dose L-AA on CIN$_{lo}$, but not on CIN$_{hi}$ HeLa cells, may be due to a difference in the oxidative status of these cell types. However, it needs to be confirmed in future studies. Moreover, our results also point toward the clastogenic potential of L-AA, as indicated by the increased MN score and increased expression of DNA damage response marker γH2AX.

However, the preliminary data obtained from the present study needs to be confirmed, using more robust studies, employing small interfering RNA (siRNA)-based methods for the induction of CIN and molecular techniques, like fluorescent in situ hybridization, for the measurement of CIN.

References

1. van Wely KM, Martinez CA. Linking stem cells to chromosomal instability. *Oncoimmunol.* 2012;1(2):195–200.
2. Cameron E, Pauling L. Supplemental ascorbate in the supportive treatment of cancer: Prolongation of survival times in terminal human cancer. *Proc Natl Acad Sci U S A.* 1976;73(10):3685–3689.
3. Hoffer LJ, Robitaille L, Zakarian R, et al. High-dose intravenous vitamin C combined with cytotoxic chemotherapy in patients with advanced cancer: A phase I-II clinical trial. *PLoS ONE.* 2015;10(4): e0120228. doi: 10.1371/journal.pone.0120228
4. Doskey CM, Buranasudja V, Wagner BA, et al. Tumor cells have decreased ability to metabolize H_2O_2: Implications for pharmacological ascorbate in cancer therapy. *Redox Biol.* 2016;10:274–284.
5. Yun J, Mullarky E, Lu C, et al. Vitamin C selectively kills KRAS and BRAF mutant colorectal cancer cells by targeting GAPDH. *Science.* 2015;350(6266):1391–1396.
6. Bonuccelli G, De Francesco EM, de Boer R, Tanowitz HB, Lisanti MP. NADH autofluorescence, a new metabolic biomarker for cancer stem cells: Identification of vitamin C and CAPE as natural products targeting "stemness". *Oncotarget.* 2017;8(13):20667–20678. doi: 10.18632/oncotarget.1540
7. Ma Y, Chapman J, Levine M, Polireddy K, Drisko J, Chen Q. High-dose parenteral ascorbate enhanced chemosensitivity of ovarian cancer and reduced toxicity of chemotherapy. *Sci Transl Med.* 2014;6(222):222ra18. doi: 10.1126/scitranslmed.3007154
8. Kundu LM, Ray S. Mitotic abnormalities and micronuclei inducing potentials of colchicine and leaf aqueous extracts of *Clerodendrum viscosum* Vent. in *Allium cepa* root apical meristem cells. *International Journal of Cytology, Cytosystematics and Cytogenetics.* 2016;70:7–14.
9. Nefic H. The genotoxicity of vitamin C in vitro. *Bosn J Basic Med Sci.* 2008;8(2):142–146.
10. Madhuri K, Vani K, Syed R, Alshatwi AA. Role of ascorbic acid as an antioxidant in gastric cancer patients in South Indian population. *Int J Pharm Pharm Sci.* 2011;3:179–181.
11. Azqueta A, Costa S, Lorenzo Y, Bastani NE, Collins AR. Vitamin C in cultured human (HeLa) cells: Lack of effect on DNA protection and repair. *Nutrients.* 2013;5(4):1200–1217.
12. Weaver BA, Silk AD, Montagna C, Verdier-Pinard P, Cleveland DW. Aneuploidy acts both oncogenically and as a tumor suppressor. *Cancer Cell.* 2013;11(1):25–36.
13. Thomas CG, Vezyraki PE, Kalfakakou VP, Evangelou AM. Vitamin C transiently arrests cancer cell cycle progression in S phase and G2/M boundary by modulating the kinetics of activation and the subcellular localization of Cdc25C phosphatase. *J Cell Physiol.* 2005;205(2):310–318.
14. Guerriero E, Sorice A, Capone F, et al. Vitamin C effect on mitoxantrone-induced cytotoxicity in human breast cancer cell lines. *PLoS ONE.* 2014;9(12):e115287. doi: 10.1371/journal.pone.0115287
15. Hahm E, Jin DH, Kang JS, et al. The molecular mechanisms of vitamin C on cell cycle regulation in B16F10 murine melanoma. *J Cell Biochem.* 2007;102(4):1002–1010.
16. Sajadian SO, Tripura C, Samani FS, et al. Vitamin C enhances epigenetic modifications induced by 5-azacytidine and cell cycle arrest in the hepatocellular carcinoma cell lines HLE and Huh7. *Clin Epigenetics.* 2016;8:46. doi: 10.1186/s13148-016-0213-6
17. Verrax J, Cadrobbi J, Delvaux M, et al. The association of vitamins C and K3 kills cancer cells mainly by autoschizis, a novel form of cell death: Basis for their potential use as coadjuvants in anticancer therapy. *Eur J Med Chem.* 2003;38(5):451–457.
18. Chen Q, Espey MG, Krishna MC, et al. Pharmacologic ascorbic acid concentrations selectively kill cancer cells: Action as a pro-drug to deliver hydrogen peroxide to tissues. *Proc Natl Acad Sci U S A.* 2005;102(38):13604–13609.

Progesterone decreases the extent of ovarian damage caused by cisplatin in an experimental rat model

Saim Ozdamar[1,E,F], Mine Islimye Taskin[2,A,F], Gozde Ozge Onder[1,B], Emin Kaymak[1,B], Munevver Baran[3,C], Arzu Yay[1,A–F]

[1] Department of Histology and Embryology, Medicine Faculty, Erciyes University, Kayseri, Turkey

[2] Department of Obstetrics and Gynecology, Medicine Faculty, University of Balikesir, Turkey

[3] Department of Pharmaceutical Basic Science, Faculty of Pharmacy, Erciyes University, Kayseri, Turkey

A – research concept and design; B – collection and/or assembly of data; C – data analysis and interpretation;
D – writing the article; E – critical revision of the article; F – final approval of the article

Address for correspondence
Arzu Yay
E-mail: arzu.yay38@gmail.com

Abstract

Background. Apart from the role of progesterone in reproductive physiology, the protective role of exogenously administered progesterone was observed in various injuries, such as neurologic defects and acute kidney injury.

Objectives. The aim of the present study was to investigate the effects of progesterone therapy on the immunoexpression of anti–Müllerian hormone (AMH) and the number of apoptotic cells in ovarian damage induced with cisplatin, a chemotherapeutic agent, in an experimental rat model.

Material and methods. Forty rats were randomly divided into 4 groups; the control group (the saline group), the cisplatin-treated group (rats were injected with 5 mg/kg/week cisplatin intraperitoneally (i.p.)), the cisplatin + progesterone-treated group (the rats were pretreated with 8 mg/kg progesterone intramuscularly (i.m.) (8 mg/kg) before they were injected with 5 mg/kg/week cisplatin i.p.), and the progesterone-treated group (the rats were treated with 8 mg/kg progesterone i.m.). The ovaries were removed from the rats in all groups 5 days after the final injection of cisplatin.

Results. Histopathologic examination and follicle counting were performed. The immunoreactivity intensity of AMH and apoptosis were compared. Histological analysis of the ovaries treated with cisplatin showed ovarian damage. Immunohistochemical analysis showed that the immunoreactivity intensity of AMH, a biomarker that discriminates the degree of ovarian damage, was lower in the cisplatin-treated groups than in other groups. Terminal deoxynucleotide transferase-mediated 20-deoxyuridine 50-triphosphate nick end-labeling (TUNEL) assays showed that the increase in the number of apoptotic cells was statistically significant in the cisplatin-treated group compared to the control group ($p < 0.05$). Progesterone administration with cisplatin resulted in decreases in TUNEL-positive cells. The decrease in the number of apoptotic cells was statistically significant in the cisplatin + progesterone-treated group compared to the control group ($p < 0.001$).

Conclusions. Our results showed that using progesterone as an adjuvant agent against ovarian damage in patients undergoing cancer chemotherapy with cisplatin is beneficial.

Key words: apoptosis, cisplatin, anti–Müllerian hormone, ovarian damage, progesterone

Introduction

Chemotherapy and radiotherapy are the most common modalities of cancer treatment and they have substantially increased the survival period and quality of life in patients with cancer. One of the most important chemotherapeutic agents is cisplatin (cis-diamminedichloroplatinum(II) – CDDP), which is currently used in the treatment of a wide range of human tumors, and particularly solid tumors occurring in reproductive structures, like the testes and ovaries.[1] Unfortunately, chemotherapy treatment strategies give rise to other problems, especially in the reproductive age group, where prolonged chemotherapy exposes a large proportion of these patients to complications that can include infertility, ovarian dysfunction and increased follicular apoptosis.[2] The use of cisplatin may, therefore, lead to side effects, such as ovarian failure, which limits proper administration of this anticancer drug.[3] However, the mechanisms that give rise to cisplatin side effects are not clearly understood. For this reason, experimental studies have been initiated to explore methods for preventing reproductive damage in patients who must undergo extensive chemotherapy.[4] The current literature indicates that the use of antioxidants might be helpful in preventing infertility caused by cisplatin-induced ovarian damage.[5]

Progesterone, a steroid hormone, is necessary for the retention of reproductive functions, such as ovulation and implantation, in females and it organizes the reproductive system. Besides this role in reproductive physiology, progesterone administration is reported to have a protective function against damage occurring during cerebral ischemia reperfusion and due to neurologic defects.[6] Progesterone is well-documented to protect against injuries of various organs, including the kidney.[7] For example, exogenously administered progesterone has a protective effect against acute kidney injury in rats subjected to ischemia reperfusion.[8] Therefore, progesterone may have a similar protective effect in the ovary, and particularly on the ovarian reserve, during chemotherapy.

The status of the ovarian reserve is commonly monitored by anti-Müllerian hormone (AMH).[9] Also known as Müllerian inhibiting substance, AMH is a 140 kDa polypeptide responsible for multiple reproductive functions. Yeh et al. recently showed that AMH is a better indicator of the ovarian reserve during the aging process than certain other ovarian hormones, as it is a necessary hormone for the growing follicular pool.[10] Recent AMH studies suggest that chemotherapeutic drugs might cause ovarian damage and play a role in the failure of the ovarian reserve.[3] However, in humans, few approaches are available that can protect patient's fertility and ovaries while applying chemotherapy.[11]

For these reasons, we hypothesized that progesterone might exert a protective effect on cisplatin-induced ovarian damage. The protective effects of progesterone have been previously studied, but no animal model has yet been developed for the study of the potential protective effect of progesterone on cisplatin-induced ovarian damage. Therefore, this study aimed to establish a rat model for the assessment of the effects of progesterone on cisplatin-induced ovarian damage via histopathological evaluation. The overall goal of the present study was to investigate whether progesterone can protect the ovaries of female rats against follicular damage during cisplatin chemotherapy.

Material and methods

Animals and drug administration

All experimental protocols were conducted in accordance with the institutional guidelines for the experimentation on animals at Erciyes University, Faculty of Medicine (Kayseri, Turkey), and the study was approved by the research ethics board of Erciyes University. For this study, 36 healthy female adult Wistar rats were obtained from Hakan Cetinsaya Experimental and Clinical Research Center of Erciyes University. All the animals were housed in plastic cages placed in a well-ventilated rat house, given ad libitum access to food and water, and subjected to a natural photoperiod of a 12-hour light/12-hour dark cycle. The animals were treated in accordance with the Guidelines for Animal Experimentation of Jichi Medical University (Shimotsuke, Japan), based on the National Institutes of Health Guidelines for the Care and Use of Laboratory Animals.

The rats were randomly assigned to 4 groups: the saline group (n = 8), the cisplatin-treated group (n = 10), the progesterone + cisplatin-treated group (n = 10), and the progesterone-treated group (n = 8). The rats in the cisplatin group were administered a single intraperitoneal (i.p.) injection of cisplatin (5 mg/kg; Eczacibasi, Istanbul, Turkey). The rats in the control group were similarly administered the same volume of 0.9% sodium chloride (NaCL). Rats subjected to progesterone treatment were administered progesterone (8 mg/kg; Kocak Farma, Istanbul, Turkey) intramuscularly (i.m.) 30 min before the injection of cisplatin in the progesterone + cisplatin-treated group, or saline in the progesterone-treated group. All injections were repeated 1 week later. Five days after the 2nd injection, the rats were sacrificed by decapitation under i.p. ketamine (50 mg/kg) xylazine (10 mg/ kg) anesthesia. After decapitation, the right and left ovaries were immediately excised.

Histological analysis

A morphological overview of the structure of the ovarian tissue was obtained using routine histological methods. Specimens were fixed in 10% formalin solution for 24–48 h, embedded in paraffin wax and cut into 5-μm thick sections. The slides were cleared in xylene, dehydrated in an ascending alcohol chain, and stained with

hematoxylin–eosin (H&E) for the evaluation of the tissue morphology and structure. Photographs were taken with a photomicroscope (Olympus BX51; Olympus, Tokyo, Japan) and analyzed.

The evaluation scale suggested by Li et al. was applied, with some modifications, for the histopathological evaluation of the ovarian tissues.[12] The histological sections were examined for the presence of vascular congestion, hemorrhage, follicular degeneration, leukocyte infiltration, and interstitial edema. The histological changes were scored from 0 to 3 according to the histological findings, where 0 represents no pathological findings, and 1, 2 and 3 represent pathological findings in <33%, 33–66% and >66% of the ovary, respectively. The scores for each parameter were calculated and the total scores were obtained.

Follicle counting and classification were performed on every 12th section stained with H&E. All measurements were carried out only in follicles with an obvious nucleus, using ImageJ software (ImageJ, Bethesda, USA). The assessment of follicular quality was based on the cellular density and the integrity of the basement membrane and the oocyte. The follicles were classified as morphologically normal and only normal follicles were quantified according to these criteria. They were then classified in the histological preparations, based on stage, into primordial, primary, secondary, or antral follicles. Briefly, primordial follicles were defined as an oocyte surrounded by 1 single epithelial cell layer; primary follicles were characterized by a single cell layer with cubic or high-prismatic cells; secondary follicles consisted of multiple layers of granulosa cells; and Graafian follicles were defined as those with antrum folliculi, stratum granulosum and cumulus oophorus.

Immunohistochemistry

The immunoexpression of AMH within the follicles of the ovaries was detected using the avidin-biotin-peroxidase method (ImmunoCruz™ Staining System, Sc:2053; Santa Cruz Biotechnology Inc., Santa Cruz, USA), following the manufacturer's recommendations. Briefly, serial 5-µm thick paraffin-embedded sections were deparaffinized, rehydrated in graded alcohol and incubated for 5 min in phosphate buffered saline (PBS) at room temperature. Antigen retrieval was carried out by microwave treatment in 0.01M sodium citrate buffer (pH 6.0) at 95°C for 15 min. The specimens were washed several times with PBS and endogenous peroxidase activity was inhibited with 3% hydrogen peroxide in methanol for 10 min. The specimens were incubated with a serum-blocking agent to block nonspecific staining. The histological sections were then incubated overnight at 4°C with a 1/50 dilution of goat polyclonal anti-AMH antibody (MIS (C-20): sc-6886; Santa Cruz Biotechnology Inc.). For immunostaining assays, primary antibodies were omitted as a negative control. After washing with PBS, the sections were incubated for 15 min with the biotinylated secondary antibodies. The sections were visualized by treatment for 3–5 min at room temperature with 3,3-P-diaminobenzidine tetrahydrochloride (DAB) as a chromogen and then lightly counterstained with hematoxylin. Images were taken using an immunofluorescence microscope (Olympus BX51; Olympus). We selected primordial, primary, preantral, secondary, and mature or Graafian follicles in sections from each experimental group at the same magnification (×40). The mean immunoreactivity intensity for each follicle in an ovarian section was measured using ImageJ software (ImageJ).

TUNEL staining

In situ detection of apoptosis was performed in the sections by terminal deoxynucleotide transferase-mediated 20-deoxyuridine 50-triphosphate nick end-labeling (TUNEL), using an In situ Cell Death Detection Kit (Chemicon, Temecula, USA), according to the manufacturer's instructions. Briefly, paraffin sections (5-µm) from the ovarian tissues were deparaffinized, rehydrated and washed twice in PBS for 5 min. The TUNEL reaction mixture was added to each slide and incubated in a humidified atmosphere for 60 min at 37°C in the dark. After washing with PBS, the sections were then incubated with a converter reagent for 30 min. Color development for the localization of cells containing labeled DNA strand breaks was performed by incubating the slides with Fast Red Substrate System (F4648; Sigma-Aldrich Chemie GmbH, Taufkirchen, Germany) for 5 min. Finally, the association with the number of TUNEL-positive cells in the rats from the experimental groups was evaluated by identifying apoptotic cells by morphology. At least 3 randomly chosen fields in each slide were counted at the original ×20 magnification. All slides were examined and photographed using an Olympus BX51 microscope (Olympus). The numbers of apoptotic cells were determined by carefully counting the TUNEL-positive cells, using ImageJ software (ImageJ) at the same magnification.[2]

Statistical analysis

Statistical significance was evaluated using GraphPad Prism v. 5.01 (Graph Pad Software Inc., San Diego, USA). The one-way analysis of variance (ANOVA) was followed by an appropriate post hoc comparison (depending on the given Gaussian distribution) and all the data was presented as the mean of normalized data ± standard error of the mean (SEM). The results were considered significant if the p-value was <0.05.

Results

The histological sections stained with H&E revealed that the control and progesterone-treated groups had normal ovarian architecture with no considerable pathologic
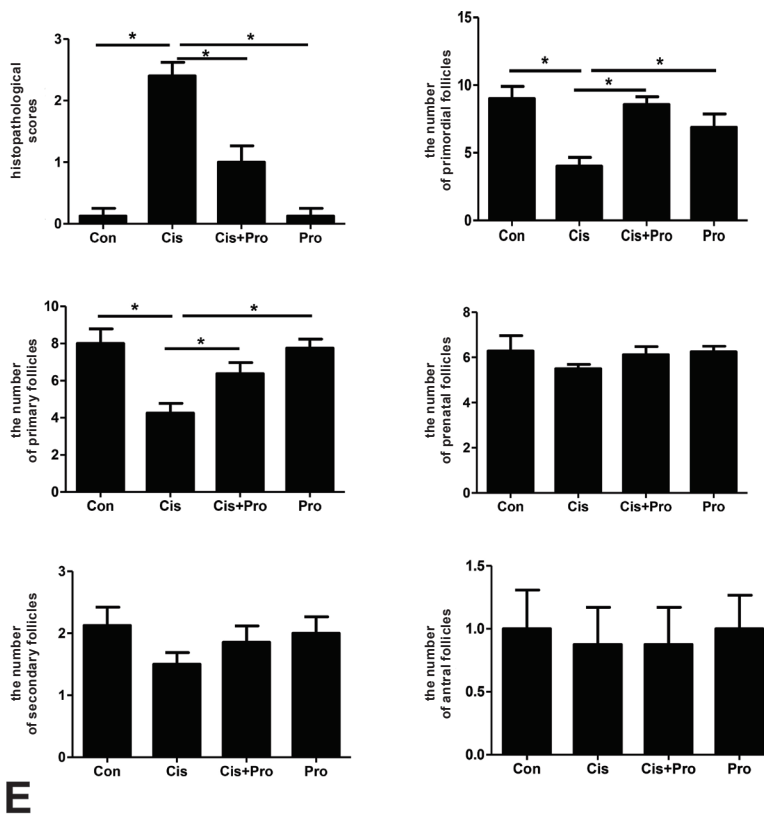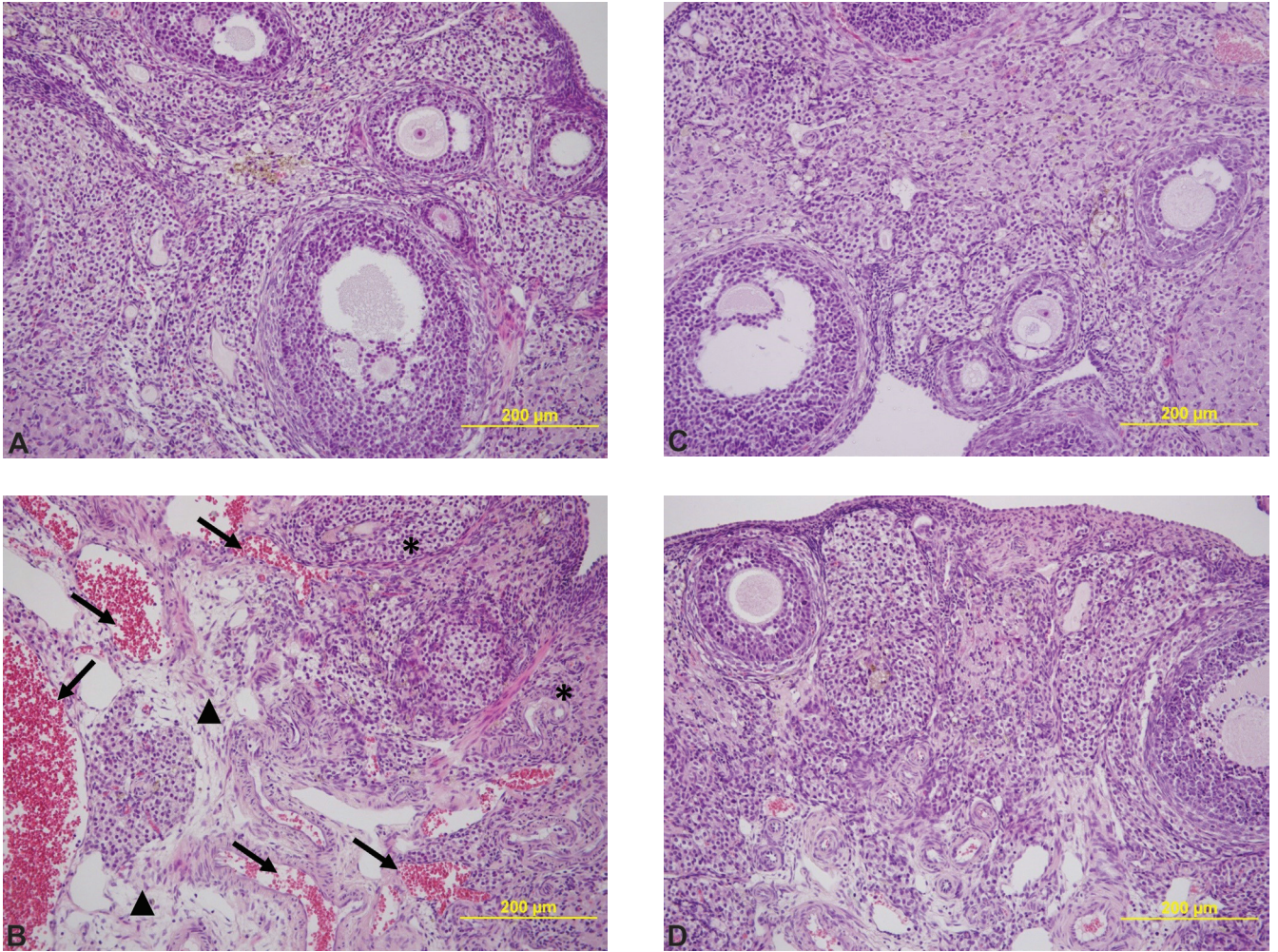
Fig. 1. Representative photomicrographs of H&E-stained sections of rat ovaries in each experimental group: A – light microscopy of the ovarian tissue with developing follicles in many different stages in the control group; B – histopathologic injury was more obvious in the cisplatin-treated groups than in other groups, degenerative changes, such as hemorrhage, follicular degeneration and edema, were evident; C – a histological image of the progesterone + cisplatin-treated group shows a significant amelioration of the ovarian histoarchitecture when compared to the disrupted histology observed in the cisplatin-treated group; D – the progesterone-treated group displayed an improved histological appearance with an orderly arrangement of follicles; E – quantification of histopathological scores and number of each type of follicles in the ovarian sections from the experimental groups

Original magnification ×200; star – follicular degeneration; arrow – hemorrhage; head of arrow – edema (E); H&E – hematoxylin/eosin; Con – control; Cis – cisplatin; Pro – progesterone; * p < 0.05.

alteration (Fig. 1). Ovarian follicles in various stages of development and with normal appearance were observed in the ovarian cortex, and the cuboid germinal or follicular cells around the oocyte were examined. The cisplatin-injected group showed the absence of Graafian follicles and the presence of the corpus luteum (CL), whereas the sections taken from the control ovarian tissues exhibited the presence of follicles at different stages of maturation. Cisplatin treatment also resulted in microscopy findings of hemorrhage and vascular congestion, as well as follicular degeneration and edema in the ovarian tissue when compared to the control group. The group that was administered cisplatin + progesterone showed more moderate, but morphologically similar, histological findings of degeneration, hemorrhage and edema. Overall, progesterone markedly decreased cisplatin-induced ovarian damage.

For follicle counting at different stages in each experimental group, unhealthy follicles were distinguished from healthy follicles by nuclear pyknosis and the disappearance of granulosa cells, whereas healthy follicles were classified considering their different developmental stages. The control group showed a number of follicles at various stages, whereas significantly fewer primordial, secondary and Graafian follicles were found in the cisplatin group than in the control group (p < 0.05), indicating substantial damage to the quality of the follicle in the cisplatin group. Primordial and primary follicle counts were higher in the control group than in the cisplatin group, and this difference was statistically significant (p < 0.05). Primordial and primary follicle counts were similar in the cisplatin + progesterone-treated group and the cisplatin group (p < 0.05). The numbers of preantral, secondary and Graafian follicles did not differ among the groups. Preantral, secondary and Graafian follicle counts were lower in the cisplatin + progesterone-treated group than in the cisplatin-treated group. No statistically significant differences were seen between the control and progesterone groups regarding the follicle numbers (Fig. 1E). All histological scores are listed in Table 1. The histopathological differences were marked as follows: 0 – normal; 1 – moderate (moderate vascular congestion, edema, no hemorrhage, and no follicular degeneration); 2 – moderate (moderate vascular congestion, edema, no hemorrhage, and no follicular degeneration); and 3 – severe (severe vascular congestion, edema, hemorrhage, follicular degeneration, and leukocyte infiltration).

Table 1. Histopathological grading of rat ovary lesions in the treatment groups

Groups	Histopathological scores			
	0	1	2	3
Control	8	–	–	–
Cisplatin	–	1	4	5
Cisplatin + progesterone	2	4	2	2
Progesterone	7	1	–	–

The influence of progesterone on AMH immunoreactivity intensity in the ovaries of the rats in all experimental groups is shown in Fig. 2. Anti-Müllerian hormone immunohistochemistry was analyzed by follicle class. No AMH was detected in atretic follicles, theca cells and the oocytes of follicles in the ovarium. Anti-Müllerian hormone was primarily expressed in granulosa cells of primary, preantral and small antral follicles. Anti-Müllerian hormone immunoreactivity intensity progressively decreased in the subsequent phases of follicle development in the control and progesterone-treated groups, whereas the immunoreactivity intensity of AMH was consistently lower in the ovaries of the cisplatin-treated group. The immunoreactivity intensity of AMH was lower, especially in primordial and primary follicles at early development stages, in the cisplatin-administered group than in the control group, but the differences were not statistically significant. The immunoreactivity intensity of AMH did not differ between secondary and tertiary follicles (Fig. 2E).

The TUNEL evaluations for DNA fragmentation in cell nuclei in each group are shown in Fig. 3. The control group showed no increases in the numbers of apoptotic cells in follicles at different stages. By contrast, the numbers of TUNEL-positive cells were significantly higher in the cisplatin-treated groups than in the control group (p < 0.001). The cisplatin group showed badly damaged follicle structures, resulting in a significant rise in the number of TUNEL-positive cells. Markedly lower numbers of TUNEL-positive cells were seen in follicles of the progesterone-treated groups than in the cisplatin-treated group (p < 0.001). Thus, the induction of large numbers of TUNEL-positive cells in the ovarian tissue by cisplatin treatment was significantly suppressed by pretreatment with progesterone (Fig. 3).

Discussion

The present study investigated whether progesterone could protect against cisplatin-induced ovarian damage in a rat model. We demonstrated that an injection of progesterone 30 min prior to cisplatin administration attenuated the cisplatin-induced ovarian injury by reducing cellular apoptosis. Progesterone also positively modulated AMH expression, indicating a possible protection of the ovarian reserve against cisplatin-induced injury. In addition, administration of progesterone led to partial protection. Evaluation of the ovarian reserve following chemotherapy is vital to ensure adequate subsequent fertility.

The targets of the chemotherapeutic drugs might be the granulosa cells in developing follicles, which may affect oocyte maturation and cause follicular destruction, followed by ovarian failure as the result of any damage to these cells. Follicle damage induced by chemotherapy is likely the main cause of infertility. For example, Meirow et al. reported that chemotherapy, in a drug- or dose-addiction, causes
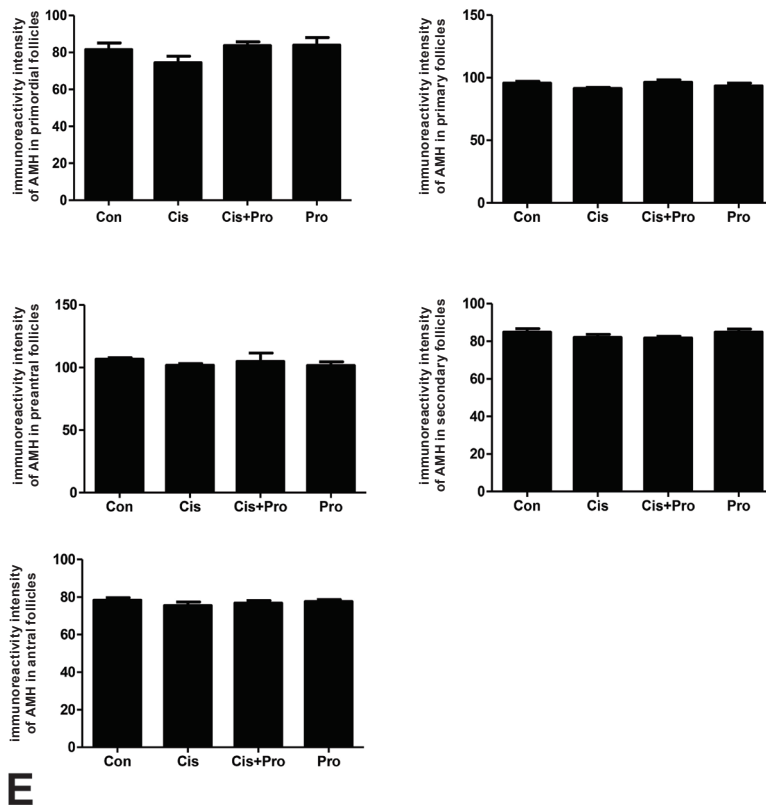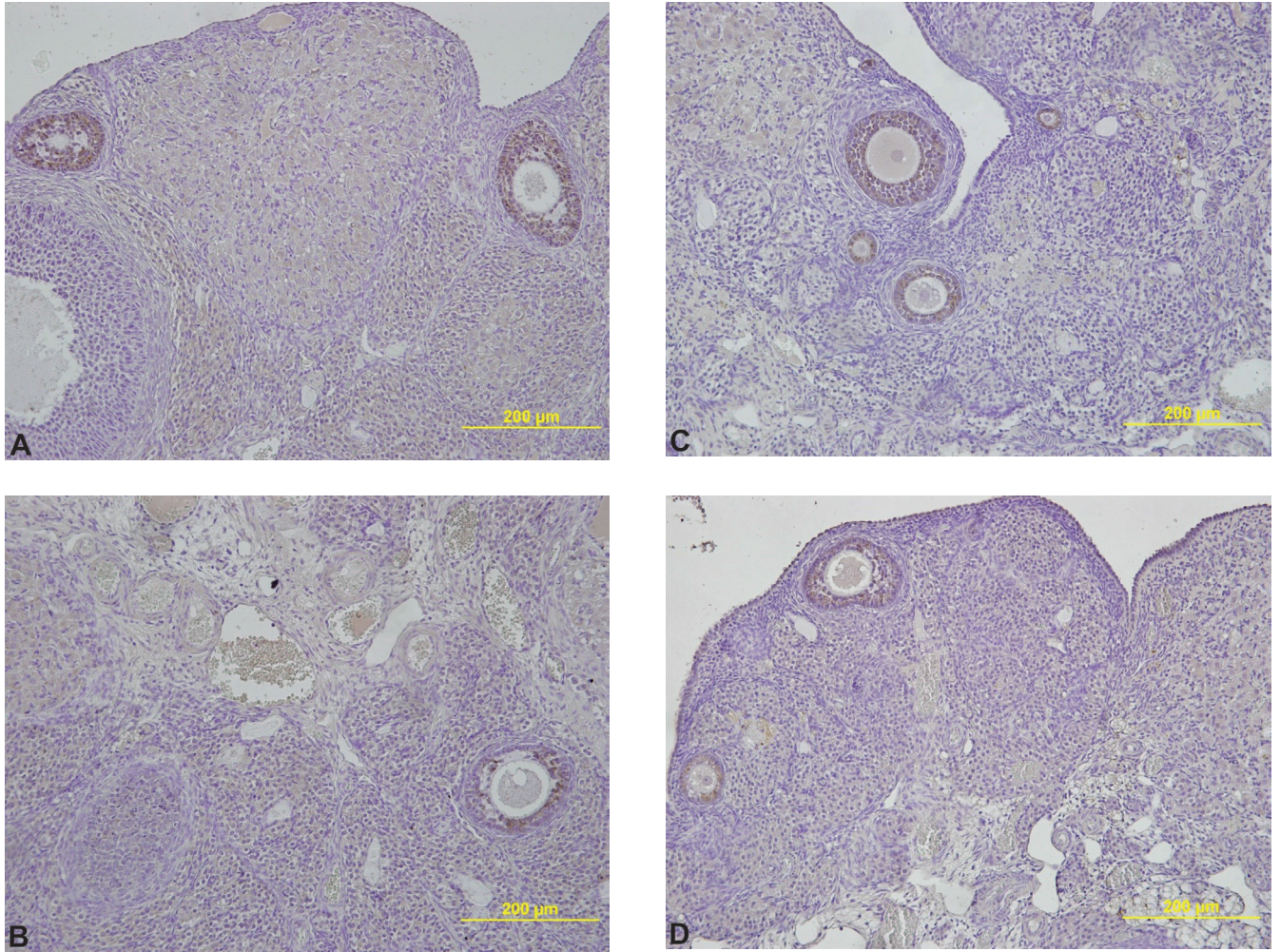
Fig. 2. Photomicrographs of rat ovarian sections and immunostaining of AMH in the different groups:
A – the control group showed AMH staining in granulosa cells surrounding the oocyte in early primary, preantral and small antral follicles; B – the positive staining for AMH was decreased in the cisplatin-treated group; C – AMH-positive staining of the ovary in the progesterone + cisplatin-treated group; D – similar AMH immunoreactivity was evident in the progesterone-treated group and in the control group; E – quantification of AMH immunoreactivity intensity in ovarian sections from the experimental groups

Original magnification ×200; AMH – anti-Müllerian hormone; Con – control; Cis – cisplatin; Pro – progesterone.
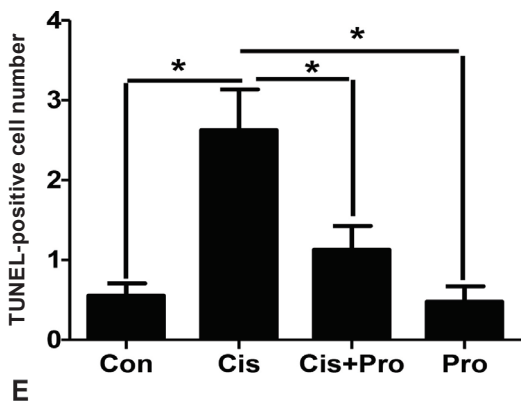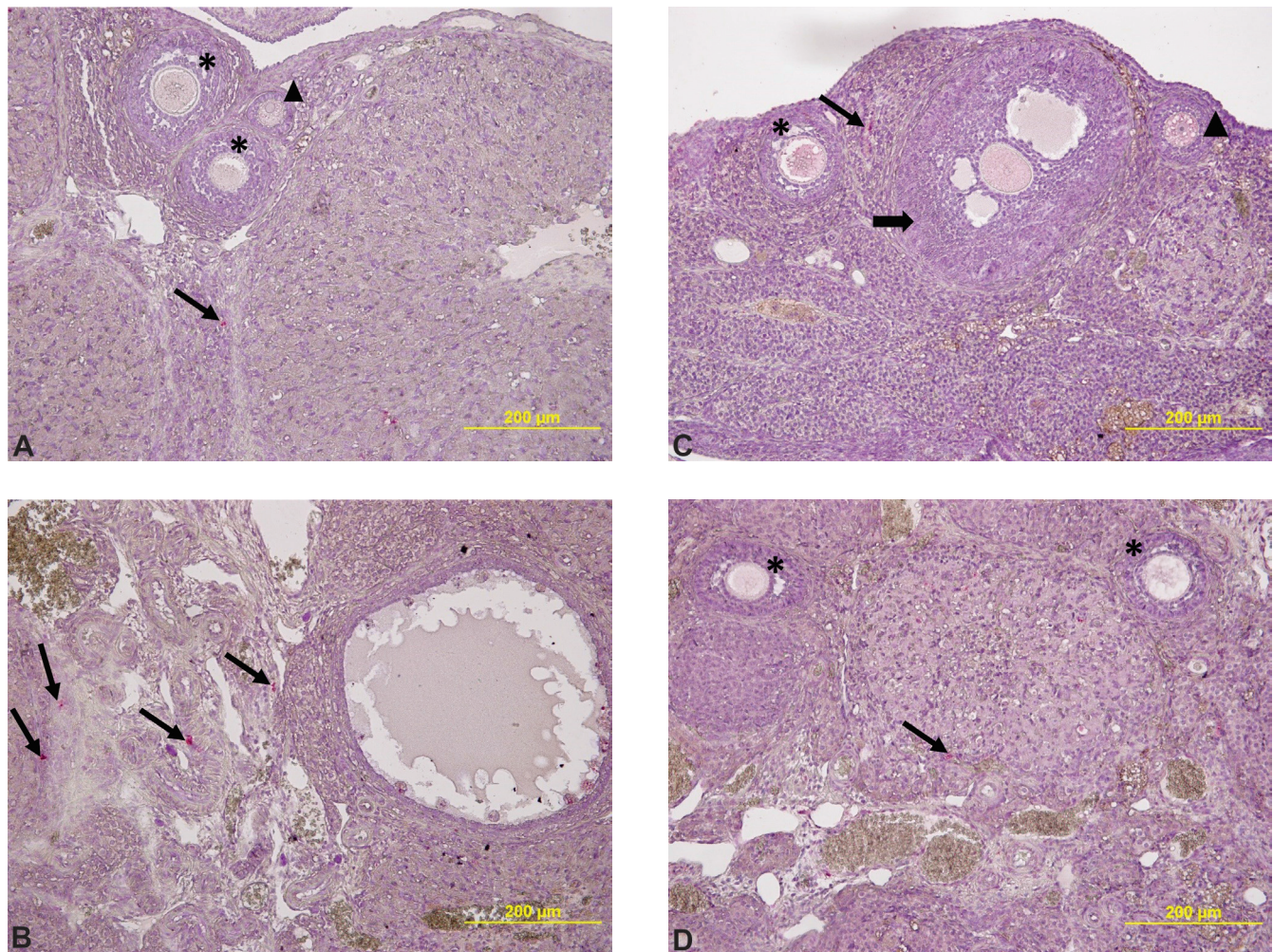
Fig. 3. Progesterone pretreatment inhibits the development of TUNEL-positive cells in the rat ovary due to cisplatin-induced ovarian damage: A – only a few TUNEL-positive cells were evident in the ovaries in the control group; B – the TUNEL-positive cell number increased in the cisplatin-treated group; C – effects of progesterone on TUNEL-positive cells in cisplatin injury in rats, a marked decrease was evident in the number of TUNEL-positive cells when compared with the cisplatin-treated group; D – the progesterone-treated group had also fewer TUNEL-positive cells than were observed in the control group; E – graph showing quantification of the different groups. The number of TUNEL-positive cells was higher in the ovarian tissues of the cisplatin-treated group than in the control group and in other groups

Arrow – TUNEL-positive cell; star – preantral follicle; head of arrow – primary follicle; thick arrow – secondary follicle; TUNEL – terminal deoxynucleotide transferase-mediated 20-deoxyuridine 50-triphosphate nick end-labeling; Con – control; Cis – cisplatin; Pro – progesterone; TUNEL staining ×200; * p < 0.001.

a depletion of the primordial follicle pool.[13] Treatment with cisplatin causes an increased prevalence of premature ovarian failure in humans.[14] In rats, cisplatin can cause ovarian damage, decreased immunoreactivity intensity of AMH and changes in the estrous cycle.[15]

Cisplatin is the commonly preferred anticancer agent for treatment of a wide range of cancer types, ranging from sarcomas and small cell lung cancer to ovarian cancer, cervical cancer and lymphomas.[16] The antitumor effect of cisplatin depends on the formation within the cell of a platinum complex that participates in DNA cross-linking and apoptosis.[17] In addition, cisplatin is thought to trigger DNA damage, failure of mitochondrial function and a hindrance in protein synthesis.[1,18,19] However, these effects on dividing cancer cells may also adversely occur in healthy dividing cells, such as the granulosa cells of follicles, thereby leading to ovarian failure, and ultimately, infertility.[12]

A positive role of progesterone has been indicated in some disorders, such as traumatic brain and spinal cord injury, neuroinflammation, stroke, ischemia, diabetic neuropathy, and neurodegeneration.[20,21] The granulosa cells and the CL in the ovary produce progesterone, which is necessary in mammals for the establishment and maintenance of pregnancy.[22] The production of interleukin (IL)-6 can

also be inhibited by progesterone, suggesting a probable immunosuppressive and anti-inflammatory role as well.[23] He et al. showed that progesterone reduces brain edema, ameliorates brain complications with its anti-inflammatory effects and reduces the levels of inflammatory cytokines.[24] Progesterone also suppresses the production of proinflammatory cytokines and chemokines in monocytes, and appears to play an important anti-inflammatory role.[25,26] Ghasemi et al. demonstrated a beneficial and dose-dependent effect of progesterone on cisplatin-induced nephrotoxicity.[7] However, the protective effect of progesterone against cisplatin-caused ovarian damage has not been studied extensively.

In the present study, AMH expression was significantly increased in the progesterone + cisplatin-treated group when compared to the cisplatin-treated group, indicating that progesterone can preserve the granulosa cells in growing follicles. No significant increase was observed in AMH immunoreactivity intensity in the progesterone-treated group when compared to the control group. Our results indicated that pretreatment with progesterone before the administration of cisplatin could have protected the follicle cells from the adverse effects of cisplatin, as indicated by the higher AMH immunoreactivity intensity in the progesterone + cisplatin-treated group as compared to the cisplatin-treated group. Anti-Müllerian hormone knockout mouse studies have shown that AMH functions as a negative stimulator of follicular maturation and an inhibitor of follicle-stimulating hormone (FSH) sensitivity.[27]

Analyzing the apoptotic mechanism is crucial in explaining the adverse cisplatin effects and the mechanisms underlying the action of possible protective agents against these effects. The ideal preventative or protective agents also must not disturb the antitumor effects of chemotherapeutics. Cisplatin can cause the generation of oxygen-free radicals, which then induce oxidative stress that gives rise to cisplatin-induced tissue damage.[28] Progesterone used together with chemotherapeutic drugs clearly decreased apoptosis in the present study. Devarajan et al. demonstrated that cisplatin induced both the intrinsic and the extrinsic apoptotic pathways.[29] Progesterone may decrease apoptosis by decreasing pro-apoptotic enzymes and increasing anti-apoptotic proteins.[30] In the present study, the anti-apoptotic effect of progesterone on cisplatin-induced ovarian damage was confirmed by the reduction in the number of TUNEL-positive apoptotic cells in the progesterone + cisplatin-treated group.

This study provides additional details about the damage caused by cisplatin to the ovary. It also presents methods for determining the protective effect of progesterone against this damage and would appear to be the first report on the effect of progesterone on cisplatin-induced ovarian damage and the immunoreactivity intensity of AMH. Taken together, our results indicate that progesterone partially prevents the damage caused by cisplatin. This finding could be crucial for women cancer patients to maintain their fertility.

In summary, we obtained data from a rat model that support the hypothesis that apoptosis can be regulated by the natural sex steroid progesterone. Additional clinical and immunohistochemical research should be carried out to confirm this conclusion about the ameliorating effect of progesterone on ovarian tissue damage, and to evaluate the efficacy, safety and potential use of progesterone.

References

1. Wang D, Lippard SJ. Cellular processing of platinum anticancer drugs. *Nat Rev Drug Discov.* 2005;4(4):307–320.
2. Taskin MI, Yay A, Adali E, Balcioglu E, Inceboz U. Protective effects of sildenafil citrate administration on cisplatin-induced ovarian damage in rats. *Gynecol Endocrinol.* 2015;31(4):272–277.
3. Yeh J, Kim BS, Liang YJ, Peresie J. Gonadotropin stimulation as a challenge to calibrate cisplatin induced ovarian damage in the female rat. *Reprod Toxicol.* 2009;28:556–562.
4. Yazici A, Sari ES, Yay A, et al. The protective effect of selenium in cisplatin-related retinotoxicity. *Cutan Ocul Toxicol.* 2014;33(4):327–332.
5. De Castilhos J, Hermel EE, Rasia-Filho AA, Achaval M. Influence of substitutive ovarian steroids in the nuclear and cell body volumes of neurons in the posterodorsal medial amygdala of adult ovariectomized female rats. *Neurosci Lett.* 2010;469(1):19–23.
6. Cheng J, Zhang J, Ma X, Su D. Frequency-dependent acceleration of cardiac repolarization by progesterone underlying its cardiac protection against drug-induced proarrhythmic effects in female rabbits. *Eur J Pharmacol.* 2012;689(1–3):172–178.
7. Ghasemi M, Nematbakhsh M, Pezeshki Z, Soltani N, Moeini M, Talebi A. Nephroprotective effect of estrogen and progesterone combination on cisplatin-induced nephrotoxicity in ovariectomized female rats. *Indian J Nephrol.* 2016;26(3):167–175.
8. Sandhi J, Singh JP, Kaur T, Ghuman SS, Singh AP. Involvement of progesterone receptors in ascorbic acid-mediated protection against ischemia-reperfusion-induced acute kidney injury. *J Surg Res.* 2014;187(1):278–288.
9. Themmen AP. Anti-Müllerian hormone: Its role in follicular growth initiation and survival and as an ovarian reserve marker. *J Natl Cancer Inst Monogr.* 2005;34:18–21.
10. Yeh J, Kim BS, Peresie J, Liang YJ, Arroyo A. Serum and ovarian Müllerian inhibiting substance, and their decline in reproductive aging. *Fertil Steril.* 2007;87(5):1227–1230.
11. Lee SJ, Schover LR, Partridge AH, et al.; American Society of Clinical Oncology. American Society of Clinical Oncology recommendations on fertility preservation in cancer patients. *J Clin Oncol.* 2006;24(18):2917–2931.
12. Li X, Kang X, Deng Q, Cai J, Wang Z. Combination of a GnRH agonist with an antagonist prevents flare-up effects and protects primordial ovarian follicles in the rat ovary from cisplatin-induced toxicity: A controlled experimental animal study. *Reprod Biol Endocrinol.* 2013;11:16. doi: 10.1186/1477-7827-11-16
13. Meirow D, Lewis H, Nugent D, Epstein M. Subclinical depletion of primordial follicular reserve in mice treated with cyclophosphamide: Clinical importance and proposed accurate investigative tool. *Hum Reprod.* 1999;14(7):1903–1907.
14. Meirow D. Reproduction post-chemotherapy in young cancer patients. *Mol Cell Endocrinol.* 2000;169(1–2):123–131.
15. Yucebilgin MS, Terek MC, Ozsaran A, et al. Effect of chemotherapy on primordial follicular reserve of rat: An animal model of premature ovarian failure and infertility. *Aust N Z J Obstet Gynaecol.* 2004;44(1):6–9.
16. Erken HA, Koç ER, Yazıcı H, et al. Selenium partially prevents cisplatin-induced neurotoxicity: A preliminary study. *Neurotoxicology.* 2014;42:71–75.
17. Meraner V, Gamper EM, Grahmann A, et al. Monitoring physical and psychosocial symptom trajectories in ovarian cancer patients receiving chemotherapy. *BMC Cancer.* 2012;12:77. https://doi.org/10.1186/1471-2407-12-77
18. Dasari S, Tchounwou PB. Cisplatin in cancer therapy: Molecular mechanisms of action. *Eur J Pharmacol.* 2014;740:364–378.

19. Lomeli N, Di K, Czerniawski J, Guzowski JF, Bota DA. Cisplatin-induced mitochondrial dysfunction is associated with impaired cognitive function in rats. *Free Radic Biol Med*. 2017;102:274–286.

20. Coronel MF, Labombarda F, Roig P, Villar MJ, De Nicola AF, González SL. Progesterone prevents nerve injury-induced allodynia and spinal NMDA receptor upregulation in rats. *Pain Med*. 2011;12(8):1249–1261.

21. Liu A, Margaill I, Zhang S, et al. Progesterone receptors: A key for neuroprotection in experimental stroke. *Endocrinology*. 2012;153(8):3747–3757.

22. Graziano V, Check JH, Dietterich C, Choe JK, Yuan W. A comparison of luteal phase support in graduated estradiol/progesterone replacement cycles using intramuscular progesterone alone versus combination with vaginal suppositories on outcome following frozen embryo transfer. *Clin Exp Obstet Gynecol*. 2005;32(2):93–94.

23. Li S, Yixi S, Feng M, Lü P, Huang H, Zhou J. Progesterone inhibits Toll-like receptor 4-mediated innate immune response in macrophages by suppressing NF-KB activation and enhancing SOCS1 expression. *Immunol Lett*. 2009;125(2):151–155.

24. He J, Evans CO, Hoffman SW, Oyesiku NM, Stein DG. Progesterone and allopregnanolone reduce inflammatory cytokines after traumatic brain injury. *Exp Neurol*. 2004;189(2):404–412.

25. Miller L, Hunt JS. Regulation of TNF alpha production in activated mouse macrophages by progesterone. *J Immunol*. 1998;160: 5098–5104.

26. Hardy DB, Janowski BA, Corey DR, Mendelson CR. Progesterone receptor plays a major anti-inflammatory role in human myometrial cells by antagonism of nuclear factor-kappaB activation of cyclooxygenase 2 expression. *Mol Endocrinol*. 2006;20(11):2724–2733.

27. Visser JA, Themmen AP. Anti-Müllerian hormone and folliculogenesis. *Mol Cell Endocrinol*. 2005;234(1–2):81–86.

28. Cepeda V, Fuertes MA, Castilla J, Alonso C, Quevedo C, Pérez JM. Biochemical mechanisms of cisplatin cytotoxicity. *Anticancer Agents Med Chem*. 2007;7(1):3–18.

29. Devarajan P, Savoca M, Castaneda MP, et al. Cisplatin-induced apoptosis in auditory cells: Role of death receptor and mitochondrial pathways. *Hear Res*. 2002;174(1–2):45–54.

30. Yao XL, Liu J, Lee E, Ling GS, McCabe JT. Progesterone differentially regulates pro- and antiapoptotic gene expression in cerebral cortex following traumatic brain injury in rats. *J Neurotrauma*. 2005;22(6):656–668.

Evaluation of the Sensory Organization Test to differentiate non-fallers from single- and multi-fallers

Katarzyna Pierchała[A–F], Magdalena Lachowska[C–F], Jarosław Wysocki[D,E], Krzysztof Morawski[E,F], Kazimierz Niemczyk[E,F]

Department of Otolaryngology, Medical University of Warsaw, Poland

A – research concept and design; B – collection and/or assembly of data; C – data analysis and interpretation;
D – writing the article; E – critical revision of the article; F – final approval of the article

Abstract

Background. Among the elderly, instability leading to falls (and consequences of them) is one of the most important problems. The etiology of falls is usually complex, but balance, posture and gait problems are considered to be the most important risk factors.

Objectives. The objective of this study was to assess the usefulness of the Sensory Organization Test (SOT) in differentiating multi-fallers from single-fallers.

Material and methods. The studied group included 92 patients aged >60 years with balance disorders and falls in their history. The patients were divided into 2 groups: multi-fallers and single-fallers. The control group (non-fallers) included 21 individuals. The SOT was performed on the 1st day (SOT1) and on the last day (SOT2) of rehabilitation. Mean equilibrium score (ES) of 1–3 and 4–6 sensory conditions and composite score (CS) of the SOT1 and SOT2 were analyzed. The falls were analyzed as a total number of falls while performing SOT and a number of falls in all 3 repetitions of both conditions 5 and 6 separately. In SOT conditions 1–4 there were no falls observed.

Results. The importance of SOT to differentiate fallers from non-fallers and single-fallers from multi-fallers is ambiguous.

Conclusions. The SOT may or may not indicate the differences between the groups – it does not fully explain those differences. It shows only postural dysfunction without indicating any localization in particular part of vestibular organ. The basic diagnostic evaluation in the elderly with a proneness to falls should include clinical examination and the Dix-Hallpike maneuver, supplemented with a videonystagmography (VNG), which would assess the structure of damage in vestibular organ. Posturography is of less validity in the differentiation of fallers from non-fallers.

Key words: posture, benign paroxysmal positional vertigo, gait, dizziness, inner ear

Introduction

Among the elderly, instability leading to falls (and consequences of them) is one of the most important problems. The etiology of falls is usually complex, but balance, posture and gait problems are considered the most important risk factors.[1,2] The age-dependent changes in the balance system play an important role in the incidence of dizziness in the elderly; they may be caused by pathological processes.[3] Various pathological processes cause damage to the vestibular organ at any age, both in young people and the elderly.[4] Increased prevalence of risk factors that cause damage to the vestibular organ in the elderly may result from a greater vulnerability of the ageing vestibular system, or from a more extended time of exposure to them in younger people.[3,4] Indeed, as dizziness is reported by about 20–30% of the general population,the same ailment is reported by 40% of men and 60% of women at the age of over 70 years.[5,6]

Among people over the age of 65 years that fall, 15–23% report an episode of vertigo as the cause of the collapse.[6] The relationship between falls and vestibular system dysfunction, however, is ambiguous. The factors that lead to its complexity are: a variety of dizziness descriptions reported by patients, the extent of damage in the vestibular system and vestibular compensation.[7] Damage to the upper part of the labyrinth (e.g., after previous vestibular neuritis), manifested by weakness or absence of a response in caloric test, initiates the process of degeneration of otolithic organs. It leads to canalo- or cupulolithiasis, clinically manifested as benign paroxysmal positional vertigo (BPPV), which is the most common type of vestibular ailment.[8] It may occur at any age, but its incidence in the elderly population is many times greater than in younger patients,and the peak of those incidences is between the 5th and 7th decade of life.[8,9]

Benign paroxysmal positional vertigo can be idiopathic or secondary to changes in the inner ear and/or the central nervous system (CNS), and may, therefore, be present independently, or as a consequence of the inner ear and/or CNS diseases.[10] In addition to typical dizziness when changing positions, which may persist for up to 12 weeks, positional vertigo can cause long-lasting instability in about 50% of individuals,or in severe cases, hypersensitivity to almost any head movement.[8–11] Considering that the recurrences of BPPV concern about 50–55% of patients, with a recurrence rate of approx. 15% per year, it seems likely that more than half of the patients with BPPV experience prolonged instability even for many months.[8,12] Thus, it seems that BPPV and consequent instability, as an independent pathology or an effect of previous pathological processes in the vestibular system (that intensifies even age-related postural control disorders), should be treated as the most important cause of imbalance and tendency to falls among the elderly.[10,11]

An important component of therapy and strategies of preventing falls in patients with vestibular pathology is the vestibular rehabilitation. Its beneficial effect has been shown also in the age-related imbalance.[13] While effectiveness of reposition maneuvers in the treatment of BPPV is undeniable, the postural training is recommended in the treatment of instability.[14] In older patients, with a variety of different health problems, postural rehabilitation improves the maintenance of balance in more than 60% of them, decreasing the intensity of symptoms and reducing disability in everyday life.[15]

One of the methods of rehabilitation is postural training, based on sensory conflicts and conducted on the basis of computer dynamic posturography (CDP) described by Nashner.[16] Computer dynamic posturography is recognized as a useful diagnostic method, evaluating the sensory and motor skills as well as biomechanical aspects of balance. Sensory conflicts used in CDP rehabilitation are similar to those in Sensory Organization Test (SOT), the most important test in CDP. The SOT indicates the nature of the deficit in the balance system. It is a commonly used test to facilitate the selection of the proper vestibular rehabilitation method and to assess its effectiveness. The 6 SOT conditions that progress from the most stable (eyes open and solid stable platform) to the least stable (sway-referenced platform and visual screen) allow for the detection of body sway. With the ability to test the patient under varying sensory conditions, SOT allows the assessment of a patient's ability to use visual, vestibular and proprioceptive information, and to suppress incorrect information in order to maintain static balance.[17] The SOT is an method often used for assessing the efficiency of postural control in different groups of pathology, as well as the assessment of the effectiveness of rehabilitation carried out by different methods.[18–21]

In its assumptions, rehabilitation based on sensory conflicts strengthens and accelerates the integration processes in the CNS.[15] A patient learns to suppress irrelevant or erroneous information coming from dysfunctional channels and to focus on stimuli that come from an undisturbed channel.[22,23] Conducting exercises in varying sensory conditions (e.g., unstable platform, altered visual stimuli) forces a patient to select the sensory information that is necessary for the maintenance of static equilibrium, and to generate appropriate motor responses. The possibility to gradually increase the difficulty of exercises puts the patient's balance against growing challenges and serves to intensify the learning process. Computer-navigated rehabilitation program provides visual feedback in real time, which makes it easier for a patient to understand the essence of the exercises, as well as to control and correct their performance, and creates the favorable conditions for "motor learning." In addition, it offers the medical personnel a possibility of supervision and constant monitoring of the treatment progress.[24]

The aim of the study was to assess the usefulness of the SOT as a method that differentiates multi-fallers from single-fallers. The additional aim was to evaluate the effectiveness of rehabilitation based on sensory conflicts in the studied populations.

Material and methods

As observed in everyday clinical practice and as described in the literature, healthy elderly individuals fall, patients with vestibular pathology fall and patients with balance problems coming from nonvestibular pathology also fall.[3,4,10–12] Therefore, in our material, the fallers group included patients who presented imbalance and falls in their medical history, regardless of etiology. The control group consisted of healthy individuals who described the state of their balance as appropriate to their age and without any falls. All subjects included in the study were people living in their own homes, and independent in basic life and social activities.

The studied group included 92 patients aged over 60 years who were referred by their family doctors, otolaryngologists or neurologists to our otoneurological outpatient unit due to balance disorders and falls in their medical history. Based on the number of falls during the last year, the patients were divided into the 2 following groups: multi-fallers (Multi-F, n = 47) with a mean age of 73.6 years (min 60, max 80; standard deviation (SD) 6.3), and single-fallers (Single-F, n = 45) with a mean age of 67.5 years (min 60, max 80; SD 5.9). The Single-F group included patients with 1 fall in the medical history and the Multi-F group included those with 2 or more falls in their history, but none of them were subjected to vestibular rehabilitation before this study. In both groups, some patients reported episodes of acute vertigo in the past over a period of at least 6 months before the beginning of this study. Outside the mentioned conditions, each patient from both groups had to meet the following additional criteria for inclusion in the study: the ability to move and the lack of serious conditions in the locomotor system, as well as no serious conditions in the circulatory system, respiratory system or CNS that could interfere with everyday rehabilitation training program.

The control group (Non-F) included 21 individuals (mean age: 67 years; min 60; max 80; SD 5.8) considered healthy from an otoneurological point of view. They did not report imbalance or falls in their history. They were volunteers interested in their state of health and were recruited from retiree clubs operating within our city.

In each patient, a clinical otoneurological evaluation was performed, including the Dix-Hallpike maneuver. The presence of typical nystagmus and/or a sensation of vertigo, even without coexisting nystagmus, were considered as an abnormal test result. After the Hallpike maneuver yielded a positive test result, the Semont maneuver was performed and the patient was scheduled for the next visit after a week; then again the diagnostic Hallpike maneuver was performed. After finding the Hallpike maneuver yielded a negative result in the next visit or a negative test result in the 1st visit, the patient was scheduled for the essential tests of the study that started another week later. In the case of a positive Hallpike maneuver test result in the 2nd visit, the whole procedure was repeated. The principle was that the main research project started 2 weeks after the Semont maneuver and 1 week after a negative Hallpike maneuver test result.

A videonystagmography (VNG) using Micromedical system (Micromedical Technologies Inc., Chatham, USA) was performed to assess the location of the damage in the vestibular system. The applied evaluation protocol was the one routinely used in our neurotological lab and included the following: spontaneous, gaze, positional, and positioning nystagmus test, saccade test, smooth pursuit eye movements test, optokinetic test, and caloric testing. To avoid the impact of VNG on CDP results, the VNG test was carried out 2 days before the start of the essential study, and after the preliminary SOT examination (SOT0).

The SOT was conducted using a computer program that is part of the Smart Equitest system (NeuroCom International Inc., Clacamas, USA). It was performed on the 1st day (SOT1) and on the last day (SOT2) of rehabilitation. The SOT and vestibular rehabilitation using sensory conflicts are very similar. In order to eliminate SOT learning effect that might influence the effectiveness of rehabilitation, we conducted a preliminary SOT 2 days before starting rehabilitation and those results were not analyzed.

The SOT included 6 sensory conditions. The 1st 3 conditions (1–3) (3 trials per condition (Cond.)) were performed on a stable platform and included: Cond. 1: stable platform, eyes open, stable visual surrounding; Cond. 2: stable platform, eyes closed; Cond. 3: stable platform, eyes open, moving visual surrounding with the subject's anterior-posterior sway. The next 4–6 conditions (3 trials per condition) were performed on a moving platform, with the range of its motion dependent on the patient's sway: Cond. 4: moving platform, eyes open; Cond. 5: moving platform, eyes closed; Cond. 6: moving platform, eyes open, moving visual surrounding dependent on the patient's sway. During the examination patients were protected against falling with special safety harness.

Analyzed parameters of the SOT were:
– mean equilibrium score (mean ES), which is the average score of the 3 trials in each of the 6 sensory conditions. Equilibrium score is based on the assumption that the swing of a healthy person in the anterior-posterior plane does not exceed 12.5°. The result of balance for each trial is calculated separately by comparing the angular difference between the maximum sways of the patients and the sways of a healthy person. The result is presented as a reversed percentage between 0 and 100 – the result close to 0 indicates the limits of postural stability and the result close to 100 means almost complete stability that theoretically indicates no anterior-posterior excursion;
– composite score (CS) is a computer-generated score of the 6 SOT conditions;

– loss of balance (LOB) in all 3 trials of each sensory condition (18 trials).

Mean ES of 1–3 and 4–6 sensory conditions and CS of the SOT1 and SOT2 were analyzed in all 3 studied groups (Single-F, Multi-F and Non-F). The falls (LOB) were analyzed as a total number of falls while performing SOT and a number of falls in all 3 repetitions of both Cond. 5 and 6 separately. No falls were observed in SOT conditions 1–4.

Vestibular rehabilitation based on the CDP was conducted using a computer program Smart Equitest System (NeuroCom International Inc.). The rehabilitation was based on daily 30-min sessions performed on weekdays for 2 weeks (a total of 10 sessions for each patient). Patients were protected against falling with a special safety harness. The rehabilitation protocol was the same for all patients with the difficulty of the task gradually increasing over time. Each rehabilitation session included 1-min exercises. The degree of exercise difficulty started from the easiest (20%) and increased gradually to 100% with 20% steps for each next exercise. It was repeated in the described manner during every rehabilitation session for the entire period of the treatment. To assess the rehabilitation effect in each group, SOT1 and SOT2 were compared. To evaluate differences between the groups, the difference between SOT2 and SOT1 in each group was calculated (SOT2–SOT1) and then compared between groups.

The project was approved by the local Ethics Committee Review Board.

Statistical analysis of SOT data was performed using STATISTICA v. 10 software (StatSoft Inc., Tulsa, USA). The data were tested for normality, parametric and nonparametric criteria. To analyze the data, the following tests were used: Kruskal-Wallis test, Pearson's χ^2 test and Wilcoxon test. A p-value <0.05 was considered statistically significant.

Results

Sensory Organization Test 1 results

Significant differences were found in Cond. 1–3, Cond. 4–6 and CS between Non-F and Multi-F groups ($p < 0.05$), and between Non-F and Single-F groups ($p < 0.05$) (Table 1). The results between Single-F and Multi-F groups were similar in Cond. 1–3 and Cond. 4–6 ($p > 0.05$); only CS results were found to be significantly different ($p < 0.05$).

Rehabilitation effect within every group

The rehabilitation effect showed a significant improvement in Cond. 4–6 and in CS in all analyzed groups ($p < 0.05$) (Table 2). Rehabilitation effect did not significantly change the results in Cond. 1–3 in all analyzed groups ($p > 0.05$).

Table 2. Rehabilitation effect within every group (Non-F, Single-F and Multi-F) in SOT Cond. 1–3, 4–6 and CS

Analyzed parameter	Wilcoxon test (p-value)		
	Non-F	Single-F	Multi-F
Rehab. effect SOT Cond. 1–3	0.0962	0.0784	0.7613
Rehab. effect SOT Cond. 4–6	0.0030*	0.0000*	0.0000*
Rehab. effect SOT CS	0.0021*	0.0000*	0.0000*

Single-F – single-fallers; Multi-F – multi-fallers; Non-F – non-fallers; SOT – Sensory Organization Test; Rehab. – rehabilitation; Cond. – condition; CS – composite score; * significant difference (p < 0.05).

Sensory Organization Test 2 results

Significant differences were found in Cond. 1–3, Cond. 4–6 and in CS between Non-F and Multi-F groups ($p < 0.05$) and between Single-F and Multi-F groups ($p < 0.05$) (Table 1). Between Non-F and Single-F groups the differences were significant in Cond. 1–3 ($p < 0.05$). The results in Cond. 4–6 and CS between those 2 groups were minor.

Table 1. Differences between all analyzed groups (Single-F, Multi-F and Non-F) in SOT1, SOT2 and rehabilitation effect

Analyzed parameter	Kruskal-Wallis test (p-value)	Mann-Whitney U test (p-value)		
	Non-F vs Single-F vs Multi-F	Non-F vs Single-F	Non-F vs Multi-F	Single-F vs Multi-F
SOT1 Cond. 1–3	0.0022*	0.0013*	0.0018*	0.5739
SOT1 Cond. 4–6	0.0000*	0.0000*	0.0000*	0.0552
SOT1 CS	0.0000*	0.0000*	0.0000*	0.0439*
SOT2 Cond. 1–3	0.0000*	0.0116*	0.0000*	0.0072*
SOT2 Cond. 4–6	0.0000*	0.1335	0.0000*	0.0016*
SOT2 CS	0.0000*	0.0831	0.0000*	0.0010*
Rehab. effect Cond. 1–3	0.7161	0.9814	0.5645	0.4559
Rehab. effect Cond. 4–6	0.0402*	0.0075*	0.0607	0.8089
Rehab. effect CS	0.1498	0.0467*	0.1413	0.7471

Single-F – single-fallers; Multi-F – multi-fallers; Non-F – non-fallers; SOT – Sensory Organization Test; Rehab. – rehabilitation; Cond. – condition; CS – composite score; * significant difference (p < 0.05).

Number of falls (LOB) in SOT1 and SOT2

The total number of falls (LOB) in SOT1 Cond. 5 and Cond. 6 as well as the number of falls in all 3 repetitions of each of those SOT1 conditions were significantly different between Non-F and Multi-F groups (p < 0.05), and between Non-F and Single-F groups (p < 0.05). No such differences were found between Single-F and Multi-F groups (Table 3).

The number of falls was significantly reduced after rehabilitation in both SOT2 conditions (Cond. 5 and 6) in the Single-F group (p < 0.05), and in Cond. 6 in Multi-F group (p < 0.05).

Only in SOT2 Cond. 5 LOB results (number of falls) between Single-F and Multi-F groups were different (p < 0.05). In all other results (number of falls) of Cond. 5 and Cond. 6 there were minor differences between all groups (Table 3).

Differences in rehabilitation effect between the groups

There were no significant differences between Non-F and Multi-F groups, nor between Single-F and Multi-F groups. Significant differences were found only in Cond. 4–6 and in CS between Non-F and Single-F groups (p < 0.05) (Table 1).

Structure of the vestibular organ damage

The incidence of a spontaneous peripheral and central gaze, as well as positional and positioning nystagmus (PPN) is presented in Table 4. The major differences were found between Non-F and Single-F groups in spontaneous nystagmus (p < 0.05), between Non-F and Multi-F groups in positional nystagmus (p < 0.005) and in both those nystagmus types between Single-F and Multi-F groups (p < 0.005 and p < 0.05, respectively) (Table 3).

Location of damage in the vestibular organ

In Single-F group, 34 patients were diagnosed with peripheral deficits, 2 patients with central deficits and 9 subjects presented normal VNG test results. In Multi-F

Table 3. Differences between all analyzed groups (Single-F, Multi-F and Non-F) in number of falls and nystagmus

Analyzed parameter	Pearson's χ^2 test (p-value)		
	Non-F vs Single-F	Non-F vs Multi-F	Single-F vs Multi-F
LOB in SOT1 Cond. 5	0.0435*	0.0004*	0.1095
LOB in SOT1 Cond. 6	0.0120*	0.0002*	0.3669
LOB in SOT2 Cond. 5	0.5067	0.1214	0.0311*
LOB in SOT2 Cond. 6	0.4985	0.1660	0.4246
Gaze nystagmus	0.4912	0.2363	0.3280
Spontaneous nystagmus	0.0274*	0.2299	0.0029*
Positional nystagmus	0.0747	0.0004*	0.0427*

Single-F – single-fallers; Multi-F – multi-fallers; Non-F – non-fallers; SOT – Sensory Organization Test; LOB – loss of balance; Cond. – condition; * significant difference (p < 0.05).

Table 4. Structure of the vestibular organ damage in Non-F, Single-F and Multi-F groups (number of patients) – types of nystagmus observed in analyzed patients

Group of patients	Gaze		Spontaneous			Positional		
	no	yes	no	yes (peripheral)	yes (central)	no	yes (peripheral: Nylen type II or PPN)	yes (central: Nylen type I or vertical)
Non-F	21	–	–	–	–	14	7 (Nylen II –1; PPN – 6)	–
Single-F	44	1	36	9	–	17	26 (Nylen II – 15; PPN – 11)	2 (Nylen I – 2)
Multi-F	44	3	41	1	5	9	30 (Nylen II – 7; PPN – 23)	8 (Nylen I – 14; Vertical – 4)

Single-F – single-fallers; Multi-F – multi fallers; Non-F – non-fallers; PPN – positional and positioning nystagmus.

Table 5. Location of damage in the vestibular organ in Single-F and Multi-F groups (number of patients)

Group of patients	Peripheral				Mixed		Central	Normal
	not compensated	compensated	compensated + PPN	normal + PPN	central + peripheral	central + PPN		
Single-F	15	8	6	5	–	–	2	9
Multi-F	7	7	9	12	4	2	2	4

Single-F – single-fallers; Multi-F – multi-fallers; PPN – positional and positioning nystagmus.

group, 35 patients were diagnosed with peripheral deficits, 2 patients with central deficits, 4 with mixed deficits, and 4 subjects presented normal VNG test results (Table 5).

Discussion

Our results indicated that neither the balance results in Cond. 1–3 and Cond. 4–6, nor the number of falls in Cond. 5 and 6 differentiated Single-F group from Multi-F group. Only CS results were significantly different between those 2 groups. However, the SOT did differentiate Non-F group from the other 2 groups (fallers groups). Whitney et al. also found no significant differences in CS between the Single-F and Multi-F results, but the results between Non-F and Single-Multi-F groups were also significantly different.[25] However, in their study, Non-F were a non-falling group with vestibular pathology present. In our study, Non-F group consisted of healthy individuals (seniors) with no report of falls and no balance problems in their history. Contrary to Whitney et al., in our study, neither the total number of LOB in SOT1 Cond. 5 and Cond. 6, nor the a number of LOB in all 3 repetitions of each of those SOT1 conditions differentiated Single-F group from Multi-F group.[25] The cause might be probably the similar structure of damage in the vestibular organ in both groups (peripheral damage in 75% of Single-F patients and in 74% of Multi-F patients), despite the significant age difference between them. Wallmann showed significant differences in CS between fallers and non-fallers.[26] However, those authors did not disclose the structure of the groups: how many individuals suffered from peripheral vestibular organ damage, and how many from central vestibular organ damage, which could be the basis to explain the differences between the groups.

Butaois et al. performed the SOT in a group of healthy people over the age of 65 years and divided them into 3 groups: Non-F, Single-F and Multi-F.[27] These groups were similar in age. The authors found worse outcomes of Cond. 2 and R^{som} (patient's ability to use inputs from somatosensory system to maintain balance; it is determined by dividing performance in Cond. 2 by performance in Cond. 1) results in Multi-F group than in Single-F and Non-F groups, and the factor that differentiated Single-F and Non-F groups was the number of LOB in the 3rd repetition of Cond. 6. Girardi et al. in their study did not show any significance of the SOT as a method for differentiating fallers from non-fallers among vestibular pathology patients.[28] However, they conducted their research on the Balance Track System that contains only 4 out of 6 SOT conditions. The authors demonstrated that the test with the most prognostic importance was limits of stability (LOS) test rather than the SOT.

Baloh et al. evaluated the sway velocity using Chattecx Balance System in the elderly with and without balance problems.[29] They found a significantly greater sway velocity in patients with impaired balance than in the control group, and in those who presented the fear of falling, compared to those who did not reported such fears. However, the authors did not find any major differences in tests results neither between fallers and non-fallers, nor among those who fell as a result of loss of balance, those falling as a result of tripping or slipping and those who did not fall at all.

In our study, we expected the results between Non-F and Multi-F groups to be different. We did not expect relevant or significant differences between Non-F and Single-F groups, given that the Single-F group consisted mostly of patients with peripheral vestibular pathology (only 2 patients were diagnosed with central deficit), that the in those patients loses its vestibular pattern after a couple of weeks and that both groups were similar in age.[30] In Non-F group, 6 cases of PPN and 1 case of Nylen type II nystagmus were found; however, those subjects did not report any balance disorders or dizziness. This may suggest that even among elderly healthy, asymptomatic individuals, the VNG tests show some symptoms of disorders in the vestibular system. On the other hand, this confirms the opinion of Norre et al. that some people with pure PPN can present a normal posturographic test result.[31]

In our study, statistically significant differences in the SOT results between Non-F group and both groups of fallers, and no significant differences between Single-F and Multi-F groups occurred probably due to the structure of the 2 groups and the type of damage in the vestibular organ. As mentioned before, patients with peripheral impairment of vestibular organ formed a dominant and almost equal number in both groups of fallers. In addition, both groups presented similar number of patients with positional nystagmus typical for peripheral damage.

Due to a different compensation pattern of vestibulo-ocular reflex (VOR) and vestibulo-spinal reflex (VSR) that progresses in different ways, even in the case of compensated peripheral deficit, the vestibulo-spinal compensation might not take place.[7] Therefore, the patients with peripheral deficit may present instability, independently of the level of VOR compensation.[31] Despite the opinion that patients with a central vestibular deficit show more abnormal gait than patients with peripheral damage, our observations indicate that patients with central damage often present less instability than patients with uncompensated peripheral damage, as shown in our previous study.[32,33] Despite the fact that the SOT was performed at least 2 weeks after the Semont maneuver, another reason for the increased body sway while standing on stable platform among our study of both fallers groups might be BPPV. Many authors have demonstrated greater sway on a stable platform, both in the frontal and sagittal plane, in patients with BPPV than in the healthy subjects, along with long-term instability, even after resolution of the typical positional vertigo.[11,34] Giacomini et al. demonstrated that Epley maneuver causes the normalization of body sway only in the frontal plane, whereas in the sagittal plane,

body sway did not undergo normalization until a period of 12 weeks.[11] Stambolieva and Angov found that patients with a short history of BPPV presented visual dependence, which in these cases has been the source of acute sensory conflict, causing a significant increase in body sway with eyes open, which was not noted among patients with long duration of BPPV.[34] The authors also showed that the duration of symptoms also determines the effect of reposition maneuver. In patients with a short history of BPPV, the reposition maneuver caused a significant decrease in body sway in both planes while standing on a platform with eyes open. However, with eyes closed, the decrease was observed only in frontal plane.

Theories about the mechanism of long-term instability after the reposition maneuver are varied. Giacomini et al. showed that the presence of otoliths within the posterior semi-circular canal causes disorders similar to proprioceptive ones, which temporarily alter the VSR, resulting in long-term increase of body sway in the sagittal plane.[11] Stambolieva and Angov did not exclude the presence of residual otoliths that modified the dynamics of an affected semicircular canal, but the authors' study about smaller spectral density in the low frequency range of the spectrum confirmed the hypothesis that the alteration of the otolithic functions might be due to some unequal loading of the utricular macula.[34,35] This means that as long as the Epley maneuver causes only the resolution of typical vertigo and decrease of body sway in the frontal plane, the resolution of long-term instability as a consequence of impaired dynamics in the semi-circular canal and damaged utricle requires stimulation of other sensory systems and central postural adaptation mechanisms. Thus, those patients after the Epley maneuver should be referred to postural training.[14]

In our study, rehabilitation based on sensory conflicts significantly improved results in SOT2 Cond. 4–6 and CS in all studied groups. In SOT2 Cond. 1–3, there was no substantial improvement. Significant differences were found between Non-F and Multi-F groups and between Single-F and Multi-F groups in all SOT2 conditions and in CS. It is interesting that the significant differences in SOT2 between Non-F and Single-F groups concerned only the equilibrium results in Cond. 1–3, probably because both groups improved results in these conditions by almost the same amount, which still makes the results significantly different between the 2 groups, as in the SOT1. The lack of significant differences between Non-F and Single-F groups in SOT2 Cond. 4–6 and in CS indicates that patients in Single-F group improved their SOT performance in Cond. 4–6 due to rehabilitation and approached the results of Non-F group, which contributed to the improvement of the overall result of the CS and, therefore, no significant differences in these parameters (SOT2 Cond. 4–6 and CS) between these groups were found.

It appears that the significant differences in all SOT2 conditions and in CS between Single-F and Multi-F groups might be due to several factors: 1) a significant difference in age between the 2 groups; 2) more patients with BPPV in Multi-F group, which does not diminish easily with short time rehabilitation; and/or 3) more patients with central and mixed disorders in Multi-F group, because people with those deficits benefit less from vestibular rehabilitation than those with peripheral deficit.[36] The analysis of LOB in Cond. 5 and 6 in both SOT1 and SOT2 confirms those assumptions. While in SOT1 the number of LOB in Cond. 5 and 6 did not differentiate those 2 groups, in SOT2 significant differences were found in Cond. 5 in all its 3 trials. This demonstrates that in Multi-F group, the patients did not present any learning effect within the trial, were not able to use residual information from the vestibular system and their adaptation process to repeated stimuli was interfered.[37]

The rehabilitation effect was evaluated in all studied groups. A more distinct effect was expected in Multi-F and Single-F groups than in Non-F group, due to the vestibular organ pathology documented in these groups. However, no significant differences in the effect of rehabilitation was found between Non-F and Multi-F groups in all SOT conditions and CS, which only confirms the low adaptive capacity in Multi-F group. The effect of rehabilitation between Single-F and Multi-F groups also did not differ significantly. Significantly different results, however, were found between Non-F and Single-F groups in terms of Cond. 4–6 and in CS. After an initial elimination of learning effect, patients in Single-F group achieved an improvement in Cond. 4–6 that exceeded the learning effect according to the suggestions of Ford-Smith et al., but only by 3 points; however, this improvement contributed to the improvement of the overall result of the CS.[38]

It is not known, however, whether the improved performance in SOT2 Cond. 4–6 and in CS in Single-F group is actually the result of rehabilitation or further learning effect. Sensory conflicts used during rehabilitation are similar to those used in the SOT. Since Wrisley et al. showed the effect of learning in SOT results in a group of young healthy people, the interpretation of SOT results, after completed rehabilitation based on sensory conflicts, must take into account the impact of learning effect on the final result of the test.[39] Taking into account the large number of patients with peripheral vestibular deficit in Single-F group in our study, the mentioned better results of the SOT after rehabilitation may be partly due to the progress of compensation started by vestibular rehabilitation itself, and partly due to the further learning effect. Another important factor is forced motor activity in these patients resulting from the need to report daily for vestibular rehabilitation conducted in our department. On the other hand, the small effect of rehabilitation and the short duration of its conduct led us to the assumption that improved results of SOT2 Cond. 4–6 and CS in Single-F group might be caused mainly by the further learning effect.

In our study, both the results of SOT1 (Cond. 1–3 and 4–6) and LOB (in Cond. 5 and 6) did not differentiate Single-F group from Multi-F group, probably due to the similarity of the structure and the contribution of peripheral vestibular deficit and/or BPPV in both groups. The factor that showed the differences between the groups was rehabilitation. It revealed different results in all SOT2 conditions, CS and change in LOB in Cond. 5, indicating lower adaptive capacity in Multi-F group than in Single-F group. This may be the result of reverse changes in the vestibular organ, depending on the age and the presence of mixed and central deficits in Multi-F group.

In conclusion, the results of this study and the results of other authors suggest that the importance of the SOT to differentiate fallers from non-fallers and single-fallers from multi-fallers is ambiguous, which results from a diversity of groups, study inclusion criteria and research methodology applied. It might be hypothesized that different results can be expected even when testing groups that have the same type of pathology (i.e., vestibular organ pathology) because it is difficult to collect patients with an identical degree and extent of damage, the same duration of symptoms and identical degree of vestibular compensation and central adaptation. The SOT may indicate the differences between the groups, but it does not fully explain those differences – it only shows postural dysfunction without indicating its localization in particular part of vestibular organ. Moreover, the principal disadvantage of the SOT and CDP is that body sway measurements are restricted to the anterior-posterior direction. This may be crucial for patients with peripheral vestibular pathology, when interpreting their tests results to distinguish between fallers and non-fallers.[40] We believe that the basic standard diagnostic evaluation in the elderly with a proneness to falls should include medical history and clinical examination supplemented by the Hallpike maneuver and VNG. The SOT for the differentiation of fallers and non-fallers does not provide any valid information.

References

1. Rubenstein LZ, Josephson KR. The epidemiology of falls and syncope. *Clin Geriatr Med*. 2002;18(2):141–158.
2. Overstall PW, Exton-Smith AN, Imms FJ, Johnson AL. Falls in the elderly related to postural imbalance. *Br Med J*. 1977;1(6056):261–264.
3. Barin K, Dodson EE. Dizziness in the elderly. *Otolaryngol Clin North Am*. 2011;44(2):437–454.
4. Katsarkas A. Dizziness in aging: The clinical experiences. *Geriatrics*. 2008;63(11):18–20.
5. Yardley L, Owen N, Nazareth I, Luxon L. Prevalence and presentation of dizziness in a general practice community sample of working age people. *Br J Gen Pract*. 1998;48(249):1131–1135.
6. National Institute on Deafness and other Communication Disorders. *National Strategic Research Plan. Balance and the Vestibular System*. Washington, DC: US Department of Health and Human Services; 1993:153–196.
7. Schaefer KP, Meyers DL. Aspects of vestibular compensation in guinea pigs. In: Flohr H, Precht W, eds. *Lesion-Induced Neuronal Plasticity in Sensimotor Systems*. New York, NY: Springer; 1981:197–207.
8. von Brevern M, Radtke A, Lezius F, et al. Epidemiology of benign paroxysmal positional vertigo: A population study. *J Neurol Neurosurg Psychiatry*. 2007;78(7):710–715.
9. Bhattacharyya N, Baugh RF, Orvidas L, et al.; American Academy of Otolaryngology – Head and Neck Surgery Foundation. Clinical practice guideline: Benign paroxysmal positional vertigo. *Otolaryngol Head Neck Surg*. 2008;139(5 Suppl 4):47–81.
10. Parnes LS, Agrawal SK, Atlas J. Diagnosis and management of benign paroxysmal positional vertigo (BPPV). *CMAJ*. 2003;169(7):681–693.
11. Giacomini PG, Alessandrini M, Magrini A. Long-term postural abnormalities in benign paroxysmal positional vertigo. *ORL J Otorhinolaryngol Relat Spec*. 2002;64(4):237–241.
12. Brandt T, Hupert D, Hecht J, Karch C, Strupp M. Benign paroxysmal positional vertigo: A long-term follow-up (6–17 years) of 125 patients. *Acta Otolaryngol*. 2006;126(2):160–163.
13. Kao CL, Chen LK, Chern CM, Hsu LC, Chen CC, Hwang SJ. Rehabilitation outcome in home-based versus supervised exercise programs for chronically dizzy patients. *Arch Gerontol Geriatr*. 2010;51(3):264–267.
14. Han BI, Song HS, Kim JS. Vestibular rehabilitation therapy. Review of indications, mechanisms, and key exercises. *J Clin Neurol*. 2011;7(4):184–196.
15. Gauchard GC, Jeandel C, Tessier A, Perrin P. Beneficial effect of proprioceptive physical activities on balance control in elderly human subjects. *Neurosci Lett*. 1999;273(2):81–84.
16. Nashner LM. Computerized dynamic posturography. In: Jacobson GP, Newman CW, Kartush JM, eds. *Handbook of Balance Function Testing*. St. Louis, MO: Mosby Year Book; 1993:280–307.
17. Nashner LM, Peters JF. Dynamic posturography in the diagnosis and management of dizziness and balance disorders. *Neurol Clin*. 1990; 8(2):331–349.
18. Badke MB, Miedaner JA, Shea TA, Grove CG, Pyle GM. Effects of vestibular and balance rehabilitation on sensory organization and dizziness handicap. *Ann Otol Rhinol Laryngol*. 2005;114(1 Pt 1):48–54.
19. Bittar RSM, de Giacomo Carneiro Barros C. Vestibular rehabilitation with biofeedback in patients with central imbalance. *Braz J Otorhinolaryngol*. 2011;77(3):356–361.
20. Cohen H, Kimball KT. Decreased ataxia and improved balance after vestibular rehabilitation. *Otolaryngol Head Neck Surg*. 2004;130(4):418–425.
21. Rossi-Izquierdo M, Ernst A, Soto-Varela A, et al. Vibrotactile neurofeedback balance training in patients with Parkinson's disease: Reducing the number of falls. *Gait Posture*. 2013;37(2):195–200.
22. Bogaerts A, Verschueren S, Delecluse C, Claessens AL, Boonen S. Effects of whole body vibration training on postural control in older individuals: A 1 year randomized controlled trial. *Gait Posture*. 2007: 26(2):309–316.
23. Seidler RD, Martin PE. The effects of short term balance training on the postural control of older adults. *Gait Posture*. 1997;6(3):224–236.
24. Balance Manager Systems. *Clinical Interpretation Guide 2009*. Clackamas, OR: NeuroCom International Inc.; 2009.
25. Whitney SL, Merchetti GF, Schade AI. The relationship between falls history and computerized dynamic posturography in persons with balance and vestibular disorders. *Arch Phys Med Rehabil*. 2006;87(3):402–407.
26. Wallmann HW. Comparison of elderly nonfallers and fallers on performance measures of functional reach, sensory organization and limits of stability. *J Gerontol A Biol Sci Med Sci*. 2001;56(9):M580–M583.
27. Butaois S, Gueguen R, Gauchard GC, Benetos A, Perrin PP. Posturography and risk of recurrent falls in healthy non-institutionalized persons aged over 65. *Gerontology*. 2006;52(6):345–352.
28. Girardi M, Konrad HR, Amin M, Hughes LF. Predicting fall risk in an elderly population: Computer dynamic posturography versus electonystagmography test results. *Laryngoscope*. 2001;111(9):1528–1532
29. Baloh RW, Jacobson KM, Enrietto JA, Corona S, Honrubia V. Balance disorders in older persons: Quantification with posturography. *Otolaryngol Head Neck Surg*. 1998;119(1):89–92.
30. El-Kahky AM, Kingma H, Dolmans M, de Jong I. Balance control near the limit of stability in various sensory conditions in healthy subjects and patients suffering from vertigo or balance disorders: Impact of sensory input on balance control. *Acta Otolaryngol*. 2000;120(4):508–516.

31. Norre ME, Forrez G. Posture testing (posturography) in the diagnosis of peripheral vestibular pathology. *Arch Otorhinolaryngol*. 1986; 243(3):186–189.
32. Furman JM, Whitney SL. Central causes of dizziness. *Phys Ther*. 2000; 80(2):179–187.
33. Pierchała K, Lachowska M, Morawski K, Niemczyk K. Does effect of rehabilitation based on sensory conflicts in patients with vestibular deficits exceed learning effect? *NeuroRehabilitation*. 2014;34(2):343–353.
34. Stambolieva K, Angov G. Postural stability in patients with different durations of benign paroxysmal positional vertigo. *Eur Arch Otorhinolaryngol*. 2006;263(2):118–122.
35. Nashner LM. A model describing vestibular detection of body sway motion. *Acta Otolaryngol*. 1971;72(6):429–436.
36. Shepard NT, Telian SA. Programmatic vestibular rehabilitation. *Otolaryngol Head Neck Surg*. 1995;112(1):173–182.
37. Rosengren KS, Rajendran K, Contakos J, et al. Changing control strategies during assessment using computerized dynamic posturography with older women. *Gait Posture*. 2007;25(2):215–221.
38. Ford-Smith ChD, Wyman JF, Elswick RK, Fernandez T, Newton RA. Test-retest reliability of the sensory organization test in noninstitutionalized older adults. *Arch Phys Med Rehabil*. 1995;76(1):77–81.
39. Wrisley DM, Stephens MJ, Mosley S, Wojnowski A, Duffy J, Burkard R. Learning effects of repetitive administration of the sensory organization test in healthy young adults. *Arch Phys Med Rehabil*. 2007;88(8): 1049–1054.
40. Allum JHJ, Adkin AL, Carpenter MG, Held-Ziółkowska M, Honneger F, Pierchała K. Trunk sway measures of postural stability during clinical balance tests: Effect of a unilateral vestibular deficit. *Gait Posture*. 2001;14(3);227–237.

Cajanine promotes osteogenic differentiation and proliferation of human bone marrow mesenchymal stem cells

Zi-Yi Zhao[1,A,E,F], Lei Yang[2,B], Xiaohong Mu[2,C], Lin Xu[1,B], Xing Yu[1,C], Yong Jiao[1,B], Xiaozhe Zhang[1,D], Lingling Fu[1,B]

[1] Department of Orthopedics, Dongzhimen Hospital, Beijing University of Chinese Medicine, China

[2] Cancer Center, 1st Hospital of Jilin University, Changchun, China

A – research concept and design; B – collection and/or assembly of data; C – data analysis and interpretation;
D – writing the article; E – critical revision of the article; F – final approval of the article

Abstract

Background. Seed cells — mesenchymal stem cells (MSCs) — appear to be an attractive tool in the context of tissue engineering. Bone marrow represents the main source of MSCs for both experimental and clinical studies. However, the number limitation of bone marrow MSCs (BMSCs) and decreased function caused by proliferation make the search for adequate alternative sources of these cells for autologous and allogenic transplant necessary.

Objectives. This study was aimed to investigate the roles of cajanine isolated from the extracts of *Cajanus cajan* L. Millsp. in the proliferation and differentiation of BMSCs, and to discover the mechanism of proliferation of BMSCs promoted by cajanine.

Material and methods. Bone marrow mesenchymal stem cells were cultured in high-glucose Dulbecco's Modified Eagle's Medium (DMEM) and osteogenic differentiation was induced by adding dexamethasone, ascorbic acid and β-glycerophosphate supplements. Bone marrow MSCs were cultured in medium without cajanine or supplemented with cajanine. The information about the proliferation and osteogenic differentiation of BMSCs was collated. The osteogenic differentiation potential of BMSCs was also assessed at the 3rd passage by Von Kossa staining. To observe cell signal transduction changes of BMSCs after culturing them with cajanine for 24 h, the western blot analysis was performed to detect phosphorylated cell cycle proteins and activated cyclins.

Results. After osteogenic induction, the differentiation of BMSCs was accelerated by cajanine treatment. Osteogenesis markers were upregulated by cajanine treatment at both protein and mRNA levels. Cajanine obviously promoted the proliferation of BMSCs. After BMSCs were cultured with cajanine for 24 h, the cell cycle regulator proteins were phosphorylated or upregulated.

Conclusions. Cajanine can promote the expansion efficiency of BMSCs, at the same time keeping their multi-differentiation potential. Cajanine can activate the cell cycle signal transduction pathway, thus inducing cells to enter the G1/S phase and accelerating cells entering the G2/M phase. This study can contribute to the development of cajanine-based drugs in tissue engineering.

Key words: mesenchymal stem cells, placenta, *Cajanus cajan* L., tissue engineering

Introduction

Cajanus cajan (cajanine) is a perennial legume from the family Fabaceae.[1] It is extracted from pigeon pea leaves and has been reported to exhibit a variety of bioactivities, including antimalaria, hypolipidemia and cytotoxicity effects, as well as reducing bone loss and promoting bone-like tissue formation.[1–7] Moreover, a recent study revealed that cajanine could increase tibial bone density and improve bone metabolism as well as lipid metabolism in ob/ob mice with osteoporosis and hyperlipidemia symptoms, indicating that cajanine might be a promising drug candidate due to its broad range of bioactivities.[8]

Mesenchymal stem cells (MSCs) are a small population of multipotent stromal cells that are present in practically all tissues.[9] Mesenchymal stem cells are maintained in a relative state of quiescence in vivo; however, they are capable of proliferating and then differentiating into osteoblasts, chondrocytes, adipocytes, or other mesoderm-type lineages when stimulated by a variety of physiological and pathological signals.[9] Multiple signaling networks have been demonstrated for the development and differentiation of MSCs into functional mesenchymal lineages. The transforming growth factor-β (TGF-β) signal pathway has been studied as a key regulator in the self-renewal, maintenance and differentiation of stem cells.[10–12] It has been reported that TGF-β1 plays an important role in cartilage development and is an important chondrogenic factor.[12,13] Moreover, some studies have demonstrated that cajanine has anti-tumor and anti-oxidant functions.[14] Despite evidence revealing that cajanine has potential to be a therapeutic agent, the detailed mechanisms of anti-tumor effects are still under investigation.

In this study, the roles of cajanine in the proliferation and differentiation of bone marrow MSCs (BMSCs) were investigated. The osteogenesis markers and cell cycle were further assessed.

Material and methods

Bone marrow mesenchymal stem cells culture

Human bone marrow aspirates were obtained from donors from Dongzhimen Hospital, Beijing, China, in the years 2012–2014, and isolated by density gradient centrifugation, utilizing Ficoll-Paque TM PLUS solution (GE Healthcare, Uppsala, Sweden), followed by cell-surface marker negative selection according to the previous report.[15] Bone marrow MSCs isolated from donors were used within 4 passages. Briefly, cells were harvested using 0.25% trypsin with 1.0 M ethylenediaminetetraacetic acid (EDTA), centrifuged and expanded in basal medium, consisting of high-glucose Dulbecco's Modified Eagle's Medium (DMEM), supplemented with 10% fetal bovine serum (FBS),

100 unit/mL penicillin and 100 unit/mL streptomycin (basal medium). Basal medium contained high-glucose DMEM, FBS, penicillin and streptomycin (all from Gibco, Gaithersburg, USA). Cells were maintained in a 37°C incubator. The medium was changed every 3 days.

Chemicals and antibodies

Cajanine was obtained from Sigma-Aldrich (Shanghai, China). Rabbit anti-collagen I polyclonal antibody was purchased from Abcam (ab21286; Abcam, Cambridge, UK); rabbit anti-osteopontin polyclonal antibody was purchased from Abcam (ab8448); rabbit anti-Runx2 monoclonal antibody was purchased from Cell Signaling (No. 12556; Beverly, USA); phospho-Rb rabbit monoclonal antibody was purchased from Cell Signaling (No. 8516); rabbit anti-CDK2 monoclonal antibody was purchased from Cell Signaling (No. 2546); rabbit anti-CDC25A and anti-CDC25B monoclonal antibodies were purchased from Cell Signaling (No. 3652, No. 9525); rabbit anti-cyclin B1 monoclonal antibody was purchased from Cell Signaling (No. 12231); and rabbit anti-α-tubulin monoclonal antibody was purchased from Cell Signaling (No. 2144).

Osteogenic induction

Osteogenic differentiation was performed by culturing 3×10^4 human BMSCs (hBMSCs) in a 6-well plate in Poietics® osteogenic induction medium (Lonza Walkersville, Inc., Walkersville, USA), which contained dexamethasone, ascorbic acid and β-glycerophosphate supplements.

Von Kossa staining

The cells were fixed in cold methanol for 15–20 min at –20°C, followed by incubation with 5% silver nitrate solution (ab150687; Abcam), and crosslinked under UV light for 20–30 min, then rinsed twice with distilled water. The dishes were incubated with 5% sodium thiosulfate solution for 2–3 min. After rinsing twice, the dishes were finally incubated with nuclear fast red solution for 5 min, and rinsed with distilled water to remove excess stain.

Real-time polymerase chain reaction

Total RNAs were extracted using the TRIzol® reagent (Sigma-Aldrich), according to the manufacturer's instructions. After diminishing genomic DNA contamination by Turbo DNAse (Thermo Fisher Scientific, Waltham, USA), according to the manufacturer's instructions, the purified RNA (10 ng/mL) was reverse-transcribed with the High Capacity cDNA Reverse Transcription (RT) Kit (Qiagen, Valencia, USA) under the following conditions: 25°C for 10 min, 37°C for 120 min, followed by 85°C for 5 min. The real-time polymerase chain reaction (RT-PCR) was performed on an Applied Biosystems StepOnePlus™ PCR

machine (Applied Biosystems, Foster City, USA), using 5 µL SYBR® Green PCR Master Mix (Life Technologies, Grand Island, USA), 2 µL sequence specific primers (0.5 mM; glyceraldehyde-3-phosphate dehydrogenase (GAPDH) was used at the amount of 0.25 mM) and 3 µL cDNA under the following conditions: 95°C for 10 min, followed by 40 cycles of 15 s of denaturation at 95°C and 60 s of annealing and elongation at 60°C. A melting curve analysis was performed after each run to confirm the product specificity. The 2Δ Ct method was employed to determine the relative gene expression level of the gene of interest, normalized to the endogenous controls.[5]

Cell proliferation assays

Cell proliferation rates were measured by a methylthiazol tetrazolium (MTT) assay, using Cell Proliferation Assay Kit (Thermo Fisher). After the cells were treated with cajanine, MTT was added to each well and the cells were incubated at 37°C for 2 h. The plates were centrifuged at $450 \times g$ for 5 min at room temperature and the medium was removed. To solubilize the crystals, dimethyl sulfoxide (DMSO) was added to each well and the plates were read at 570 nm, using a microplate reader (Molecular Devices, Sunnyvale, USA). The same experiment was repeated 3 times.

Immunofluorescence

The cells were fixed in 4% paraformaldehyde, rinsed with 1× phosphate-buffered saline (PBS) and incubated with 3% bovine serum albumin (BSA) blocking solution for 60 min on a shaker. Runx2 antibody (1:500 dilution) was added directly to the blocking solution and the samples were further incubated for 3 h at room temperature. The samples were washed with 1× PBS and incubated with 5 µL AlexaFluor® 488-labeled goat anti-rabbit secondary antibody (2 mg/mL; Molecular Probes, Carlsbad, USA) in 1× PBS at room temperature, protected from light. After 60 min of incubation, the cells were washed with 1× PBS for 3 times of 5 min each. 4′,6-diamidino-2-phenylindole (DAPI) was added to PBS for nuclear staining at 1 × 5000, followed by washing by PBS. Images were taken with an Olympus IX70 inverted microscope (Olympus, Tokyo, Japan) and processed, using ImageJ software (National Institutes of Health, Bethesda, USA).

Western blot

After the cajanine treatment, the cells were collected and the harvested proteins were first separated by 10% sodium dodecyl sulfate-polyacrylamide gel electrophoresis (SDS-PAGE), and then transferred to nitrocellulose membranes (Bio-Rad Laboratories, Hercules, USA). The membranes were blocked with 5% non-fat milk and incubated with primary antibodies at a dilution of 1:1000. The membranes were subsequently incubated with a horseradish peroxidase secondary antibody (Sigma-Aldrich). The protein complex was detected, using enhanced chemiluminescence reagents (Pierce Biochnology Inc., Rockford, USA). Endogenous α-tubulin was used as the internal control.

Statistical analysis

Statistical analyses were performed with Student's t-test or one-way analysis of variance (ANOVA), using Prism v. 5.0 (GraphPad Software, La Jolla, USA).

Results

Cajanine promotes the osteogenic differentiation of bone marrow mesenchymal stem cells

It has been well recognized that the human bone marrow stroma contains multipotent mesenchymal cells that give rise to adipocytes and osteoblasts, as well as many other lineages.[9] To assess the roles of cajanine in the differentiation of BMSCs, we started to investigate whether cajanine isolated from the plant *Cajanus cajan* L. Millsp. could regulate the osteogenesis of BMSCs in vitro. Bone marrow MSCs were isolated and cultured with or without cajanine for 24 h, then the cells were cultured in regular osteogenic differentiation medium for 16 days. Interestingly, our results show that BMSCs treated with cajanine achieved dramatic increases in extracellular calcium deposits (Fig. 1). Consistently, the results described above were confirmed by Von Kossa staining, which is used for histological visualization of calcium deposits. After 3 weeks of osteogenic induction, the cajanine-treated BMSCs displayed higher

Table 1. The proliferation rates for BMSCs increased by cajanine treatments, measured using an MTT assay

Group	MTT assay/OD 570 nm				
	3 days	6 days	9 days	12 days	15 days
Control	0.13 ±0.01	0.21 ±0.02	0.27 ±0.02	0.34 ±0.01	0.39 ±0.03
1×10^9 g/mL	0.20 ±0.02	0.48 ±0.01	0.67 ±0.01	0.72 ±0.01	0.81 ±0.01
1×10^8 g/mL	0.21 ±0.01	0.51 ±0.04	0.73 ±0.03	0.80 ±0.02	0.83 ±0.02
1×10^7 g/mL	0.21 ±0.03	0.52 ±0.01	0.75 ±0.01	0.81 ±0.04	0.83 ±0.03

The data is presented as means ± standard deviations (SD); BMSCs – bone marrow mesenchymal stem cells; MTT – methylthiazol tetrazolium; OD – optical density.

48

Z-Y. Zhao, et al. The effect of cajanine on hBMSCs

levels of calcine deposit than the control group (Fig. 2). Taken together, we found that cajanine promoted the osteogenic differentiation of BMSCs.

The effects of in vitro cajanine treatment on the expressions of osteogenesis markers

To investigate the mechanisms of the cajanine-stimulated osteogenesis of BMSCs, we assessed the osteogenic markers. It has been reported that the expressions of osteopontin (OPN) and type I collagen are the markers of osteogenesis.[9] As we expected, BMSCs treated with cajanine showed upregulated expressions of OPN and collage I at protein and mRNA levels (Fig. 3A–D). Moreover, Runx2, a transcription factor required for bone formation and the differentiation of BMSCs into osteoblasts, is primarily controlled by the activation of Runx2.[16] As we expected, cajanine promoted the nuclear translocation of Runx2 in BMSCs (Fig. 3E), suggesting that the cajanine-activated BMSCs had higher Runx2 activity.
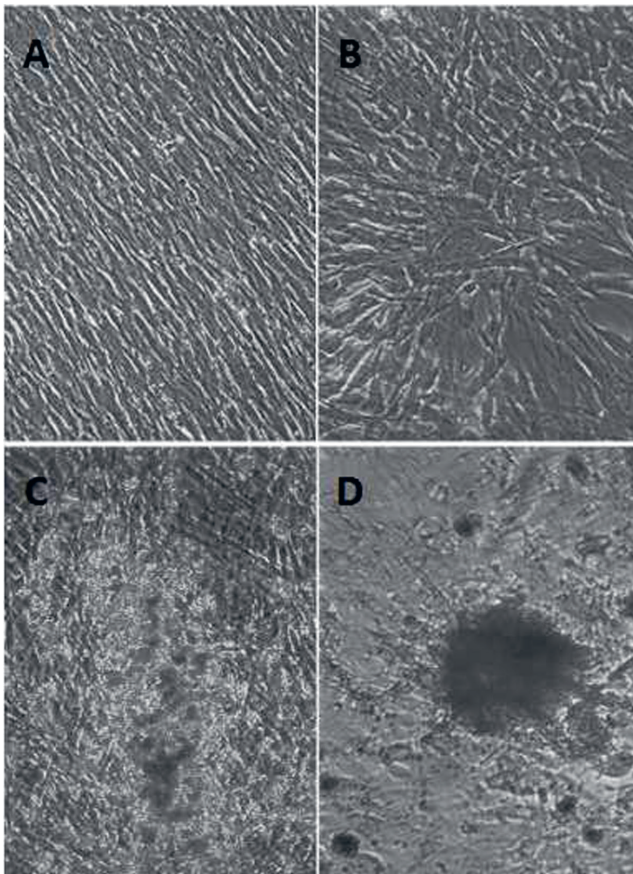
Fig. 1. Cajanine promotes osteogenic differentiation of BMSCs

A – BMSCs treated with PBS as a control; B – BMSCs treated with cajanine for 24 h; C – cells from A incubated in osteogenic induction medium for 2 weeks; D – cells from B incubated in osteogenic induction medium for 2 weeks.
BMSCs – bone marrow mesenchymal stem cells; PBS – phosphate-buffered saline.
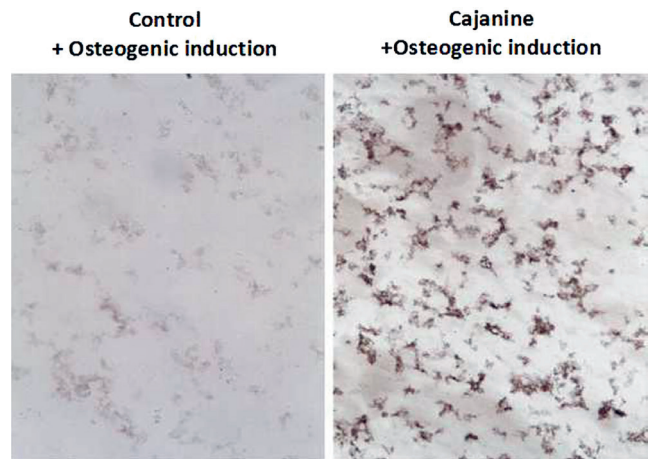
Fig. 2. Von Kossa staining of BMSCs with or without cajanine treatment under the osteogenic induction conditions

A – BMSCs treated with PBS for 24 h before osteogenic induction;
B – BMSCs treated with cajanine for 24 h, and then incubated with osteogenic induction medium for 2 weeks.
BMSCs – bone marrow mesenchymal stem cells; PBS – phosphate-buffered saline.

The proliferation rate of bone marrow mesenchymal stem cells is stimulated by cajanine

We next investigated the effects of cajanine on the proliferation of BMSCs in vitro. Bone marrow MSCs were left untreated or were treated with cajanine at 1, 10 or 100 ng/mL for 3, 6, 9, 12, and 15 days. The MTT assays were performed to measure the cell proliferation ratio. Our data in Table 1 and Fig. 4 demonstrate that cajanine treatment at low concentrations (1 ng/mL) could significantly increase the cell proliferation after 6 days. At higher concentrations (10 and 100 ng/mL), the cell proliferation rates were similar as in the case of low concentrations. Taken together, our results revealed that cajanine promoted both the osteogenic differentiation and proliferation of BMSCs, suggesting cajanine might contribute to the development of therapeutic agents for the clinical applications of tissue engineering.

Cajanine activates cell cycle regulators of bone marrow mesenchymal stem cells

Our abovementioned results demonstrated that cajanine promotes the proliferation of BMSCs in vitro. We then assessed the cell cycle markers of BMSCs in response to cajanine treatment. To determine the cell cycle consequences of cajanine, we analyzed cell cycle regulators in cajanine-treated BMSCs. Interestingly, our data showed that the phosphorylation of retinoblastoma (Rb) is responsible for a major G1 checkpoint, which was increased by cajanine stimulation, suggesting that cajanine might contribute to the G1 to S phase transition (Fig. 5). In addition, we found that the expressions of CDK2, cyclin B1 and CDC 25A&B
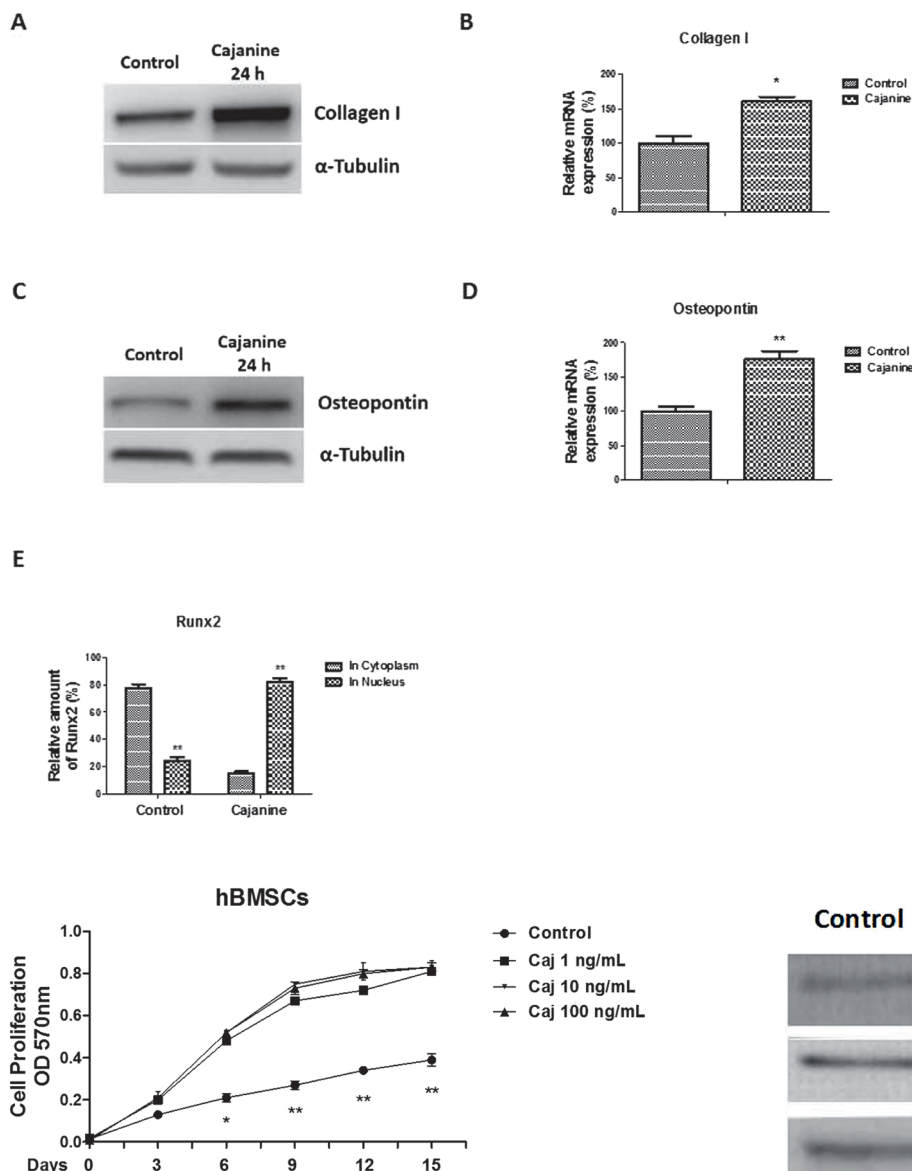
Fig. 3. Cajanine treatment upregulates the osteogenic differentiation markers of BMSCs

A – BMSCs left untreated or treated with cajanine for 24 h, then total cell lysates collected and subjected to a western blot analysis, with α-tubulin as a loading control; B – BMSCs left untreated or treated with cajanine for 24 h, then the mRNA level of collagen I detected using qRT-PCR; C – BMSCs left untreated or treated with cajanine for 24 h, then the protein level of OPN detected using western blot with α-tubulin as a loading control; D – the mRNA level of OPN detected using qRT-PCR in cajanine-treated or untreated BMSCs.
BMSCs – bone marrow mesenchymal stem cells; qRT-PCR – quantitative reverse transcription polymerase chain reaction; OPN – osteopontin.

Fig. 4. Cajanine promotes BMSCs proliferation

Bone marrow mesenchymal stem cells treated with a control solution, 1, 10 or 100 ng/mL of cajanine for 3, 6, 9, 12, and 15 days; the cell proliferation rates measured using a MTT assay.
BMSCs – bone marrow mesenchymal stem cells; MTT – methylthiazol tetrazolium.

Fig. 5. Cajanine upregulates cell cycle regulators

Bone marrow mesenchymal stem cells treated with cajanine for 24 h, then collected and subjected to a western blot analysis, with α-tubulin as a loading control.
BMSCs – bone marrow mesenchymal stem cells.

were upregulated by cajanine treatment (Fig. 5), which shows that cajanine promoted the proliferation of BMSCs through the modulation of cell cycle progressions.

Discussion

Cajanus cajan L. Millsp. is a traditional Chinese medicine herb involved in diverse biological processes. In this study, we explored the roles of cajanine in the differentiation and proliferation of hBMSCs. We found that cajanine treatment promoted the osteogenic differentiation of BMSCs in vitro. Since BMSCs are a promising source of precursor cells, which may be applied in various tissue engineering strategies, our study focused on the regulatory functions of cajanine in relation to the osteogenic differentiation of BMSCs, providing a new approach to the development of therapeutic agents for tissue engineering.

Bone marrow MSCs can be induced to differentiate toward a variety of mature target cells by differentiation-specific

protocols. Moreover, bone differentiation and formation are regulated at the molecular level. Previous studies demonstrated that Runx2 is a transcription factor required for bone formation.[17] Runx2 is also a target of bone morphogenetic proteins (BMPs) and is induced by TGF-β in pluripotent mesenchymal precursor cells.[18] Apart from the TGF-β pathway, BMSCs osteogenic differentiation was directed through the non-SMAD signaling pathways, mitogen-activated protein kinase (MAPK) signaling and Wnt signaling cascades.[19] Our results, consistent with the previous studies, showed that the activities of Runx2, as well as other osteogenic markers, are upregulated by cajanine treatment.

Bone marrow MSCs are maintained in a relative state of quiescence until they are activated by a variety of physiological and pathological stimuli. Bone marrow MSCs are capable of proliferating and then differentiating into osteoblasts, chondrocytes, adipocytes, or other mesoderm-type lineages. Therefore, the proliferation of BMSCs is important for maintaining the biological functions of them before differentiation. We report here that cajanine promotes the proliferation of BMSCs by the upregulation of cell cycle regulators. We will continue to explore the detailed mechanisms of the cajanine-stimulated proliferation of BMSCs by measuring other cell proliferation signaling pathways, such as mTOR, Akt or MAPK, in further work. In summary, we discovered a novel function of cajanine in the regulation of osteogenic differentiation and proliferation in BMSCs. Our study will contribute to the cajanine-based drug development for tissue engineering.

References

1. Nix A, Paull CA, Colgrave M. The flavonoid profile of pigeon pea, *Cajanus cajan*: A review. *Springerplus*. 2015;4:125.
2. Duker-Eshun G, Jaroszewski JW, Asomaning WA, Oppong-Boachie F, Brogger CS. Antiplasmodial constituents of *Cajanus cajan*. *Phytother Res*. 2004;18(2):128–130.
3. Luo QF, Sun L, Si JY, Chen DH. Hypocholesterolemic effect of stilbenes containing extract-fraction from *Cajanus cajan* L. on diet-induced hypercholesterolemia in mice. *Phytomedicine*. 2008;15(11):932–939.
4. Ashidi JS, Houghton PJ, Hylands PJ, Efferth T. Ethnobotanical survey and cytotoxicity testing of plants of south-western Nigeria used to treat cancer, with isolation of cytotoxic constituents from *Cajanus cajan* Millsp. leaves. *J Ethnopharmacol*. 2010;128(2):501–512.
5. Luo M, Liu X, Zu Y, et al. Cajanol, a novel anticancer agent from pigeon pea (*Cajanus cajan* L. Millsp.) roots, induces apoptosis in human breast cancer cells through a ROS-mediated mitochondrial pathway. *Chem Biol Interact*. 2010;188(1):151–160.
6. Zhang J, Liu C, Sun J, Liu D, Wang P. Effects of water extract of *Cajanus cajan* leaves on the osteogenic and adipogenic differentiation of mouse primary bone marrow stromal cells and the adipocytic trans-differentiation of mouse primary osteoblasts. *Pharm Biol*. 2010;48 (1):89–95.
7. Bhargavan B, Gautam AK, Singh D, et al. Methoxylated isoflavones, cajanin and isoformononetin have non-estrogenic bone forming effect via differential mitogen-activated protein kinase (MAPK) signaling. *J Cell Biochem*. 2009;108(2):388–399.
8. Ye GF, Wang L, Yang RY, Tian RH, Hu YJ, Shen XL. Effects of hydrophobic fraction of *Cajanus cajan* L. Millsp. on bone density and blood lipid level in obese and diabetic mice. *Chinese Pharmacological Bulletin*. 2013;29: 961–965.
9. Pontikoglou C, Deschaseaux F, Sensebe L, Papadaki HA. Bone marrow mesenchymal stem cells: Biological properties and their role in hematopoiesis and hematopoietic stem cell transplantation. *Stem Cell Rev*. 2011;7(3):569–589.
10. Yamasaki S, Mera H, Itokazu M, Hashimoto Y, Wakitani S. Cartilage repair with autologous bone marrow mesenchymal stem cell transplantation: Review of preclinical and clinical studies. *Cartilage*. 2014;5(4): 196–202.
11. Hu J, Liao H, Ma Z, et al. Focal adhesion kinase signaling mediated the enhancement of osteogenesis of human mesenchymal stem cells induced by extracorporeal shockwave. *Sci Rep*. 2016;6:20875.
12. Sakaki-Yumoto M, Katsuno Y, Derynck R. TGF-beta family signaling in stem cells. *Biochim Biophys Acta*. 2013;1830(2):2280–2296.
13. Watabe T, Miyazono K. Roles of TGF-beta family signaling in stem cell renewal and differentiation. *Cell Res*. 2009;19(1):103–115.
14. Ji XY, Xue ST, Zheng GH, et al. Total synthesis of cajanine and its antiproliferative activity against human hepatoma cells. *Acta Pharmaceutica Sinica B*. 2011;1(2):93–99.
15. Kollmer M, Buhrman JS, Zhang Y, Gemeinhart RA. Markers are shared between adipogenic and osteogenic differentiated mesenchymal stem cells. *J Dev Biol Tissue Eng*. 2013;5(2):18–25.
16. Gao P, Zhang H, Liu Y, et al. Beta-tricalcium phosphate granules improve osteogenesis in vitro and establish innovative osteo-regenerators for bone tissue engineering in vivo. *Sci Rep*. 2016;6:23367.
17. Bruderer M, Richards RG, Alini M, Stoddart MJ. Role and regulation of RUNX2 in osteogenesis. *Eur Cell Mater*. 2014;28:269–286.
18. Chen G, Deng C, Li YP. TGF-beta and BMP signaling in osteoblast differentiation and bone formation. *Int J Biol Sci*. 2012;8(2):272–288.
19. Rahman MS, Akhtar N, Jamil HM, Banik RS, Asaduzzaman SM. TGF-beta/BMP signaling and other molecular events: Regulation of osteoblastogenesis and bone formation. *Bone Res*. 2015;3:15005.

Non-classical and intermediate monocytes in patients following venous thromboembolism: Links with inflammation

Ewa Wypasek[1,2,A,C,D], Agnieszka Padjas[2,B–D], Magdalena Szymańska[3,B,C], Krzysztof Plens[4,C], Maciej Siedlar[5,E,F], Anetta Undas[1,A,E,F]

[1] Institute of Cardiology, Jagiellonian University Medical College, Kraków, Poland

[2] Department of Medicine, Jagiellonian University Medical College, Kraków, Poland

[3] John Paul II Hospital, Kraków, Poland

[4] Data Analysis Center, Cardiovascular Research Institute, Kraków, Poland

[5] Department of Clinical Immunology, Chair of Clinical Immunology and Transplantation, Institute of Pediatrics, Jagiellonian University Medical College, Kraków, Poland

A – research concept and design; B – collection and/or assembly of data; C – data analysis and interpretation;
D – writing the article; E – critical revision of the article; F – final approval of the article

Address for correspondence
Ewa Wypasek
E-mail: ewa.wypasek@wp.pl

Abstract

Background. Monocyte subsets are involved in atherosclerotic vascular disease and its thromboembolic complications. Moreover, the role of monocytes has been suggested in the pathogenesis of venous thromboembolism (VTE).

Objectives. We hypothesized that pro-inflammatory non-classical and intermediate monocytes are increased in the first months following VTE.

Material and methods. We enrolled 70 patients aged 18–65 years (mean age 41.6 ±11.6) with the first-ever provoked (n = 32; 45.7%) or unprovoked (n = 38; 54.28%) VTE episode, and 46 healthy controls. The exclusion criteria were: acute infection, cancer, autoimmune disorders, previous myocardial infarction (MI), or stroke. Monocyte subsets were assessed 12 (8.5–21.5) months after VTE using flow cytometry and were defined as classical ($CD14^{++}CD16^{-}$), intermediate ($CD14^{++}CD16^{+}$) and non-classical ($CD14^{+}CD16^{++}$).

Results. Patients with VTE had higher intermediate and non-classical monocyte counts compared to the control group (16.8 ±9.3 vs 10.4 ±4.0 cells/µL, and 64.1 ±25.2 vs 44.1 ±19.2 cells/µL, respectively, both p < 0.001). Increased non-classical monocyte counts were observed in patients who experienced a VTE incident within 12 months prior to enrollment (71.5 ±27.4 vs 56.03 ±20.6 cells/µL; p = 0.01) and those with unprovoked VTE (70.2 ±4.1 vs 58.8 ±4.3 cells/µL; p = 0.06). There were no differences in monocyte subsets related to the current anticoagulation.

Conclusions. Our data has shown for the first time that VTE is associated with an increased number of non-classical and intermediate monocytes, which may indicate the involvement of monocyte-related mechanisms in the pathophysiology of this disease.

Key words: inflammation, venous thromboembolism, non-classical monocytes, intermediate monocytes

Introduction

Venous thromboembolism (VTE), including deep vein thrombosis (DVT) and pulmonary embolism (PE), is a common disease associated with significant mortality and substantial healthcare costs. Venous thromboembolism occurs in approx. 1 to 2 per 1,000 person per year, and the overall VTE incidence is similar to that of strokes.[1] Idiopathic VTE events represent 25–40%. The morbidity rises dramatically after about 45 years of age and is slightly higher for men than for older women.[1–3] Venous thromboembolism is the 3rd most common cause of cardiovascular death worldwide, just after myocardial infarction (MI) and stroke.[4]

There is evidence that inflammation and thrombosis are closely linked, but the nature of this relationship is poorly understood. Increased level of C-reactive protein (CRP), a major marker of inflammation, has been shown to be associated with VTE in the general population as well as DVT, in particular in those with post-thrombotic syndrome that occurs in 20–50% of the patients within the first 2 years since the event.[5–9] In addition, acute infections predispose to DVT, which also supports the role of inflammation in thrombosis.[10,11] Levels of CRP and IL-6 at the time of the DVT diagnosis were associated with thrombotic disease burden, as measured by DVT extent and severity of DVT symptoms and signs.[12]

Identification of internal prothrombotic functions of cells of the innate immune system, which acts in blood vessels, resulted in an intriguing concept of immunothrombosis.[13–16] Involvement of the immune system in the thrombosis process represents a physiological mechanism, an independent line of host defense against microorganisms that mediates in the identification of and protection against pathogens by promoting microthrombi in the vessels.[7–9] Immunothrombosis is triggered and maintained by the local accumulation of innate immune cells, mainly monocytes and neutrophils. Dysregulation of immunothrombotic reactions can, therefore, contribute to thrombotic disorders, including DVT, in individuals free of infections.[7] During development of DVT, activated endothelial cells adopt a proinflammatory phenotype, which initiates the recruitment of innate immune cells, particularly monocytes and neutrophils. Active participation of cells of the innate immune system in the formation of thrombi is a specific attribute of thrombosis, as indicated by studies on mouse models of DVT.[14] It has been demonstrated in animals that the DVT begins as a sterile inflammation characterized by a massive recruitment of neutrophils and monocytes. The role of monocytes in VTE observed in human subjects is, however, unclear.

Monocytes represent a heterogeneous cell population in both phenotype and function. Based on the expression of CD14 and CD16, 3 monocyte subsets can be differentiated: classical (CD14++CD16−), intermediate (CD14++CD16+) and non-classical (CD14+CD16++). CD16

antigen is identified as FcγRIIIA and is involved in innate immunity, while CD14 is a coreceptor of toll-like receptor 4 that binds lipopolysaccharide (LPS). The correct count of the number of individual subsets of monocytes requires staining and appropriate gating strategy, which includes a 3rd pan-monocyte marker, i.e., HLA-DR or CD86. CD16+ monocytes are the main producers of tumor necrosis factor-α (TNF-α), interleukin-1β (IL-1β) and IL-6, which indicates that intermediate or non-classical monocytes or both jointly produce the largest quantities of the proinflammatory cytokines.[17–20]

Recently, Mukherjee et al. have shown that non-classical CD14+CD16++ subtype of monocytes displays inflammatory characteristics and properties for antigen presentation.[21] In turn, intermediate CD14++CD16+ appear to be transitional monocytes that display both phagocytic and inflammatory functions, whereas classical monocytes CD14++CD16− are phagocytic with low inflammatory attributes.[21]

Growing evidence suggests that proinflammatory subsets of monocytes are involved in atherosclerosis and its thromboembolic complications. Higher numbers of proinflammatory intermediate or non-classical monocytes have been shown in patients with a stable and unstable coronary artery disease (CAD).[22,23] In patients with stable CAD, cardiovascular events can be predicted by elevated counts of intermediate monocytes.[24] Intermediate monocytes have also been shown to be positively correlated with peak cardiac troponin and inflammatory markers in patients with acute ST segment elevation MI that is caused in the vast majority of cases by a thrombus occluding a coronary artery.[25] In unstable angina patients counts of intermediate monocytes, intermediate monocyte-platelet aggregates and total monocyte-platelet aggregates are increased, and are independent of traditional risk factors.[26] Hypercholesterolemia is also associated with an elevated number of non-classical monocytes, while HDL-cholesterol showed a negative association.[27] Elevated counts of intermediate monocytes have also been demonstrated in patients during the first days after an ischemic stroke.[28]

Despite the fact that monocyte subpopulations have been assessed in various diseases and experimental studies have shown a causative role of monocytes in the pathogenesis of VTE, to our knowledge there have been no published studies assessing various subsets of circulating monocytes in patients following VTE.[29,30]

Methods

Patients

We investigated 70 consecutive Caucasian patients, aged 18–65 years, with a history of the first-ever provoked or unprovoked DVT alone or in combination with PE, referred to an outpatient clinic between October 2012

and June 2015. The diagnosis of DVT was established by a positive finding on color duplex sonography (visualization of an intraluminal thrombus in calf, popliteal, femoral, or iliac veins). The diagnosis of PE was based on the presence of typical symptoms and positive results of computed tomography pulmonary angiography (CT). Patients with signs of acute infection, known cancer, chronic inflammatory disease, or autoimmune disorders (including antiphospholipid syndrome), previous MI or stroke, serum creatinine ≥120 µM, liver injury, pregnancy were ineligible. All patients were treated with unfractionated or low-molecular-weight heparin, and then vitamin K antagonists (VKA) were continued for at least 3 months in patients with VTE triggered by transient risk factors and for 6 months or longer on the discretion of the treating physicians in patients with unprovoked VTE. A VTE episode was defined as unprovoked (idiopathic) if the patient had no history of cancer, surgery requiring general anesthesia, major trauma, a plaster cast or hospitalization within the last month, or pregnancy or delivery within the last 3 months. A proximal DVT was defined as thrombosis in the popliteal veins, including the trifurcation, the femoral and iliac veins.

Forty-six consecutive healthy volunteers served as the control group. The exclusion criteria were: personal and/or family history of cardiovascular diseases including VTE, MI, CAD, heart failure, stroke, and any of chronic diseases except for arterial hypertension, as well as age over 65 years. All subjects denied taking any medication on a long-term basis and within the previous month.

Body mass index (BMI) was calculated as weight in kilograms divided by the square of height in meters. Obesity was defined as a BMI of 30 kg/m^2 or higher. Diabetes mellitus was defined as the previous diagnosis of diabetes, or at least 2 random fasting glucose levels of >7 mmol/L. Arterial hypertension was diagnosed based systolic or diastolic pressure ≥140 mm Hg or ≥90 mm Hg, respectively, on at least 2 different occasions or the use of antihypertensive treatment. Hypercholesterolaemia was diagnosed based on low-density lipoprotein cholesterol (LDL-C) level >3.0 mmol/L or previously diagnosed hypercholesterolaemia. The diagnosis of MI was based on the 2012 American Heart Association, European Society of Cardiology, American College of Cardiology Foundation, and World Heart Federation (ESC/ACCF/AHA/WHF) guidelines. Ischemic stroke was diagnosed according to the World Health Organization criteria. Smoking was defined as the use of at least 1 cigarette per day.

The Ethical Committee by Regional Medical Council in Kraków (No. 135/KBL/OIL/2013) approved the study and all the participants provided their written informed consent.

Laboratory investigations

Fasting blood samples were drawn between 8 a.m. and 12 a.m. from an antecubital vein with minimal stasis. Serum triglycerides, total cholesterol, LDL-C, high-density lipoprotein cholesterol (HDL-C), creatinine and glucose, total protein and albumin, and complete blood count were assayed using a biochemical analyser Cobas 6000™ (Roche Diagnostics GmbH, Mannheim, Germany). Fibrinogen was determined using the Clauss method. A high-sensitivity CRP (hs-CRP) was determined using immunoturbidimetry (Roche Diagnostics GmbH).

A complete blood count was determined using the hematological analyzer Sysmex XT2000i (Sysmex Corporation, Kobe, Japan). Anti-nuclear antibodies (ANA) were tested using indirect fluorescent assay (IFA) in sera diluted at 1:160 (Euroimmun, Lübeck, Germany).

Flow cytometry

The number of monocytes was assessed in blood samples an average of 12 months after the incident of VTE. Whole blood samples were drawn into EDTA-K3 collection tubes and were prepared for flow cytometry within 30 min. Briefly, 50 µL of whole blood was incubated with antibody mix containing 10 µL of FITC-labeled anti-human CD14 (B36297, Beckman Coulter, Brea, USA), 10 µL PE-labeled anti-human CD16 (332779, BD Biosciences, San Jose, USA), 10 uL PerCP-labelled anti-human HLA-DR (347402, BD Biosciences), 5 µL APC-labeled anti-human CD45 (340910, BD Biosciences) in BD Trucount tubes (all from BD Bioscience) for 30 min in room temperature in the dark. The isotype control was run in parallel. Lysis of erythrocytes was performed using 450 µL of BD FACS Lysing Solution (BD Bioscience) for 5 min. Determination of monocytes subsets were performed on FACSCanto II flow cytometry (BD Bioscience) and analyzed by FACSDiva software v. 7.0 (BD Biosciences). The following calculation has been performed: [(number of events in quadrant containing cell population)/(number of events in absolute-count bead region)] × [(number of beads per test defined by manufacturer)/(test volume)], to obtain the number of monocytes per microliter.

Monocyte subpopulation identification

The absolute number of monocyte subpopulations was determined as described previously.[31] Briefly, based on CD45-positive and SSC characteristics, monocytes were gated together with adjacent lymphocytes, including NK cells (Fig. 1A). Then, to exclude CD14-negative and HLA-DR-negative NK cells (gate "d"), a gate "c" was defined including CD14-positive and HLA-DR-positive events (Fig. 1B). All events from gate "c" were then divided based on CD14 and CD16 expression into: classical monocytes CD14^{++}CD16$^-$ (gate "e") expressing high levels of CD14 but no CD16; intermediate monocytes CD14^{++}CD16$^+$ (gate "f") expressing high levels of CD14 and low CD16; and non-classical monocytes CD14$^+$CD16^{++} (gate "g") expressing low CD14 but high CD16 (Fig 1C).
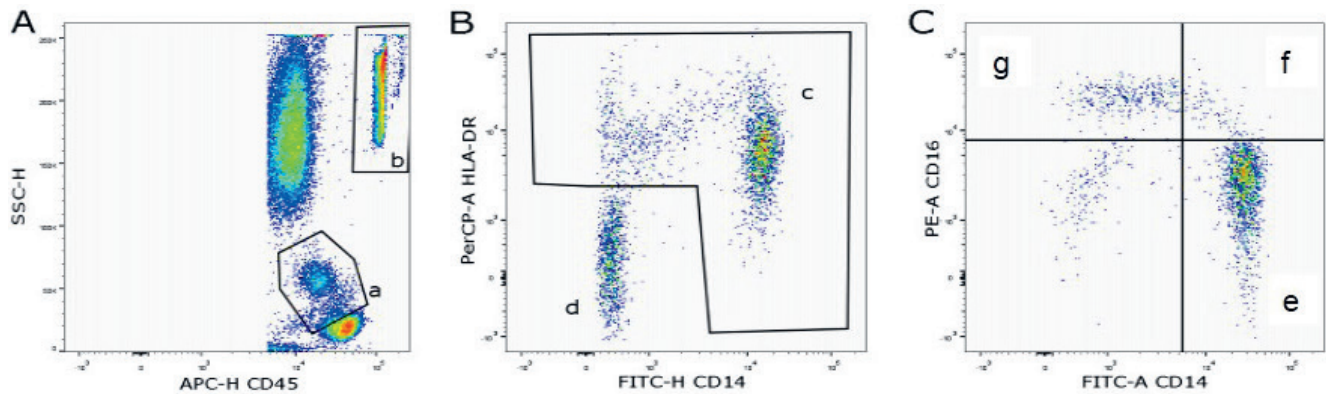
Fig. 1. Gating strategy of monocytes subsets analysis by flow cytometry. Monocytes were gated as (A) CD45-positive cells vs side scatter (SSC) plot: ("a") monocytes, ("b") counting beads for determination of the absolute cell count. (B) CD14-positive cells from gate "a" were then gated ("c") to exclude CD14-HLA-DR-negative NK cells ("d") and finally analyzed for CD14 and CD16 expression (C) as: classical monocytes (CD14++CD16−, "e"), intermediate monocytes (CD14++CD16+, "f") and non-classical monocytes (CD14+CD16++, "g")

Statistical analysis

Assuming a standard deviation (SD) for non-classical monocytes of 25/µL, the study would require a sample size of 44 for each group to demonstrate 2-sided equality and to achieve a power of 0.8 and a level of significance of 0.05, for detecting a difference in means of this monocyte subset between the VTE and the control group of 15/µL.[32]

Categorical variables are presented as numbers and percentages. Continuous variables are expressed as mean ± SD or median and interquartile range (IQR). Normality was assessed by the Shapiro-Wilk test. Equality of variances was assessed using Levene's test. Differences between groups were compared using the Student's or the Welch's t-test depending on the equality of variances for normally distributed variables. The Mann-Whitney U test was used for non-normally distributed continuous variables. Categorical variables were compared by Fisher's exact test. The Pearson's correlation coefficient was computed to measure the linear association between 2 variables. The Spearman's rank correlation coefficient was calculated to measure the monotonic trend between 2 variables. Multivariate logistic regression models were used to adjust the results to age and BMI. Two-sided p-values < 0.05 were considered statistically significant. All calculations were done with JMP v. 9.0.0 (SAS Institute Inc., Cary, USA).

Results

Study participants

The characteristics of VTE patients and healthy controls are presented in Table 1.

Venous thromboembolism patients were slightly older and more overweight. The age range for the control group was 20–58 years and 18–64 years for the VTE patients. Twenty-three (32.8%) of VTE subjects had isolated DVT

and 24 (34.3%) subjects had symptomatic PE with concomitant DVT. Proximal DVT occurred in 56 (80.0%) subjects. More than 80% of VTE patients were treated with oral anticoagulants (Table 1). One patient with VTE (1.4%) had a history of previous MI and another one (1.4%) experienced ischemic stroke in the past.

Most laboratory investigations were similar in both groups. Fibrinogen was higher in VTE patients, while CRP concentrations were similar (Table 1). However, the proportion of VTE patients with CRP >3 mg/L was 2-fold larger compared to that found in healthy volunteers (Table 1). The difference remained significant after adjustment for age and BMI. In VTE patients, glucose was slightly higher; while creatinine and albumin concentrations were lower (Table 1). Only the relative frequency, but not the absolute count of monocytes and lymphocytes, was lower in VTE patients, which seems to be due to the increase in neutrophils without changes in the absolute blood level of monocytes and lymphocytes (Table 1).

Positive ANA was detected more commonly among VTE patients compared to the controls (Table 1).

Monocyte characteristics

Patients with VTE had higher intermediate CD14++CD16+ and non-classical CD14+CD16++ monocyte counts compared to the control group (Table 1). These differences remained significant after adjustment for age and BMI. There were no intergroup differences in classical monocyte CD14++CD16− counts (Table 1).

The absolute number of all 3 monocyte subsets in VTE patients was not associated with comorbidities, type of VTE or the medications used. Among the VTE patients, the non-classical CD14+CD16++ monocytes were positively associated with age (r = 0.33; p = 0.008), weight (r = 0.33; p = 0.005) and BMI (r = 0.31; p = 0.009), while in the control group the only significant association was found for this monocyte subpopulation and age

Table 1. Characteristics of the study participants

Parameters	Control (n = 46)	VTE (n = 70)	p-value
Age [years]	36.98 ±10.09	41.61 ±11.55	0.03
Male sex, n [%]	22 (47.83)	23 (32.86)	0.12
Body mass index [kg/m²]	24.19 ±3.78	26.82 ±5.25	0.004
Obesity, n [%]	3 (6.52)	15 (21.43)	0.04
Clinical characteristics, n [%]			
Current smoking	6 (13.04)	14 (20.00)	0.25
Arterial hypertension	0	17 (24)	–
Diabetes mellitus	0	5 (7.14)	–
Hypercholesterolemia	20 (43)	36 (51.42)	0.31
Unprovoked VTE	0	38 (54.28)	–
DVT alone	0	23 (32.85)	–
PE + DVT	0	24 (34.28)	–
Proximal DVT	0	56 (80.00)	–
Family history of VTE	0	25 (35.71)	–
Time from the last VTE event [months]	n.a.	12.0 (8.5–21.5)	–
Laboratory parameters			
Glucose [mmol/L]	4.98 ±0.55	5.38 ±0.66	0.002
Creatinine [μmol/L]	77.17 ±13.01	71.27 ±14.16	0.01
Total cholesterol [mmol/L]	4.88 ±0.86	5.13 ±0.95	0.11
HDL cholesterol [mmol/L]	1.64 ±0.32	1.60 ±0.41	0.31
LDL cholesterol [mmol/L]	3.08 ±0.83	3.31 ±0.89	0.10
Triglycerides [mmol/L]	1.13 ±0.68	1.24 ±0.79	0.62
Total protein [g/L]	74.84 ±4.41	74.49 ±4.34	0.83
Albumin [g/L]	40.80 ±2.63	39.40 ±2.80	0.007
Albumin/globulin ratio	1.21 ±0.16	1.14 ±0.17	0.01
ANA, n [%]	9 (19.57)	24 (42.11)	0.004
Blood cell variables			
Red blood cells [10⁶/μL]	4.83 ±0.46	4.76 ±0.38	0.36
Hemoglobin [g/dL]	13.70 ±1.43	13.81 ±1.33	0.66
Hematocrit [%]	40.76 ±3.59	41.21 ±3.30	0.48
Platelets [10³/μL]	237 ±54	255 ±59	0.16
Leukocytes [10³/μL]	5.81 ±1.29	6.53 ±1.91	0.045
Neutrophils [10³/μL]	3.20 ±0.94	4.05 ±1.65	0.004
Lymphocytes [10³/μL]	1.94 ±0.49	1.79 ±0.54	0.08
Monocytes [10³/μL]	0.55 ±0.26	0.60 ±0.77	0.41
Eosinophils [10³/μL]	0.15 ±0.09	0.14 ±0.09	0.62
Basophils [10³/μL]	0.03 ±0.02	0.03 ±0.01	0.40
Neutrophils [%]	54.34 ±7.12	60.80 ±9.49	<0.001
Lymphocytes [%]	33.68 ±6.35	28.63 ±8.50	<0.001
Monocytes [%]	8.82 ±1.54	7.78 ±1.96	<0.001
Eosinophils [%]	2.53 ±1.56	2.22 ±1.34	0.36
Basophils [%]	0.43 ±0.28	0.43 ±0.24	0.70
Inflammatory markers			
Fibrinogen [g/L]	2.66 ±0.57	3.24 ±0.90	<0.001
hsCRP [mg/L]	1.11 (0.70–1.98)	1.23 (0.69–2.59)	0.27
hsCRP >3 mg/L, n [%]	5 (10.87)	17 (24.29)	0.02

Table 1. Characteristics of the study participants (cont.)

Parameters	Control (n = 46)	VTE (n = 70)	p-value
Monocyte subsets [10³/μL]			
Classical	370.48 ±113.04	363.90 ±143.71	0.43
Intermediate	10.43 ±4.01	16.79 ±9.29	<0.001
Non-classical	44.09 ±19.21	64.09 ±25.21	<0.001
Non-classical/classical monocytes ratio	0.14 (0.11–0.18)	0.18 (0.13–0.23)	0.003
Treatment			
Vitamin K antagonists	n.a.	30 (42.86)	–
Rivaroxaban	n.a.	24 (34.28)	–
No anticoagulation	n.a.	10 (14.29)	–

Data is shown as mean ± standard deviation (SD) or a median (interquartile range (IQR)) or number (percentage). VTE – venous thromboembolism; DVT – deep vein thrombosis; PE – pulmonary embolism; HDL – high-density lipoprotein; LDL – low-density lipoprotein; ANA – anti-nuclear antibodies, hsCRP – high sensitivity C-reactive protein; n.a. – not applicable.

(r = 0.39; p = 0.01). Additionally, the non-classical CD14⁺CD16⁺⁺ monocyte counts showed positive correlations with glucose (r = 0.26; p = 0.03) and albumin to globulin ratio (r = 0.26; p = 0.03).

Classical CD14⁺⁺CD16⁻ and intermediate CD14⁺⁺CD16⁺ monocyte counts were positively associated with leukocyte counts (r = 0.67 and r = 0.51, respectively, p < 0.0001 for both). Classical CD14⁺⁺CD16⁻ and non-classical CD14⁺CD16⁺⁺ monocyte counts showed positive correlations with hsCRP (r = 0.25 and r = 0.27, respectively, p = 0.03 for both). However, after removing of 3 outliners, only the trend towards correlation between non-classical monocytes and CRP was found (r = 0.2; p = 0.08).

Only intermediate CD14⁺⁺CD16⁺ monocyte counts were positively associated with FVIII activity (r = 0.5; p = 0.03). There was no correlation of these counts with D-dimer and ANA antibody. Interestingly, the patients who had a VTE incident within 12 months prior to enrollment (9 (6–10) months) were characterized by an increased number of non-classical CD14⁺CD16⁺⁺ monocytes as compared to those who experienced a VTE event at an earlier, more distant time point (21 (15–29) months) (71.5 ±27.4 vs 56.03 ±20.6 cells/μL, p = 0.01; Fig. 2).

As shown in Fig. 3, non-classical CD14⁺CD16⁺⁺ monocyte counts tended to be higher in patients following unprovoked VTE as compared to individuals with provoked VTE (70.2 ±4.1 vs 58.8 ±4.3 cells/μL; p = 0.06).

Discussion

This study shows that a history of VTE, regardless of the type of thrombotic event and anticoagulant treatment, is associated with increased counts of non-classical CD14⁺CD16⁺⁺ and intermediate CD14⁺⁺CD16⁺ monocytes.
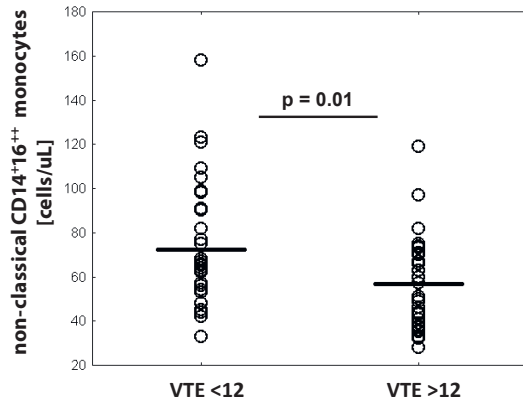
Fig. 2. The absolute number of non-classical CD14+CD16++ monocytes in venous thromboembolic patients (VTE) who experienced a last VTE event <12 and >12 months

This effect was not associated with unprovoked or provoked VTE.
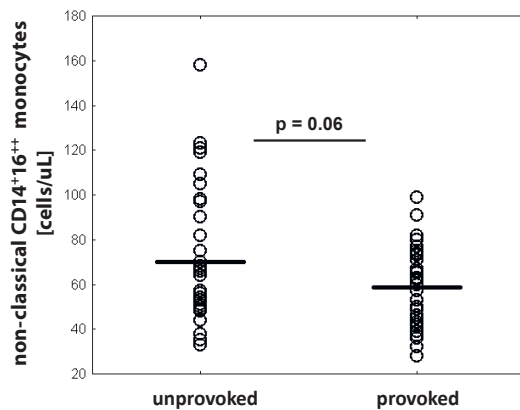
Fig. 3. Non-classical CD14+CD16++ monocyte counts in patients with unprovoked and provoked venous thromboembolism (VTE)

This phenomenon is more pronounced in our patients aged 65 years or less assessed in the first 12 months from the VTE event, and it is in partly driven by inflammation, reflected by positive correlations with elevated hsCRP.

The pattern of monocytes counts in peripheral venous blood observed following VTE is similar to that found in patients with atherosclerotic vascular disease.[25,26] It may be speculated that the non-classical and intermediate monocytes are involved in the similar processes in patients with VTE and those with atherosclerosis. The recent data has suggested that VTE and atherothrombosis share similar pathophysiological pathways like low-grade systemic inflammation and hypercoagulability state.[33] The mechanisms typical of atherosclerosis like platelet activation and neutrophil recruitment with the formation of neutrophil extracellular traps are also involved in the pathogenesis of DVT.[34] The same coagulation proteins which play a crucial role in the pathophysiology of VTE are also expressed in the atherosclerotic arterial walls enhancing the inflammatory and immune processes characteristic of atherosclerosis.[33] Additionally, the clinical association of VTE and atherothrombosis has been shown for the first time by Prandoni et al., who demonstrated that patients with idiopathic VTE were more likely to have carotid artery plaque (47%) than patients with provoked VTE (27%) or age- and sex-matched controls (32%).[35] Further studies have reported an increased risk of acute MI and stroke among patients with a prior history of VTE than among those without such a history.[36,37] Also, symptomatic cardiovascular events may precede the incident of VTE.[33] Our findings suggest that monocytes might contribute to the links between atherosclerosis and VTE.

Molecular mechanisms underlying the current findings study are likely complex. Increased numbers of non-classical monocytes, which are primary producers of TNF-α and IL-1β, may regulate the immune response by enhancing cells proliferation, migration and receptor expression in VTE patients. Accordingly, it has been shown that the gene expression profile exhibited by non-classical monocytes showed the highest expression of *TNF-α* and the metalloprotease *ADAM17* gene, which are involved in the processing of TNF-α from the cell surface.[38] Moreover, an in vitro study demonstrated that only non-classical CD14+CD16++ monocytes are able to produce high levels of IL-6, CCL2 chemokine and matrix metalloproteinase-9.[39] Thus, their increased number and accumulation onto endothelium may result in the recruitment of monocytes and T cell subsets at sites of inflammation in response to CCL2 and IL-6-induced cell activation and/or differentiation, and MMP-9-mediated vascular and tissue injury.[39]

It should be also underlined that TNF-α may exert procoagulant activity and its expression by non-classical monocytes may lead to enhanced thrombin formation. It has been shown that TNF-α may downregulate thrombomodulin, a cofactor in protein C activation.[40] Moreover, a study performed in healthy volunteers showed that TNF-α is able to induce a rapid inhibition of fibrinolysis mediated by a delayed increase in plasminogen activator inhibitor-1.[41] It may be speculated that in VTE patients non-classical monocytes may play a role in immunothrombosis. In the mouse model of flow restriction-induced DVT, it has been shown that the rapid accumulation of neutrophils and monocytes is observed within a forming thrombus and innate immune cells initiate local fibrin formation predominantly through the delivery of TF.[17] Further studies are needed to elucidate monocyte-derived mediators involved in VTE and the consequences of elevated non-classical monocytes.

In the current study we also found the associations between non-classical monocytes and age. It has been shown earlier that aging is associated with significant changes in monocyte subsets, which may have implications for the development of age-related diseases.

In a cross-sectional study involving 91 healthy individuals, age was associated with an increased proportion of intermediate and non-classical monocytes.[42] Most recently, it has been shown by Puchta et al. that intermediate human and mice monocytes produced more of the inflammatory cytokines IL-6 and TNF-α with age, both in the steady state and when stimulated with bacterial products.[43]

Moreover, we found that non-classical monocytes correlated positively with BMI and glucose, which is in line with the previous findings.[44,45] It has been shown that the proportion of intermediate and non-classical monocyte positively correlated with BMI and fasting glycemia in obese and type 2 diabetic patients.[44] Moreover, it has been shown that CD16 positive monocyte subsets were reduced by drastic fat mass loss. This feature suggests that increased glycemia could be a parameter regulating intermediate and non-classical monocytes numbers.[44] Furthermore, the I LIKE HOMe study reveals a significant association between counts of non-classical monocytes but not of total monocytes or classical monocytes, and both obesity as well as subclinical atherosclerosis in a large cohort in low-risk individuals.[45]

Of note, we observed that the elevated number of non-classical monocytes is decreased after 12 months of the VTE event, when the inflammatory process is resolved. This suggests the involvement of this subset in the acute thrombosis and the subsequent thrombus resolution.

We also showed a positive correlation of non-classical monocytes with elevated hsCRP level.

Data on the relationship between monocyte subsets and inflammatory markers yielded inconsistent findings. In patients with unstable angina, CD16-positive monocytes were associated with hsCRP levels, but no such association was found in stable angina.[22,23] Similar to our observations, an association of CRP levels and non-classical monocyte counts has been found in patients with rheumatoid arthritis and type 1 diabetes mellitus.[46,47] It should also be noted that specific single nucleotide polymorphisms in the *CRP* gene and other inflammatory and coagulation biomarkers are strongly associated with their plasma concentrations and may regulate the inflammatory processes.[48]

The present findings increase our knowledge on the role of immune responses in the pathophysiology of VTE by providing a new, monocyte-associated aspect of immunothrombosis, which suggests the involvement of non-classical and intermediate monocytes in the early phase following an acute VTE episode.

Several study limitations should be acknowledged. The number of patients with VTE and healthy controls was limited; however, the study was sufficiently powered. Nevertheless, the subgroup analysis should be interpreted with caution. A well-matched control group is recommended to be used for future study on this topic. Furthermore, we determined each variable at a single time point. Our findings cannot be easily extrapolated to the elderly or patients with severe comorbidities, in particular cancer, who

were excluded from our study. Associations reported here do not necessarily mean the cause-effect relationship and should be regarded as the hypothesis-generating investigation, which can, however, have important implications. Moreover, observation at different time intervals after VTE event would introduce additional information on the presence and proportion of each subpopulation of monocytes. Finally, a long-term follow-up study is needed to assess a potential prognostic role of the current findings and investigate whether and when the intermediate and non-classical monocyte subset populations can normalize.

To our knowledge, this is the first study which shows increased counts of non-classical and intermediate monocyte subsets in patients following VTE, suggesting a new role of the immune system in this disease. Monocyte-related immunothrombotic mechanisms of VTE, that are more pronounced within the first months since the event, in particular that of unprovoked nature, provide new insights into the pathophysiology of this common disease.

References

1. Heit JA, Spencer FA, White RH. The epidemiology of venous thromboembolism. *J Thromb Thrombolysis*. 2016;41(1):3–14.
2. Zhu T, Martinez I, Emmerich J. Venous thromboembolism risk factors for recurrence. *Arterioscler Thromb Vasc Biol*. 2009;29(3):298–310.
3. Cushman M. Epidemiology and risk factors for venous thrombosis. *Semin Hematol*. 2007;44(2):62–69.
4. Goldhaber SZ, Bounameaux H. Pulmonary embolism and deep veins thrombosis. *Lancet*. 2012;379(9828):1835–1846.
5. Folsom AR, Lutsey PL, Astor BC, Cushman M. C-reactive protein and venous thromboembolism. A prospective investigation in the ARIC cohort. *Thromb Haemost*. 2009;102(4):615–619.
6. Zacho J, Tybjaerg-Hansen A, Nordestgaard BG. C-reactive protein and risk of venous thromboembolism in the general population. *Arterioscler Thromb Vasc Biol*. 2010;30(8):1672–1678.
7. Roumen-Klappe EM, den Heijer M, van Uum SH, van der Ven-Jongekrijg J, van der Graaf F, Wollersheim H. Inflammatory response in the acute phase of deep vein thrombosis. *J Vasc Surg*. 2002;35(4):701–716.
8. Pesavento R, Villalta S, Prandoni P. The post-thrombotic syndrome. *Intern Emerg Med*. 2010;5(3):185–192.
9. Rabinovich A, Kahn SR. How to predict and diagnose postthrombotic syndrome. *Pol Arch Med Wewn*. 2014;124(7–8):410–416.
10. Bucek RA, Reiter M, Quehenberger P, Minar E. C-reactive protein in the diagnosis of deep vein thrombosis. *Br J Haematol*. 2002;119(2):385–389.
11. Smeeth L, Cook C, Thomas S, Hall AJ, Hubbard R, Vallance P. Risk of deep vein thrombosis and pulmonary embolism after acute infection in a community setting. *Lancet*. 2006;367(9516):1075–1079.
12. Rabinovich A, Cohen JM, Cushman M. BioSOX Investigators. Association between inflammation biomarkers, anatomic extent of deep venous thrombosis, and venous symptoms after deep venous thrombosis. *J Vasc Surg Venous Lymphat Disord*. 2015;3(4):347–353.
13. Engelmann B, Massberg S. Thrombosis as an intravascular effector of innate immunity. *Nat Rev Immunol*. 2013;13(1):34–45.
14. von Bruhl ML, Stark K, Steinhart A, et al. Monocytes, neutrophils, and platelets cooperate to initiate and propagate venous thrombosis in mice in vivo. *J Exp Med*. 2012;209(4):819–835.
15. Pfeiler S, Massberg S, Engelmann B. Biological basis and pathological relevance of microvascular thrombosis. *Thromb Res*. 2014;133(Suppl 1):S35–37.
16. van der Poll T, Herwald H. The coagulation system and its function in early immune defense. *Thromb Haemost*. 2014;112(4):640–648.
17. Passlick B, Flieger D, Ziegler-Heitbrock HW. Identification and characterization of a novel monocyte subpopulation in human peripheral blood. *Blood*. 1989;74(7):2527–2534.

18. Ziegler-Heitbrock L, Ancuta P, Crowe S , et al. Nomenclature of mono-cytes and dendritic cells in blood. *Blood.* 2010;116(16):74–80.

19. Ziegler-Heitbrock L. Blood monocytes and their subsets: Established features and open questions. *Front Immunol.* 2015;6:423.

20. Belge KU, Dayyani F, Horelt A, et al. The proinflammatory CD14+CD16+DR++ monocytes are a major source of TNF. *J Immunol.* 2002; 168(7):3536–3542.

21. Mukherjee R, Kanti Barman P, Kumar Thatoi P, Tripathy R, Kumar Das B, Ravindran B. Non-classical monocytes display inflammatory features: Validation in sepsis and systemic lupus erythematous. *Sci Rep.* 2015;5:13886.

22. Schlitt A, Heine GH, Blankenberg S, et al. CD14+CD16+ monocytes in coronary artery disease and their relationship to serum TNF-alpha levels. *Thromb Haemost.* 2004;92(2):419–424.

23. Imanishi T, Ikejima H, Tsujioka H, et al. Association of monocyte sub-set counts with coronary fibrous cap thickness in patients with unsta-ble angina pectoris. *Atherosclerosis.* 2010;212(2):628–635.

24. Rogacev KS, Cremers B, Zawada AM , et al. CD14++CD16+ monocytes independently predict cardiovascular events: A cohort study of 951 patients referred for elective coronary angiography. *J Am Coll Cardiol.* 2012;60(16):1512–1520.

25. Tapp LD, Shantsila E, Wrigley BJ, Pamukcu B, Lip GY. The CD14++CD16+ monocyte subset and monocyte-platelet interactions in patients with ST-elevation myocardial infarction. *J Thromb Haemost.* 2012; 10(7):1231–1241.

26. Zeng S, Zhou X, Ge L, et al. Monocyte subsets and monocyte-platelet aggregates in patients with unstable angina. *J Thromb Thrombolysis.* 2014;38(4):439–446.

27. Rothe G, Gabriel H, Kovacs E, et al. Peripheral blood mononuclear phagocyte subpopulations as cellular markers in hypercholesterol-emia. *Arterioscler Thromb Vasc Biol.* 1996;16(12):1437–1447.

28. Kaito M, Araya S, Gondo Y, et al. Relevance of distinct monocyte sub-sets to clinical course of ischemic stroke patients. *PLoS One.* 2013;8(8): e69409.

29. Maldonado-Peña J, Rivera K, Ortega C, Betancourt M, Lugo JE, Camar-go E. Can monocytosis act as an independent variable for predicting deep vein thrombosis? *Int J Cardiol.* 2016;219:282–284.

30. Go SI, Kim RB, Song HN, et al. Prognostic significance of the absolute monocyte counts in lung cancer patients with venous thromboem-bolism. *Tumour Biol.* 2015;36(10):7631–7639.

31. Siedlar M, Strach M, Bukowska-Strakova K, et al. Preparations of intra-venous immunoglobulins diminish the number and proinflammato-ry response of CD14+CD16++ monocytes in common variable immu-nodeficiency (CVID) patients. *Clin Immunol.* 2011;139(2):122–132.

32. Chow S, Shao J, Wang H. *Sample Size Calculations in Clinical Research*. 2nd ed. New York-Basel: Marcel Dekker Inc.; 2008.

33. Riva N, Donadini MP, Ageno W. Epidemiology and pathophysiology of venous thromboembolism: Similarities with atherothrombosis and the role of inflammation. *Thromb Haemost.* 2015;113(6):1176–1183.

34. Fuchs TA, Brill A, Wagner DD. Neutrophil extracellular trap (NET) impact on deep vein thrombosis. *Arterioscler Thromb Vasc Biol.* 2012; 32(8):1777–1783.

35. Prandoni P, Bilora F, Marchiori A, et al. An association between ath-erosclerosis and venous thrombosis. *N Engl J Med.* 2003;348(15):1435–1441.

36. Prandoni P, Ghirarduzzi A, Prins MH, et al. Venous thromboembolism and the risk of subsequent symptomatic atherosclerosis. *J Thromb Haemost.* 2006;4(9):1891–1896.

37. Sørensen HT, Horvath-Puho E, Pedersen L, et al. Venous thrombo-embolism and subsequent hospitalization due to acute arterial car-diovascular events: A 20 year cohort study. *Lancet.* 2007;370(9601): 1773–1779.

38. Gren ST, Rasmussen TB, Janciauskiene S, Håkansson K, Gerwien J, Grip O. A single-cell gene-expression profile reveals inter-cellular heterogeneity within human monocyte subsets. *PLoS One.* 2015; 10(12):e0144351.

39. Ancuta P, Wang J, Gabuzda D. CD16+ monocytes produce IL-6, CCL2, and matrix metalloproteinase-9 upon interaction with CX3CL1-expressing endothelial cells. *J Leukoc Biol.* 2006;80(5):1156–1164.

40. Nawroth PP, Stern DM. Modulation of endothelial cell hemostatic properties by tumor necrosis factor. *J Exp Med.* 1986;163(3):740–745.

41. van der Poll T, Levi M, Büller HR, et al. Fibrinolytic response to tumor necrosis factor in healthy subjects. *J Exp Med.* 1991;174(3):729–732.

42. Hearps AC, Martin GE, Angelovich TA, et al. Aging is associated with chronic innate immune activation and dysregulation of monocyte phenotype and function. *Aging Cell.* 2012;11(5):867–875.

43. Puchta A, Naidoo A, Verschoor CP, et al. TNF drives monocyte dys-function with age and results in impaired anti-pneumococcal immu-nity. *PLoS Pathog.* 2016;12(1):e1005368.

44. Poitou C, Dalmas E, Renovato M, et al. CD14dimCD16+ and CD14+CD16+ monocytes in obesity and during weight loss: Rela-tionships with fat mass and subclinical atherosclerosis. *Arterioscler Thromb Vasc Biol.* 2011;31(10):2322–2330.

45. Rogacev KS, Ulrich C, Blomer L, et al. Monocyte heterogeneity in obe-sity and subclinical atherosclerosis. *Eur Heart J.* 2010;31(3):369–376.

46. Kawanaka N, Yamamura M, Aita T, et al. CD14+, CD16+ blood mono-cytes and joint inflammation in rheumatoid arthritis. *Arthritis Rheum.* 2002;46(10):2578–2586.

47. Myśliwska J, Smardzewski M, Marek-Trzonkowska N, Myśliwiec M, Raczyńska K. Expansion of CD14+CD16+ monocytes producing TNF-α in complication-free diabetes type 1 juvenile onset patients. *Cyto-kine.* 2012;60(1):309–317.

48. Montagnana M, Danese E, Lippi G. Genetic risk factors of athero-thrombosis. *Pol Arch Med Wewn.* 2014;124(9):474–482.

Expression of caspase 1 and histomorphology of lung after cladribine treatment

Marta Lis-Sochocka[B–D], Patrycja Chylińska-Wrzos[B–D], Ewelina Wawryk-Gawda[B–D], Barbara Jodłowska-Jędrych[A,E,F]

Department of Histology and Embryology with Experimental Cytology Unit, Medical University of Lublin, Poland

A – research concept and design; B – collection and/or assembly of data; C – data analysis and interpretation;
D – writing the article; E – critical revision of the article; F – final approval of the article

Abstract

Background. Cladribine is a useful immunosuppressive drug for the treatment of autoimmune diseases, leukemias and multiple sclerosis (MS). Despite the drug having low toxicity, side effects have been reported connected with myelosuppression, neutropenia and severe anemia.

Objectives. The objective of this study was to investigate the influence of cladribine on lung pathomorphology and the expression of caspase 1 using immunohistochemistry method.

Material and methods. The study was conducted on Wistar rats, which were divided into a control group (C) and an experimental group (E). In group C, the rats were given a 0.9% NaCl solution by a subcutaneous injection, at the same dose as the dose of drug used in the experiment. In group E, the animals received cladribine at a dose of 0.07 mg/kg/24 h by a subcutaneous injection. The animals were decapitated 24 h following the last dose. To detect collagen deposition, we utilized Masson's trichrome staining. To evaluate the intensity of the inflammatory process in the lung, an immunohistochemistry reaction was carried out with the use of caspase 1.

Results. In group E, we observed an increase in the thickness of space between the alveoli. A statistically significant ($p < 0.017243$) difference between the thicknesses of the interalveolar septum was seen between the research groups. In E group, we observed regions with collagen deposition, alveolar epithelial cell hyperplasia, hyperemia and inflammatory cell infiltration. Caspase 1 activity was higher in group E. The immunohistochemical reaction with caspase 1 was positive in 49% of all the interalveolar cells in group E; however, in group C about 13% of the interalveolar cell showed positive immunohistochemistry (IHC) response.

Conclusions. Cladribine-based therapy might have negative influence on lung morphology. The interstitial changes in the lung tissue suggest that cladribine is a drug that may be the cause of drug-induced lung disease and may lead to several respiratory disorders.

Key words: inflammation, lung, caspase 1, cladribine

Introduction

Lungs are composed of very sensitive tissue. Their large surface has contact with many substances from the environment and with substances that are used incorporeally. Indeed, the list of drugs which can be the cause of lung toxicity is long. Furthermore, the clinical, radiological and histological symptoms are nonspecific; therefore, the diagnostic and recognition of drug-induced lung disease is difficult.[1]

Cladribine (2-CdA), a purine analog which acts as antineoplastic and immunosuppressive agent, has been used in the treatment of malignances, autoimmune and degenerative diseases. The drug, 2-CdA, is a deoxyadenosine analog which is used in experimental multiple sclerosis (MS) treatment as it exhibits selective toxicity relative to lymphocytes and monocytes.[2] According to the study undertaken by Leist and Weissert, the administration of the oral form of 2-CdA abates the number of lymphocytes for up to 6–12 months after the end of treatment.[3] What is more, although 2-CdA mainly negatively affects the number of CD4^{+}/CD8^{+} lymphocytes, it has been seen particularly as being effective in minimizing the CD4^{+} class.[3–5] Cladribine is considered to be of relatively low toxicity in therapeutic doses, and any side effects have been seen only in the first 14 days of therapy or in the first month of treatment. In individual studies, the drug is generally well-tolerated by MS patients. Reported side-effects are connected with myelosuppression, neutropenia and severe anemia, and with the complications that come about as a result of opportunistic infections. Infections of upper respiratory tract, infections of urinary tract, herpes zoster and HBV virus infections are among the most commonly reported side effects. In addition, patients have complained about general disorders such as fever, lack of appetite, tiredness, chills and general weakness. These clinical symptoms can be brought about by mucosa damage.[2,4,6]

Cladribine could also destroy healthy, functional cells, especially those which are rapidly dividing (the mucosa cells of the digestive system, the bone-marrow cells or the skin cells).[7] Previous studies have shown that cladribine could initiate apoptosis in the epithelial cells covering the ovary, the uterine epithelial cells, the fallopian tube epithelium and in the epidermal cells.[8–12] Literature reports suggest that patients may be susceptible to opportunistic infections during cladribine treatment due to the reduced number of immune system cells.

Multiple sclerosis is classified as an autoimmune disease,and autoreactive T cells, mainly of the CD4^{+} type, are involved in the development of it.[13–15] Herein, activated T cells penetrate the blood–brain barrier and permeate to the central nervous system. Here, they stimulate other immune cells such as the macrophages. As a result of these multidirectional immune responses, foci of demyelination in white matter and the degeneration of axons will be seen.[16,17] Moreover, the resulting errors that come about in the apoptosis and which interfere with the destruction of cytotoxic T cells also play an important role in MS pathogenesis.[16] Immunomodulatory and immunosuppressive therapies have been commonly applied in MS treatment.[18] In these therapeutic methods, certain oral anti proliferative drugs are prescribed, while other medicaments are being researched.[19–22]

Considering the results of our previous studies, and because there is no data on the impact of 2-CdA on the histology of the lung, the aim of the authors' study is to ascertain the effect of 2-CdA on the lung pathomorphology. In our study, we used cladribine at a dosage that is normal for treating MS in people. Our intent is ascertain whether 2-CdA at this dose may be the cause of interstitial lung disease. In addition, by way of employing the immunohistochemistry method, we intend to study caspase 1 expression (a marker of inflammation).

Material and methods

The study was conducted on 10 female white Wistar rats (weighing about 250–300 g each), which were placed within one control group (C) and one experimental group (E), 5 animals in each. The animals were kept according to ethical standards set out by the National Institute of Health Guidelines for the Care and Use of Laboratory Animals and the European Community Council Directive of 24 November 1986, for Care and Use of Laboratory Animals (86/609/EEC), and accepted by the local ethics committee (Medical University of Lublin, Poland). Furthermore, consent no 126/2001 was obtained from the local bioethical committee.

In group E, the animals received cladribine (Biodribin; Institute of Biotechnology and Antibiotics, Warszawa, Poland) at a dose of 0.07 mg/kg/day by way of a subcutaneous injection for 6 successive days (in the morning), in 3 courses, with 5 weeks break between each (such scheme of dosage is normal for treating MS in people).[23,24] In group C, the rats were given a 0.9% NaCl solution by way of a subcutaneous injection at the same dose as the dose of drug used in the experiment.

The animals of both groups were decapitated 24 h following the last injection.

During the experiment, the rats resided in cages (Techniplast®; Techniplast Kukuczka, Ustroń, Poland) of 0.5 m[2] area. They were fed granulated fodder (LSM; AnimaLab, Poznań, Poland) and had free access to normal water. The air humidity was 50–60%, the temperature of their environment was 20 ±1°C, and a 24 h cycle was kept (12 h day, 12 h night). All stress factors were reduced to a minimum. In the time period of the experiment, we saw no symptoms of infection.

At the end of experiment (89 days), the animals were killed by decapitation, and lung samples (about 1 cm[2] area) were taken for histological and immunohistochemical examination.

For a histological investigation, the material was fixed in Baker's solution, after which they were dehydrated in alcohol with increasing concentration, placed in xylene and put in paraffin. The paraffin blocks were cut utilizing a rotational microtome Leica (Leica Biosystems, Nussloch, Germany) RM 2135, in 5 μm sections, and the prepared samples were colored with hematoxylin and eosin (H&E). To detect collagen deposition, we utilized Masson's trichrome staining. To evaluate the intensity of the inflammatory process in the lung, an immunohistochemistry reaction was carried out by way of using primary antibodies (Sigma®; Sigma-Aldrich, Poznań, Poland). In this, caspase 1 (ANTI-CASP1, HPA008936-100UL, antibody produced in rabbit, dilution: 1:50) was employed. The IHC study was conducted via the indirect immunoperoxidase method. In this way, 5 μm thickness paraffin fragments were placed on slides (Polysine®; VWR International, Poznań, Poland) and incubated all night at a 58°C temperature. Next, the specimens were dehydrated with increasing concentrations of ethyl alcohol, and then immersed in xylene. Following this, the activity of the endogenous peroxidase was blocked for 5 min by way of immersion in a 3% hydrogen peroxide in methanol solution. Afterwards, the slides were rinsed in distilled water and subsequently in a solution of TBS. Next, the places of active antigen were unmasked by applying a thermal process. Herein, specimens were microwaved (800 V) while in a 0.01 M citrate buffer, pH 6.0, by way of 3 × 5-min cycles. After washing in distilled water, the samples were then incubated with inactive serum (normal diluted serum) for 30 min to mask all places which could connect with caspase 1. Following a rinsing in a TBS solution, the samples were incubated for 24 h at 8°C, with the primary antibodies. To make the reaction visible, NovoLink™ Polymer Detection Systems (Leica Microsystems, Wetzlar, Germany) was used. After this, the samples were re-rinsed in a solution of TBS and mottled by chromogen – 3-3'diaminobenzidine (Novolink DAB; Vector Laboratories Inc., Burlingame, USA), which indicated a positive reaction by turning the brown. Finally, the cell nuclei of the samples were stained through the application of Mayer's hematoxylin. A negative control was put into place for all sections of all the groups by the same method. This was without the primary antibody.

The study's material was evaluated using an Olympus BX41 with digital camera image DP25 (Olympus, Tokyo, Japan). Calculations were made in Cell^D (Olympus, Tokyo, Japan).

In both research groups, 40 measurements of the thickness of the interalveolar septum were made in different view areas.

To assess the intensity of the immunohistochemistry reaction in the alveolar interstitial cells, different areas of ×400 vision were selected, and 300 cell-counts were analyzed. The places of different intensity of immunohistochemistry reaction were reported as: 1 (+) – a weak reaction, 2 (++) average response and 3 (+++) – strong reaction. Areas with a negative response were marked as 0 (–).

The statistical results surveys were analyzed in STATISTICA v. 10.0 (StatSoft Polska, Kraków, Poland).

The statistical differences of intensity of caspase 1 expression between examined groups were assessed with the Kruskal-Wallis nonparametric test. In addition, statistical correlations between the thicknesses of the interalveolar septum, and between the research groups, were calculated utilizing Student's t-test. An overall p-value of less than 0.05 was considered to show a statistically significant result.

Results

Hematoxylin and eosin stain

In the control group (C), specimen tissue showed visible bronchioles of a different diameter which were easily differentiated as respiratory bronchioles, alveolar ducts and alveoli (Fig. 1). The alveoli are lined by 2 types of cells: pneumocytes type I (squamous) and pneumocytes type II
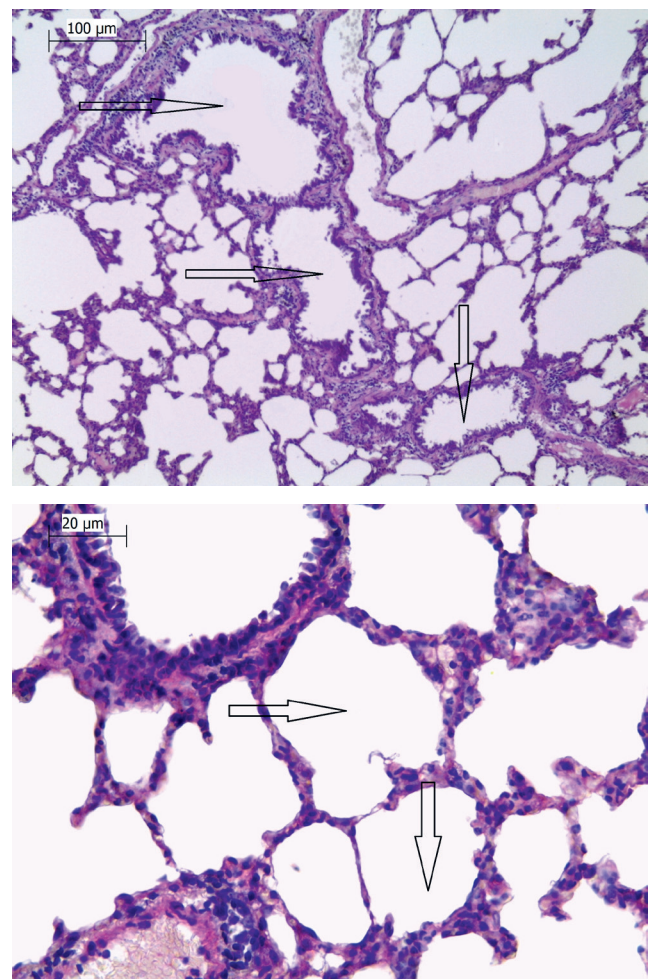
Fig. 1,2. Control group

H&E staining. Bronchioles (arrows) of different diameter giving rise to an alveolar duct and alveoli (arrows) composed of squamous pneumocytes type I and cuboidal pneumocytes type II. Thin layers of connective tissue and capillaries can be seen between them.
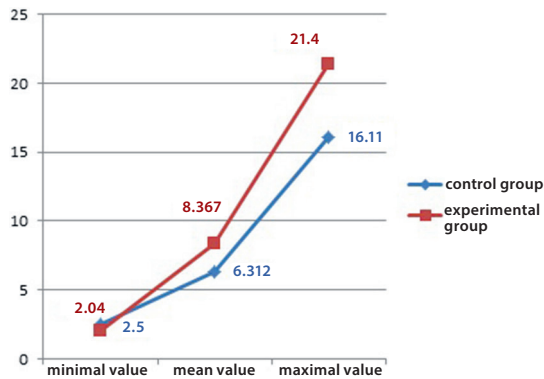
Fig. 3. Statistical values of interalveolar septum thicknesses among alveoli in the research groups.

Our study demonstrated statistically significant differences (p < 0.017243) between the thicknesses of the interalveolar septum in the 2 research groups. The minimal value of thickness of the interalveolar septum in both groups was similar: in the control group – 2.5 μm; in the experimental group – 2.04 μm. However, the maximal value of thickness of the interalveolar septum (21.4 μm) was observed only in the experimental group. All values are given in μm.

(cuboidal). Between the alveoli, were thin bands of connective tissue and blood vessels (Fig. 2). The mean value of the thickness between the alveoli was 6,312 μm, with the maximum and minimum value of 2.50 and 16.11 μm, respectively (Fig. 3). In the experimental group (E), we found evidence of nonspecific interstitial pneumonia (NSIP).[1] A significant increase in the thickness of alveolar spaces was observed, and leukocytes, as well as macrophages and eosinophils, were detected in these spaces (Fig. 4). Inflammatory infiltrates with a predominance of lymphocytes were also recognizable around the blood vessels (Fig. 5). Furthermore, a mild hyperplasia of type II pneumocytes was observed. The mean value of the thickness of the interalveolar septum was 8.367 μm, while the minimum and maximum thicknesses were 2.04 μm and 21.40 μm, respectively. A statistically significant (p < 0.017243) difference between the thicknesses of the interalveolar septum was seen between the research groups.

Masson's trichrome staining

In the experimental group (E), we observed regions with collagen deposition in their lung tissue, especially in the alveolar septa. What is more, alveolar epithelial cell hyperplasia, hyperemia and inflammatory cell infiltration were found (Fig. 6,7).

The immunohistochemical study

Regarding group C, the immunohistochemical reaction with caspase 1 was negative in most interstitial cells (over 87%) (Fig. 8,9). Moreover, only a few interalveolar cells showed a weak (8% of all cells) or a moderate (4% of all cells) IHC response. A strong expression of the caspase 1 protein, assessed as 3 (+++), was only visible in 0.67% of all
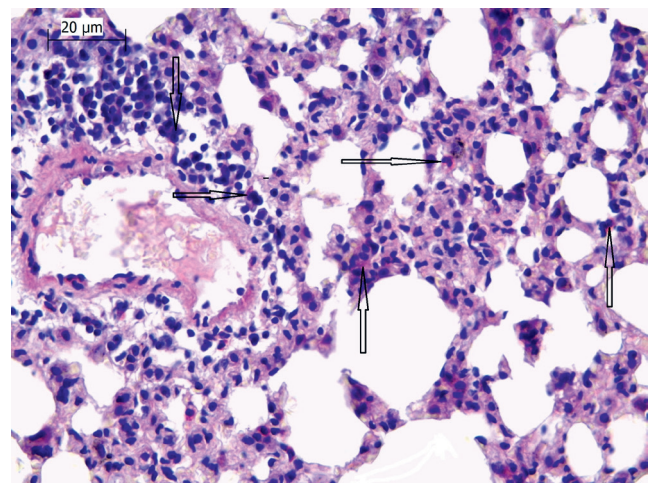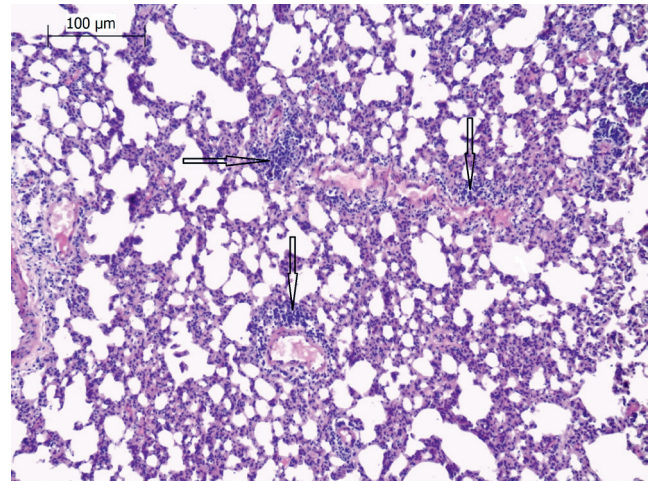
Fig. 4,5. Experimental group

H&E staining. The increased thickness of the space between the alveoli is evident. This is occupied mainly by leukocytes (arrows). Inflammatory infiltrates are visible around the blood vessels (arrows).
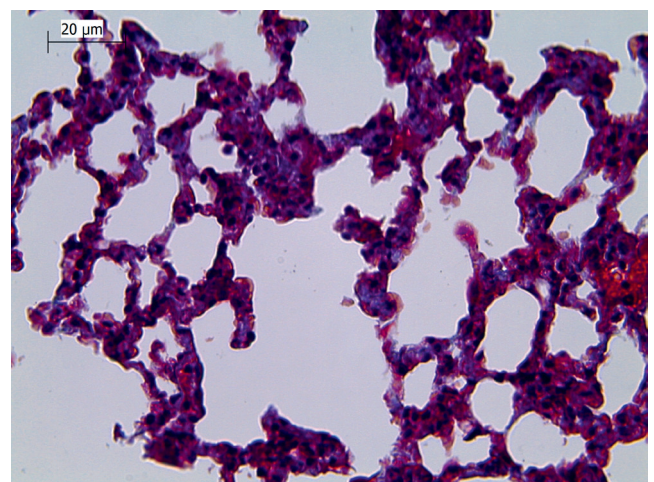
Fig. 6. Control group, normal lung tissue

Masson's trichrome staining (objective ×40).

the observed cells (Fig. 10). However, in group E, a positive, cytoplasmic immunohistochemical reaction was seen in 49% of all the interalveolar cells. Of this, more than 30%
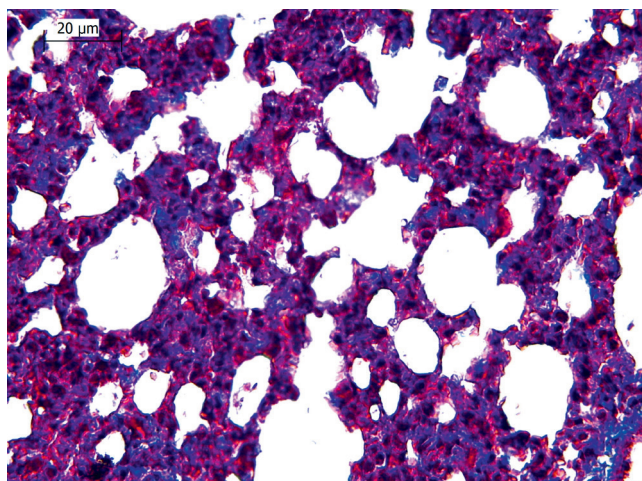
Fig. 7. Experimental group

Masson's trichrome staining. The blue collagen deposition in the lung tissue is especially evident in the alveolar septa. Hyperplasia of type II pneumocytes, hyperemia and inflammatory cell infiltration can be seen (objective ×40).

Fig. 9. The intensity of the caspase 1 expression in the alveolar interstitial cells, in the studied groups

0 (–) – no reaction, 1 (+) – weak reaction, 2 (++) – average reaction, 3 – (+++) strong reaction. Our study revealed a statistically significant difference (p < 0.000001) in the expression of caspase 1 between the control group and the experimental group. In the work, the interstitial cells of the control group exhibited a majority of cells (> 87%) with no immunohistochemical reaction. In the experimental group, more than 30% of all cells expressed a weak reaction, while roughly 16% of all cells showed an average reaction, and 2% of all cells expressed a strong immunohistochemical reaction.

Fig. 8. Control group

The predominance within the interalveolar cells of a negative (short and thick arrows) immunohistochemical reaction and weak (long and thin arrows) immunohistochemical reaction with caspase 1, is evident (objective ×40).
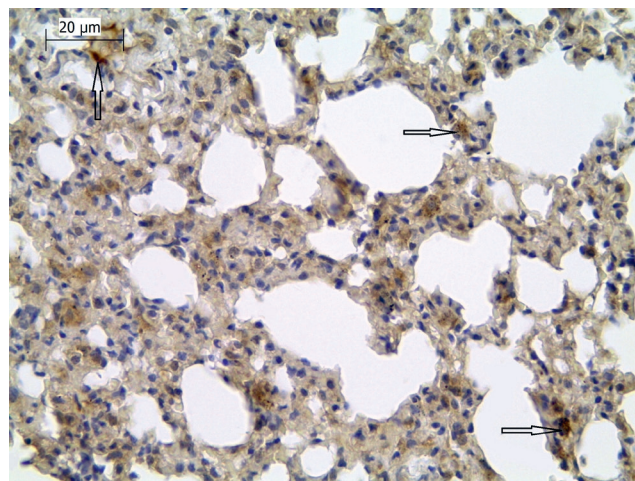
Fig. 10. Experimental group

The interalveolar cells reveal an average and strong (arrows) immunohistochemical reaction to caspase 1 (×40 magnification).

of the cells were assessed 1 (+) as revealing a weak reaction, while more than 16% of all cells showed an average of 2 (++) and 2% of the cells showed a strong 3 (+++) reaction. In the remaining cells (51%), the reaction was negative or at trace amounts (Fig. 9,10). Of note: the difference in the caspase 1 expression between the control and experimental groups was statistically significant (p < 0.000001).

Discussion

Cladribine, as an antineoplastic and immunosuppressive agent, induces apoptosis in the cells and penetrates into the cells through the cellular membrane by way of nucleoside transporters. Within the cell, 2-CdA is converted into an active 2-CdATP metabolite. Its function in the cell leads to a series of enzymatic and structural changes, which affect the stability of damaging factors and repair mechanisms. Cladribine acts on proliferating and non-proliferating cells; its cytotoxic effect is also multidirectional. Although this drug is considered to have low toxicity, it is not completely safe,[3,25,26,27] yet previous reports put forward the claim that cladribine is not associated with lung toxicity.[28] Cladribine, like other purine analogues, is an antimetabolite, which exhibits selective toxicity with respect to lymphocytes and monocytes.[2] In therapeutic doses, 2-CdA is well tolerated by patients, but some side-effects have been noticed. Betticher et al. reported that the main side effects observed in cladribine therapy were myelotoxicity and immunosuppression with regard to opportunistic infections (14%) such as pneumonia.[29] Similarly, Van Den Neste et al. also reported that 42% of patients treated with 2-CdA and cyclophosphamide

developed opportunistic infections, e.g. pneumonia caused by varicella-zoster virus.[30] Furthermore, Montillo et al. observed pneumonia due to *Enterococcus* or cytomegalovirus in patients receiving cladribine at 4 mg/m^2/day and cyclophosphamide at 350 mg/m^2/day.[31] In addition, Okawa et al. reported pneumonia induced by *Cryptococcus* after 2-CdA treatment. In this study, cladribine was administered in 4 courses.[32]

Fridrik et al. evaluated the performance of 2-CdA in the treatment of patients with advanced non-Hodgkin's lymphoma. In this study, patients received cladribine in a dose of 0.12 mg/kg intravenously daily for 5 days. This schema was repeated every 28 days for 4 cycles. During the treatment, certain side effects were observed, mainly hematological toxicity and respiratory system infections.[33] Feenstra et al. also reported pulmonary toxicity (with a diffuse interstitial pneumonitis and with hypoxaemic respiratory failure) after the first course of cladribine therapy of non-Hodgkin's lymphoma.[34] In order to assess the possible changes that could occur in the lungs after the application of 2-CdA, in our work, at first, we carried out routine histological H&E staining. In this, lung histological examination of the control group showed normal pulmonary histology. What is more, the thickness between alveoli varied between 2.50 and 16.11 μm, with the mean value of the thickness being 6,312 μm. In the experimental group, however, an increase in the thickness of alveolar spaces was observed. The mean value of the thickness of interalveolar septum was 8.367 μm, while the minimal thickness was 2.04 μm, and the maximal was 21.40 μm. Of note: a statistically significant ($p < 0.017243$) difference between the thickness of the interalveolar septum was evident between the research groups. Moreover, inflammatory infiltrates with a predominance of lymphocytes were detected around the blood vessels. In addition, a fibrotic broadening of the alveolar septa was seen, and type II pneumocyte hyperplasia was observed. We put forward that the results of H&E staining is indicative of nonspecific interstitial pneumonia. This would be consistent with the findings of other authors who described the existence of pneumonia in patients treated with 2-CdA.

In order to confirm the inflammatory reaction in lung tissue, we conducted immunohistochemistry using caspase 1, which is a major marker of inflammation.

Caspase 1 belongs to the family of cysteine proteases. In the cytosol of a cell, this enzyme is synthesized as the inactive zymogene pro-caspase 1. Caspase 1 is activated as a response to inflammation, and it is believed that it is associated with dimerization and the autoproteolysis of enzymes. With time, characteristic large and small subunits (p20 and p10) of active caspase 1 are formed.[35–37] In the first step of activation, in association with the NLR or PYHIN protein families, it forms the inflammasome complex. Proteins NLR/PYHIN are sensitive to pathogens, toxins and several sorts of infections.[35] Activated caspase 1 initiates the secretion of pro-inflammatory cytokines such as

interleukin 1β and 18.[35,38] Our work found that in the control group C, in most interstitial cells (over 87% of all cells), the immunohistochemical reaction with caspase 1 was negative. In addition, a weak or an average IHC response (respectively, 8% and 4%) was seen in the examined cells. However, in experimental group E, a positive, cytoplasmic immunohistochemical reaction was seen in 49% of all interalveolar cells that were observed. While about 30% of such cells presented a weak reaction, 16.3% of the cells showed an average reaction, and 2% of the cells reacted strongly. The dissimilarity in the occurrence of the caspase 1 expression between 2 groups: the control and the experimental, was, hence, statistically significant $p < 0.000001$. The results confirm the H&E staining observation.

Inflammatory reaction is the initial response to the lung injury. Activated inflammatory cells such as the neutrophils and the macrophages accumulate in the tissue and release harmful amounts of reactive oxygen species, as well as some pro-inflammatory cytokines that (in turn) activate collagen production in alveolar fibroblasts. The increasing amounts of matrix proteins distort the normal lung architecture and affect gas exchange.[39] The interstitial changes in the lung tissue observed in our study suggest that cladribine is a drug that may be the cause of drug-induced lung disease and may lead to several respiratory disorders.

We think that the obtained results might improve the therapy with cladribine and also reduce the risk of the adverse effects and damage of the tissues. Moreover, knowledge of how cladribine influences lung morphology might improve the design of therapeutic strategies.

References

1. Schwaiblmair M, Behr W, Haeckel T, Märkl B, Foerg W, Berghaus T. Drug induced interstitial lung disease. *Open Respir Med J*. 2012;6:63–74. doi: 10.2174/1874306401206010063
2. Spurgeon S, Yu M, Phillips JD, Epner EM. Cladribine: Not just another purine analogue? *Expert Opin Investing Drugs*. 2009;18(8):1169–1181.
3. Leist TP, Weissert R. Cladribine: Mode of action and implications for treatment of multiple sclerosis. *Clin Neuropharm*. 2011;34:28–35.
4. Hartung HP, Aktas O, Kieseier B, Comi G. Development of oral cladribine for the treatment of multiple sclerosis. *J Neurol*. 2010;257:163–170.
5. Leist TP, Vermersch P. The potential role for cladribine in the treatment of multiple sclerosis: Clinical experience and development of an oral tablet formulation. *Curr Med Res Opin*. 2007;23(11): 2667–2676.
6. Warnke C, Leussink VI, Goebels N, et al. Cladribine as a therapeutic option in multiple sclerosis. *Clin Immunol*. 2012;142:68–75.
7. Kobelska-Dubiel N, Górnaś M. Powikłania chemioterapii. http://www.amgen.pl/produkty/public/pdf/Powikania_po_chemioterapii.pdf. Accessed June 11, 2012.
8. Jędrych M, Wawryk-Gawda E, Jodłowska-Jędrych B, Chylińska-Wrzos P, Jasiński L. Immunohistochemical evaluation of cell proliferation and apoptosis markers in ovarian surface epithelial cells of cladribine-treated rats. *Protoplasma*. 2013;250:1025–1034. doi: 10.1007/s00709-012-0461-z
9. Wawryk-Gawda E, Chylińska-Wrzos P, Lis-Sochocka M, et al. P53 protein in proliferation, repair and apoptosis of cells. *Protoplasma*. 2014; 251:525–533. doi: 10.1007/s00709-013-0548-1
10. Wawryk-Gawda E, Chylińska-Wrzos P, Lis-Sochocka M, Bulak K, Jodłowska-Jędrych B. Intrinsic apoptosis pathway in fallopian tube epithelial cells induced by cladribine. *Sci World J*. 2014. doi.org/10.1155/2014/928036

11. Chylinska-Wrzos P, Wawryk-Gawda E, Lis-Sochocka M, et al. The intrinsic or the extrinsic pathways of apoptosis in the epidermis after cladribine application? *J Biomed Sci Eng.* 2013;6:265–272. doi.org/10.4236/jbise.2013.63033

12. Chylińska-Wrzos P, Lis-Sochocka M, Wawryk-Gawda E, et al. Expression of p53 protein and the histomorphological view of epidermis in experimental animals after cladribine application. *IJVR.* 2014; 15(3,48):198–205.

13. Fatima N, Toscano MP, Hunter SB, Cohen C. Controversial role of Epsein-Barr virus in multiple sclerosis. *Appl Immunohistochem Mol Morphol.* 2011;19(3):246–252. doi: 10.1097/PAI.0b013e3181fcf3b4

14. Giacomini PS, Darlington PJ, Bar-Or A. Emerging multiple sclerosis disease-modifying therapies. *Curr Opin Neurol.* 2009;22:226–232.

15. Kasper LH, Shoemaker J. Multiple sclerosis immunology. The healthy immune system vs the MS immune system. *Neurology.* 2010;74(1):S2–S8.

16. Losy J. Patogeneza oraz aktualne kryteria diagnostyczne stwardnienia rozsianego. *Neurologia i Psychiatria.* 2004;4:53–56.

17. Menge T, Weber MS, Hemmer B, et al. Disease-modifying agents for multiple sclerosis. recent advances and future prospects. *Drugs.* 2008;68(17):2445–2468.

18. Pappas DJ, Oksenberg JR. Multiple sclerosis pharmacogenomics. Maximizing efficacy of therapy. *Neurology.* 2010;74(1):S62–S69.

19. Coyle PK. Existing therapies for multiple sclerosis offer proven efficacy and safety. *Curr Opin Neurol.* 2009;22:S4–S9.

20. Montalban X. Multiple sclerosis therapy: Historical and future perspectives. *Curr Opin Neurol.* 2009;22:S1–S3.

21. Preiningerova J. Oral laquinimod therapy in relapsing multiple sclerosis. *Expert Opin Investig Drugs.* 2009;18(7):985–989.

22. Slavin A, Kelly-Modis L, Labadia M, Ryan K, Brown ML. Pathogenetic mechanism and experimental models of multiple sclerosis. *Autoimmunity.* 2010;43(7):504–513.

23. Filippi M, Rovaris M, Iannucci G, Mennea S, Sormani MP, Comi G. Whole brain volume changes in patients with progressive MS treated with cladribine. *Neurology.* 2000;55:1714–1718.

24. Rice GP, Filippi M, Comi G. Cladribine and progressive MS: Clinical and MRI outcomes of a multicenter controlled trial. Cladribine MRI Study Group. *Neurology.* 2000;54(5):1145–1155.

25. Wawryk-Gawda E, Chylińska-Wrzos P, Jodłowska-Jędrych B, Lis-Sochocka M. Use of selected purine analogs in neoplastic and autoimmune diseases. Annales UMCS, Sectio DDD. *Pharmacia.* 2011; 24(4,3):29–47.

26. Robak T, Lech-Maranda E, Korycka A, Robak E. Purine nucleoside analogs as immunosuppressive and antineoplastic agents: Mechanism of action and clinical activity. *Curr Med Chem.* 2006;13:3165–3189.

27. Robak T, Korycka A, Lech-Maranda E, Robak P. Current status of older and new purine nucleoside analogues in the treatment of lymphoproliferative diseases. *Molecules.* 2009;14:1183–1226.

28. Dimopoulou I, Bamias A, Lyberopoulos P, Dimopoulos MA. Pulmonary toxicity from novel antineoplastic agents. *Ann Oncol.* 2006;17: 372–379. doi:10.1093/annonc/mdj057

29. Betticher DC, Hsu Schmitz SF, Ratschiller D, et al. Cladribine (2-CdA) given as subcutaneous bolus injections is active in pretreated Waldenstrom macroglobulinaemia. *Br J Haematol.* 1997;99:358–363.

30. Van Den Neste E, Michaux L, Layios N, et al. High incidence of complications after 2-chloro-2'-deoxyadenosine combined with cyclophosphamide in patients with advanced lymphoproliferative malignancies. *Ann Hematol.* 2004;83:356–363. doi 10.1007/s00277-004-0858-7

31. Montillo M, Tedeschi A, O'Brien S, et al. Phase II study of cladribine and cyclophosphamide in patients with chronic lymphocytic leukemia and prolymphocytic leukemia. *Cancer.* 2003;97(1):114–120.

32. Okawa Y, Shimada T, Nagasaki E, Nozato A, Mizoroki F, Kobayashi M. Pulmonary cryptococcosis occurring 6 months after cladribine therapy for relapsed follicular lymphoma. *Jpn J Clin Oncol.* 2006;47(7): 650–655.

33. Fridrik MA, Jager G, Kienzer HR, et al. Efficacy and toxicity of 2-chlorodeoxyadenosine (Cladribine) – 2 h infusion for 5 days – as first-line treatment for advanced low grade Non-Hodgkin's lymphoma. *Eur J Cancer.* 1998;34(10):1560–1564.

34. Feenstra JF, Hickey BP, Blackwell EA. Acute respiratory failure associated with cladribine pneumonitis. *Int Med J.* 2004;34(9–10): 583–584.

35. Broz P, von Moltke J, Jones JW, Vance RE, Monack DM. Differential requirement for Caspase-1 autoproteolysis in pathogen-induced cell death and cytokine processing. *Cell Host Microbe.* 2010;8:471–483.

36. Li J, Yuan J. Caspases in apoptosis and beyond. *Oncogene.* 2008;27: 6194–6206.

37. Park HH. Structural features of Caspase-activating complexes. *Int J Mol Sci.* 2012;13:4807-4818. doi: 10.3390/ijms13044807

38. Brough D, Rothwell NJ. Caspase-1-dependent processing of pro-interleukin-1βis cytosolic and precedes cell death. *J Cell Sci.* 2007;120: 772–781. doi: 10.1242/jcs.03377

39. Cui K, Kou JQ, Gu JH, et al. Naja naja atra venom ameliorates pulmonary fibrosis by inhibiting inflammatory response and oxidative stress. *BMC Complement Altern Med.* 2014;14:461. doi: 10.1186/1472-6882-14-461

Analysis of *KRAS*, *NRAS*, *BRAF*, and *PIK3CA* mutations could predict metastases in colorectal cancer: A preliminary study

Kamila Wojas-Krawczyk[1,A,C–F], Ewa Kalinka-Warzocha[2,A,C–F], Katarzyna Reszka[3,B–D], Marcin Nicoś[1,B,C], Justyna Szumiło[4,B–D], Sławomir Mańdziuk[5,B,C], Katarzyna Szczepaniak[6,C,D], Dorota Kupnicka[7,B,C], Remigiusz Lewandowski[8,B,C], Janusz Milanowski[1,A,D–F], Paweł Krawczyk[1,A,D–F]

[1] Department of Pneumonology, Oncology and Allergology, Medical University of Lublin, Poland

[2] Polish Mother's Memorial Hospital Research Institute, Łódź, Poland

[3] Genetic and Immunology Institute GENIM Ltd., Lublin, Poland

[4] Department of Clinical Patomorphology, Medical University of Lublin, Poland

[5] Oncology and Chemotherapy Unit, Medical University of Lublin, Poland

[6] Chemotherapy Department, Regional Centre of Oncology, Nicolaus Copernicus Provincial Specialist Hospital, Łódź, Poland

[7] Pathology Laboratory Synevo, Łódź, Poland

[8] MolGenDia Ltd., Bydgoszcz, Poland

A – research concept and design; B – collection and/or assembly of data; C – data analysis and interpretation;
D – writing the article; E – critical revision of the article; F – final approval of the article

Abstract

Background. Colorectal cancer (CRC) is usually diagnosed in the metastatic stage, when chemotherapy and molecularly-targeted therapies, instead of surgery, play the most important therapeutic role. Application of anti-epidermal growth factor receptor (EGFR) therapy requires the analysis of *RAS* mutation status and only *RAS* wild-type (wt) patients are qualified for the therapy.

Objectives. The objective of this study was to analyze driver mutations in *KRAS*, *NRAS*, *BRAF*, and *PIK3CA* genes in CRC patients.

Material and methods. We assessed the *KRAS*, *NRAS*, *BRAF*, and *PIK3CA* genes in 102 inoperable, locally advanced and advanced CRC patients. Real-time polymerase chain reaction (RT-PCR) and high resolution melt PCR (HRM-PCR) techniques with DNA intercalating dye were applied in the study.

Results. Forty-six patients demonstrated the presence of examined mutations (45.1%). No significant differences in driver mutation occurrence between men and women, as well as between younger (<65 years) and older (≥65 years) patients were found. The mutations were present significantly more frequently in metastatic than in primary tumors (p = 0.039) due to the high incidence of *KRAS* gene mutations in metastatic tissue. *BRAF* and *PIK3CA* mutations were found only in primary tumors. The incidence of *PIK3CA* mutations was significantly higher (11.77%) in early than in advanced stages of the disease (1.96%; p = 0.05); *NRAS* mutations were found only in metastatic cancer (7.85%; p = 0.041). Only a single mutation of the *PIK3CA* and no mutations of *NRAS* were found in rectal cancer.

Conclusions. Our results have shown low occurrence of driver mutations in Polish CRC patients, involving also mutations in rarely tested genes. The extent of the research panel of additional mutations could contribute to creating a better method of qualifying patients for molecularly targeted therapies and obtaining a better outcome for these therapeutic strategies.

Key words: colorectal cancer, *PIK3CA*, *BRAF*, molecularly targeted therapy, *RAS* mutation

Introduction

Colorectal cancer (CRC) is one of the leading causes of cancer death and one of the most common cancers among both men and women in developed countries. In Poland, approx. 16,000 new cases of CRC are registered every year; more than 10,000 people die (approx. 5,700 men and 4,800 women), and a 5-years overall survival rate among these patients is less than 50%. The early diagnosis of cancers allows the patients to be qualified for surgery. Unfortunately, only small percentage of patients are qualified for surgical resection, and a significant proportion is diagnosed at a late stage, when, in the case of metastatic disease, surgical treatment is only a palliative procedure. Therefore, systemic treatment involving chemotherapy and molecularly targeted therapies plays an important role in the treatment of CRC.[1–3]

For several years, in many European countries, bevacizumab, cetuximab and panitumumab were the molecularly targeted drugs available for advanced CRC.[3] The first one is a monoclonal antibody directed against vascular endothelial growth factor (VEGF), which inhibits angiogenesis and leads to the increase of blood vessel pressure. Two other drugs are monoclonal antibodies against epidermal growth factor receptor (EGFR), and their mechanism of action involves blocking the proliferation signal of tumor cells by inhibiting the EGFR signaling pathway (EGFR/Pi3K/AKT/mTOR or EGFR/RAS/RAF/MAPK/ERK).[3] Application of these drugs requires an analysis of *RAS* gene mutations status and only patients with *RAS* wild-type (wt) are qualified for the therapy. However, more than 40% of patients without common *KRAS* gene mutations (codon 12 and 13) do not respond to anti-EGFR monoclonal antibody therapies. This resistance can be explained by the presence of mutations in other downstream *EGFR* signaling pathway effectors, such as *BRAF*, *PIK3CA* and *NRAS* genes, as well as rare *KRAS* gene mutations (codon 59, 61, 117, 146).[2–4]

In the present study, we assessed the occurrence of driver mutations in *KRAS*, *NRAS*, *BRAF*, and *PIK3CA* genes in inoperable, locally advanced and advanced CRC patients. We also estimated the association between the mutations incidence and clinical factors, especially tumor localization and stage of the disease.

Material and methods

The study group consisted of 102 CRC patients, including 69 (67.6%) men and 33 (32.4%) women, diagnosed in the Chemotherapy Department, Regional Centre of Oncology, Provincial Specialist Hospital in Łódź, Poland, and in the Oncology and Chemotherapy Unit of the Medical University of Lublin, Poland. The median age was 64 ±9.41 years. All patients had advanced or inoperable mucinous adenocarcinoma CRC. Colorectal cancer grading and subtypes were not possible to assess in all patients due to the availability of only small biopsy specimens. Patients were qualified for anti-EGFR therapy with monoclonal antibodies (cetuximab or panitumumab monotherapy). For the purpose of the study, the following localizations of CRC adenocarcinoma were determined: 1. rectum; 2. sigmoid colon; 3. ascending, transverse and descending colon; and 4. CRC metastases. The clinical characteristics of patients are summarized in Table 1.

Archival tumor tissue from CRC as formalin-fixed paraffin embedded (FFPE) blocks was available from all patients enrolled in the study. The FFPE blocks were archived in the Department of Clinical Pathomorphology, Medical University of Lublin, Poland, and in Pathology Laboratory Synevo in Łódź, Poland. Mutation analysis was performed after a histological confirmation of cancer and when the presence of more than 10% tumor cells was observed by a pathologist in hematoxylin and eosin (H&E)-stained slides. Genomic DNA was extracted from the FFPE tumor tissue sections using a QIAamp DNA FFPE Tissue Kit (CE-IVD-marked; Qiagen, Hilden, Germany), according to the manufacturer's instructions. DNA concentration and quality was determined by the spectrophotometry method.

The study was approved by the Ethical Committee of the Medical University of Lublin, Poland (No. KE-0254/218/2015). Informed consent was obtained from each participant.

The analysis of *KRAS* mutations was performed using *KRAS*/*BRAF* Mutation Analysis Kit for real-time polymerase chain reaction (RT-PCR) (CE-IVD; EntroGen, Woodland Hills, USA) with a Cobas 480 RT-PCR device (Roche Diagnostics, Basel, Switzerland). The following mutations in the *KRAS* (NM_004985.3) gene, according to specific codon, were analyzed: codon 12 – p.Gly12Asp (c.35G>A), p.Gly12Cys (c.34G>T), p.Gly12Ser (c.34G>A), p.Gly12Arg (c.34G>C), p.Gly12Ala (c.35G>C), p.Gly12Val (c.35G>T); codon 13 – p.Gly13Asp (c.38G>A); codon 59 – p.Ala59Thr (c.174G>A), p.Ala59Glu (c.176C>A), p.Ala59Gly (c.176C>G); codon 61 – p.Gln61His (c.183A>C & c.183A>T), p.Gln61Leu (c.182A>T), p.Gln61Arg (c.182A>G); codon 146 – p.Ala146X (c.436G>A, c.436G>C, or c.437C>T); codon 117 – p.Lys117X (c.351A>C, c.351A>T, c.350A>G, or c.349A>G). The mutation analysis was carried out in relation to the amplification of positive and negative control tests provided by the manufacturer and according to the included protocol.

The analysis of the *NRAS* mutation was performed using the *NRAS* Mutation Analysis Kit for RT-PCR (CE-IVD; EntroGen) with a Cobas 480 RT-PCR device (Roche Diagnostics). The following mutations in *NRAS* (NM_002524.2) gene, according to codon, were analyzed: codon 12 – Gly12Asp (c.35G>A), Gly12Cys (c.34G>T), Gly12Ser (c.34G>A), Gly13Arg (c.37G>C); codon 13 – Gly13Val (c.38G>T); codon 59 – Ala59Thr (c.175G>A), Ala59Asp (c.176C>A); codon 61 – Gln61His (c.183A>C & c.183A>T), Gln61Leu (c.182A>T),

Gln61Lys (c.181C>A), Gln61Arg (c.182A>G); codon 146 – Ala146Thr (c.436G>A); codon 117 – Lys117Arg (c.350A>G). The mutation analysis has been carried out in relation to the amplification of positive and negative control tests provided by the manufacturer and according to the included protocol.

The analysis of *BRAF* mutations was performed using Cobas® 480 *BRAF* V600 Mutation Test (Roche Diagnostics). with a Cobas 480 RT-PCR device (Roche Diagnostics). The test detects Val600X (c.1799T>A or c.1798_1799GT>AA) mutations in the *BRAF* (NM_004333.4) gene and does not distinguish the type of mutations. The mutation analysis was carried out in relation to the amplification of positive and negative control tests provided by the manufacturer and according to the included protocol.

Estimation of the *PIK3CA* gene mutations (substitutions Glu542Lys, Glu545Lys, His1047Arg) was conducted using 2 methods based on a quantitative RT-PCR (qPCR). As a screening method, the high resolution melt PCR (HRM-PCR) technique was used. One pair of primers flanked the mutations located in exon 9 (substitutions Glu542Lys, c.1624G>A and Glu545Lys, c.1633G>A), and the 2nd pair of primers flanked a mutation located in exon 20 (substitution His1047Arg, c.3140A>G). The amplification of the examined region was performed using the Eco RT-PCR device (Illumina, San Diego, USA). Different genotypes of *PIK3CA* were distinguished according to the normalization data derived from the raw data plots and a difference graph derived from to the normalization data. Comparison of the amplification and melting curves in the positive and negative controls allowed us to distinguish the mutated-type (mt) and wt samples.

In the next step, the allele-specific qPCR (ASP-qPCR) method was used to define the type of mutations. The analysis was performed using the Eco RT-PCR device (Illumina). The wt and mt of the *PIK3CA* gene were tested in separate reactions with specific forward primers for these variants of the gene. Samples were assessed as positive if amplification in the ASP-qPCR was observed both for the mt and for wt of the *PIK3CA* gene. The samples with late amplification (Ct >32 cycle)

Table 1. Characteristics of the studied group and comparison of different clinical factors and driver mutations incidence

Characteristics, n (%)		*KRAS* mutations, n (%)	p-value; X^2	*NRAS* mutations, n (%)	p-value	*BRAF* mutations, n (%)	p-value	*PIK3CA* mutations, n (%)	p-value	All analyzed mutations, n (%)	p-value; X^2
Gender	male, n = 69 (67.6)	22 (31.9)	0.636; 0.224	2 (2.9)	0.593	5 (7.25)	1.000	5 (7.25)	1.000	34 (49.28)	0.717; 0.131
	female, n = 33 (32.4)	9 (27.3)		2 (6.1)		2 (6.1)		2 (6.1)		15 (45.46)	
Median age [years]					64 ±9.41 (median ±SD)						
	≥64, n = 50 (49)	13 (26)	0.344; 0.894	3 (6.0)	0.358	5 (10.0)	0.265	4 (8.0)	0.713	25 (50.0)	0.698; 0.151
	<64, n = 52 (51)	18 (34.6)		1 (1.93)		2 (3.85)		3 (5.77)		24 (46.16)	
Localization of adenocarcinoma CRC	rectum, n = 45 (44.1)	13 (28.9)		0		4 (8.89)		1 (2.23)		18 (40.0)	
	sigmoid, n = 18 (17.6)	7 (38.9)	0.039*; 8.377	1 (5.56)	NC	1 (5.56)	NC	2 (11.12)	NC	11 (61.12)	0.085; 6.614
	ascending, transverse and descending colon, n = 32 (31.5)	6 (18.8)		2 (6.25)		2 (6.25)		4 (12.5)		14 (43.75)	
	metastatic CRC, n = 7 (6.8)	5 (71.4)		1 (14.3)		0		0		6 (85.72)	
Different localization (only primary tumors)	rectum, n = 45 (44.1)	13 (28.9)	0.753; 0.099	0	0.244	4 (8.89)	0.704	1 (2.23)	0.115	18 (40.0)	0.328; 0.956
	colon and sigmoid, n = 50 (49.0)	13 (26.0)		3 (6.0)		3 (6.0)		6 (12.0)		25 (50.0)	
Tumor type	primary, n = 95 (93.14)	26 (27.37)	0.014*; 5.983	3 (3.16)	0.251	7 (7.37)	1.000	7 (7.37)	1.000	43 (45.27)	0.039*; 4.274
	metastatic, n = 7 (6.86)	5 (71.43)		1 (14.29)		0		0		6 (85.72)	
All stages of CRC	II, n = 9 (8.82)	3 (33.34)		0		1 (8.34)		1 (8.34)		5 (55.56)	
	III, n = 42 (41.18)	14 (33.34)	0.812; 0.417	0	NC	4 (9.31)	NC	5 (11.63)	NC	23 (54.77)	0.382; 1.926
	IV, n = 51 (50.00)	14 (27.45)		4 (7.85)		2 (4.26)		1 (2.13)		21 (41.18)	
Early and locally advanced vs advanced stages of CRC	II + III, n = 51 (50.00)	17 (33.34)	0.518; 0.417	0	0.117	5 (9.81)	0.436	6 (11.77)	0.112	28 (54.91)	0.165; 1.925
	IV, n = 51 (50.00)	14 (27.45)		4 (7.85)		2 (3.93)		1 (1.96)		21 (41.18)	

CRC – colorectal cancer; NC – non-calculable; SD – standard deviation; * p < 0.05.

of the wt *PIK3CA* gene were excluded from analysis, and the samples with late amplification (Ct >32 cycle) of the mt region of the *PIK3CA* gene were assessed as wt. The representative analyses of mutations in *PIK3CA* genes analyzed by HRM-PCR and by ASP-qPCR were presented in Fig. 1 and 2, respectively.

DNA isolated from the *PIK3CA* gene mutations positive cell-lines (SW48 cell-line for Glu542Lis; MCF10A cell-line for substitutions Glu545Lys and His1047Arg; Horizon Discovery, Cambridge, UK) served as a positive control. The negative control was determined with DNA isolated from the peripheral blood leukocytes of healthy individuals.

Statistical analysis was performed using STATISTICA, v. 10 (StatSoft Inc., Tulsa, USA). Associations between driver mutation occurrence and clinical factors were examined using Fisher's χ^2 test if the expected values were greater than 5. Fisher's exact test was used if the expected values ranged from 0 to 4. Student's t-test was used for testing the equality of population medians among groups (median age between groups); p-values below 0.05 were considered significant.

Results

The median age was similar in the groups of patients with different clinical characteristics. Forty-six patients demonstrated the presence of any of the examined mutations (45.1%). We found 53 driver mutations in the following genes: 35 mutations in *KRAS* gene, 4 mutations in *NRAS* gene, 7 mutations in *BRAF* gene, and 7 mutations in *PIK3CA* gene (Fig. 3).

In 2 cases, the coexistence of 3 of the examined mutations was found. *KRAS* codon 12 gene (Gly12Val) mutation coexisted with *KRAS* codon 117 (Lys117X) and *PIK3CA* codon 542 (Glu542Lys) mutations. In the 2nd case, *KRAS* codon 12 gene (Gly12Val) coexisted with *KRAS* codon 12 (Gly12Cys) and *PIK3CA* codon 1047 (His1047Arg) mutations. Moreover, in 3 cases we found the coexistence of 2 of the following mutations: *KRAS* codon 12 (Gly12Asp) mutation coexisted with *KRAS* codon 12 (Gly12Val) mutation, *KRAS* codon 12 (Gly12Cys) mutation coexisted with *KRAS* codon 146 (Ala146X) mutation, and *KRAS* codon 146 (Ala146X) mutation coexisted with *PIK3CA* codon 1047 (His1047Arg) mutation.

No differences in the incidence of driver mutations between men (49.28%) and women (45.46%) were found. The occurrence of mutations in *KRAS*, *NRAS* and *BRAF* genes as well as in *PIK3CA* gene were very similar in men (31.9%, 2.9%, 7.25%, and 7.25%, respectively) and in women (27.3%, 6.1%, 6.1%, and 6.1%, respectively) (Table 1).

Depending on the age group, the incidence of *KRAS* mutations was insignificantly higher, while the incidence of *NRAS*, *BRA*F and *PIK3CA* gene mutations was
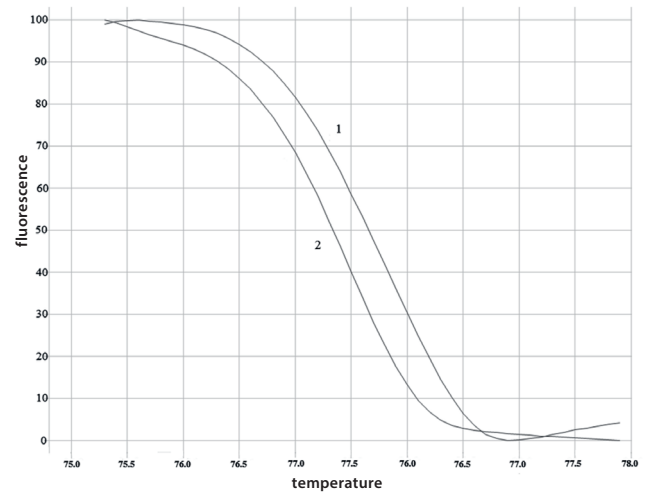
Fig. 1. Differences in melting curves of *PIK3CA* wt and mt genotypes. The H1047R mutation involves replacing of histidine (wt) by arginine (mt) in the 1047 position in the polypeptide chain. The mutation is caused by substitution of adeninie to guanine in the 3140 position of *PIK3CA* gene (exon 20). Comparison of melting temperatures and analysis of normalized data plots allowed distinguishing the wt and mt of *PIK3CA* gene

The melting curve 1 represents mt *PIK3CA* region, which corresponds to guanine in the position 3140 that needs higher temperature to melt the quantitative real-time polymerase chain reaction (qPCR) products; the melting curve 2 represents wt *PIK3CA* region, which corresponds to adenine in the position 3140 that needs lower temperature to melt the qPCR products.
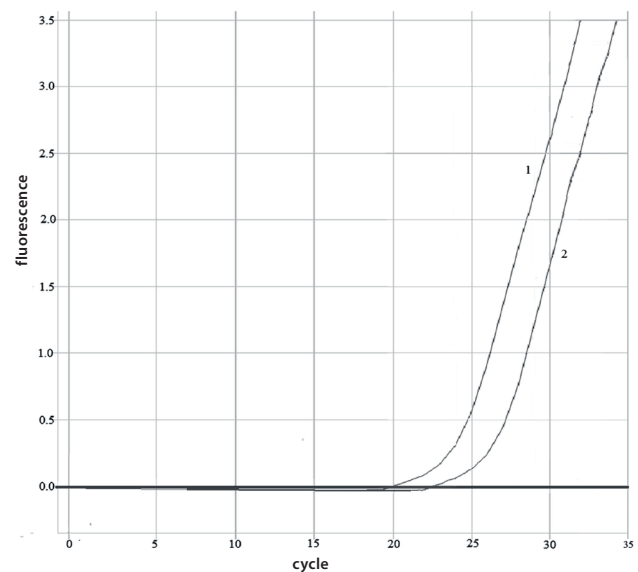
Fig. 2. Amplification curves of *PIK3CA* gene in allele-specific quantitative polymerase chain reaction (ASP-qPCR) analysis

Curve 1 represents amplification of wt *PIK3CA* region in negative control; curve 2 represents amplification of mt *PIK3CA* region in a positive patient.

insignificantly lower in younger patients, when compared to patients ≥64 years old (Table 1).

There were no statistically significant differences in the incidence of analyzed mutations in rectal and colon cancer. However, only a single mutation of *PIK3CA* gene and no mutations of *NRAS* gene were found in rectal cancer.

Doublet/triplet mutations:
1) *KRAS* Ala146X and *PIK3CA* His1047Arg
2) *KRAS* Gly12Asp and *KRAS* Gly12Val
3) *KRAS* Gly12Cys and *KRAS* Ala146X
4) *KRAS* Gly12Val and *KRAS* Lys117X and *PIK3CA* Glu542Lys
5) *KRAS* Gly12Val and *KRAS* Gly12Cys and *PIK3CA* His1047Arg
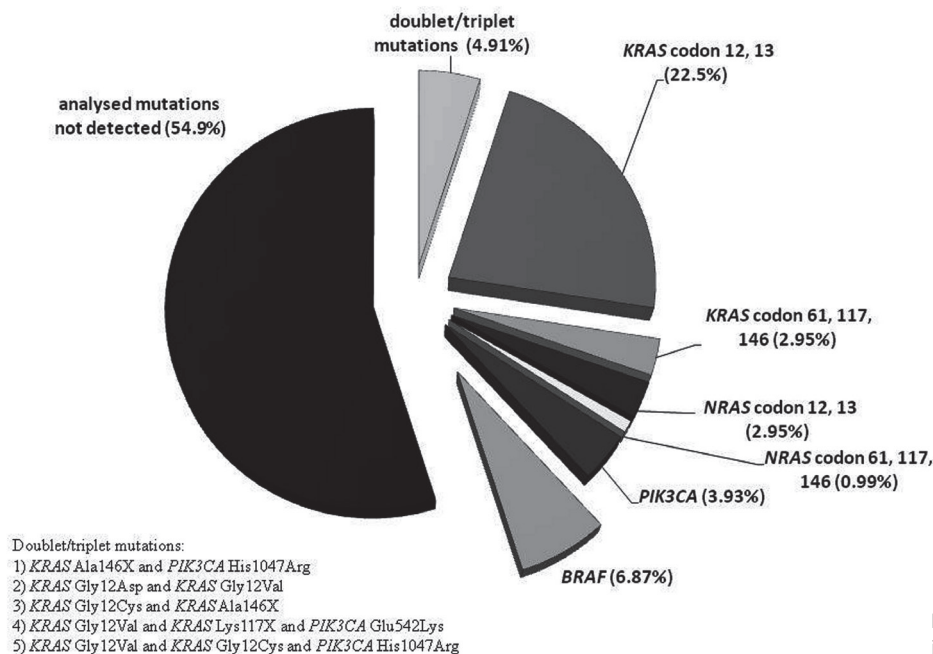
Fig. 3. The percentage of detected mutations in colorectal cancer (CRC) patients

The molecular profile of metastases seems to be different from the primary one. We found that the driver mutations were present significantly more frequently in metastatic tissue compared to primary tissue (p = 0.039; χ^2 = 4.274). Specifically, a significantly higher incidence of *KRAS* mutations was observed in metastatic tissue (p = 0.014; χ^2 = 5.983) when compared to primary CRC (71.43% vs 27.37%, respectively); similar insignificant differences were observed for *NRAS* mutations (14.29% vs 3.16%). Moreover, *BRAF* as well as *PIK3CA* mutations were observed only in primary tumor tissue (Table 1).

The incidence of the examined mutations was also analyzed according to CRC stages, and we found that it was similar for stages II and III of CRC (55.56% and 54.77%, respectively) and for the metastatic stage IV of CRC (41.18%). When the earlier CRC stages were analyzed together, the incidence of *PIK3CA* mutations was insignificantly higher (11.77%; p = 0.112) in stages II and III of CRC when compared to metastatic CRC (1.96%). On the other hand, *NRAS* gene mutations were found only in the advanced stage of CRC (7.85%; p = 0.112) (Table 1).

Discussion

Nowadays, personalized cancer therapy rapidly becomes the standard care not only for CRC patients, but also in terms of therapies in other cancer patients. New molecular biology techniques are widely used for this purpose.[3–5]

De Sousa et al. distinguished 3 types of colon cancer subtypes using the whole-genome gene expression data and noticed that each type of cancer was associated with a different dominant feature and prognosis for the patient: CCS1 (epithelial type) and CCS2 (microsatellite instability – MSI type) were characterized by a rather good disease outcome, while CCS3 is of the mesenchymal dominant and had a bad prognosis.[6] Nagtegaal and van Krieken proposed that CRC could be molecularly divided into 3 groups based on the epigenetic markers: chromosomal instability (CIN), MSI and CpG island methylation phenotype.[4] It is also postulated that these types of tumors differ in terms of pathology, outcome and response to therapy, but this distinction is not used in clinical practice.[4]

From a practical point of view, it is difficult to require such wide molecular testing for CRC. In clinical practice, there are very few genetics laboratories where such broad molecular diagnostics could be performed. Therefore, we promote here an extended panel of *RAS* gene mutations that could be helpful in a better qualification of CRC patients for molecularly targeted therapy. Furthermore, the use of diagnostic kits (CE-IVD-marked) for the determination of a wide panel of *RAS* mutations should result in faster test release and a quicker decision in molecularly targeted therapy qualification. It could also help to understand the metastasis process and provide new prognostic factors in patients with CRC.

It is widely known that mutations in *KRAS* codons 12 and 13 predict the lack of response to anti-EGFR therapies. Vaughn et al. postulated that not only those mutations are responsible, but also additional, rarely tested activating mutations could play a role in treatment resistance.[7] They found that 27.3% of tumors with *KRAS* wild-type codons 12 and 13 harbored mutation in codons 59, 61, 117, and 147 of the *KRAS* gene. In *RAS* wild-type CRC

patients, *PIK3CA* mutations have been associated with a worse clinical outcome and with a negative prediction of response to targeted therapy with anti-EGFR monoclonal antibodies.[7–9] Authors suggested that accurate testing of *RAS* genes could be useful in identifying patients who may also be resistant to anti-EGFR therapies.[7–9]

In our examined population, we proved that driver mutations are present in relatively low numbers in CRC patients due to a low incidence of common *KRAS* mutations (codon 12 and 13). We analyzed 102 CRC patients and 46 (45.1%) of them were found to carry 1 of the analyzed genes aberrations. Moreover, 5 patients were found to carry more than 1 mutation, including patients with coexistence of *KRAS* and *PIK3CA* genes mutations. This resulted in the inability to use monoclonal anti-EGFR therapy for those patients, but they had the possibility to be treated in specialized clinical trials.

In the Cetuximab Combined with Irinotecan in First-Line Therapy for Metastatic Colorectal Cancer (CRYSTAL)study, a clinical benefit was observed for FOLinic acid-Fluorouracil-IRInotecan (FOLFIRI) scheme together with cetuximab addition in metastatic CRC patients with *KRAS* codon 12/13 wild-type. Moreover, the patients with the extended *RAS* wild-type profile derived significant benefit from such therapy, while patients with any *RAS* mutation did not.[10,11] Based on the CRYSTAL study results, Van Cutsem et al. postulated that molecular testing for all activating *RAS* mutations is essential for considering anti-EGFR therapy.[12] Similar results were obtained in Oxaliplatin and Cetuximab in First-Line Treatment of Metastatic Colorectal Cancer (OPUS) (FOLFOX4 and cetuximab) as well as Panitumumab Efficacy in combination with mFOLFOX6 Against bevacizumab plus mFOLFOX6 in mCRC subjects with wild-type KRAS tumors (PEAK) (FOLFOX6 and panitumumab) and PRIME (FOLFOX and panitumumab) studies.[13–15]

There are only few reports in the literature concerning the differences between some genetic alterations and CRC localization. Slattery et al. analyzed the differences in the occurrence of driver mutations in colon and rectal tumors, and found that proximal colon cancers expressed more frequently microsatellite instability and had more *KRAS* gene mutations than rectal and distal colon tumors, which are more likely to express *p53* gene mutations.[16]

We analyzed the incidence of driver mutations according to the localization of cancer as well as the type of tumor. When only primary tumors were considered, we found that *KRAS* driver mutations are more likely to localize in sigmoid colon cancer than in other tumor sites. Moreover, at this tumor location we observed the incidence of different mutations in any gene loci, including a rare mutation in *KRAS* codon 146, and *NRAS* codon 61 as well as the *PIK3CA* Glu542Lys mutations, which could indicate a preferential location of genetic changes at this site. Moreover, the predominant mutations found in rectal tumors were *KRAS* codon 12 and *BRAF* Val600X. However, our

work was carried out on a relatively small number of patients and confirmation of this thesis requires an extended study group. The coexistence of *KRAS* with different other mutations could be related to the heterogeneity of the tumor and to the presence of these mutations in different clones of cancer cells. These clinical cases are especially difficult to treat with molecularly targeted therapy.

What is more interesting, we postulated that primary CRC seems to be different in terms of molecular profiling from metastatic tumors. Based on the very preliminary results, we tried to define the molecular profile of CRC metastases, which contain mutations in *KRAS* and *NRAS* genes, while they contain neither *BRAF* nor *PIK3CA* gene mutations. In contrast, the presence of *BRAF* and *PKI3CA* mutations is characteristic for primary, early stages of CRCs.

Driver mutation status correlates not only with the response to anti-EGFR therapies, but also with metastatic spread. According to Lipsyc and Yaeger, the presence of *KRAS* mutation is associated with an increased risk of lung, brain and bone metastases. *BRAF* and *KRAS* genes mutations are rarely associated with the development of CRC liver metastases. *BRAF* mutation, a poor prognostic factor in metastatic CRC (mCRC), is associated with increased peritoneal and distant lymph node metastases.[17] Moreover, the assessment of mutations in the *RAS/BRAF* and *PIK3CA* genes can not only be a predictor of the response to anti-EGFR antibody treatment, but these mutations could also help select patients who would achieve a better response to bevacizumab treatment.[18] In the context of widening the routine molecular diagnostics, the meta-analysis conducted by Therkildsen et al. should be mentioned.[19] The authors suggest that the biomarker analysis beyond *KRAS* exon 2 should be implemented for clinical benefit prediction from anti-EGFR antibodies in metastatic CRC.[19]

Summarizing, our preliminary study has shown a lower incidence of driver mutations in CRC patients, involving mutations not only in the widely studied *KRAS* codon 12 and 13, but also in rarely tested genes such as *PIK3CA*. Therefore, an in-depth molecular diagnosis seems to be necessary for proper qualifications to anti-EGFR therapy and for understanding the mechanisms of resistance to such therapies.

References

1. Akkad J, Bochum S, Martens UM. Personalized treatment for colorectal cancer: Novel developments and putative therapeutic strategies. *Langenbecks Arch Surg.* 2015;400(2):129–143.
2. Coppedè F, Lopomo A, Spisni R, Migliore L. Genetic and epigenetic biomarkers for diagnosis, prognosis and treatment of colorectal cancer. *World J Gastroenterol.* 2014;20(4):943–956.
3. Linnekamp JF, Wang X, Medema JP, Vermeulen L. Colorectal cancer heterogeneity and targeted therapy: A case for molecular disease subtypes. *Cancer Res.* 2015;75(2):245–249.
4. Nagtegaal ID, van Krieken JH. Colorectal cancer: Is the new era of colorectal cancer classification finally here? *Nat Rev Gastroenterol Hepatol.* 2013;10(7):391–393.

5. Kim TM, Lee SH, Chung YJ. Clinical applications of next-generation sequencing in colorectal cancers. *World J Gastroenterol.* 2013;19(40):6784–6793.

6. De Sousa E, Melo F, Wang X, et al. Poor-prognosis colon cancer is defined by a molecularly distinct subtype and develops from serrated precursor lesions. *Nat Med.* 2013;19(5):614–618.

7. Vaughn CP, Zobell SD, Furtado LV, Baker CL, Samowittz WS. Frequency of *KRAS*, *NRAS* and *BRAF* mutations in colorectal cancer. *Genes Chromosomes Cancer.* 2011;50(5):307–312.

8. Cathomas G. *PIK3CA* in colorectal cancer. *Front Oncol.* 2014;4:35. doi: 10.3389/fonc.2014.00035

9. Sartore-Bianchi A, Martini M, Veronese FMS, et al. *PIK3CA* mutations in colorectal cancer are associated with clinical resistance to EGFR-targeted monoclonal antibodies. *Cancer Res.* 2009;69(5):1851–1857.

10. De Roock W, Claes B, Bernasconi D, et al. Effects of *KRAS*, *BRAF*, *NRAS* and *PIK3CA* mutations on the efficacy of cetuximab plus chemotherapy in chemotherapy-refractory metastatic colorectal cancer: A retrospective consortium analysis. *Lancet Oncol.* 2010;11(8):753–762.

11. Loupakis F, Ruzzo A, Cremolini C, et al. *KRAS* codon 61, 146 and *BRAF* mutations predict resistance to cetuximab plus irinotecan in *KRAS* codon 12 and 13 wild-type metastatic colorectal cancer. *Br J Cancer.* 2009;101(4):715–721.

12. Van Cutsem E, Lenz HJ, Köhne CH, et al. Fluorouracil, leucovorin, and irinotecan plus cetuximab treatment and *RAS* mutations in colorectal cancer. *J Clin Oncol.* 2015;33(7):692–700.

13. Bokemeyer C, Kohne CH, Ciardiello F, et al. Treatment outcome according to tumour *RAS* mutation status in OPUS study patients with metastatic colorectal cancer (mCRC) randomized to FOLFOX4 with/without cetuximab. *J Clin Oncol.* 2014;32(15 Suppl):abstr 3505.

14. Oliner K, Douillard J, Siena S, et al. Analysis of *KRAS/NRAS* and *BRAF* mutations in the phase III PRIME study of panitumumab and FOLFOX vs FOLFOX as first line treatment for metastatic colorectal cancer. *J Clin Oncol.* 2013;31(15 Suppl):abstr 3511.

15. Schwartzberg LS, Rivera F, Karthaus M, et al. PEAK: A randomized, multi-centre phase II study of panitumumab plus modified fluorouracil, leucovorin, and oxaliplatin (mFOLFOX6) or bevacizumab plus mFOLFOX6 in patients with previously untreated, unresectable, wild-type *KRAS* exon 2 metastatic colorectal cancer. *J Clin Oncol.* 2014;32(21):2240–2247.

16. Slattery ML, Curtin K, Wolff RK, et al. A comparison of colon and rectal somatic DNA alterations. *Dis Colon Rectum.* 2009;52(7):1304–1311.

17. Lipsyc M, Yaeger R. Impact of somatic mutations on patterns of metastasis in colorectal cancer. *J Gastrointest Oncol.* 2015;6(6):645–649.

18. Nakayama I, Shinozaki E, Matsushima T, et al. Retrospective study of *RAS/PIK3CA/BRAF* tumor mutations as predictors of response to first-line chemotherapy with bevacizumab in metastatic colorectal cancer patients. *BMC.* 2017;17(1):38–46.

19. Therkildsen C, Bergmann TK, Henrichsen-Schnack T, Ladelund S, Nilbert M. The predictive value of *KRAS*, *NRAS*, *BRAF*, *PIK3CA* and *PTEN* for anti-EGFR treatment in metastatic colorectal cancer: A systemic review and meta-analysis. *Acta Oncol.* 2014;53(7):852–864.

An initial evaluation of cytotoxicity, genotoxicity and antibacterial effectiveness of a disinfection liquid containing silver nanoparticles alone and combined with a glass-ionomer cement and dentin bonding systems

Alicja Porenczuk[1,A–D], Anna Grzeczkowicz[2,A,B], Izabela Maciejewska[3,C–F], Marlena Gołaś[4,D], Katarzyna Piskorska[4,D], Adam Kolenda[5,C,D], Dariusz Gozdowski[6,C], Ewa Kopeć-Swoboda[4,E,F], Ludomira Granicka[2,E,F], Dorota Olczak-Kowalczyk[1,E,F]

[1] Department of Pediatric Dentistry, Medical University of Warsaw, Poland

[2] The Maciej Nałęcz Institute of Biocybernetics and Biomedical Engineering, Polish Academy of Sciences, Warszawa, Poland

[3] Department of Molecular Medicine, Medical University of Gdańsk, Poland

[4] Department of Medical Microbiology, Medical University of Warsaw, Poland

[5] Department of Prosthetic Dentistry, Medical University of Warsaw, Poland

[6] Department of Experimental Design and Bioinformatics, Faculty of Agriculture and Biology, Warsaw University of Life Sciences, Poland

A – research concept and design; B – collection and/or assembly of data; C – data analysis and interpretation;
D – writing the article; E – critical revision of the article; F – final approval of the article

Address for correspondence
Alicja Porenczuk
E-mail: alicja.mackiewicz@wum.edu.pl

Abstract

Background. Bacterial reinfection of dental cavities remains an unsolved clinical problem. The search for methods enabling the limitation of the bacterial factor has become the fundamental goal of the dental materials research. Silver nanoparticles (AgNPs) are used as disinfection agents. An incomplete polymerization of the polymer resins combined with AgNPs, along with the increase of the release of the unbound monomers, have been found.

Objectives. The aim of this study was to evaluate the vitality of the human dental pulp stem cells (DPSCs) in response to a disinfection agent containing silver and gold nanoparticles (NPs), different bonding systems, glass-ionomer cement (GIC), and their combinations with the disinfection agent. Also, the influence of these materials both on the secretory function of DPSCs and on their antibacterial properties was established.

Material and methods. Cytotoxicity (MTT assay) and genotoxicity (enzyme-linked immunosorbent assay – ELISA) assays were used in the study. Antibacterial features were assessed with the optical density (OD) measurement of the bacteria (*Streptococcus mutans, Streptococcus salivarius* and *Lactobacillus acidophilus*) kept in dental materials.

Results. The disinfection liquid proved to be biocompatible. However, it relevantly interfered with the total-etch bonding system in terms of vitality, which may have serious clinical implications. Its combination with the self-etching system was biocompatible, yet it impaired the antibacterial action of the system. An enhancement of antibacterial action of GIC with AgNPs was found.

Conclusions. The disinfection liquid and GIC were biocompatible toward the DPSCs in terms of cytotoxicity and genotoxicity. Simultaneous usage of AgNPs with other dental materials did not affect the biocompatibility of the used materials. The disinfection liquid and GIC acted as antibacterial agents against all studied bacteria species. Used together with GIC and the total-etch bonding system, the disinfection liquid seemed to be efficient toward bacteria, yet it relevantly impaired the antibacterial action of self-etching systems.

Key words: cytotoxicity, silver nanoparticles, glass-ionomer cement, antibacterial properties, adhesives

Introduction

Bacterial reinfection of dental cavities, caused by the microgap between the tooth and the filling material, remains an unsolved clinical problem. Therefore, the search for methods enabling the limitation of the bacterial factor has become the fundamental goal of science dealing with dental materials. Recurrent caries development along the edges of the polymer resin fillings can be attributed to the presence of Gram-positive bacteria, such as *Streptococcus mutans* (*S. mutans*), so called non-mutans streptococci group, *Actinomyces* spp. and *Lactobacillus* spp., in dental plaque. It has been established that caries-associated species possess the ability to survive underneath these restorations for even a few months.[1] Thus, the application of the dental materials providing bacterial clearance and a proper seal is recommended. Among them, glass-ionomer cement (GIC) may be chosen due to its remineralizing and antibacterial properties.[2] The factors defining its usefulness in the cavity restorations include chemical composition (fluoride ions content, their release to and uptake from the surrounding environment) and low pH during setting.[2] However, the differences in bacteria susceptibility to fluoride and the strength of the antibacterial action of GIC are still a subject of dispute. Due to its poor physical properties, GIC cannot be considered long-term restoration, so new methods of modifying dental materials with antibacterial agents are being introduced, among them: antibacterial monomers (12-methacryloyloxydodecylpyridinium bromide – MDPB, dimethylamino dodecyl methacrylate – DMADDM and quaternary ammonium-methacrylate – QAMP), inorganic silver compounds (silver nanoparticles – AgNPs) and organic silver compounds (AgNPs bound to oleic acid – Ag-NCs).[3–5]

The organic matrix of adhesive bonding systems and polymer restorative materials is responsible for their cytotoxicity on pulpal cells. The cytotoxicity of the total-etch bonding systems is very high, as they leak into opened and widened dentinal tubuli after aggressive etching with 32–38% phosphoric acid.[6] Furthermore, due to the incomplete polymerization process enhanced by an oxygen inhibition phenomenon, the level of unbound monomer release remains high after curing.[6] Also, the compatibility of 2-hydroxyethyl methacrylate (HEMA) with water contributes to the degradation of the created bond over time, thus leading to the release of continuous monomers.[7] This phenomenon is partially eradicated in self-etching bonding systems, the composition of which makes them more compatible with a wetted dentin surface and the collagen matrix. The primer of the self-etching adhesive is acidic in nature and thus acts also as the antibacterial agent.[8] In order to minimize the cytotoxicity of the bonding systems, a liner is usually administered in deep cavities; however, its application may reduce the adhesion zone and does not always protect the pulp from the bacterial microleakage. There is no stated cavity restoration procedure that would be equally advantageous in all aspects (simultaneous disinfection, proper seal and low cytotoxicity). The usage of either the self-etching bonding systems, total-etch technique and/or antimicrobial agents has to be considered individually.

The clinical utilization of nanoparticles (NPs) and their antibacterial efficiency rely not only on their physicochemical characteristics (sizes, shapes, concentrations of released silver ions), but also on the type of bacteria (species, cell structure, sensitivity).[9–12] It is known that silver ions are toxic to aquatic organisms even at minor concentrations.[13] Silver-containing products gradually release cationic silver produced in a redox reaction with water.[13] The aqueous cellular environment favors this reaction. It remains unknown whether cytotoxicity manifested by the AgNPs results from the silver ions release or from the action of the whole particle.[13] The scientific research focuses on establishing the features of AgNPs combinations with the polymer resins, which are supposed to broaden the antibacterial range of AgNPs.[14–18] However, the incomplete polymerization of the polymer resins combined with AgNPs, along with the increase of the release of the unbound monomers, have been pointed out.[14] Taking all aspects into consideration, the literature does not clearly state if and how AgNPs can be used with the polymer resins in restorative dentistry.

Broad research on the antibacterial properties of AgNPs proved that bacteria do not show or develop drug resistance to them, so their application in dentistry might be particularly advantageous.[10,12] The level of the released silver ions is determined by the sizes of AgNPs. It was shown that 10 nm AgNPs freed many active ions, in contrast to larger AgNPs, which released only small amounts of them.[19] The sizes of AgNPs also determine their surface energy, which decides on their binding to the bacteria surface.[10,20] The mechanism of action of AgNPs against bacteria is manifested in their interactions with disulphide groups of glycoproteins blocking the bacteria living functions (providing constriction of the synthesis of the cellular wall, nucleic acids and ribosome 30S-induced proteins).[20] Furthermore, silver ions destabilize the cellular membrane (by inducing changes of its chemical potential) and reduce the level of intracellular adenosine triphosphate (ATP), the main cellular energy source.[21] An in vitro study proved that AgNPs act against *S. mutans*, *Streptococcus sobrinus* (*S. sobrinus*) and *Lactobacillus acidophilus* (*L. acidophilus*).[22] Moreover, a suppressive effect of the bacterial biofilm formation on the AgNPs-enriched surface of polymer fillings was detected, which, presumably, may minimize the risk of the recurrent caries incidence.[10,17]

To estimate the influence of silver-containing materials on the dental pulp cells, possible biological drawbacks of their application and their impact on the restorative dental materials, in vitro testing on the dental pulp stem cells (DPSCs) in needed. They are specialized adult stem cells capable of differentiating into a variety of cell types,

such as odontoblasts, osteoblasts and chondrocytes.[23] In the mature pulp tissue, the amount of the DPSCs remains stable and the division process is actuated in the case of inflammation or other dangers.[23] In laboratory conditions, the 9th passage of the DPSCs exhibits properties of an adult odontoblast.[24] Therefore, DPSCs from the 9th passage and above can be used in laboratory testing of the dental materials without the fear of the disturbances of the results. Differentiated into odontoblasts, the DPSCs secrete dentin building proteins comprising 2 main elements – dentin sialoprotein (DSP) and dentin phosphoprotein (DPP), both encoded by the same dentin sialophosphoprotein gene (*DSPP*).[24]

The aim of this study was to evaluate the vitality and secretory function of the DPSCs in response to a disinfection agent containing silver and gold NPs, different bonding systems, GIC and their combinations with the disinfection agent. Antibacterial properties of these materials were also assessed.

Material and methods

The dental materials (dentin bonding systems, GIC and disinfection liquid with NPs) used in the study are described in Table 1. Short names of the materials used alone and combined with the disinfection liquid are given in Table 2.

Nanoparticles characteristics

The evaluation of the internal structure of Nanocare Gold (NG) and its chemical composition was determined in a previous study.[25] The material comprises various shapes and sizes of NPs suspended in liquid (isopropyl alcohol) and solid (composition unknown) carriers. The material is mainly built of silver (91.34 wt%) and aluminum (4.53 wt%). Most of the AgNPs are spherical and 48 nm in diameter on average. Also, truncated AgNPs sized 125.3 nm in diameter on average were found. The smallest NP in the sample was 5.8 nm. The data from the physico-chemical analysis revealed that the concentration of AgNPs was 3.96 µg/µL (913,400 ppm). Gold was found only in a trace quantity (3.18 wt%) and was connected to a silver NP providing a conglomerate (Au-AgNP). The cross-section and the chemical analysis revealed that Au-AgNP is a dual particle made of silver as a base with a discoid flake of gold on its surface (silver – 56.91 wt%; gold – 33.98 wt%).[25]

Cell line

Human DPSCs from the 11th passage were used in the study. The cells were cultured to over 90% confluence, washed with calcium- and magnesium-free phosphate-buffered saline (PBS) and trypsinized with 0.25% trypsin-ethylenediaminetetraacetic acid (EDTA) solution. Afterwards, the DPSCs were seeded in sterile cell culture wells in a concentration of 2×10^4/cm^2. Cell number was estimated using a cell counter (Bürker counting chamber; BRAND GMBH + CO KG, Wertheim, Germany). After 24 h of incubation, the ex tempore prepared samples of the tested dental materials were added to the cells and incubated for the next 48 h. The negative control were the DPSCs cultured in the medium free from the extracts of the materials.

Table 1. Manufacturers, compositions and applications of the dental materials used in the study

Name of the material (manufacturer)	Type of the material	Composition	Application mode and time of light curing	LOT number
Clearfil SE Bond® (Kuraray Medical Inc., Kurashiki, Japan)	2-step self-etching dentin bonding system	primer: MDP, HEMA, hydrophilic dimethacrylate, N,N-diethanol-p-toluidine, water adhesive: MDP, Bis-GMA, HEMA, hydrophobic dimethacrylate, dl-campherquinone, N,N-diethanol-p-toluidine, silanated silicate	primer + adhesive application (drop/cavity) light curing 10 s	41956
OptiBond Solo Plus® (KerrHawe S.A., Scafati, Italy)	total-etch dentin bonding system	Bis-GMA, GPDM, HEMA, silica, barium glass, sodium hexafluorosilicate, ethanol, water	adhesive application (1 drop/cavity) light curing 20 s	4691988
Ketac Molar EasyMix® (3M ESPE AG, Seefeld, Germany)	glass-ionomer restorative material	liquid: polycarboxylic acid, tartaric acid, water powder: calcium, aluminum, silicon fluorosilicate glass, pigments	powder–liquid (1 measured portion: 1 drop/cavity) no light curing, chemical setting	549021
Nanocare Gold® (Dental Nanotechnology Ltd., Katowice, Poland)	accessory material (disinfection agent) comprised of silver and gold nanoparticles	liquid carrier: isoprophyl alcohol solid carrier: gel-like, unknown composition silver nanoparticles (91.34% MW), gold (scarce), silver-gold nanoparticles (0.03% MW)	application of the material (5 drops/cavity, must be left to evaporate for approx. 5 min) no light curing	270213

MDP – 10-methacryloxydecyl dihydrogen phosphate; HEMA – 2-hydroxyethyl methacrylate; Bis-GMA – bisphenol A glycidyl dimethacrylate; GPDM – glycero-phosphate dimethacrylate; MW – molecular weight.

78

A. Porenczuk, et al. The chosen properties of silver nanoparticles

Sample preparation

All tested materials were prepared in aseptic conditions in a laminar flow without artificial light and with working forced ventilation, strictly according to the manufacturers' instructions. Nanocare Gold was applied into each sterile well of a sterile 12-well plate in the amount of 5 drops (mean volume of 1 drop: 0.015 cm^3; mean density: 0.44 g/cm^3) per well and left undisturbed, allowing the carrier to evaporate so as to obtain AgNPs.[25] The bonding systems were added into the wells (alone and after application of NG) and cured with a diode polymerization lamp Bluephase® Style (Ivoclar Vivadent AG, Schaan, Liechtenstein; power of light 1100 mW/cm^2). OptiBond Solo Plus (OB) adhesive was applied in the amount of 1 drop per well (mean volume of 1 drop: 0.032 cm^3; mean density: 1.44 g/cm^3); a piece of Clearfil SE Bond (CSE) was prepared according to the manufacturer's instructions by mixing together 1 drop of CSE primer (mean volume of 1 drop: 0.0195 cm^3; mean density: 1.18 g/cm^3) and 1 drop of CSE adhesive (mean volume of 1 drop: 0.0205 cm^3; mean density: 0.99 g/cm^3) and applied in the wells in the amount of 1 piece per well. Ketac Molar EasyMix (KM) was hand-mixed and weighted so as to obtain a sample of mean weight 0.10 g and added to the wells (alone and after the application of NG). RPMI-1640 medium (2.5 mL per vial) was added to each material sample and incubated for 24 h (37°C; 5% CO$_2$). Extract medium was drawn and added to the cells in 1:1 ratio and left for further 48 h. Three replicate wells for each material and their combinations were prepared.

Assessment of cell vitality

The vitality of the DPSCs was assessed in the MTT assay after 24 and 48 h of culture. The MTT is a tetrazolium salt that is cleaved to formazan by the succinate dehydrogenase system, which belongs to the cellular mitochondrial respiratory chain. This enzyme is only active in viable cells and reduces the yellow tetrazolium salt into soluble purple formazan. The enzyme activity was measured at 540 nm in a spectophotometer (Hewlett Packard 8452; Agilent Technologies, Santa Clara, USA). The experiment was carried out in triplicate.

Secretory function of dental pulp stem cells

The secretory function of the DPSCs was measured using an enzyme-linked immunosorbent assay (ELISA) kit (Uscn Life Sciences Inc., Wuhan, China). DSP and DPP are the 2 odontoblast-specific gene products encoded by a single *DSPP* gene. Its expression occurs after the formation of a collagenous predentin matrix and is associated with the process of dentinogenesis. The sandwich enzyme immunoassay was used in order to detect the expression of the *DSPP* gene. The microtiter 96-well plate provided in this kit had been pre-coated with an antibody specific to *DSPP*. The DPSCs were seeded in a 96-well plate and treated with the extracts of the materials according to the procedure given for the vitality assay. Then, after 24 and 48 h of incubation, the supernatants were harvested for the cytokine test. The procedure proceeded strictly according to the instructions. The results of the study were obtained using the spectrophotometer at a wavelength of 450 nm (Hewlett Packard 8452; Agilent Technologies). The negative controls were the wells treated with the cell medium only. The experiment was carried out in triplicate.

Bacteria species

Standard carious bacteria species *S. mutans* ATCC® 35668™, *Streptococcus salivarius* (*S. salivarius*) ATCC® 13419™ and *L. acidophilus* ATCC® 314™ (Microbiologics, St. Cloud, USA) were used in the study. The bacteria were incubated in brain heart infusion (BHI) medium in standardized anaerobic conditions (37°C). The dental materials samples were prepared in test tubes according to the procedures given for the vitality assay, but without the medium addition. Part of the samples (dentin bonding agents) were polymerized with a diode polymerization lamp Bluephase® Style (Table 2).

Bacteria suspension preparation

The 0.5 (McFarland's density scale) suspensions of *S. mutans*, *S. salivarius* and *L. acidophilus* were prepared. Five mL of the BHI medium and 400 µL of the bacteria suspensions were added to each test tube containing previously applied dental materials. The specimens were kept tightly sealed and incubated for 48 h in standardized anaerobic conditions (37°C) with delicate shaking (100 rotations/min; Incu-Shaker Mini; Benchmark Scientific Inc., Sayreville, USA). The negative control were the bacteria in BHI culture medium without the dental materials addition.

Optical density assessment

The antibacterial properties of the dental materials were assessed by the optical density (OD) measurement of the bacteria kept in the dental materials (polymerized and not polymerized) extracts and the negative controls, and from spectrophotometer read-outs at 500 nm after 24 h and 48 h of incubation.

The bacterial percentage growth inhibition (IH(%)) was calculated using the formula:

$$IH(\%) = \left(\frac{OD_{contr} - OD_{exper}}{OD_{contr}} \right) \times 100$$

where: IH(%) – percentage growth inhibition; OD$_{contr}$ – OD of the negative control; OD$_{exper}$ – OD of the experimental specimens.

Table 2. Short names of the dental materials used in the study alone and in combination with the disinfection liquid

Dental materials used in the study			
name of the material		short name of the material	
Nanocare Gold		NG	
Ketac Molar EasyMix		KM	
Nanocare Gold/Ketac Molar EasyMix		NG/KM	
Dental materials used alone			
polymerized		not polymerized	
name of the material	short name of the material	name of the material	short name of the material
Clearfil SE Bond	CSEs	Clearfil SE Bond	CSEns
OptiBond Solo Plus	OBs	OptiBond Solo Plus	OBns
Dental materials used in combinations with the disinfection liquid			
polymerized		not polymerized	
name of the material	short name of the material	name of the material	short name of the material
Nanocare Gold/Clearfil SE Bond	NG/CSEs	Nanocare Gold/Clearfil SE Bond	NG/CSEns
Nanocare Gold/OptiBond Solo Plus	NG/OBs	Nanocare Gold/OptiBond Solo Plus	NG/OBns

Statistical analysis

Tukey's honest significance test was conducted at a significance level of 0.05 for all analyses. Pearson's correlation coefficient test was used to examine the relationships between vitality and the expression of the *DSPP* gene. Data processing was carried out using the statistical software STATISTICA v. 10 (Stat Soft Inc., Tulsa, USA).

Results

The statistical analyses of the obtained results of the MTT and ELISA assays are presented in Table 3.

Within 48 h, the vitality of cells in the NG group was the same as in the control group.

The comparison between OBs alone and NG/OBs results showed a significantly larger decrease of the vitality of the DPSCs after 48 h in NG/OBs group (p = 0.002).

Among all tested materials, the strongest cytotoxicity was observed in CSEs group during the whole observation time. In comparison to the control, both CSEs and NG/CSEs significantly decreased the cells number in both observation periods (CSEs 24 h p < 0.001; 48 h p = 0.006; NG/CSEs 24 h p < 0.001; 48 h p = 0.022). However, we found no differences between CSEs and NG/CSEs groups in terms of the vitality of the cells. Also, the vitality in NG/KM group was indifferent compared to KM alone group and the control group. Nanocare Gold did not cause any increase in the *DSPP* gene expression level in comparison to the control. In the whole observation time, both OBs and

NG/OBs relevantly raised the *DSPP* gene expression level in comparison to the control group (OBs 24 h p < 0.001; 48 h p = 0.003; NG/OBs 24 h p < 0.001; 48 h p = 0.001). However, we found no differences in the *DSPP* gene expression level between these groups. In CSEs group, the Pearson's correlation between ELISA/24 and ELISA/48 was relevantly negative (r = –1.000), which proved a positive correlation between the decrease in the *DSPP* gene expression level and the vitality of the cells, even though the results of ELISA were indifferent. Comparing CSEs to NG/CSEs, no relevant differences were found. Both KM and NG/KM groups showed no relevance in the results in comparison to the control group or to one another.

To sum up, NG proved to be biocompatible and had no influence on the *DSPP* gene expression level by DPSCs. In NG/OBs group, a large decrease in the vitality of the cells

Table 3. The statistical analyses of the results obtained for the groups of the materials in MTT assay and enzyme-linked immunosorbent assay (ELISA) in the Tukey's honest test at 0.05 significance level. Descriptive data was presented as mean values and standard deviations (SDs)

Name of the sample	MTT/24	MTT/48	ELISA/24	ELISA/48
	24 h	48 h	24 h	48 h
Control	0.270 (0.017)[AB]	0.200 (0.091)[CD]	0.095 (0.008)[FG]	0.081 (0.005)[HI]
NG	0.281 (0.053)	0.205 (0.055)	0.113 (0.023)	0.099 (0.023)
OBs	0.319 (0.049)	0.226 (0.083)[E]	0.341 (0.068)[F]	0.174 (0.006)[H]
NG/OBs	0.243 (0.037)	0.019 (0.019)[E]	0.257 (0.047)[G]	0.189 (0.059)[I]
CSEs	0.067 (0.002)[A]	0.014 (0.006)[C]	0.079 (0.007)	0.093 (0.004)
NG/CSEs	0.077 (0.006)[B]	0.042 (0.028)[D]	0.081 (0.010)	0.088 (0.003)
KM	0.300b (0.012)	0.232 (0.013)	0.098 (0.018)	0.093 (0.004)
NG/KM	0.326 (0.034)	0.264 (0.026)	0.090 (0.023)	0.085 (0.017)

[A] CSEs vs control, p < 0.001; [B] NG/CSEs vs control, p < 0.001; [C] CSEs vs control, p = 0.006; [D] NG/CSEs vs control, p = 0.022; [E] OBs vs NG/OBs, p = 0.002; [F] OBs vs control, p < 0.001; [G] NG/OBs vs control, p < 0.001; [H] OBs vs control, p = 0.003; [I] NG/OBs vs control, p < 0.001.

was observed after 48 h. The strongest cytotoxicity was observed in CSEs group during the whole observation time. Addition of NG to CSEs had no impact on its action. Both OBs and NG/OBs relevantly raised the *DSPP* gene expression level, with no differences between them. The positive correlation between the decrease in the *DSPP* gene expression and the vitality of the cells was seen in CSEs group. Neither KM nor NG/KM had any impact on the *DSPP* gene expression level.

The results of the statistical analyses of the bacterial IH(%) are presented in Fig. 1–3.

For all bacteria species, the results indicated that both NG and KM relevantly stopped bacteria growth only after 48 h of incubation (NG – 54.2%; KM – 53.0%) (Fig. 1–3). Among all tested materials, NG/KM combination proved to be effective against all bacteria species after 24 h, with the differences between its results and the results of KM (p < 0.001) and NG (p < 0.001) being significant (Fig. 1–3). Yet, after 48 h, there were no differences between these results (Fig. 1–3), apart from *S. salivarius* group, with the differences between NG/KM and KM still significant (p < 0.013) (Fig. 2). Among all tested materials, NG/KM combination seemed to be effective against *S. salivarius* after 24 h, with the differences between its results and the results of KM (p < 0.001), OBs (p < 0.001), CSEs (p = 0.016), and NG/CSEs (p < 0.001) being significant (Fig. 1–3). Yet, after 48 h, there were no differences between these results (Fig. 1–3); NG/OBs inhibited all bacteria growth in all observation periods. However, only for *L. acidophilus* did NG/OBs cause significant growth decrease after 24 h compared to OBs group alone (p = 0.006) (Fig. 3). For other bacteria (*S. mutans, S. salivarius*), addition of NG to OBs did not have any impact on its action (Fig. 1,2).

The CSEs inhibited all bacteria growth in all observation periods. The results of NG/CSE group showed that adding NG had an influence on the depletion of the antibacterial action of CSEs alone, but the results were significant only between CSEs and NG/CSEs groups toward *S. mutans* (24 h p = 0.999; 48 h p = 676) (Fig. 1). For other bacteria species (*S. salivarius* and *L. acidophilus*) in both observation times, addition of NG to CSEs had no relevant impact on its action (Fig. 2,3). Non-polymerized dentin bonding systems manifested no antibacterial activity against *S. mutans* after 24 h (Fig. 1). Non-polymerized dentin bonding systems, apart from CSEns, manifested no antibacterial activity against *S. salivarius* and *L. acidophilus* after 24 h (Fig. 2,3).

To sum up, the materials NG and KM, used alone, acted as antibacterial agents against all studied bacteria species only after 48 h of observation. Their connection (NG/KM) seemed to be efficient toward all bacteria species. The combination of NGs with total-etch system (NG/OBs) appeared to be successful against *L. acidophilus* in the first 24 h. The combination of NG with self-etching system (NG/CSEs) appeared to be unsuccessful against *S. mutans* in a longer observation period (48 h), indicating that it relevantly lowered its antibacterial potential.
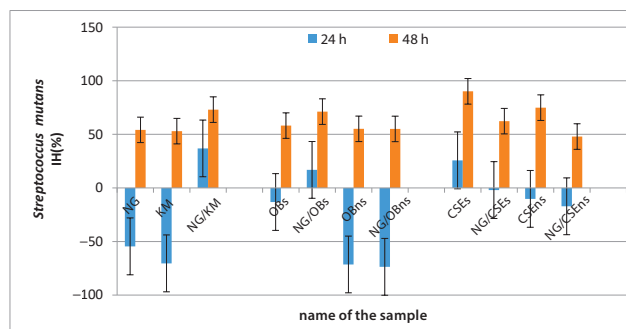
Fig. 1. The percentage growth inhibition (IH(%)) of *Streptococcus mutans* by dental materials after 24 h and 48 h of observation and the confidence intervals (CIs) based on the multiple Tukey's comparisons
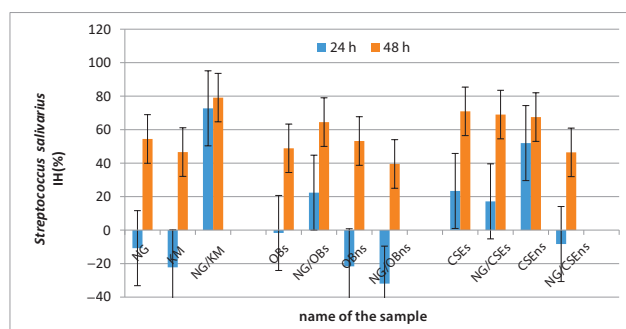
Fig. 2. The percentage growth inhibition (IH(%)) of *Streptococcus salivarius* by dental materials after 24 h and 48 h of observation and the confidence intervals (CIs) based on the multiple Tukey's comparisons
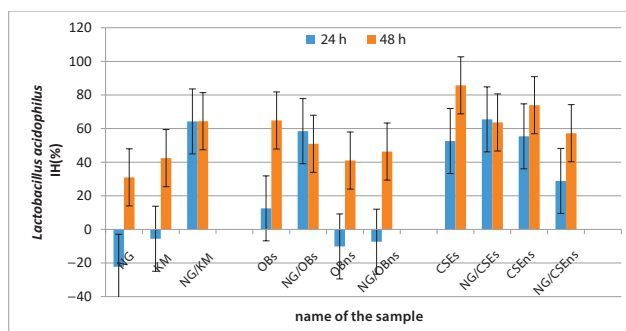
Fig. 3. The percentage growth inhibition (IH(%)) of *Lactobacillus acidophilus* by dental materials after 24 h and 48 h of observation and the confidence intervals (CIs) based on the multiple Tukey's comparisons

In the non-polymerized materials groups, only CSEns proved to act against *S. salivarius* and *L. acidophilus* for 24 h.

Discussion

Research reports indicated that AgNPs cytotoxicity was correlated with such factors as the cell line, the sizes and concentrations of NPs in the examined material, for example, NPs (1–100 nm; 100 µg/µL) were highly toxic toward

NIH3T3 mouse fibroblasts, whereas the same material was biocompatible with human colon carcinoma cells HCT116.[26] In comparison to other research on the Ag-NPs cytotoxicity, the data provided from the chemical and microscopic analysis of NG denoted that it would probably be biocompatible with the human pulp cells.[25] Nevertheless, its impact on polymer resin adhesives remained unknown. Taking different sizes, shapes and dual carriers presence into consideration, we presumed that NG might change other dental materials cytotoxicity level. In a pilot study carried out on human leukemia T lymphocyte cell line, Jurkat determined the cytotoxicity of NG alone and in combination with different adhesives. Even though NG itself proved to be biocompatible with the Jurkat cells, when mixed with polymerized OB or CSE, their cytotoxicity would rise at a statistically relevant level.[27] We concluded that these results, implying a negative impact of NG on dental adhesives, might be due to the process of NPs agglomeration interfering with the structural elements of the adhesives. This chemical reaction could possibly change the properties of polymer resins in terms of biocompatibility. Therefore, the need for research on the DPSCs arose.

The manufacturer envisaged NG to be used with the total-etch bonding systems, after the dentin etching. In this study, OB was used because it is both widely used in restorative dentistry and more biocompatible with different cell lines in comparison to other total-etch bonding systems due to smaller HEMA release after setting.[28] We also decided to include a self-etching bonding system in the study protocol. Clearfil SE Bond was thoroughly examined in various research and was proven to be one of the mildest self-etching bonding agents.[29] Both these materials (OB and CSE) possess similar properties, such as pH, inorganic filler content and the presence of dentin surface wetting components (OB – ethanol; CSE – p-toluidyne) that would not adversely interact with isopropyl alcohol in NG.

The exposition on nanomaterials can occur through direct contact, respiration or digestion. Nanoparticles may relocate from the uptake point via blood or lymphatic vessels and cause multiple side effects, such as chronic inflammation, oxygen stress, thrombosis, and other.[11] Cellular AgNPs uptake is facilitated by a clathrin-mediated endocytosis and micropinocytosis.[11] AshaRani et al. proved that the egzocytosis of small NPs (6–20 nm) is much slower than their uptake, which explains their harmful action against cells. Only 66% of the collected NPs are excreted from the cells, while the rest groups into larger conglomerates and locates near the cellular membrane and inside the nucleus.[11] This may lead to the genetic mutations and other cell malfunctions.

Compared to the control group, no differences between the MTT assay results were found in NG group, thus the material was biocompatible with the DPSCs at the early contact stage. Of all tested materials, the lowest cytotoxicity was in KM group, which stays in agreement with other research proceeded on rat stem cells (MDPC-23), where cytotoxicity of KM was the lowest compared to the control group (cellular growth inhibition – 32.5%; metabolism inhibition – 42.5%).[30] The combination of NG with KM was seen as biocompatible up to 48 h. The DSPP gene expression level by the cells in the environment of NG was similar to the control. Based on MTT and ELISA tests, NG may, therefore, be considered biocompatible. Behavior of the DPSCs in terms of the DSPP gene expression level is a result of their primary function, which is the dentin building proteins excretion in response to multiple factors. Through a boosted dentin proteins secretion, the pulpal cells are able to separate from the irritants. Even at a minor AgNPs concentration (120 µg/mL), Miura and Shinohara observed a boosted expression of the repair DNA by HeLa S3 cells.[31] The scientists have also indicated that the cytotoxicity of silver ions was incomparably higher (IC_{50} – 17 µg/mL) than of AgNPs (IC_{50} – 92 µg/mL).[31] For NG, either the concentration of AgNPs or silver ions release may be too low to cause a severe cytotoxic effect or to interfere with the DSPP gene expression level.

Within the dentin bonding systems groups, the cell death was clearly visible in NG/OBs (48 h), which indicates that these combinations of materials may not be clinically acceptable. The comparison between OBs alone and NG/OBs presented OBs as a more biocompatible material to the DPSCs. Both groups relevantly raised the DSPP gene expression level, but with no relevant differences. The largest drop in the vitality of the cells was seen in CSEs and NG/CSEs groups, and the Pearson's test confirmed the correlation between the decrease in the DSPP gene expression level along with the cell death. Due to the fact that NG turned out to be biocompatible, the decrease in the vitality of the cells must, therefore, be linked with the action of the bonding system. On the basis of the MTT test, self-etching system CSE proved to be more cytotoxic than the total-etch system OB, which may result from the methodology of the study. The differences in the vitality of the cells stayed in contrast to an in vitro study conducted by Rathke et al., who proved that CSE released relevantly smaller amounts of HEMA than OB, even after additional etching of the samples.[32] The possible explanation of our contrary results may lie within the methodology of the study. Both primer and adhesive of CSE were applied in our study, whereas only the adhesive of OB was applied. The etching step was omitted in the protocol. Therefore, on the basis of the obtained results, we may not speculate whether CSE was more or less cytotoxic toward the DPSCs in comparison to OB. Taking only cytotoxicity into consideration, these study results indicate that it may be beneficial to use NG as a disinfection agent, particularly with CSE system, as their combination had no relevant impact neither on the cytotoxicity nor on genotoxicity parameters. In contrast, addition of NG to OB does not seem satisfactory in the clinical practice, mainly because of their impact on the vitality of the cells, which was lower

in NG/OBs group indicating fast (within first 48 h) cell death. This is in agreement with the results of our pilot study, where the combination of NG and OB was also unfavorable toward the Jurkat cells.[27]

A ligand-bound NP is capable of penetrating through the bacterial cell wall, which mechanically damages it and changes its permeability. The AgNPs may lead to the damage of the respiratory chain, as well as to DNA synthesis and cell divisions disorders through their impact on the reactive oxygen species (ROS) formation.[10,12,20] Liu et al. bound AgNPs to the organic ligand (Ag-NCs) and proved that their antibacterial activity against *L. acidophilus* was directly proportional to silver concentration. At 50 ppm, the bacteria growth inhibition was 57.9% after 12 h, whereas at 100 ppm it was 66.5%.[3] This study was conducted using the same OD technique as in our study. Our results obtained for NG group indicated that the material lacked the immediate antibacterial action. The growth suppression of *S. mutans* (54.2%), *S. salivarius* (54.5%) and *L. acidophilus* (31.0%) was eminent only after 48 h, which may confirm the antibacterial property of the AgNPs composing the disinfection liquid. The differences between our percentage results and those gained by Liu et al. may lie in the amount of silver ions released from AgNPs bound to different ligands. Hernández-Sierra et al. showed that spherical AgNPs of different sizes (25, 80 and 125 nm) were capable of inhibiting *S. mutans* growth just at the concentration of 4.86 ±2.71 μg/μL, in contrast to AuNPs of the same sizes and spherical shape, which killed the bacteria only at a high concentration (197 μg/μL).[33] Nanocare Gold is an accessory liquid used for disinfecting cavities after their mechanical preparation. Our own research on its chemical composition revealed that AgNPs were tightly set and had different shapes (mostly spherical), sizes (5.8–125.3 nm) and the concentration of 3.96 μg/μL.[25] These characteristics suggest mediocre antibacterial potential (large diameters of particles, potentially low silver ions release and low wt% of gold ions). Heterogeneous sizes and shapes of the AgNPs and the presence of the Au-AgNPs conglomerates point out that there are various energy surfaces within the material, which may have an unexpected influence on other dental materials used with it. Due to the small amount of the Au-AgNPs conglomerates in NG, the impact of gold on its antibacterial features may be considered additional to that of AgNPs. Our study results remain in correlation with those obtained by Hernández-Sierra et al. due to the similarities of shapes, sizes and concentration of AgNPs. The efficacy of NG toward different carious-associated bacteria seems surprisingly similar to that of KM. Both materials used separately lowered the bacteria density only after 48 h of observation, but when used together, they demonstrated to be very powerful in bacteria growth suppression. This combination was also biocompatible with the DPSCs and had no influence on the *DSPP* gene expression. Łuczaj-Cepowicz et al. proved that KM inhibited the growth

of *S. salivarius* and *Streptococcus sanguinis* (*S. sanguinis*) after 7 days, but it had no effect on *S. mutans*.[2] The researchers emphasized that antibacterial activity of KM was aligned to many factors, including the exact chemical composition, concentration of the released fluoride ions and bacteria sensitivity.[2] Our study results confirmed the lack of antibacterial potential of KM against *S. mutans* and *S. salivarius*, yet when used together with NG, the IH(%) of *S. mutans* (IH(%)/48 = 73%) and *L. acidophilus* (IH(%)/48 = 64.4%) was relevantly higher. In the case of *L. acidophilus* and *S. mutans*, addition of NG eminently impaired antibacterial action of CSE, which may have a serious clinical impact. Therefore, their simultaneous usage cannot be considered clinically approvable. In the case of the total-etch bonding system OB, its primary antibacterial power was only slightly suppressed by the addition of the NPs. The results imply that NG boosted action of OB; NG/OBs was particularly competent against *L. acidophilus* (IH(%)/24 = 58.5%).

The polymerization process relies on the monomers cross-linking, an irreversible process that impairs the release of the monomers to the surrounding environment. Studies evaluating the differences in biological behavior of polymerized and not polymerized resins suggested that their antibacterial features were different.[34] Kim and Shin emphasized that non-polymerized dentin bonding systems performed stronger antibacterial activity than the polymerized ones, which may be explained by the lack of full cross-linking and by undisturbed free monomers release to the environment.[34] They also pointed out that some of the dentin bonding systems comprising of the antibacterial agents also acted as antibacterial agents after polymerization, but their efficiency was decreased.[34] Our study data confirms this hypothesis, particularly after 48 h of observation, where there were no differences between the results gained by the corresponding groups (polymerized and not polymerized).

Conclusions

The disinfection liquid containing silver and gold NPs and GIC proved to be biocompatible and had no effect on the secretory function of the DPSCs. The studied adhesive systems were cytotoxic and boosted the secretory function of the cells. The addition of the disinfection liquid to the dental materials had no relevant effect on their biocompatibility.

The disinfection liquid as well as the GIC acted as antibacterial agents against all studied bacteria species. The polymerized self-etching bonding system inhibited the bacteria growth. The disinfection liquid used together with the GIC seemed to be efficient toward all bacteria species. Also, its combination with the total-etch system was efficient, but it significantly impaired the antibacterial action of the self-etching bonding system.

References

1. Gonzàles-Cabezas C, Li Y, Gregory RL, Stookey GK. Distribution of three cariogenic bacteria in secondary carious lesions around amalgam restorations. *Caries Res.* 1999;33(5):357–365.
2. Łuczaj-Cepowicz E, Marczuk-Kolada G, Zalewska A, Pawińska M, Leszczyńska K. Antibacterial activity of selected glass ionomer cements. *Postepy Hig Med Dosw (Online).* 2014;68:23–28.
3. Liu F, Wang R, Shi Y, Jiang X, Sun B, Zhu M. Novel Ag nanocrystals--based dental resin composites with enhanced mechanical and antibacterial properties. *Pro Nat Sci-Mater.* 2013;23(6):573–578.
4. Zhang K, Cheng L, Wu EJ, Weir MD, Bai Y, Xu HHK. The effect of water-ageing on dentine bond strength and anti-biofilm activity of bonding agent containing new monomer dimethylaminododecyl methacrylate. *J Dent.* 2013;41(6):504–513.
5. Pupo YM, Farago PV, Nadal JM, et al. Effect of a novel quaternary ammonium methacrylate polymer (QAMP) on adhesion and antibacterial properties of dental adhesives. *Int J Mol Sci.* 2014;15(5):8998–9015.
6. Kusdemir M, Gunal S, Ozer F, et al. Evaluation of cytotoxic effects of six self-etching adhesives with direct and indirect contact tests. *Dent Mater J.* 2011;30(6):799–805.
7. Çetingüç A, Ölmez S, Vural N. HEMA diffusion from dentin bonding agents in young and old primary molars in vitro. *Dent Mater.* 2007;23(6):302–307.
8. Gondim JO, Duque C, Hebling J, Giro EMA. Influence of human dentine on the antibacterial activity of self-etching adhesive systems against cariogenic bacteria. *J Dent.* 2008;36(4):241–248.
9. Yen HJ, Hsu SH, Tsai CL. Cytotoxicity and immunological response of gold and silver nanoparticles of different sizes. *Small.* 2009;5(13):1553–1561.
10. Pal S, Tak YK, Song JM. Does the antimicrobial activity of silver nanoparticles depend on the shape of the nanoparticle? A study of the Gram-negative bacterium *Escherichia coli. Appl Environ Microbiol.* 2007;73(6):1712–1720.
11. AshaRani PV, Hande MP, Valiyaveettil S. Anti-proliferative activity of silver nanoparticles. *BMC Cell Biol.* 2009;10:65. doi: 10.1186/1471-2121-10-65
12. Prabhu S, Poulose EK. Silver NPs: Mechanism of antimicrobial action, synthesis, medical applications, and toxicity effects. *Int Nano Lett.* 2012;2:32.
13. Lee YJ, Kim J, Oh J, et al. Ion-release kinetics and ecotoxicity effects of silver nanoparticles. *Environ Toxicol Chem.* 2012;31(1):155–159.
14. Durner J, Stojanovic M, Urcan E. Influence of silver nano-particles on monomer elution from light-cured composites. *Dent Mater.* 2011;27(7):631–636.
15. Krämer N, Möhwald M, Lücker S, et al. Effect of microparticulate silver addition in dental adhesives on secondary caries in vitro. *Clin Oral Invest.* 2015;19(7):1673–1681.
16. Sokołowski K, Szynkowska MI, Pawlaczyk A, Łukomska-Szymańska M, Sokołowski J. The impact of nanosilver addition on element ions release form light-cured dental composite and compomer into 0.9% NaCl. *Acta Biochim Pol.* 2014;61(2):317–323.

17. Zhang K, Cheng L, Imazato S, et al. Effects of dual antibacterial agents MDPB and nano-silver in primer on microcosm biofilm, cytotoxicity and dentine bond properties. *J Dent.* 2013;41(5):464–474.
18. Sokołowski J, Szynkowska MI, Kleczewska J, et al. Evaluation of resin composites modified with nanogold and nanosilver. *Acta Bioeng Biomech.* 2014;16(1):51–61.
19. Li Q, Mahendra S, Lyon DY, Brunet L, Li D, Alvarez PJJ. Antimicrobial nanomaterials for water disinfection and microbial control: Potential applications and implications. *Water Res.* 2008;42(18):4591–4602.
20. Lara HH, Garza-Trevino EN, Ixtepan-Turrent L, Singh DK. Silver NPs are broad-spectrum bactericidal and virucidal compounds. *J Nanobiotechnology.* 2011;9:30. doi: 10.1186/1477-3155-9-30
21. Dibrov P, Dzioba J, Gosink KK, Hase CC. Chemiosmotic mechanism of antimicrobial activity of Ag(+) in *Vibrio cholerae. Antimicrob Agents Chemother.* 2002;46(8):2668–2670.
22. Allaker RP. The use of nanoparticles to control oral biofilm formation. *J Dent Res.* 2010;89(11):1175–1186.
23. Kacprzyńska E, Maciejewska I. Dental pulp stem cells. Possibilities of application in contemporary dentistry and future directions: Review [in Polish]. *Postepy Biologii Komorki.* 2011;38(3):467–473.
24. Feng JQ, Luan X, Wallace J, et al. Genomic organization, chromosomal mapping, and promoter analysis of the mouse dentin sialophosphoprotein (*Dspp*) gene, which codes for both dentin sialoprotein and dentin phosphoprotein. *J Biol Chem.* 1998;273(16):9457–9464.
25. Mackiewicz A, Olczak-Kowalczyk D. Microscopic evaluation of surface topography and chemical composition of Nanocare Gold. *Czas Stomatol.* 2014;6(67):826–840.
26. Hsin YH, Chen CF, Huang S, Shih TS, Lai PS, Chueh PJ. The apoptotic effect of nanosilver is mediated by a ROS- and JNK-dependent mechanism involving the mitochondrial pathway in NIH3T3 cells. *Toxicol Lett.* 2008;179(3):130–139.
27. Mackiewicz A, Grzeczkowicz A, Granicka L, et al. Cytotoxicity of Nanocare Gold® in in vitro assay: A pilot study. *Dent Med Probl.* 2015;52(2):167–173.
28. Szep S, Kunkel A, Ronge K, Heidemann D. Cytotoxicity of modern dentin adhesives: In vitro testing on gingival fibroblasts. *J Biomed Mater Res.* 2002;63(1):53–60.
29. Huang FM, Chang YC. Cytotoxicity of dentine-bonding agents on human pulp cells in vitro. *Int Endod J.* 2002;35(11):905–909.
30. De Souza Costa CA, Hebling J, Garcia-Godoy F, Hanks CT. In vitro cytotoxicity of five glass-ionomer cements. *Biomaterials.* 2003;24(21):3853–3858.
31. Miura N, Shinohara Y. Cytotoxic effect and apoptosis induction by silver nanoparticles in HeLa cells. *Biochem Biophys Res Commun.* 2009;390(3):733–737.
32. Rathke A, Alt A, Gambin N, Haller B. Dentin diffusion of HEMA released from etch-and-rinse and self-etch bonding systems. *Eur J Oral Sci.* 2007;115(6):510–516.
33. Hernández-Sierra JF, Ruiz F, Pena DCC, et al. The antimicrobial sensitivity of *Streptococcus mutans* to nanoparticles of silver, zinc oxide, and gold. *Nanomedicine.* 2008;4(3):237–240.
34. Kim SR, Shin DH. Antibacterial effect of self-etching adhesive systems on *Streptococcus mutans. Restor Dent Endod.* 2014;39(1):32–38.

MiR-494 alleviates lipopolysaccharide (LPS)-induced autophagy and apoptosis in PC-12 cells by targeting IL-13

Wei Geng[1,A,C–F], Lei Liu[2,B,D,F]

[1] Department of Spine Surgery, Liaocheng People's Hospital, China
[2] Department of Orthopedic Surgery, Liaocheng 3rd People's Hospital, China

A – research concept and design; B – collection and/or assembly of data; C – data analysis and interpretation;
D – writing the article; E – critical revision of the article; F – final approval of the article

Address for correspondence
Wei Geng
E-mail: gengwei159@126.com

Abstract

Background. MiR-494 is reported to act as a tumor-suppressive factor that inhibits the proliferation and colony formation of some cancer cells. However, there is still no report available on miR-494 functions in spinal cord injury (SCI) until now.

Objectives. The objective of this study was to examine the status of miR-494 in PC-12 cells injury induced by lipopolysaccharide (LPS), as well as its mechanism.

Material and methods. The cell counting kit-8 (CKK-8) assay and apoptosis assay were respectively used to determine the proliferation and apoptosis of PC-12. The reverse transcription polymerase chain reaction (RT-PCR) analysis and western blot analysis displayed the expression of related factors at mRNA and protein level, respectively.

Results. The results showed that LPS could significantly decrease cell viability, and promote the cell apoptosis and autophagy of PC-12 in a dose-dependent manner (p < 0.05). The overexpression of miR-494 could protect PC-12 cells from LPS-induced injury, as miR-494 overexpression increased cell viability, and reduced cell apoptosis and autophagy (p < 0.05). MiR-494 played a negative regulatory role in interleukin (IL)-13, and IL-13 was a direct target of miR-494. The overexpression of IL-13 could significantly aggravate LPS-diminished cell viability, and LPS-induced apoptosis and autophagy (p < 0.05). Besides, the overexpression of miR-494 did not attenuate LPS-induced injury when IL-13 was overexpressed. Furthermore, we found that the overexpression of miR-494 could significantly promote the phosphorylation of STAT6/MAPK and ERK/JNK signaling pathway.

Conclusions. MiR-494 could protect PC-12 cells from LPS-induced cell damage by targeting IL-13, and the activation of STAT6/MAPK and ERK/JNK pathways.

Key words: apoptosis, interleukin-13, autophagy, miR-494, PC-12

Introduction

Spinal cord injury (SCI), characterized by a high disability rate, high mortality rate and poor prognosis, is a serious disease of the central nervous system.[1,2] It is caused by lateral bending, axial loading, rotation, dislocation, and hyperextension or hyperflexion of the spinal cord, leading to the dysfunction of locomotion and paralysis. Spinal cord injury can cause damage to body functions, such as loss of feeling, abnormal reflexes, movement disorders, impairment of bowel and bladder control, and other changes. This damage cause permanent disability and many people are unable to take care of themselves. In China, nearly 60,000 new cases occur annually and the figure is rising. Unfortunately, the majority of the victims are young, between 15 and 40 years of age. Spinal cord injury brings enormous emotional and financial burdens to the patients, their families and the society.[1] The precautions, treatment and rehabilitation of SCI have been a question for study in the domain of medical science.

The pathological process of SCI involves the primary injury and secondary injury.[3] The primary injury is defined as damage to the spinal cord by mechanical force directly, such as distraction, transaction, compression, and laceration. The secondary injury that results in the evolution of physiological and biochemical reactions, such as edema, ischemia, immune responses, excitotoxicity, and electrolyte disturbances, follows the primary injury.[4] Both hypoxia-ischemia and inflammation can cause the production and release of reactive oxygen species (ROS), and massive accumulation of ROS, which leads to the oxidative injury of local tissues, as well as the apoptosis and necrosis of neurons. Therefore, it is of extreme importance to study the molecular mechanism of ROS damage following SCI.

In normal tissue, cell proliferation and growth should coexist with aging and death. There are 3 categories of cell death: apoptosis, autophagic cell death and necrosis. The former 2 deaths are also known as programmed cell death. Large empirical studies have confirmed that apoptosis and autophagy were the significant cell death form in secondary SCI.[5] Apoptosis is a process of programmed cell death, which is accurately regulated by genetic information. Once the balance between cell proliferation and apoptosis has been broken, it leads to a tumor or autoimmunity disease, or other diseases.

Caspase-3, also named as cysteine protease P32, is generally accepted as the key protease in cell apoptosis. Posttranslational activation of caspase-3 requires proteolytic cleavage of the precursor protein and is generated into 2 subunits, which leads to enzyme polymerase activation and the initialization of apoptosis. According to previous reports, caspase-3 involves neuronal apoptosis in secondary SCI, and the expression level of caspase-3 is positively correlated with the apoptosis level of nerve cells.[6] In addition, the anti-apoptotic Bcl-2 and the pro-apoptotic Bax also play important roles in regulating cell death.[7,8] Several lines of evidence indicate that the relative ratio of these 2 proteins can determine, to a great extent, the response of an individual cell to the apoptotic process.[9,10] The expression of Bcl-2 and Bax, and the ratio between Bcl-2 and Bax could regulate the apoptosis.

MicroRNAs (miRNAs) are a class of short non-coding RNAs, in the size range of 19–25 nucleotides, which regulate the expression of target genes at the post-transcriptional level by combining 3' UTR of target genes and causing translational inhibition and mRNA degradation.[11] Several studies have demonstrated that miRNAs play a key role in various cellular processes, such as cell cycle, proliferation, migration, differentiation, and tumorigenesis.[12] In recent years, a large number of researches have shown that miRNA plays important roles in the development and progression of malignant tumors.[13–15] Of note are the miRNAs that play important roles not only in human cancers, but also in cardiovascular disease, including cardiac hypertrophy, heart failure and ischemic heart disease.[16]

It has been reported that miR-494 could suppress the proliferation of some cancer cells, such as gastric cancer, lung cancer,and head and neck squamous cell carcinoma cells.[17–19] However, there has been no report available on miR-494 functions in SCI until now. In this study, we aimed to explore the effects of miR-494 on lipopolysaccharide (LPS)-injured PC-12 cells by the detection of cell viability and apoptosis, autophagy, as well as STAT6/MAPK and ERK/JNK signaling pathways. The findings of this study can provide us with a new perspective suggesting that miR-494 might exert a protective role in LPS-damaged PC-12 cells.

Material and methods

Cell culture and treatment

The PC-12 cells were purchased from the Kunming Institute of Zoology (China) and used throughout the study. The cells were seeded onto flasks at a density of 1×10^4 cells/mL in Dulbecco's Modified Eagle Medium (DMEM) (Sigma-Aldrich, St. Louis, USA) with 10% (v/v) fetal bovine serum (FBS), 100 U/mL penicillin and 100 µg/mL streptomycin. The culture was maintained at 37°C in a humidified incubator containing 5% carbon dioxide (CO_2). The culture medium was changed every other day. The 3% and 21% oxygen (O_2) concentration were as the hypoxia and normoxia culture conditions. The culture medium was changed every other day.

Cells were treated by LPS in a series of concentrations for 12 h.

Cells were treated with STAT6 inhibitor AS1517499 (100 nM), p38-MAPK inhibitor SB203580 (20 µM), JNK inhibitor SP600125 (100 nM), or ERK inhibitor PD98059 (20 µM) for 1 h.

Cell counting kit-8 assay

Cells were seeded in a 96-well plate with 5000 cells/well. Cell proliferation was assessed by a cell counting kit-8 – CCK-8 (Dojindo Molecular Technologies, Gaithersburg, USA). Briefly, after stimulation, the CCK-8 solution was added to the culture medium, and the cultures were incubated for 1 h at 37°C in humidified 95% air and 5% CO_2. The absorbance was measured at 450 nm using a microplate reader (Bio-Rad Laboratories, Hercules, USA).

Apoptosis assay

Flow cytometry analysis was performed to identify and quantify the apoptotic cells by using the Annexin-V-fluorescein isothiocyanate (FITC)/propidium iodide (PI) apoptosis detection kit (Beijing Biosea Biotechnology, Beijing, China). The cells (100,000 cells/well) were seeded in a 6-well plate. Treated cells were washed twice with cold phosphate-buffered saline (PBS) and resuspended in a buffer. The adherent and floating cells were combined and treated according to the manufacturer's instruction, and measured with a flow cytometer (Beckman Coulter, Brea, USA) to differentiate apoptotic cells (Annexin-V-positive and PI-negative) from necrotic cells (Annexin-V and PI-positive).

Transfection and generation of stably transfected cell lines

MiR-494 mimics, inhibitors and their respective negative controls (NC) were synthesized (Life Technologies Corporation, Carlsbad, USA) and transfected into cells in the study. The sequences of the oligonucleotides used were as follows: miR-494 mimic; sense 5'-UGAAACAUACACGGGAAACCUC-3'; antisense 5'-GGUUUCCCGUGUAUGUUUCAUU-3'; mimic control; sense 5'-UUCUCCGAACGUGUCACGUUU-3'; antisense 5'-ACGUGACACGUUCGGAGAAUU-3'; miR-494 inhibitor 5'-GAGGUUUCCCGUGUAUGUUUCA-3'; and inhibitor control 5'-UUCUCCGAACGUGUCACGUUUC-3'. For the analysis of the interleukin (IL)-13 functions, the full-length IL-13 sequences and short-hairpin RNA directed against IL-13 were constructed in pEX-2 and U6/GFP/Neo plasmids (GenePharma, Shanghai, China), respectively. They were referred as to pEX-IL-13 and sh-IL-13. The Lipofectamine 3000 reagent (Life Technologies Corporation) was used for the transfection of the cells according to the manufacturer's instructions. The plasmid carrying a non-targeting sequence was used as the NC of sh-IL-13 that was referred as to sh-NC. The sequences of the shRNAs used were as follows: sh-IL-13, 5'-AATGCCATCTACAGGACCCAG-3'; sh-NC, 5'-AAAGGTATGGTACGACGGCGT-3'. Since the highest transfection efficiency occurred at 48 h, a 72-hour post-transfection was considered as the harvest time in the subsequent experiments. The stably transfected cells were selected by the culture medium containing 0.5 mg/mL G418 (Sigma-Aldrich). After approx. 4 weeks, G418-resistant cell clones were established.

Qualitative reverse transcription polymerase chain reaction

Total RNA was extracted from cells and tissues using Trizol reagent (Life Technologies Corporation), according to the manufacturer's instructions. The TaqMan MicroRNA Reverse Transcription Kit and TaqMan Universal Master Mix II with the TaqMan MicroRNA Assay of miR-494 and U6 (Applied Biosystems, Foster City, USA) were used for testing the expression levels of miR-494 in cells.

Dual luciferase activity assay

The 3'UTR target site was generated by polymerase chain reaction (PCR) and the luciferase reporter constructs with IL-13 3'UTR, carrying a putative miR-494 binding site into pMiR-report vector, were amplified by PCR. Cells were co-transfected with the reporter construct, control vector and miR-494 or scramble, using Lipofectamine 3000. Reporter assays were done using the dual luciferase assay system (Promega, Madison, USA), following the manufacturer's information.

Western blot

The protein used for western blotting was extracted using Radio Immunoprecipitation Assay (RIPA) lysis buffer (Beyotime Biotechnology, Shanghai, China) supplemented with protease inhibitors (Roche, Guangzhou, China). The proteins were quantified using the BCA™ Protein Assay Kit (Pierce, Appleton, USA). The western blot system was established using a Criterion XT Bis-Tris Gel system (Bio-Rad Laboratories), according to the manufacturer's instructions. The glyceraldehyde 3-phosphate dehydrogenase (GAPDH) antibody was purchased from Sigma-Aldrich. Primary antibodies were prepared in 5% blocking buffer at a dilution of 1:1,000. Anti-Bcl-2 (ab59348), anti-Bax (ab32503), anti-pro-caspase-3 (ab32150), anti-cleaved-caspase-3 (ab13847), anti-caspase-9 (ab202068), anti-LC3B (ab48394), anti-Beclin-1 (ab62557), anti-p62 (ab56416), anti-IL-13 (ab106732), anti-STAT6 (ab32520), anti-p-STAT6 (ab28829), anti-p38MAPK (ab197348), anti-p-p38MAPK (ab47363), anti-ERK (ab54230), anti-p-ERK (ab214362), anti-p-c-Jun (ab32385), anti-c-Jun (ab31419), and anti-GAPDH (ab8245) were all obtained from Abcam (Cambridge, UK). Primary antibody was incubated with the membrane at 4°C overnight, followed by wash and incubation with secondary antibody, marked by horseradish peroxidase for 1 h at room temperature. After rinsing, the polyvinylidene difluoride (PVDF) membrane carried blots and the antibodies were transferred into the Bio-Rad ChemiDoc™ XRS system (Bio-Rad, Shanghai, China), and

then 200 µL of Immobilon Western Chemiluminescent HRP Substrate (Merck Millipore, Burlington, USA) was added to cover the membrane surface. The signals were captured and the intensity of the bands was quantified using Image Lab™ Software (Bio-Rad, Shanghai, China).

Statistical analysis

All the experiments were repeated 3 times. Data is presented as the mean ± standard deviation (SD). Statistical differences between the mean values of multiple groups were analyzed using SPSS v. 19.0 statistical software (IBM Corp., Armonk, USA). Statistical significance was analyzed by using analysis of variance (ANOVA), followed by the least significant difference (LSD(L)) test post-hoc. A p-value <0.05 was considered to indicate statistical difference.

Results

Lipopolysaccharide inhibited cell proliferation, and promoted cell apoptosis and autophagy of PC-12

As shown in Fig. 1A, the cell viability of PC-12 was significantly decreased as the concentrations of LPS increased (p < 0.05). On the contrary, the cell apoptosis rate of PC-12 was significantly increased as the concentrations of LPS increased (p < 0.05) (Fig. 1B). Western blot analysis (Fig. 1C) showed that the expression of Bcl-2 was decreased, and the expression of Bax and cleaved-caspase-3/9 was increased as the concentrations of LPS increased. Moreover, we detected the expression of autophagy-related proteins. The results (Fig. 1D) showed that the expression of LC-II and Beclin-1 was increased, and the expression of p62 was decreased as the concentrations of LPS increased. This data indicated that LPS could promote cell apoptosis and autophagy of PC-12 in a dose-dependent manner, and 5 ug/mL was selected as a LPS-stimulatory condition which was used in this study.

Overexpression of miR-494 alleviated cell damage induced by lipopolysaccharide

As shown in Fig. 2A, transfection with miR-494 mimic could significantly increase the expression of miR-494, while miR-494 inhibitor could significantly decrease the expression of miR-494 (p < 0.05). To test the role of miR-494 in LPS-stimulated PC-12, the CCK-8 and apoptosis assays were performed (Fig. 2B,C). We found that miR-494 overexpression significantly increased cell viability and decreased apoptosis under LPS treatment conditions (p < 0.05). Contrastingly, miR-494 suppression decreased cell viability and increased apoptosis under LPS exposure (p < 0.05). Western blot analysis showed that the over-expression of miR-494 could increase the expression of Bcl-2 and p62, and decrease the expression of Bax, cleaved-caspase-3/9, LC3-II, and Beclin-1 (Fig. 2D,E). On the contrary, the expression of these proteins in miR-494 knock-down group showed the reverse trend. These results indicated that the overexpression of miR-494 could reduce the cell damage induced by LPS, while miR-494 knock-down could aggravate it.
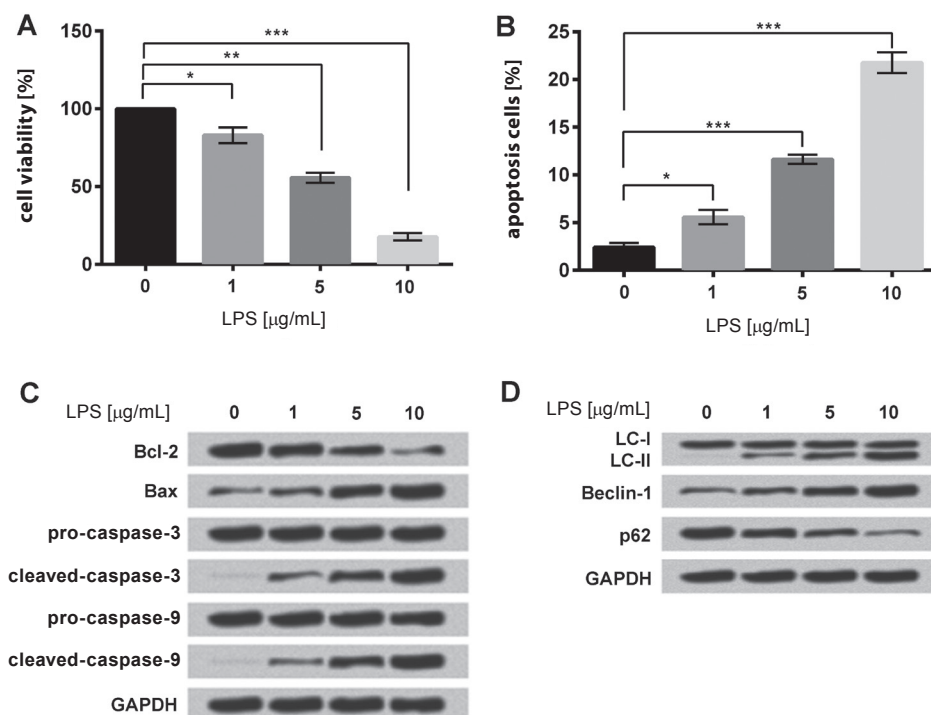
Fig. 1. Lipopolysaccharide affects cell proliferation, apoptosis and autophagy of PC-12

A – cell viability detected using MTT assay; B – apoptosis of PC-12 detected using apoptosis assay; C – apoptosis-related proteins detected using western blot; D – autophagy-related proteins detected using western blot.

LPS – lipopolysaccharide; MTT – methylthiazol tetrazolium; GAPDH – glyceraldehyde 3-phosphate dehydrogenase; data presented as mean ±SD; * p < 0.05; ** p < 0.01; *** p < 0.001.
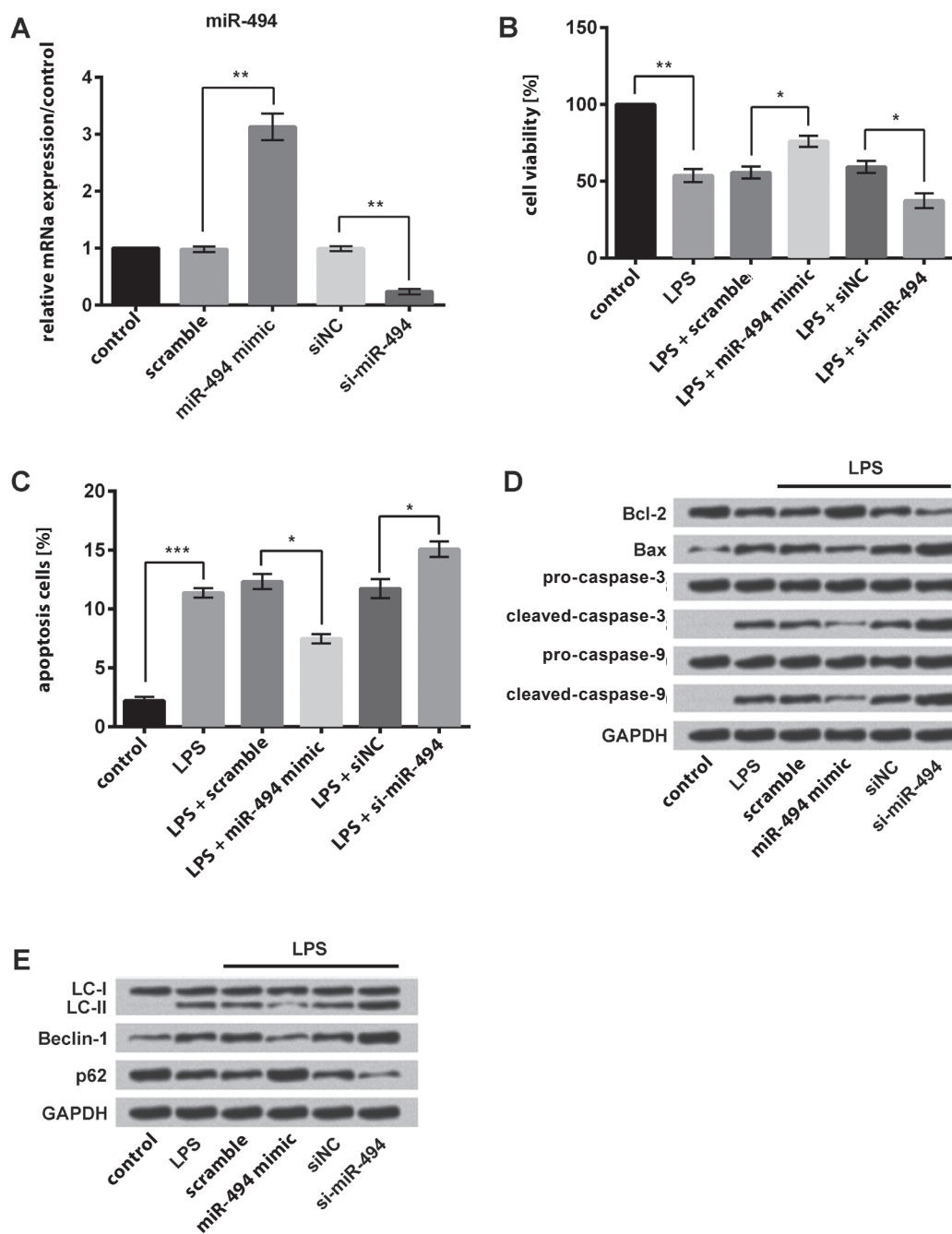
Fig. 2. MiR-494 affects cell proliferation, apoptosis and autophagy of PC-12

A – expression of miR-494 detected using RT-PCR;
B – cell viability detected using MTT assay;
C – apoptosis of PC-12 detected using apoptosis assay; D – apoptosis-related proteins detected using western blot; E – autophagy-related proteins detected using western blot.

RT-PCR – reverse transcription polymerase chain reaction; MTT – methylthiazol tetrazolium; GAPDH – glyceraldehyde 3-phosphate dehydrogenase; data presented as mean ±SD; * $p < 0.05$; ** $p < 0.01$; *** $p < 0.001$.

Interleukin-13 was a direct target of miR-494

As shown in Fig. 3A and 3B, the overexpression of miR-494 could significantly decrease the expression of IL-13, while miR-494 knock-down could significantly increase the expression of IL-13 ($p < 0.05$), indicating that miR-494 acted as a negative regulation of IL-13. In addition, we found that the overexpression of miR-494 inhibited the luciferase activity of Wt-3'UTR of IL-13 by about 70% compared to the mutated miR-494 binding site (Fig. 3C). These results indicated that IL-13 was a direct target of miR-494.

Overexpression of miR-494 protected PC-12 cells from lipopolysaccharide-induced cell damage via targeting interleukin-13

As shown in Fig. 4A and 4B, transfection with the IL-13 expressing vector, pEX-IL-13, could significantly increase the expression of IL-13, while transfection with IL-13 targeted shRNA, sh-IL-13, could significantly decrease the expression of IL-13 ($p < 0.05$). We found that miR-494 overexpression did not prevent LPS-induced cell damage when IL-13 was overexpressed, as cell viability was reduced, Bcl-2 was downregulated, and Bax, cleaved-caspase-3/9 were upregulated after the addition of pEX-IL-13 ($p < 0.05$) (Fig. 4C,E).
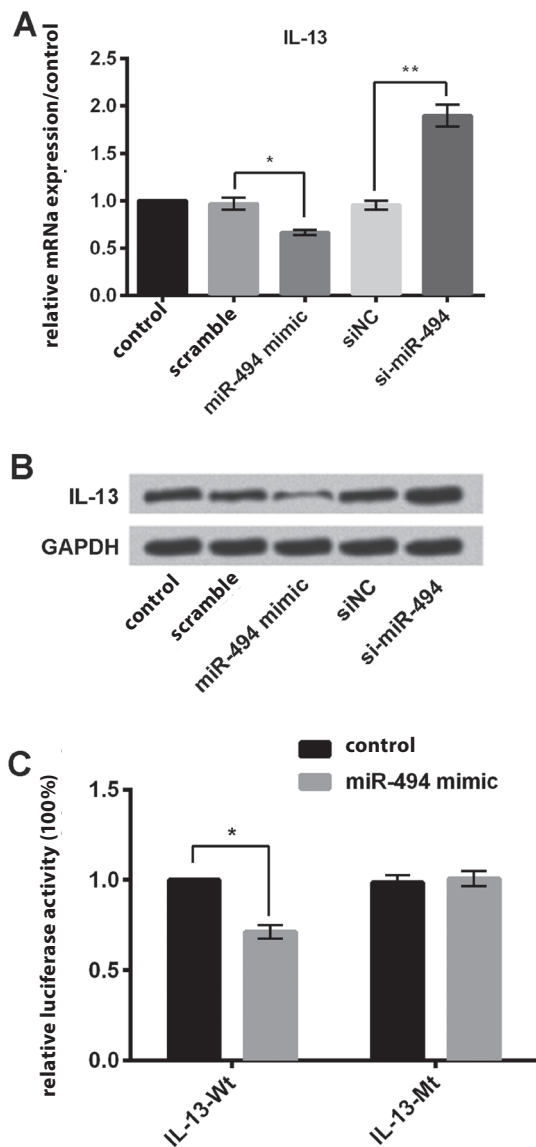
Fig. 3. IL-13 is a direct target of miR-494

A, B – expression of IL-13 detected with RT-PCR; C – dual luciferase assay performed on PC-12 cells transfected with luciferase construct alone or co-transfected with miR-494 mimics.

IL-13 – interleukin-13; RT-PCR – reverse transcription polymerase chain reaction; data presented as mean ±SD; * p < 0.05; ** p < 0.01.

Meanwhile, miR-494 knock-down could not aggravate LPS-induced cell damage when IL-13 was silenced, as cell apoptosis was reduced, LC3-II and Beclin-1 were down-regulated, while p65 was upregulated after the addition of sh-IL-13 (p < 0.05) (Fig. 4D,E). This data indicated that the overexpression of miR-494 protected PC-12 cells from LPS-induced cell damage via targeting IL-13.

Interleukin-13 regulated cell damage of PC-12 induced by lipopolysaccharide

As shown in Fig. 5A, the overexpression of IL-13 could significantly aggravate the proliferation inhibition of PC-12 induced by LPS (p < 0.05), while the knock-down of IL-13

could significantly reduce the proliferation inhibition of PC-12 induced by LPS (p < 0.05). Figure 5B showed that the overexpression of IL-13 could significantly promote the cell apoptosis of PC-12 induced by LPS (p < 0.05), while the knock-down of IL-13 could significantly inhibit the cell apoptosis of PC-12 induced by LPS (p < 0.05). Western blot analytical results showed that IL-13 silence exerted the same effects as miR-494 overexpression on the expression of apoptosis and autophagy-related proteins (Fig. 5C,D), indicating the pro-apoptotic and pro-autophagic roles of IL-13 in PC-12 cells.

MiR-494 activated the STAT6/MAPK and ERK/JNK signaling pathways

Western blotting was used to examine the phosphorylation state of STAT6/MAPK and ERK/JNK in PC-12 cells that were treated with LPS (Fig. 6A,B). The results showed that the overexpression of miR-494 could significantly increase the expression of p-STAT6, p-p38MAPK, p-ERK, and p-c-Jun, while its knock-down could significantly decrease the expression of p-STAT6, p-p38MAPK, p-ERK, and p-c-Jun. These findings indicated that the knock-down of miR-494 inhibited STAT6/MAPK and ERK/JNK signaling pathway through upregulating the expression of IL-13, thus promoting the cell damage of PC-12 induced by LPS. Furthermore, to confirm this hypothesis, we measured the effect of miR-494 on the expression of p-STAT6, p-p38MAPK, p-ERK, and p-c-Jun after the inhibition of STAT6/MAPK and ERK/JNK pathways. As indicated by the results in Fig. 6C and 6D, miR-494 overexpression did not upregulate p-STAT6, p-p38MAPK, p-ERK, or p-c-Jun when they were respectively exposed to STAT6 inhibitor AS1517499, p38-MAPK inhibitor SB203580, ERK inhibitor PD98059, or JNK inhibitor SP600125.

Discussion

Spinal cord injury is a common traumatic neuronal injury that imposes several complications and is a severe threat to human health.[20] The microenvironment after SCI in adults is much less receptive to regrowth, thus hindering the regeneration of the damaged nerve.[21] Therefore, the key method of improving SCI patient's outcomes is by utilizing protecting neurons, promoting the axonal regeneration. PC-12 cells are widely used as an in vitro neuron model for research on neurobiology, central nervous system diseases and neuro-toxins. In the present study, we found that LPS could induce the cell damage of PC-12 via inhibiting cell proliferation, and promoting cell apoptosis and autophary, and the damage degree increased with increasing LPS concentration.

According to our data mentioned above, we found that LPS had a remarkable inhibition effect on the cell proliferation of PC-12, while promoting cell apoptosis and autophagy (Fig. 1). Apart from that, we found that LPS
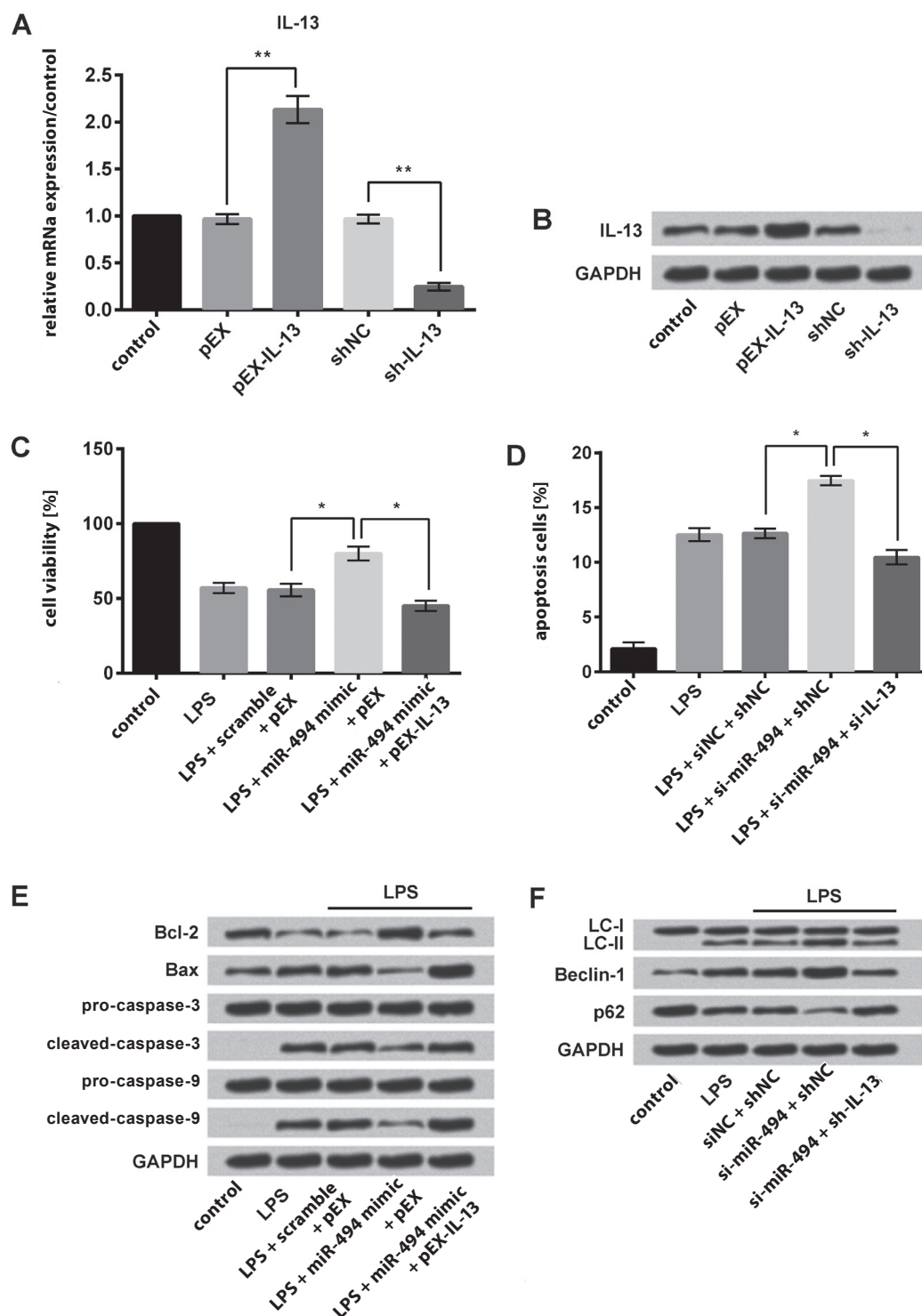
Fig. 4. Overexpression of miR-494 protected PC-12 cells from LPS-induced cell damage via targeting IL-13

A, B – expression of IL-13 detected with RT-PCR; C – cell viability detected with MTT assay; D – apoptosis of PC-12 detected with apoptosis assay; E – apoptosis-related proteins detected with western blot; F – autophagy-related proteins detected with western blot.

LPS – lipopolysaccharide; IL-13 – interleukin-13; RT-PCR – reverse transcription polymerase chain reaction; MTT – methylthiazol tetrazolium; GAPDH – glyceraldehyde 3-phosphate dehydrogenase; data presented as mean ±SD; * p < 0.05; ** p < 0.01.

could decrease the expression of Bcl-2, and increase the expression of Bax and caspase-3/9, thus promoting the apoptosis of PC-12. However, miR-494 could protect PC-12 cells from LPS-induced cell damage, as miR-494 overexpression increased cell viability, reduced apoptosis and autophagy, as well as increase the expression of Bcl-2 and decrease the expression of Bax and caspase-3/9.

MiR-494, first reported to have a high expression in retinoblastoma, has been found to be implicated in various types of human cancers.[22] In cancer, miR-494 functions as a tumor suppressor or oncogenic gene, dependent on different cell types.[23] Apart from that, miR-494 was reported to act as a pivotal factor in regulating cell proliferation and apoptosis.[24] In terms of SCI, miR-494 was reported to improve recovery from SCI and to attenuate apoptosis in SCI rats.[25] Our study was consistent with this previous study, indicating that miR-494 exerted a protective function in SCI by reducing apoptosis, while our study provided the first evidence that miR-494 affected PC-12 cells also by controlling cell autophagy.

A

B
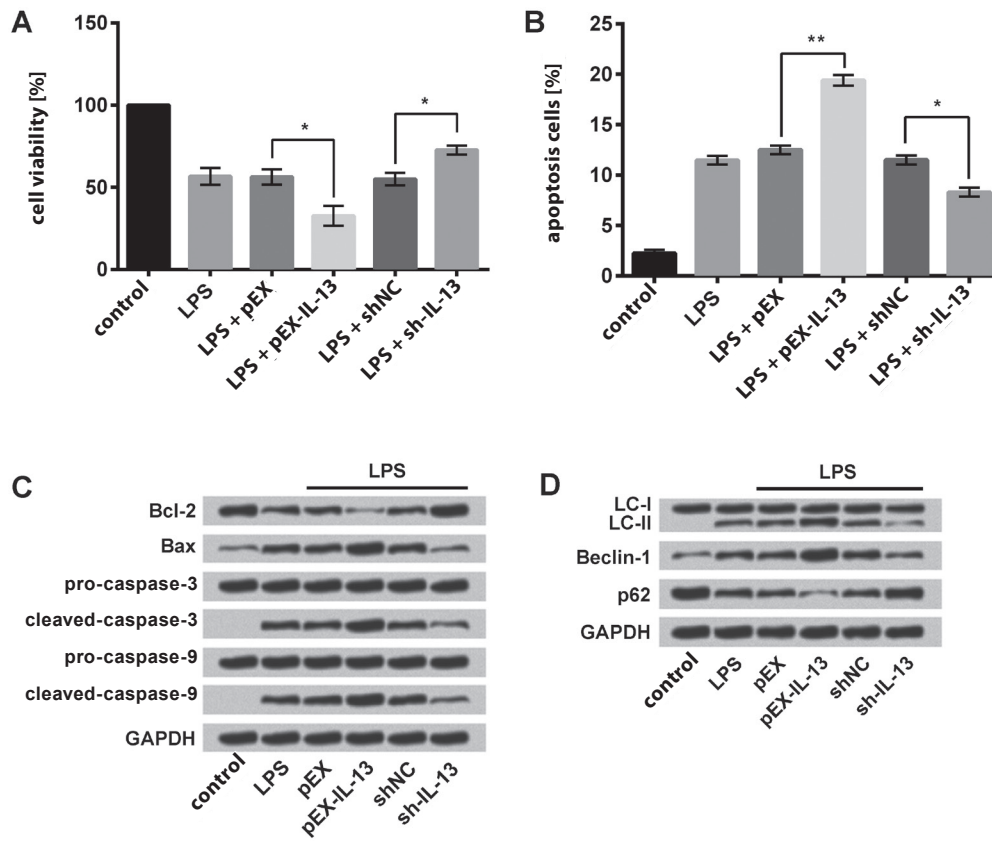
Fig. 5. IL-13 regulated cell damage induced by LPS

A – cell viability detected with MTT assay; B – apoptosis of PC-12 detected with apoptosis assay; C – apoptosis-related proteins detected with western blot; D – autophagy-related proteins detected with western blot.

IL-13 – interleukin-13; LPS – lipopolysaccharide; MTT – methylthiazol tetrazolium; GAPDH – glyceraldehyde 3-phosphate dehydrogenase; data presented as mean ±SD; * p < 0.05; ** p < 0.01.

C

D

A

B
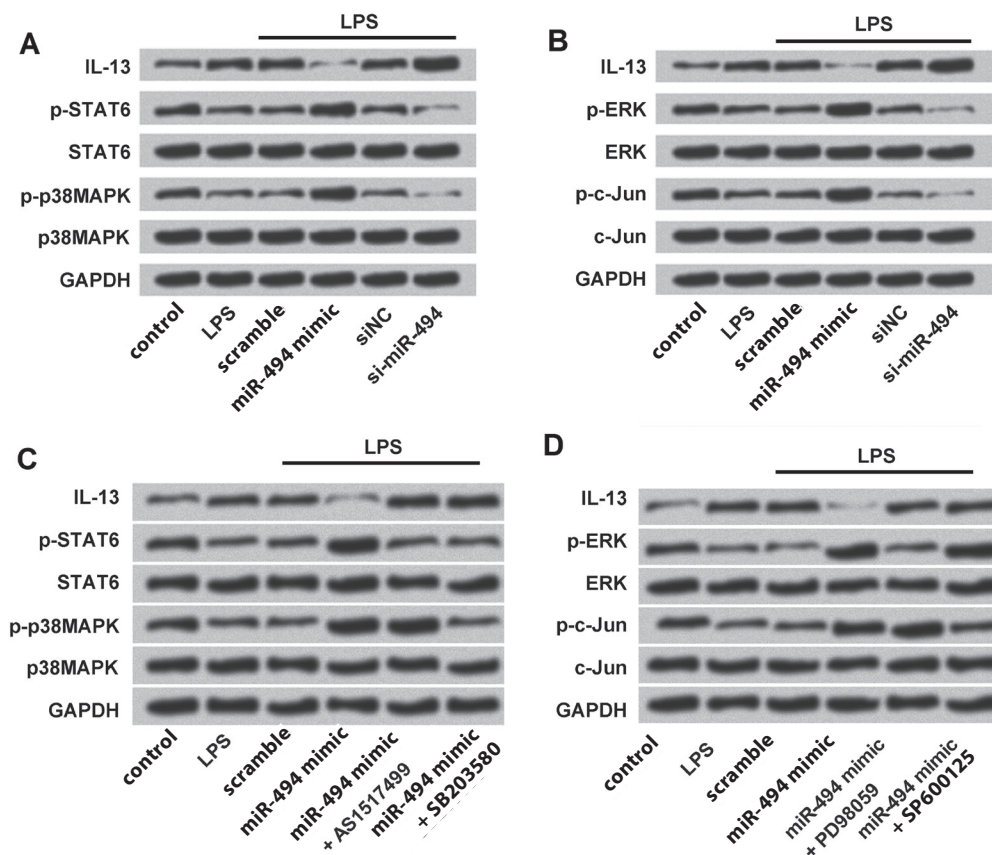
Fig. 6. MiR-494 affected expression of STAT6/MAPK and ERK/JNK pathways

A, C – STAT6/MAPK signaling pathway-related proteins detected using western blot; B, D – ERK/JNK signaling pathway-related proteins detected using western blot.

GAPDH – glyceraldehyde 3-phosphate dehydrogenase; LPS – lipopolysaccharide; MAPK – mitogen-activated protein kinase; ERK – extracellular signal transduction kinase.

C

D

Autophagy is a unique life phenomenon of eukaryotes, which can degrade and recycle unnecessary or dysfunctional components.[26,27] It plays an important role in the occurrence, development and treatment of the nervous system, digestive system and immune system diseases. Beclin-1 is an important factor in the initial period of autophagy, which is a mammalian ortholog of the yeast Atg6.[28] With the action of Atg4, LC3 precursor is processed into soluble LC3-I, which combines with PE on the autophagic membrane, and then changes into LC3-II, which then attaches to the intracellular autophagic membrane until the autophagy-lysosome is formed. The LC3-II expression level is positively related to the sum of phagophores, suggesting that autophagy activity is closely related to the expression intensity of LC3-II.[29,30] In addition, p62 located in the cytoplasm forms complexes by combining with ubiquitin protein and LC3-II protein. The complexes will eventually be degraded in the lysosome.[31] Therefore, p62 is constantly consumed in the process of autophagy. These 3 proteins are usually recognized as the markers of the autophagy level.[32–34] The above-mentioned results showed that LPS increased the expression of LC3-II and Beclin-1, and decreased the expression of p62, suggesting that LPS promoted PC-12 autophagy. However, the overexpression of miR-494 decreased the expression of LC3-II and Beclin-1, and increased the expression of p62, indicating that miR-494 could reduce the autophagy of PC-12 induced by LPS.

Mitogen-activated protein kinase (MAPK) is one kind of serine/threonine protein kinase which widely exists in eukaryotic cells. The family consists of extracellular signal transduction kinase (ERK), c-Jun-N-terminal kinase (JNK) and p38 kinase, etc.[35] Extracellular signal transduction kinase mainly participates in cell proliferation, differentiation and transformation, while JNK and p38 are associated with intracellular and extracellular damage, infarct, inflammation, and oxidative stress reaction.[36–38] It has been reported that MAPK pathways have anti-apoptotic effects in C6 glioma cells.[39] In this paper, we found that the knock-down of miR-494 could inhibit the activation of STAT6/MAPK and ERK/JNK pathways, thus promoting LPS-induced cell damage.

In conclusion, our study suggested that miR-494 could protect PC-12 cells from LPS-induced cell damage by controlling cell proliferation, cell apoptosis and autophagy. The protective role of miR-494 in PC-12 cells might be carried out via targeting IL-13, and thus through the activation of STAT6/MAPK and ERK/JNK pathways. Our findings might provide better insight into the function of miR-494 in LPS-induced cell damage, which could contribute to clinical treatment of SCI.

References

1. Ackery A, Tator C, Krassioukov A. A global perspective on spinal cord injury epidemiology. *J Neurotrauma*. 2004;21(10):1355–1370.
2. Böthig R, Fiebag K, Thietje R, Faschingbauer M, Hirschfeld S. Morbidity of urinary tract infection after urodynamic examination of hospitalized SCI patients: The impact of bladder management. *Spinal Cord*. 2013;51(1):70.
3. Li S, Tator CH. Spinal cord blood flow and evoked potentials as outcome measures for experimental spinal cord injury. In: Stålberg E, Shanker Sharma H, Olsson Y, eds. *Spinal Cord Monitoring: Basic Principles, Regeneration, Pathophysiology, and Clinical Aspects*. Vienna, Austria: Springer; 1998:365–392.
4. Jones TB. Lymphocytes and autoimmunity after spinal cord injury. *Exp Neurol*. 2014;258:78.
5. Yune TY, Kim SJ, Lee SM, et al. Systemic administration of 17beta-estradiol reduces apoptotic cell death and improves functional recovery following traumatic spinal cord injury in rats. *J Neurotrauma*. 2004;21(3):293–306.
6. Springer JE. Apoptotic cell death following traumatic injury to the central nervous system. *J Biochem Mol Biol*. 2002;35(1):94–105.
7. Kroemer G, Galluzzi L, Brenner C. Mitochondrial membrane permeabilization in cell death. *Physiol Rev*. 2007;87(1):99–163.
8. Green DR, Kroemer G. The pathophysiology of mitochondrial cell death. *Science*. 2004;305(5684):626–629.
9. Boise LH, González-García M, Postema CE, et al. Bcl-x, a Bcl-2-related gene that functions as a dominant regulator of apoptotic cell death. *Cell*. 1993;74:597–608.
10. Oltvai ZN, Milliman CL, Korsmeyer SJ. Bcl-2 heterodimerizes in vivo with a conserved homolog, Bax, that accelerates programmed cell death. *Cell*. 1993;74(4):609–619.
11. Garzon R, Pichiorri F, Palumbo T, et al. MicroRNA gene expression during retinoic acid-induced differentiation of human acute promyelocytic leukemia. *Oncogene*. 2007;26(28):4148–4157.
12. Schickel R, Boyerinas B, Park SM, Peter ME. MicroRNAs: Key players in the immune system, differentiation, tumorigenesis, and cell death. *Oncogene*. 2008;27(45):5959–5974.
13. Huang Y, Dai Y, Yang J, et al. Microarray analysis of microRNA expression in renal clear cell carcinoma. *Eur J Surg Oncol*. 2009;35(10):1119–1123.
14. Shenouda SK, Alahari SK. MicroRNA function in cancer: Oncogene or a tumor suppressor? *Cancer Metastasis Rev*. 2009;28(3-4):369–378.
15. Calin GA, Croce CM. MicroRNA signatures in human cancers. *Nat Rev Cancer*. 2006;6(11):857–866.
16. Lv G, Shao S, Dong H, Bian X, Yang X, Dong S. MicroRNA-214 protects cardiac myocytes against H2 O2-induced injury. *J Cell Biochem*. 2014;115(1):93–101.
17. Kim WK, Park M, Kim YK, et al. MicroRNA-494 downregulates KIT and inhibits gastrointestinal stromal tumor cell proliferation. *Clin Cancer Res*. 2011;17(24):7584–7594.
18. Ohdaira H, Sekiguchi M, Miyata K, Yoshida K. MicroRNA-494 suppresses cell proliferation and induces senescence in A549 lung cancer cells. *Cell Prolif*. 2012;45(1):32.
19. Chang SS, Jiang WW, Smith I, et al. MicroRNA alterations in head and neck squamous cell carcinoma. *Int J Cancer*. 2008;123(12):2791.
20. Kang N, Hai Y, Yang J, Liang F, Gao CJ. Hyperbaric oxygen intervention reduces secondary spinal cord injury in rats via regulation of HMGB1/TLR4/NF-κB signaling pathway. *Int J Clin Exp Pathol*. 2015;8(2):1141–1153.
21. Nakamura M, Bregman B. Differences in neurotrophic factor gene expression profiles between neonate and adult rat spinal cord after injury. *Exp Neurol*. 2001;169(2):407–415.
22. Zhao JJ, Yang J, Lin J, et al. Identification of miRNAs associated with tumorigenesis of retinoblastoma by miRNA microarray analysis. *Childs Nerv Syst*. 2009;25(1):13–20.
23. Zhan MN, Yu XT, Tang J, et al. MicroRNA-494 inhibits breast cancer progression by directly targeting PAK1. *Cell Death Dis*. 2017;8(1):e2529.
24. Romano G, Acunzo M, Garofalo M, et al. MiR-494 is regulated by ERK1/2 and modulates TRAIL-induced apoptosis in non-small-cell lung cancer through BIM down-regulation. *Proc Natl Acad Sci U S A*. 2012;109(41):16570–16575.

25. Gu S, Xie R, Liu X, Shou J, Gu W, Che X. Long coding RNA XIST contributes to neuronal apoptosis through the downregulation of AKT phosphorylation and is negatively regulated by miR-494 in rat spinal cord injury. *Int J Mol Sci*. 2017;18(4):732–748.

26. Mizushima N, Levine B, Cuervo AM, Klionsky DJ. Autophagy fights disease through cellular self-digestion. *Nature*. 2008;451(7182): 1069–1075.

27. Ding WX. Role of autophagy in liver physiology and pathophysiology. *World J Biol Chem*. 2010;1(1):3–12.

28. Sui YQ, Feng YZ. Expression and clinical significance of autophagy-related genes LC3, Beclin-1 and apoptosis-related genes p53, BCL-2 in colorectal carcinoma. *J Clin Exp Pathol*. 2012;28:282–286.

29. Mizushima N. Methods for monitoring autophagy. *Int J Biochem Cell Biol*. 2005;36(12):2491–2502.

30. Kabeya Y, Mizushima N, Ueno T, et al. LC3, a mammalian homologue of yeast Apg8p, is localized in autophagosome membranes after processing. *EMBO J*. 2000;19(21):5720–5728.

31. Pankiv S, Clausen TH, Lamark T, et al. p62/SQSTM1 binds directly to Atg8/LC3 to facilitate degradation of ubiquitinated protein aggregates by autophagy. *J Biol Chem*. 2007;282(33):24131–24145.

32. Mai S, Muster B, Bereiterhahn J, Jendrach M. Autophagy proteins LC3B, ATG5 and ATG12 participate in quality control after mitochondrial damage and influence life span. *Autophagy*. 2012;8(1):47–62.

33. Backer JM. The regulation and function of Class III PI3Ks: Novel roles for Vps34. *Biochem J*. 2008;410(1):1–17.

34. Klionsky DJ, Abeliovich H, Agostinis P, et al. Guidelines for the use and interpretation of assays for monitoring autophagy in higher eukaryotes. *Autophagy*. 2015;8(4):445–544.

35. Keren A, Tamir Y, Bengal E. The p38 MAPK signaling pathway: A major regulator of skeletal muscle development. *Mol Cell Endocrinol*. 2006; 252(1–2):224.

36. Huppertz B, Kingdom JCP. Apoptosis in the trophoblast: Role of apoptosis in placental morphogenesis. *J Soc Gynecol Investig*. 2004; 11(6):353–362.

37. Davis RJ. Signal transduction by the JNK group of MAP kinases. *Cell*. 2000;103(2):239.

38. Dhanasekaran DN, Reddy EP. JNK signaling in apoptosis. *Oncogene*. 2008;27(48):6245–6251.

39. Feng Y, Huang J, Ding Y, Xie F, Shen X. Tamoxifen-induced apoptosis of rat C6 glioma cells via PI3K/Akt, JNK and ERK activation. *Oncol Rep*. 2010;24(6):1561–1567.

Dorsal and volar wrist ganglions: The results of surgical treatment

Sebastian Kuliński[1,A–D], Olga Gutkowska[1,B,C,E], Sylwia Mizia[2,C,F], Jacek Martynkiewicz[1,B,C,E], Jerzy Gosk[1,A,C,E,F]

[1] Clinic of Traumatology and Hand Surgery, Department of Traumatology, Wroclaw Medical University, Poland
[2] Division of Organization and Management, Department of Public Health, Faculty of Health Sciences, Wroclaw Medical University, Poland

A – research concept and design; B – collection and/or assembly of data; C – data analysis and interpretation;
D – writing the article; E – critical revision of the article; F – final approval of the article

Address for correspondence
Sebastian Kuliński
E-mail: sebastiankulinski@wp.pl

Abstract

Background. The wrist, especially its dorsal surface, is the most common location of ganglion cysts in the human body.

Objectives. The purpose of this study was to present our experience in the treatment of wrist ganglions and to evaluate the results obtained with the operative management of this type of lesion.

Material and methods. A total of 394 patients (289 females and 105 males, aged 10–83 years) treated operatively for wrist ganglions between 2000 and 2014 were included in the study. The results of surgical treatment were evaluated after a minimal 2-year-long follow-up in 69.4% of patients operated on for dorsal wrist ganglions and in 70.6% of patients after the excision of volar wrist ganglions. The shape and size of postoperative scar, range of motion of the wrist, grip strength, severity of pain, and presence/absence of ganglion recurrence were assessed. The influence of demographic factors on the risk of recurrence was statistically analyzed.

Results. Persistent limitation of wrist palmar flexion was observed in 6 patients after the removal of dorsal wrist ganglions. There were no cases of postoperative grip strength weakening. An unesthetic scar developed in 15 patients after the excision of dorsal wrist ganglions and in 6 patients after the removal of volar wrist ganglions. Postoperative pain was observed in 7 patients with ganglion recurrence and in 17 patients without recurrence. Ganglion cysts recurred in 12.1% of patients treated for dorsal wrist ganglions and in 10.4% of patients operated on for volar wrist ganglions. No influence of patient gender, age, body side, or cyst location on ganglion recurrence was detected.

Conclusions. Operative treatment is a widely recognized method of management of wrist ganglions. The rate of resulting persistent complications is low. Recurrence of ganglion cysts is unpredictable and independent of patient demographic factors. It can be observed even in cases, in which a perfect surgical technique has been used.

Key words: surgery, wrist, ganglion cysts, benign tumors

Introduction

Ganglion cysts can develop in close proximity to any joint or tendon sheath in the human body.[1–4] They are most commonly located around the wrist and its dorsal aspect is affected more often.[1] The majority of dorsal wrist ganglions have a connection with the scapholunate ligament; they are located between the tendons of the extensor digitorum communis and the extensor pollicis longus muscles.[5–7] Volar wrist ganglions are most often found at the radial side of the wrist between the tendons of flexor carpi radialis and abductor pollicis longus muscles.[5,6] These ganglion cysts usually communicate with the radioscaphoid-scapholunate interval, scaphotrapezial joint or metacarpotrapezial joint.[1,3,8] The purpose of this work was to present our experience in the treatment of wrist ganglions and to evaluate the results obtained with operative management of this type of lesion.

Material and methods

The study group consisted of 394 patients: 289 females and 105 males, aged from 10 to 83 years (mean age: 39.2 ±16.2 years). The patients were treated operatively at the Clinic of Traumatology and Hand Surgery in Wrocław, Poland, for ganglion cysts located in the wrist region between the years 2000–2014. The subjects were scheduled for an operation on the basis of the presence of a tumor mass around the wrist. Many patients had an X-ray and ultrasound examination or a magnetic resonance imaging (MRI) of the wrist performed on the outpatient basis, but these imaging studies were not mandatory before the operative treatment. A medical history was collected, with the emphasis on the time the tumor first appeared, the dynamics of its growth, the character and severity of symptoms (including pain), previous injuries, and conservative or operative treatment. Preoperative clinical examination consisted of: evaluation of the tumor size in palpation, assessment of its mobility against the underlying tissue, the appearance of the skin overlying the tumor and its mobility against the tumor, range of motion of the wrist joint in comparison to the opposite side, and evaluation of grip strength in comparison to the healthy side.

Operative technique

The operations were performed mostly using conduction anesthesia, and in exceptional cases using general or local anesthesia, with the use of an arm tourniquet. The type of surgical incision used depended on the location of the ganglion cyst. In operative treatment of dorsal wrist ganglions, a longitudinal or transverse incision directly above the tumor was used. An attempt was made to dissect the cyst as a whole, without perforation of its wall. Dissection was continued along the ganglion stalk to the joint capsule. The capsule of the joint communicating with the ganglion cyst was incised in a semicircular fashion, and the capsule flap was raised. Small intraarticular cysts were excised along with the duct connecting the ganglion with the joint. The defect in the joint capsule created after the resection of the basis of the cyst, measuring approx. 1 cm in diameter, was left without repair. (Fig. 1,2)
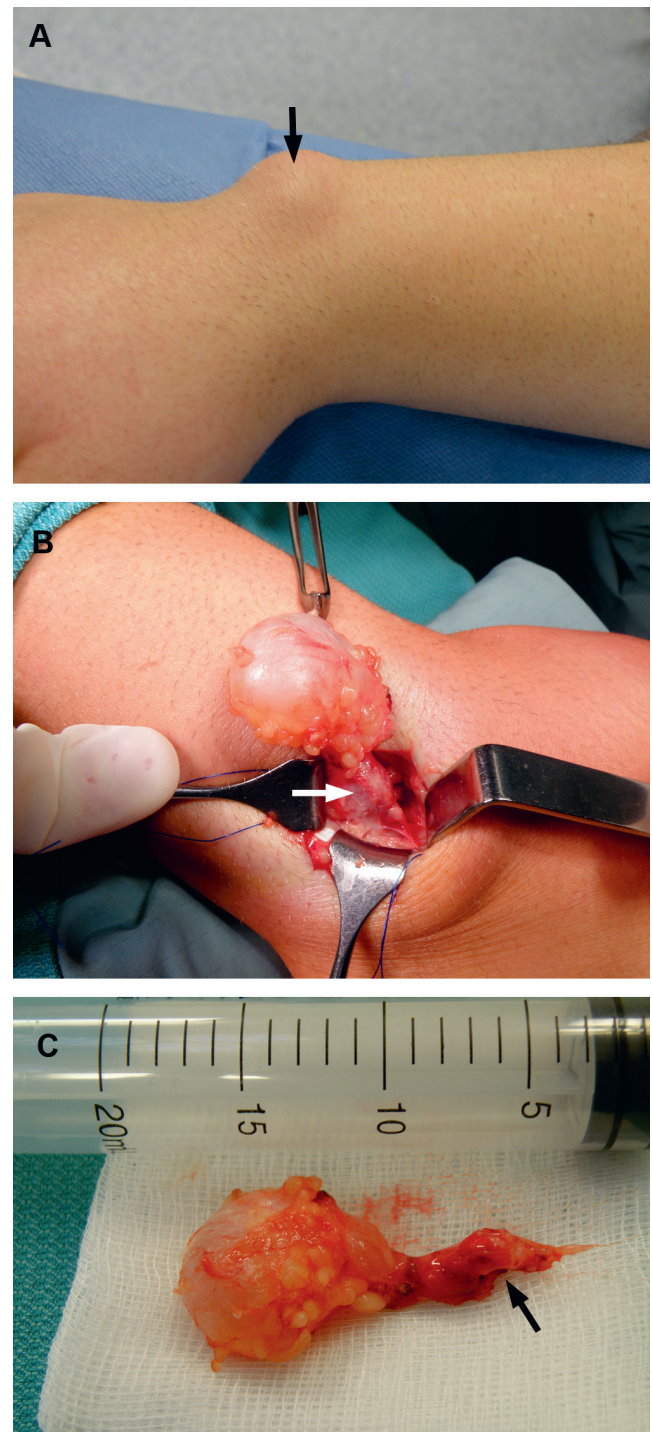

Fig. 1. Dorsal wrist ganglion

A – clinical appearance of a dorsal wrist ganglion (black arrow);
B – intraoperative view: exposure of the ganglion cyst along with the duct (white arrow); C – postoperative view: appearance of the ganglion cyst along with the duct (black arrow) after resection.
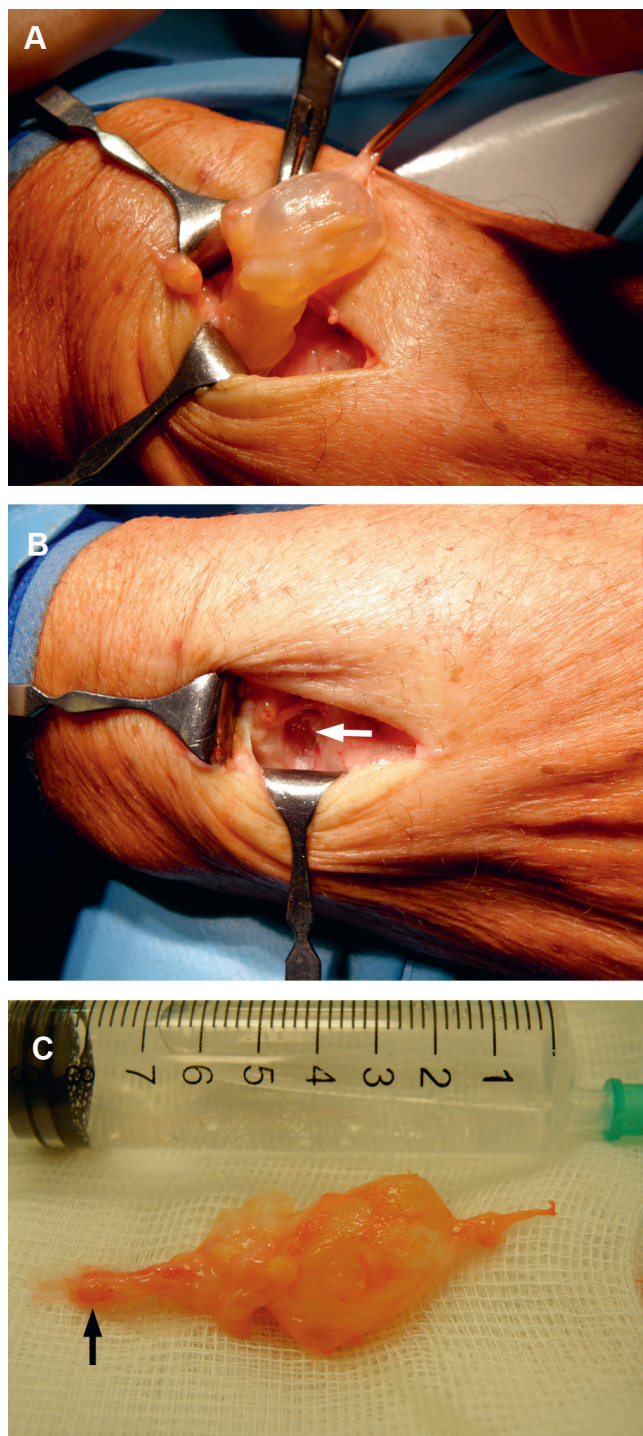
Fig. 2. Dorsal wrist ganglion

A – intraoperative view: exposure of the ganglion cyst; B – intraoperative view: exposure of the site of origin of the ganglion (where the stalk of the ganglion is connected with the scapholunate ligament), along with the defect in the joint capsule (white arrow); C – postoperative view: appearance of the ganglion cyst along with the duct (black arrow) after resection.

In the cases of volar wrist ganglions, a longitudinal or arcuate incision was used, usually on the radial side of the cyst. During ganglion dissection, radial artery or ulnar artery and ulnar nerve, depending on the ganglion cyst location, were identified and secured. Continuing the dissection along the stalk, the joint capsule was reached and

incised. The duct and the capsular attachments were resected, which resulted in a joint capsule defect, not exceeding 5 mm in diameter. If leakage of gelatinous substance was observed as a result of applying pressure to the surrounding tissues, the decision was made to resect them. The defect in the joint capsule was left without repairing (Fig. 3).

Wounds were closed with single 4–0 or 5–0 non-absorbable sutures. In the postoperative period, immobilization in a short plaster splint, reaching distally to the level of metacarpophalangeal joints, was used for 5–7 days. Afterwards, a rehabilitation program was started with a gradually increasing range of wrist joint motion. Resected tissue was subjected to a histopathological analysis.

Postoperative assessment

The final results of the treatment after the follow-up period of min 2 years (mean: 38 months; range: 24–118 months) were evaluated in 198 patients operated on for dorsal wrist ganglions (69.4% of all patients treated operatively for this type of ganglion cysts) and 77 patients with volar wrist ganglions (70.6% of all patients operated on for this type of lesion). The following criteria were considered during follow-up examinations: the presence/absence of ganglion recurrence, size and shape of postoperative scar, range of motion of the wrist joint in comparison to the opposite side, evaluation of grasp strength in comparison to the healthy side, presence/absence of pain.

Statistical analysis

Statistical analysis was performed with the use of STATISTICA software v. 12 (StatSoft Inc., Tulsa, USA). The risk factors for recurrence were identified using the χ^2 test or its modifications (Fisher's exact test, χ^2 test with Yates' correction and V^2 test) for the categorical variables and the Mann-Whitney U test for the continuous variables. The level of statistical significance was set at 0.05 ($p < 0.05$).

Results

Preoperative examination results

Ganglion cysts of the wrist were found significantly more often in females (73.3%) than in males (26.7%), with a 2.75:1 ratio. The right wrist was affected in 178 patients (45.2%) and the left wrist in 216 patients (54.8%). Dorsal wrist ganglions were diagnosed in 285 patients, in whom a total number of 286 ganglions (constituting 72.4% of all ganglion cysts) were removed. Two lesions were observed in the dorsal aspect of the left wrist of a 25-year-old male,
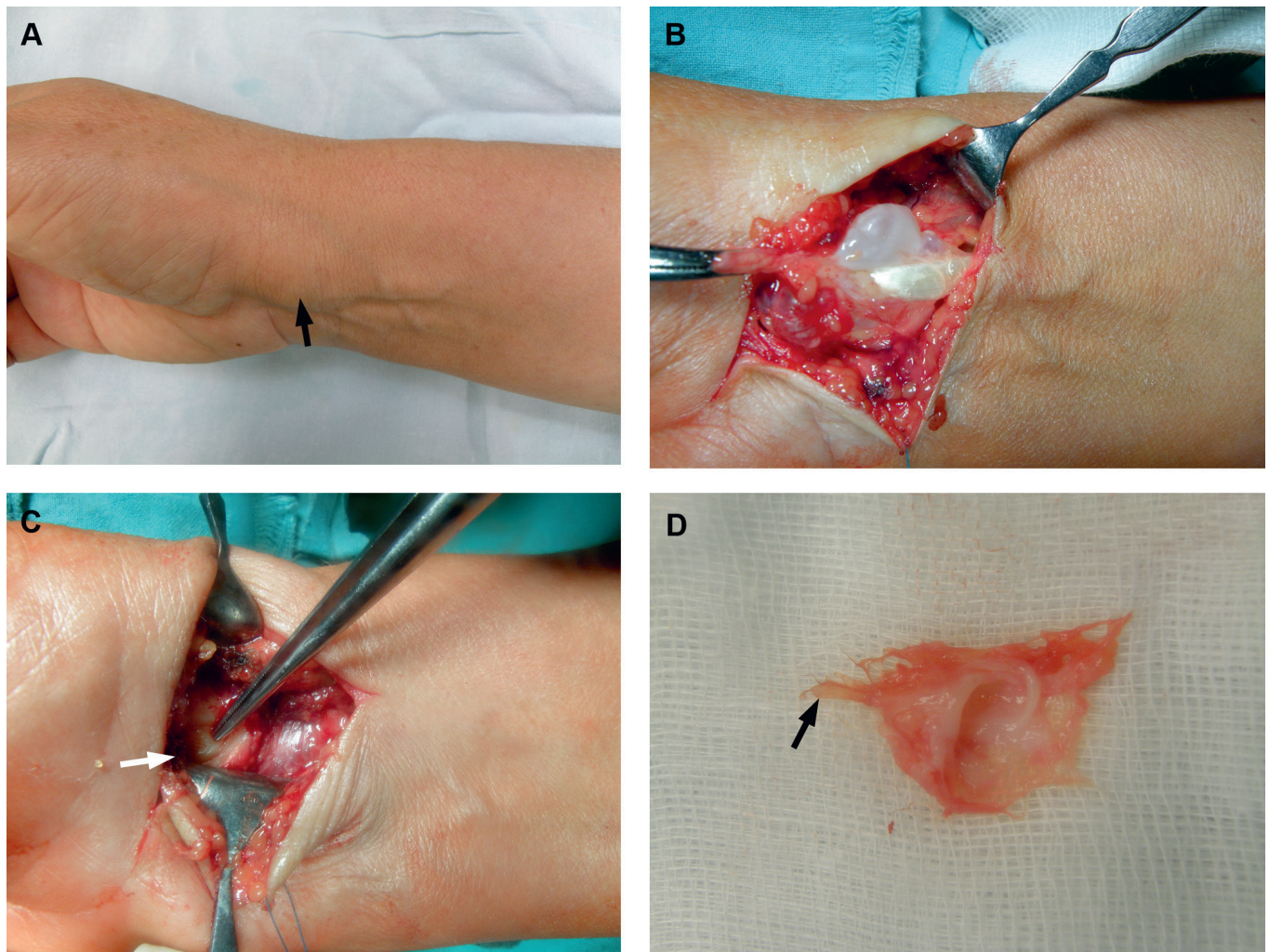
Fig. 3. Volar wrist ganglion

A – clinical appearance of a volar wrist ganglion located at the radial side of the wrist (black arrow); B – intraoperative view: exposure of the ganglion cyst; C – intraoperative view: the site of connection of the stalk of the ganglion with the radiocarpal joint (white arrow); D – postoperative view: appearance of the ganglion cyst along with the duct (black arrow) after resection.

one of which was located at the radial and the other at the ulnar side of the wrist. Volar wrist ganglions, all manifested as solitary tumors, were found in 109 patients (27.6% of all ganglions). A visible and palpable tumor mass was found during preoperative clinical examination in all of the patients. The majority of the patients reported moderate pain on palpation of the tumor and at end ranges of wrist motion. In the study, 280 patients (71% of the studied group) complained of pain on exertion (elicited by sporting activities or overworking) and the maximal severity of pain reported was 4 on the Visual Analogue Scale (VAS). About 35% of the patients (138 persons) noticed changes in ganglion volume dependent on their level of activity (increase in ganglion cyst dimensions after overworking and decrease in its dimensions after a period of rest). Slight weakening of grip strength in comparison to the healthy side was found in 28% of the patients (111 subjects). Limitation of dorsiflexion or palmar flexion not exceeding 10° in comparison to the opposite side was found in 32% of the patients (127 persons).

Histopathological examination results

The size of ganglions removed as a whole varied from 0.5 cm to 3 cm in diameter. The cyst wall was built of collagen fibers organized in layers, and the inside of the cysts was filled with gelatinous matter.

Operative treatment results

No intraoperative complications were observed during the removal of dorsal wrist ganglions. Excision of volar wrist ganglions was, however, associated with injury to the radial artery, resulting in its complete disruption in 3 cases. The artery was reconstructed in 2 cases; in the remaining case, the stumps were ligated. No insufficient blood supply to the upper limb was observed in any of these patients during the postoperative course. In 10 patients operated on for dorsal wrist ganglions, symptoms of irritation of the superficial branch of the radial nerve were observed in the early postoperative period. Eight patients, who had volar wrist

ganglions located at the radial portion of the wrist removed, complained of symptoms of dysfunction of the cutaneous branch of the median nerve, while 3 patients after excision of volar wrist ganglions located at the ulnar portion of the wrist manifested symptoms of the ulnar nerve irritation. The symptoms resolved in all of the patients within 6 months after the operation. Limitation of the wrist joint range of motion was often observed in the early postoperative period, and in the majority of the cases it was caused by pain. Wrist joint function gradually improved in most patients after several weeks of rehabilitation. Swelling and redness of postoperative wound was observed in 10 patients after the removal of dorsal wrist ganglions and in 6 patients after the excision of volar wrist ganglions. Moreover, dorsal wrist ganglion removal was complicated by purulent infection in 2 patients, which resolved after intravenous antibiotic therapy. Persistent limitation of palmar flexion of the wrist ranging from 10° to 15° was observed in 6 patients in a minimal 2-year-long follow-up after resection of dorsal wrist ganglions. Volar wrist ganglion removal did not cause limitation of wrist joint motion in any patient. None of the patients manifested evident weakening of the grip strength in comparison to the healthy subjects. Excision of dorsal wrist ganglions left a widened, unesthetic postoperative scar in 15 patients, and the removal of volar wrist ganglions was associated with the formation of such a scar in 6 patients. Keloid formation was observed in 4 patients after resection of dorsal wrist ganglions.

About 75% of the patients (206 out of 275 persons subjected to follow-up) reported preoperative pain: 152 in the dorsal wrist ganglion group and 54 in the volar wrist ganglion group. None of the patients who did not report preoperative pain (46 patients diagnosed with dorsal wrist ganglions and 23 patients with volar wrist ganglions) complained of pain during the follow-up examinations. In the group of patients operated on for dorsal wrist ganglions, pain was reported in 5 patients with ganglion recurrence and in 12 patients without recurrence. Out of the patients treated operatively for volar wrist ganglions, 2 persons with ganglion recurrence and 5 persons without recurrence complained of pain. The intensity of pain was not greater than 3 according to the VAS in any of the patients.

Ganglion cysts recurred in 24 patients operated on for dorsal wrist ganglions (12.1% of the studied group) and in 8 patients treated surgically for volar wrist ganglions (10.4% of the study group). Recurrences were observed between 7 and 22 months after operative treatment. Dorsal wrist ganglions recurred in 8 males and 16 females aged 19–83 years (mean age: 40.2 ±18.8 years). Recurrences were observed in the left wrist in 15 patients and in the right wrist in 9 patients. Volar wrist ganglions recurred in 2 males and 6 females aged 33–54 years (mean age: 43.0 ±7.2 years). The right wrist was affected in 5 patients and the left wrist in 3 patients. Statistical analysis did not confirm the influence of such factors as patient age, gender, body side (Tables 1,2), and ganglion location at the volar or dorsal aspect of the wrist on ganglion recurrence (Table 3).

Table 1. The influence of age, gender and body side on recurrence in the volar wrist ganglion (VWG) group

| Variable | Recurrence | | p-value |
	yes n = 8	no n = 69	
Gender male female	2 6	20 49	0.859*
Age x ±SD Me (range)	43.0 ±7.2 44.5 (33–54)	41.1 ±12.3 39.0 (19–68)	0.493**
Age <39 years ≥39 years	3 5	34 35	0.797*
Side left right	3 5	33 36	0.857*

x – mean; SD – standard deviation; Me – median; * χ^2 test with Yates's correction; ** Mann-Whitney U test.

Table 2. The influence of age, gender and body side on recurrence in the dorsal wrist ganglion (DWG) group

| Variable | Recurrence | | p-value |
	yes n = 24	no n = 174	
Gender male female	8 16	40 134	0.269*
Age x ±SD Me (range)	40.2 ±18.8 32.5 (19–83)	35.4 ±16.7 30 (11–82)	0.192**
Age <35 years ≥35 years	13 11	97 77	0.884***
Side left right	15 9	92 82	0.375***

x – mean; SD – standard deviation; Me – median; * V^2 test; ** Mann-Whitney U test; *** χ^2 test.

Table 3. The influence of ganglion location (volar or dorsal aspect of the wrist) on recurrence

| Variable | Recurrence | | p-value |
	yes n = 32	no n = 243	
Location VWG DWG	8 24	69 174	0.688*

VWG – volar wrist ganglion; DWG – dorsal wrist ganglion; * V^2 test.

Discussion

The analysis of relevant literature revealed huge differences in the intensity of preoperative symptoms manifested by patients in the studied groups. Reported symptoms included pain, limitation of wrist joint motion and weakening of grip strength. Pain can be elicited by applying

pressure to the tumor mass, overworking or by placing the wrist joint at the end rages of motion (maximal palmar flexion or dorsiflexion). The frequency and severity of this symptom can vary significantly. Among our patients, 71% complained of pain, but its intensity was rated as low. In the study by Dermon et al. on 119 patients operated on for dorsal wrist ganglions (94 cysts), volar wrist ganglions (28 cysts) and ganglions located at the ulnar aspect of the wrist (2 cysts) over a period of 6 years, pain was reported by 79.8% of the patients. The intensity of persistent pain was high and reached levels 7–9 according to the VAS.[1] Similar percentage of patients (79%) suffering from pain in the preoperative period was observed by Craik and Walsh in their study group comprising 59 patients.[9] Dias and Buch reported preoperative pain in 84% of their 79 patients treated for volar wrist ganglions.[10] Out of 103 patients treated by Wong et al. (61 patients diagnosed with dorsal wrist ganglions and 42 patients with volar wrist ganglions), 44 complained of pain in the preoperative period.[11] In the patient group studied by Limpaphayom and Wilairatana, pain was reported in 58.3% of the total number of 24 patients.[12] Pain was the most common preoperative complaint among 26 patients treated by Singhal et al., observed in 46.2% of cases.[13] According to Rocchi et al., in their patient group, only 6 out of 50 subjects operated on for volar wrist ganglions with the arthroscopic or open method complained of pain in the preoperative period.[14] Out of 114 patients analyzed by Gallego and Mathoulin, 51 complained of pain ranging in severity from 1 to 6 according to the VAS. The remaining 63 patients (55.2%) did not report any pain, which corresponds to 0 according to the VAS.[15]

Other symptoms like wrist stiffness and weakness can also be manifested with varying severity. In our patients, these symptoms were found in 32% and 28% of cases, respectively. In the patient group studied by Craik and Walsh, comprising 59 cases, wrist stiffness was observed preoperatively in 31% of patients and weakness in 44% of patients. Moreover, 27% of the study participants complained of the presence of paresthesia and numbness.[9] Dias and Buch reported the presence of preoperative weakness in 26% and wrist stiffness in 10% of the 79 patients with volar wrist ganglions.[10] In 114 patients diagnosed with dorsal wrist ganglions, described by Gallego and Mathoulin, the mean palmar flexion deficit observed in the preoperative period was 15.2° when compared with the healthy subjects (59.9° vs 75.1°), while the mean dorsiflexion deficit was 8.3° in comparison to the healthy side (69.7° vs 78°). Moreover, the mean grip strength was diminished by 22% when compared with the opposite side.[15] By contrast, none of the 50 patients with volar wrist ganglions treated by Rocchi et al. manifested a limitation of wrist range of motion or grip strength weakening in the preoperative period.[14] Considering the discussed data, it should be noted that in many cases, the main indication for operative treatment was the presence of a tumor. Other motivations for

seeking operative treatment included concerns about the malignant character of the tumor and cosmetic aspects.[9,16]

Surgical treatment of ganglion cysts carries the inherent risk associated with operative intervention in the intraoperative as well as early and late postoperative period. Careful preoperative planning and preparation is essential in surgical management of ganglion cysts. Surgical procedures should be performed using conduction anesthesia and tourniquet ischemia. The surgeon must have excellent knowledge on the operative anatomy of the hand and wrist as well as on the possible connections ganglion cysts may have with the neighboring joints. This ensures radical excision of the cyst and lowers the risk of recurrence.

Injury to the radial artery is a potential intraoperative complication associated with the removal of volar wrist ganglions located at the radial side of the wrist. Jacobs and Govaers observed the existence of a direct connection between the ganglion cyst wall and the arterial wall in 38 out of 72 patients operated on (54%).[17] In the patient group described by Aydin et al., cysts adhered tightly to the arterial wall in 65% of patients, and in 5% of patients, the radial artery entered the ganglion.[18] Iatrogenic injury to the radial artery occurred in 2 out of 40 patients treated operatively (5%).[18] Rocchi et al. described iatrogenic arterial injury in 4 out of 20 patients treated surgically with the open method (20%).[14] The incidence of this complication varies from 1% to 20% in the literature.[14,19] In order to decrease the risk of arterial injury, Lister and Smith suggested a modification of the operative technique, in which a fragment of the cyst wall closely connected with the artery is retained.[20] This complication cannot always be prevented, despite the awareness of the risk of arterial injury associated with the dissection of volar wrist ganglions, as in the case of the 3 patients who suffered such a complication in our patient group.

Another possible complication is the formation of an overgrown scar or a keloid. In order to prevent it, adequate surgical incision is essential. Angelides recommended transverse skin incision in all cases of dorsal wrist ganglions.[6] Other authors used horizontal as well as transverse incisions in operative treatment of dorsal wrist ganglions, without noticeable differences in wound healing.[1,19] Our observations regarding this aspect are similar. The use of either of the 2 approaches did not influence scar formation in our patient group. The process of wound healing and scar remodeling was undisturbed in the majority of the patients. Wound closure with the use of thin, atraumatic sutures could have contributed to uneventful healing.

Other possible postoperative complications are wrist stiffness and weakness. The presence of such symptoms in the postoperative period may represent a lack of clinical improvement in comparison to the preoperative state.[10,21] Such symptoms can also be observed after surgery in patients who did not manifest them preoperatively.[1,6,18] In the group of 50 patients treated by Dermon et al., postoperative

wrist stiffness was present in 3 patients (4.5%) and weakness in 2 patients (3%).[1] Aydin et al. observed wrist stiffness in 5 out of 40 operatively treated patients (12.5%).[18] Two out of 25 patients (8%) operated with the open method, described by Rocchi et al. manifested postoperative wrist stiffness.[14] In our study group, the limitation of palmar wrist flexion was observed in 6 out of 198 patients (3%) after the excision of dorsal wrist ganglions. Most authors agree that short-term immobilization after surgery and early rehabilitation decrease the risk of postoperative stiffness. Another important factor is adequate operative technique without attempts to suture the joint capsule or close its defect.[1,6,13]

Surgical excision of a ganglion cyst is associated with the risk of recurrence. According to different authors, recurrence rate ranges from 1% to almost 50%.[1,6,9,10,12,14,18,19,21–25] The frequency of ganglion recurrence observed in our patient group (12.1% for dorsal wrist ganglions and 10.4% for volar wrist ganglions) is acceptable. Huge differences in recurrence rates reported by different authors are the result of the heterogeneity of the studied patient groups, including different numbers of patients included in particular studies, varying postoperative follow-up periods, as well as different levels of surgeon experience, etc. It is currently believed that there is a close connection between the operative technique employed and the risk of ganglion recurrence. Removal of the main cyst along with the duct connecting it to the adjacent joint, a fragment of the joint capsule and microcysts located around the duct is essential.[1,6] It must be emphasized, however, that even a perfect surgical technique does not eliminate the risk of ganglion recurrence completely.[1,6] At the same time, the comparison of different methods used in the treatment of ganglion cysts (observation, aspiration, administration of an obliterating agent into the cyst, operative management) reveals that the highest patient satisfaction is associated with surgical treatment, even in the cases in which recurrence occurred.[19,21] Operative treatment allows for fast tumor removal and carries a lower risk of recurrence than other methods.[19,21]

Arthroscopic treatment can constitute an alternative to open surgery. Arthroscopic resection of a wrist ganglion was first conducted by Osterman and Raphael in 1995.[26] This method is used in the management of both dorsal and volar wrist ganglions.[27–29] Like every operative treatment method, arthroscopy carries the risk of certain complications. Hematoma, injury to the vessels and nerves, wrist stiffness and weakness, tendinitis, paratenonitis, and ganglion recurrence are among the most common ones.[15] In some situations, conversion to open surgery may be necessary.[14,28,30] Neither of the methods has been proven to be evidently superior. Such factors as the patient's preference and surgeon's experience should be taken into consideration when choosing the optimal operative technique.[27]

Conclusions

Operative treatment is a widely recognized method of managing wrist ganglions and it is characterized by a low rate of resulting persistent complications. Recurrence of ganglion cysts after surgery is unpredictable and independent of patient demographic factors. It can be observed even in the cases, in which perfect surgical technique has been employed during the initial excision of the ganglion cyst.

References

1. Dermon A, Kapetanakis S, Fiska A, Alpantaki K, Kazakos K. Ganglionectomy without repairing the bursal defect: Long-term results in a series of 124 wrist ganglia. *Clin Orthop Surg*. 2011;3(2):152–156. doi:10.4055/cios.2011.3.2.152
2. Teefey SA, Dahiya N, Middleton WD, Gelberman RH, Boyer MI. Ganglia of the hand and wrist: A sonographic analysis. *AJR Am J Roentgenol*. 2008;191(3):716–720. doi:10.2214/AJR.07.3438
3. Shoaib A, Clay NR. Ganglions. *Curr Orthop*. 2002;16(6):451–461. doi:10.1054/cuor.2002.0289
4. Azzopardi EA, Gujral S, Mandal A, Kulkarni M. Rapidly expanding thenar eminence ganglion: A case report. *Cases J*. 2009;2:129. doi:10.1186/1757-1626-2-129
5. Minotti P, Taras JS. Ganglion cysts of the wrist. *Journal of the American Society for Surgery of the Hand*. 2002;2:102–107.
6. Angelides AC. Ganglions of the hand and wrist. In: Green DP, Hotchkiss RN, Pederson WC, eds. *Green's Operative Hand Surgery*. 3rd ed. Philadelphia, PA: Churchill Livingstone; 1998:2171–2183.
7. Gude W, Morelli V. Ganglion cysts of the wrist: Pathophysiology, clinical picture, and management. *Curr Rev Musculoskelet Med*. 2008;1(3–4):205–211. doi:10.1007/s12178-008-9033-4
8. Burke FD, Melikyan EY, Bradley MJ, Dias JJ. Primary care referral protocol for wrist ganglia. *Postgrad Med J*. 2003;79(932):329–331.
9. Craik JD, Walsh SP. Patient outcomes following wrist ganglion excision surgery. *J Hand Surg Eur Vol*. 2012;37(7):673–677. doi:10.1177/1753193411434376
10. Dias J, Buch K. Palmar wrist ganglion: Does intervention improve outcome? A prospective study of the natural history and patient-reported treatment outcomes. *J Hand Surg Br*. 2003;28(2):172–176.
11. Wong AS, Jebson PJ, Murray PM, Trigg SD. The use of routine wrist radiography is not useful in the evaluation of patients with a ganglion cyst of the wrist. *Hand (N Y)*. 2007;2(3):117–119. doi:10.1007/s11552-007-9032-8
12. Limpaphayom N, Wilairatana V. Randomized controlled trial between surgery and aspiration combined with methylprednisolone acetate injection plus wrist immobilization in the treatment of dorsal carpal ganglion. *J Med Assoc Thai*. 2004;87(12):1513–1517.
13. Singhal R, Angmo N, Gupta S, Kumar V, Mehtani A. Ganglion cysts of the wrist: A prospective study of a simple outpatient management. *Acta Orthop Belg*. 2005;71(5):528–534.
14. Rocchi L, Canal A, Fanfani F, Catalano F. Articular ganglia of the volar aspect of the wrist: Arthroscopic resection compared with open excision. A prospective randomised study. *Scand J Plast Reconstr Surg Hand Surg*. 2008;42(5):253–259. doi:10.1080/02844310802210897
15. Gallego S, Mathoulin C. Arthroscopic resection of dorsal wrist ganglia: 114 cases with minimum follow-up of 2 years. *Arthroscopy*. 2010;26(12):1675–1682. doi:10.1016/j.arthro.2010.05.008
16. Westbrook AP, Stephen AB, Oni J, Davis TR. Ganglia: the patient's perception. *J Hand Surg Br*. 2000;25(6):566–567.
17. Jacobs LG, Govaers KJ. The volar wrist ganglion: Just a simple cyst? *J Hand Surg Br*. 1990;15(3):342–346.
18. Aydin A, Kabakaş F, Erer M, Ozkan T, Tunçer S. Surgical treatment of volar wrist ganglia. *Acta Orthop Traumatol Turc*. 2003;37(4):309–312.
19. Finsen V, Håberg O, Borchgrevink GE. Surgery for ganglia of the flexor tendon sheath. *Orthop Rev (Pavia)*. 2013;18;5(1):e6. doi:10.4081/or.2013.e6

20. Lister GD, Smith RR. Protection of the radial artery in the resection of adherent ganglions of the wrist. *Plast Reconstr Surg*. 1978;61(1): 127–129.

21. Dias JJ, Dhukaram V, Kumar P. The natural history of untreated dorsal wrist ganglia and patient reported outcome 6 years after intervention. *J Hand Surg Eur Vol*. 2007;32(5):502–508.

22. Lidder S, Ranawat V, Ahrens P. Surgical excision of wrist ganglia: Literature review and nine-year retrospective study of recurrence and patient satisfaction. *Orthop Rev (Pavia)*. 2009;1(1):e5. doi:10.4081/or.2009.e5

23. Rollins KE, Ollivere BJ, Johnston P. Predicting successful outcomes of wrist and finger ganglia. *Hand Surg*. 2013;18(1):41–44. doi:10.1142/S021881041350007X

24. Humail SM, Abidi AR, Haq SNU, Mustafa GKK. Comparative study of two methods for treatment of dorsal wrist ganglion. *J Pak Orthop Assoc*. 2010;22:53–57.

25. Yamamoto M, Natsume T, Kurimoto S, et al. Patients with benign hand tumors are indicated for surgery according to patient-rated outcome measures. *J Plast Reconstr Aesthet Surg*. 2017;70(4):487–494. doi:10.1016/j.bjps.2016.12.010

26. Osterman AL, Raphael J. Arthroscopic resection of dorsal ganglion of the wrist. *Hand Clin*. 1995;11(1):7–12.

27. Kang L, Weiss APC, Akelman E. Arthroscopic versus open dorsal ganglion cyst excision. *Oper Tech Orthop*. 2012;22(3);131–135.

28. Rocchi L, Canal A, Pelaez J, Fanfani F, Catalano F. Results and complications in dorsal and volar wrist ganglia arthroscopic resection. *Hand Surg*. 2006;11(1–2):21–26.

29. Rizzo M, Berger RA, Steinmann SP, Bishop AT. Arthroscopic resection in the management of dorsal wrist ganglions: Results with a minimum 2-year follow-up period. *J Hand Surg Am*. 2004;29(1):59–62.

30. Chassat R, Nourissat G, Chaumeil G, Dumontier C. Arthroscopic treatment of dorsal ganglion cyst at the wrist. About 54 cases. *Chir Main*. 2006;25(3–4):146–151.

Gastric band migration to gastrointestinal lumen and possibilities of its surgical treatment

Anna Sawicka-Pierko[1,A–D], Jacek Pierko[2,A–D], Monika Krawczyk[2,B], Jerzy R. Ładny[2,E,F], Jacek Dadan[2,E,F], Hady Razak Hady[2,A,E,F]

[1] Department of Ophthalmology, Medical University of Bialystok, Poland

[2] 1st Clinical Department of General and Endocrine Surgery, Medical University of Bialystok, Poland

A – research concept and design; B – collection and/or assembly of data; C – data analysis and interpretation;
D – writing the article; E – critical revision of the article; F – final approval of the article

Address for correspondence
Jacek Pierko
E-mail: jacekpierko@gmail.com

Abstract

Background. Due to numerous late complications after laparoscopic adjustable gastric banding (LAGB), leading to band removal, a significant decrease of its application has been observed.

Objectives. The objective of this study was to present complications after LAGB in our own material.

Material and methods. The study included 152 obese patients who underwent LAGB between 2005 and 2012. The group of women consisted of 91 patients (60%) with the following preoperative parameters: average body mass index (BMI) 42 ±3.66 kg/m^2 and average body mass 122 ±12.8 kg. The group of men included 61 patients (40%) with a preoperative average BMI 43 ±3.81 kg/m^2 and average body mass 125 ±13.02 kg. The average age of women was 35.02 ±11.6 years and of men 36.18 ±10.5 years.

Results. Among 152 patients after LAGB due to morbid obesity, in 7 (4.6%) migration of the band to the stomach lumen was observed, in 4 port wound purulence occurred, in 3 stomach mucosa ulceration was diagnosed in the band pressure area, 3 reported heartburn and hyperacidity, and 4 suffered from emesis. In all aforementioned patients, body mass loss stopped and they reported lack of restriction after last band regulation.

Conclusions. Surgical or endoscopic treatment in patients with a migrated band is an individual matter depending on the type and size of band dislocation, its clinical symptoms and the general state of the patient, but also on the experience of the operating team and the quality of the equipment.

Key words: band migration, obesity, laparoscopic adjustable gastric banding, bariatric surgery

Introduction

The number of cases of morbid obesity is constantly growing – it is estimated that in 2016 the number of adults with overweight will oscillate around 2.3 billion and of obese adults will exceed 70 million.[1,2] In almost every country, obesity is an epidemic, which explains the recent intensive development of bariatric surgery. Surgical treatment is now a method of choice in obese patients who did not reveal satisfying effects after preservative treatment.[3]

In our department, the following procedures are performed as a routine: sleeve gastrectomy (SG), gastric bypass (GBP) and laparoscopic adjustable gastric banding (LAGB); however, in the last 3 years, there has been an 80% decrease in gastric banding procedures. It is worth mentioning that we performed an endoscopic evacuation of a migrated band for the first time in Poland. As with every surgical intervention, bariatric surgery brings the risk of perioperative complications; however, obese patients are a very specific group, according to the rule: big patient – big risk.[4]

Surgical treatment of obesity using the adjustable gastric band (AGB) became possible after research commenced in the 1980s. Laparoscopic adjustable gastric banding, started and developed by Guy-Bernard Cadière and Franco Favretti, is the least invasive method among bariatric procedures.

In Poland, this procedure was applied for the first time in 1998. Currently, it is estimated that adjustable gastric banding is the most frequently applied procedure in the USA and Australia, while in Europe, a significant decrease in its application has been noted due to numerous late complications, leading to band removal.

The undisputed advantages of this procedure are the following: lack of anatomy alteration, the possibility of band removal if needed, no necessity of nutritional supplementation in the postoperative period, and low frequency of complications occurrence, comparable to other bariatric procedures despite their different characteristic.[3,5]

A possible early complication after LAGB is bleeding from the port-site incision. The following perioperative complications are also worth noting: damage and bleeding from the diaphragm and organs such as stomach, liver and spleen. Late postoperative complications include band slippage, its migration to the gastrointestinal lumen, pouch dilatation, mucositis and esophagus dilatation, stomach mucosa ulceration in the place of band pressure, heartburn, hyperacidity, emesis, lost connection between band and its port, as well as body mass loss discontinuance.[6,7]

Material and methods

The study included 152 obese patients who underwent LAGB between 2005 and 2012. The group of women consisted of 91 patients (60%) with the following preoperative parameters: average body mass index (BMI) 42 ±3.66 kg/m^2

and average body mass 122 ±12.8 kg. The group of men included 61 patients (40%) with a preoperative average BMI 43 ±3.81 kg/m^2 and average body mass 125 ±13.02 kg. The average age of women was 35.02 ±11.6 years and of men 36.18 ±10.5 years (Table 1).

Patients were qualified for LAGB according to Polish recommendations based on European guidelines taking into account principles of evidence-based medicine (EBM)[8,9] after an analysis of the results of precise laboratory tests and a series of multispecialistic consultations.

An abdominal medical ultrasonography (USG) and a gastroscopy allowed us to exclude any pathologies which would disqualify the patient from the surgery. Furthermore, the following examinations had been conducted in order to exclude other contraindications for surgical treatment: endocrinological examination, cardiological examination in patients with cardiovascular dysfunction, gynecological examination in women, dietetic examination, and psychological examination. The aforementioned consultations minimized the perioperative risk and intensified the postsurgical effect.

Adjustable gastric banding was performed laparoscopically with general anesthesia, using 4–5 trocars. A pars flaccida approach and multiple banding-perigastric technique was applied as a method of entrance. The further stage of the operation involved exposing the posterior wall of the stomach and reaching the His angle using the Goldfinger device or a grasper and, lastly, introducing a silicone ring and closing it under the cardia by creating a small pouch (approx. 25 mL).

Finally, the ring was connected with a regulation port, placed in subcutaneous tissue under the left costal arch, using a drain. In the majority of cases, the average time of hospitalization was 3 days. One of the postoperative recommendations was a 2-week semi-liquid, low-calorie and low-carbohydrate. Further recommendations included a control visit in an outpatient clinic once a month. The first regulation was conducted 6 weeks after the surgery and further regulations were applied every 3–6 months.

Results

Among 152 patients after LAGB due to morbid obesity, in 7 (4.6%) migration of the band to the stomach lumen was observed, port wound purulence occurred in 4 patients,

Table 1. Characteristics of patients

Variables	Female	Male
Number of patients	91	61
Body mass [kg]	122 ±12.8	125 ±13.02
Age [years]	35 ±11.6	36.18 ±10.05
BMI [kg/m^3]	42 ±3.66	43 ±3.81

Data presented as mean ± standard deviation (SD);
BMI – body mass index.

Fig. 1. X-ray. Migration of the band to the stomach lumen followed by its replacement to the small intestine
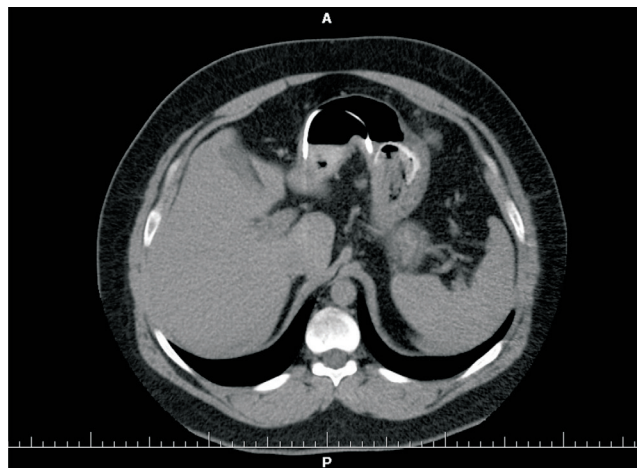

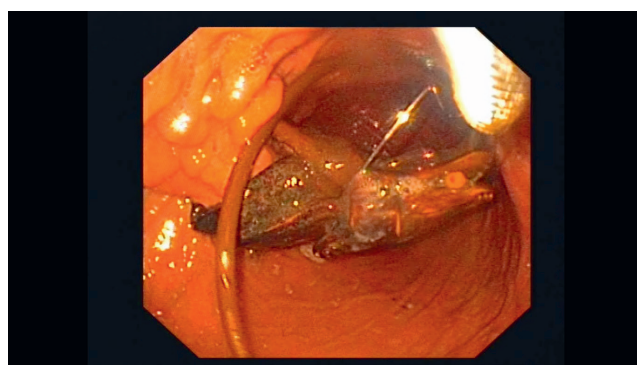Fig. 2. Computed tomography (CT). Partial migration of the band to the stomach

Fig. 3. Gastroscopy. Removal of the relocated band

stomach mucosa ulceration was diagnosed in the band pressure area in 3 patients, 3 patients reported heartburn and hyperacidity, and 4 patients suffered from emesis (Table 2).

In all the aforementioned patients, body mass loss stopped, even weight gain was observed, and they reported lack of restriction after the last band regulation. The following imaging diagnostics were conducted: thorax and abdominal X-ray, esophagus and stomach contrast X-ray, gastroscopy, abdominal USG, and computed tomography (CT). Further treatment depended on the general condition of the patient, clinical symptoms of gastric band migration and the type of band allocation.

We observed 1 case of a 27-year-old patient who suffered from pain, port infection and symptoms of peritonitis 38 months after LAGB. In this period, she underwent 9 band regulations. Abdominal X-ray revealed band migration to the lower pelvis (Fig. 1). The patient underwent reconnoitering laparoscopy showing the presence of a 12-centimeter linear perforation of the anterior wall of the stomach and band migration to the small intestine, 50–60 cm from Treitz ligament, with partial necrosis of the intestinal wall in this area (10–15 cm). The operating team decided perioperatively to continue with the classical method. The band was removed

with a partial small intestine resection and end-to-end anastomosis; perforation of the stomach wall was dressed surgically. What is more, the abscesses created between the intestines were evacuated, and the abdominal cavity was rinsed and drained (3 drains were applied).

In 4 out of 7 patients in this group, a partial dislocation of AGB occurred. In 3 cases 2/3 (Fig. 2) and in 1 case 3/4 of the band migrated to the stomach lumen (Fig. 3).

Treatment included port removal from the abdomen, introduction of a drain connecting the port and the band with the peritoneal cavity, and finally, endoscopic removal of the band from the stomach lumen. Postoperative

Table 2. Migration of the band to the stomach lumen including number of regulations and percentage of excess weight loss (%EWL)

Patient number	Patient	Age	BMI	%EWL year 1/2/3	Migration month	Number of regulations
1	F	47	45	64/61/45	36	8
2	F	27	43	66/58/38	38	9
3	F	44	42	61/54/34	32	4
4	F	36	41	70/56/28	36	10
5	M	35	44	51/63/49	38	9
6	M	41	42	84/68/58	42	18
7	M	32	46	74/70/--	28	10

BMI – body mass index; %EWL – percentage of excess weight loss; F – female, M – male.

observation lasted 3 days and each of the 4 patients underwent control abdominal contrast X-ray in order to check stomach tightness.

Two patients, in whom 28 and 32 months after LAGB body mass gain was observed along with lack of restriction after band regulation, heartburn, hyperacidity, and emesis, were referred for abdominal X-ray and CT.

Diagnostics were performed by means of an endoscopy of the upper gastrointestinal tract repeated several times. It revealed a partial migration of the gastric band (1/4–1/3) and its migration outside the stomach lumen was the cause of the aforementioned symptoms.

The patients were qualified for laparoscopic surgery, which was performed using 2 trocars (10 mm and 15 mm) along with a harmonic knife or LigaSure[TM]. In both cases, the band was removed. In 1 case, stomach wall perforation was stitched and in another case, due to its location (the posterior stomach wall), it was impossible.

In both cases, a tube was placed into the stomach in order to drain the area of band migration. In the case where the perforation of the posterior wall of the stomach was impossible to stitch, lack of tightness lasted for 15 days.

Discussion and conclusions

The most effective treatment of obesity is surgery.[10] It leads to permanent body mass loss, improves the quality of life and, in the majority of cases, eliminates co-morbidities such as diabetes, hypertension or hyperlipidemia.[11] Due to the increase of demand, new bariatric centers are launched both worldwide and in Poland, and, along with that fact, the number of reports about the efficiency of obesity treatment and specialization is constantly growing.

The first LAGB was performed by Hallberg and Forsell in 1993.[12] Between 2003 and 2008, this was the most frequently applied method worldwide.[13] In 2011, Roux-en-Y gastric bypass (RYGB) was a leading procedure – 46.6% of surgeries, followed by sleeve gastrectomy (SG) – 27.8%. The number of performed LAGB procedures has decreased within the last 4 years to 17.8%.[14]

Complications after LAGB include:
– those connected with port – disconnection from the drain, purulence in the place of port implantation;
– those connected with band – band slippage, pouch dilatation, migration to the stomach lumen, and band erosion;
– other – heartburn and hyperacidity, emesis.

Cobourn et al. from Surgical Weight Loss Clinic in Mississauga, Canada, conducted an analysis of the results based on an observation of 2815 obese patients after LAGB between May 2005 and January 2011. It was stated that complications occurred in 238 (8.5%) patients, including 118 (4.2%) patients experiencing band slippage, 14 (0.5%) with band migration and erosion, and 35 (1.2%) with symptoms of port and drain disconnection.[15] Other complications included wound infection near the port (0.4% of cases), and intraperitoneal bleeding (0.1%).

In comparison, Mittermair et al. from Medical University of Innsbruck, Austria, published in 2008 their own results – the percentage of 107 patients under 25 years of age who underwent LAGB and suffered from band migration was 2.78%.[16]

A significantly higher number of patients after LAGB who suffered from band migration to the stomach lumen was noticed by Lanthaler et al. in another center in Innsbruck. According to their data from 2010, the aforementioned complication occurred in 20.5% of cases. The examined group consisted of 276 patients after LAGB between 1996 and 2000.[17]

The causes of band migration formulated on the basis of own experience include:
– band migration to the gastrointestinal tract is connected with the fact that the band is produced from plastics and tissues in different patients react differently to such a product; it is manifested in, perioperatively noted, numerous peritoneal adhesions, fibrosis or scarring in the area of the implemented band;
– complications caused by the operating team – frequency of complications is strictly connected with the "learning curve" and the number of procedures performed by the operator;
– causes connected with the producer – a manufacturing defect;
– causes connected with the patient – lack of proper cooperation with the physician and neglecting postoperative recommendations.

The aforementioned complications indicate that the removal of a migrated band requires a multispecialistic operating team in case of surgical method alteration.

Therapeutic proceedings – surgical or endoscopic treatment in patients with a migrated band – is an individual matter depending on the type and the size of band dislocation. Treatment also depends on clinical symptoms and the general state of the patient. The experience of the operating team and the quality of the equipment also are important factors.

References

1. Bużga M, Holéczy P, Švagera Z, Švorc P Jr, Zavadilová V. Effects of sleeve gastrectomy on parameters of lipid and glucose metabolism in obese women – 6 months after operation. *Wideochir Inne Tech Maloinwazyjne*. 2013;8(1):22–28.
2. James WP. The epidemiology of obesity: The size of the problem. *J Intern Med*. 2008;263(4):336–352.
3. Szydłowski K, Frask A, Michalik M, Ciesielski M, Budziński R, Orłowski M. Complications after surgical treatment of obesity based on own material. *Wideochir Inne Tech Maloinwazyjne*. 2008;3(2):45–52.
4. Fernandez AZ Jr, Demaria EJ, Tichansky DS, et al. Multivariate analysis of risk factors for death following gastric bypass for treatment of morbid obesity. *Ann Surg*. 2004;239(5):698–702.
5. Chakravarty PD, McLaughlin E, Whittaker D, et al. Comparison of laparoscopic adjustable gastric banding (LAGB) with other bariatric procedures: A systematic review of the randomized controlled trials. *Surgeon*. 2012;10(3):172–182.

6. Póvoa AA, Soares C, Esteves J, et al. Simultaneous gastric and colic laparoscopic adjustable gastric band migration: Complication of bariatric surgery. *Obes Surg*. 2010;20(6):796–800.
7. Hady RH, Dadan J, Sołdatow M, et al. Complications after laparoscopic gastric banding in own material. *Wideochir Inne Tech Maloinwazyjne*. 2012;7(3):166–174.
8. Wierzbicki Z, Lisik W. Przygotowanie chorego do operacji bariatrycznej. *Medycyna Praktyczna Chirurgia*. 2011;5:19–21.
9. Frieda M, Hainerb V, Basdevantc A, et al. Interdisciplinary European guidelines on surgery of severe obesity. *Obes Facts*. 2008;1(1):52–59.
10. Maggard MA, Shugarman LR, Suttorp M, et al. Meta-analysis: Surgical treatment of obesity. *Ann Intern Med*. 2005;142(7):547–559.
11. Hady RH, Dadan J, Gołaszewski P, Safiejko K. Impact of laparoscopic sleeve gastrectomy on body mass index, ghrelin, insulin and lipid levels in 100 obese patient. *Wideochir Inne Tech Maloinwazyjne*. 2012;7(4):251–259.
12. Abalikšta T, Brimas G, Strupas K. Laparoscopic adjustable gastric banding. A prospective randomized study comparing the Swedish adjustable gastric band and the MiniMizer Extra: One-year results. *Wideochir Inne Tech Maloinwazyjne*. 2011;6(4):207–216.
13. Buchwald H, Oien DM. Metabolic/bariatric surgery worldwide 2008. *Obes Surg*. 2008;19(12):1605–1611.
14. Buchwald H, Oien DM. Metabolic/bariatric surgery worldwide 2011. *Obes Surg*. 2013;23(4):427–436.
15. Cobourn C, Chapman MA, Ali A, Amrhein J. Five-year weight loss experience of outpatients receiving laparoscopic adjustable gastric band surgery. *Obes Surg*. 2013;23(7):903–910.
16. Mittermair R, Aigner F, Obermüller S. High complication rate after Swedish adjustable gastric banding in younger patients ≤25 years. *Obes Surg*. 2009;19(4):446–450.
17. Lanthaler M, Aigner F, Kinzl J, Sieb M, Cakar-Beck F, Nehoda H. Long-term results and complications following adjustable gastric banding. *Obes Surg*. 2010;20(8):1078–1085.

Corneal biomechanical properties in patients with Hashimoto's thyroiditis

Ahmet Kırgız[1,A,C,D,F], Kübra Şerefoğlu Çabuk[1,A,B], Mikail Yetmis[2,B], Kürşat Atalay[1,C,E]

[1] Department of Ophthalmology, Bağcılar Training and Research Hospital, Istanbul, Turkey
[2] Department of Internal Medicine, Bağcılar Training and Research Hospital, Istanbul, Turkey

A – research concept and design; B – collection and/or assembly of data; C – data analysis and interpretation;
D – writing the article; E – critical revision of the article; F – final approval of the article

Address for correspondence
Ahmet Kırgız
E-mail: ahmetk1@yahoo.com

Abstract

Background. Hashimoto's thyroiditis (HT) is an autoimmune endocrine disorder that results from a dys-regulation of the immune system leading to an immune attack on the thyroid gland. It has potential effects on different organs and tissues.

Objectives. The aim of the study was to investigate the effect of HT on corneal biomechanical properties using the ocular response analyzer (ORA).

Material and methods. A total of 48 patients with HT and 49 healthy subjects were enrolled in the study. The mean age of the patients and healthy subjects was 42.33 ± 11.96 and 40.20 ± 12.60 years, respectively ($p = 0.39$). All of the subjects underwent a full ophthalmological examination, including visual acuity, corneal pachymetry with topography, biomicroscopy, and funduscopy. Corneal biomechanical properties, including corneal hysteresis (CH) and corneal resistance factor (CRF), Goldmann-correlated intraocular pressure (IOPg) and corneal compensated IOP (IOPcc) were measured with the ORA.

Results. Central corneal thickness (CCT) in the patient group and the control group were not significantly different ($p = 0.65$). Corneal hysteresis of the HT patients was significantly lower than that of the control group ($p = 0.005$). There were no statistically significant differences in CRF between the 2 groups ($p = 0.53$). Goldmann-correlated IOP and IOPcc were higher in the HT patients, but only IOPcc showed a statistically significant difference ($p = 0.001$).

Conclusions. In conclusion, our data shows that HT affects corneal biomechanical properties by decreasing CH. Thus, IOPcc measured with the ORA should be taken into account when determining accurate IOP values in patients with HT.

Key words: corneal hysteresis, corneal resistance factor, Hashimoto's thyroiditis, ocular response analyzer

Introduction

Hashimoto's thyroiditis (HT) is a chronic inflammation of the thyroid gland. It is now considered the most common autoimmune disease,[1,2] the most common endocrine disorder,[3] as well as the most common cause of hypothyroidism.[4] It affects predominantly women. It is characterized by elevated levels of antithyroglobulin (Anti-Tg) antibody and antithyroid peroxidase (anti-TPO), and a characteristic hypoechogenic pattern in ultrasonography of the thyroid gland. It has different clinical stages ranging from euthyroidism to hypothyroidism.[5]

There is a relationship between thyroid diseases and the eye: so-called thyroid eye disease (TED). It is most commonly associated with Graves' disease (GD) and is occasionally seen in the euthyroid state.[6,7] The clinical manifestations include exophthalmos, conjunctival hyperemia and chemosis, soft tissue swelling, eyelid retraction, ophthalmoplegia, increases in orbital volume that may lead to increased intraorbital pressure, keratopathy, and optic neuropathy.[8,9] In contrast, TED in HT is extremely uncommon and there are limited reports of it in the literature.[10–12]

Because of the fact that one of the most important manifestations of TED is corneal and ocular surface involvement, investigators have studied alterations in corneal biomechanical properties in TED patients.[13,14] There are also some studies about corneal microstructural changes using corneal pachymetry and confocal biomicroscopy in GD.[15,16] To the best of our knowledge, alterations in corneal biomechanical properties in patients with HT have not been studied in detail before.

The ocular response analyzer (ORA) (Reichert Ophthalmic Instruments, Buffalo, USA) was introduced with the aim of providing information on corneal biomechanical factors such as hysteresis and resistance. It determines noncontact intraocular pressure (IOP) as Goldmann-correlated IOP (IOPg) and corneal-compensated IOP (IOPcc). This modality has been designed to quantify IOP by integrating corneal biomechanical factors, allowing the practitioner to reduce the margin of error in IOP measurements as compared with the conventional method, Goldmann applanation tonometry (GAT).[17]

The aim of the study was to investigate the effect of HT disease on corneal biomechanical properties using the ORA.

Material and methods

Between June 2015 and January 2016, 51 patients diagnosed with HT at the Endocrinology Department of Bağcılar Training and Research Hospital, Istanbul, Turkey, were referred to our eye clinic. Out of these 51, 48 exclusively female patients were included in this prospective observational study (Group 1) to eliminate any errors that might depend on gender differences. For the control group (Group 2), 49 healthy female subjects who visited our outpatient general clinics for routine ocular checkups or for glasses prescriptions were matched regarding age. Whenever both eyes met the criteria, the right eye of each participant was included. Patients with a history of corneal surgery, ocular trauma, corneal scarring, or any concurrent ocular disease were excluded from the study, as were contact lens wearers and women who were pregnant or lactating during the course of the study. All the patients with HT were under treatment and none of the patients had TED. The study followed the tenets of the Declaration of Helsinki and was approved by the local ethics committee.

All the subjects underwent a full ophthalmological examination including visual acuity, biomicroscopy, funduscopy, corneal pachymetry by Sirius topographer (Costruzione Strumenti Oftalmici, Florence, Italy), measurement of corneal hysteresis (CH) and corneal resistance factor (CRF), as well as IOPg and IOPcc using the ORA. All ORA measurements were obtained using the same calibrated instrument by the same masked technician. All the patients underwent measurements while sitting and were asked to fix their vision on a target light as the measurement was taken. A noncontact probe scanned the central corneal area and released an air puff. For each patient, 4 measurements with a minimum waveform score (WS) of 6.0 were obtained.[18] The best signal value was used in the statistical evaluation.

All the statistical analyses were performed with SPSS for Windows v. 21.0 (SPSS Inc., Chicago, USA). The parameters used in the study were expressed as means ± standard deviation (SD). The normality of the data was tested with the Kolmogorov-Smirnov test. Student's t-test was used to determine the significance of differences in the results. A p-value of less than 0.05 was considered statistically significant.

Results

The mean age of the patients was 42.33 ±11.96 years (range: 17–62 years) in the group with HT (Group 1) and 40.20 ±12.60 years (range: 17–61 years) in the control group (Group 2) (p = 0.39). Central corneal thickness (CCT) values were not significantly different between the groups (p = 0.65), as shown in Table 1.

Corneal hysteresis of HT patients was significantly lower than that of the control group (p = 0.005). There was no statistically significant difference in CRF between the 2 groups (p = 0.53). Goldmann-correlated IOP and IOPcc were higher in the HT patients, but only IOPcc showed a statistically significant difference (p = 0.001) (Table 1).

Discussion

The structure and the properties of soft tissue, such as the cornea, are dependent on the biochemical and physical nature of the components present. Stress

Table 1. The demographic and corneal biomechanical features of the study participants

Variable	Hashimoto's thyroiditis (n = 48)	Control (n = 49)	p-value
Age [years]	42.33 ±11.96	40.2 ±12.6	0.39
IOPg [mm Hg]	16.73 ±3.52	15.78 ±3.16	0.16
IOPcc [mm Hg]	17.89 ±3.19	15.85 ±2.81	0.001
CH [mm Hg]	9.51 ±1.31	10.27 ±1.28	0.005
CRF [mm Hg]	10.11 ±1.66	10.31 ±1.54	0.53
CCT [μm]	541.83 ±30.54	544.75 ±33.63	0.65

IOP – intraocular pressure; IOPg – Goldmann-correlated IOP;
IOPcc – corneal-compensated IOP; CH – corneal hysteresis;
CRF – corneal resistance factor; CCT – central corneal thickness.

to these components and their response to it show the biomechanical properties of the tissue. The ORA is a noncontact tonometer that uses a rapid air pulse to create stress on the cornea and an electro-optical system to record the corneal deformation.[17] In our study, we wanted to evaluate the effect of HT on corneal biomechanical properties measured with the ORA, and we found that the CH of HT patients was significantly lower than that of the healthy control group.

Corneal hysteresis is a quantification of the ability of the cornea to absorb and/or dissipate energy: so-called viscous dampening. Low values of CH indicate a floppy cornea and less corneal viscous dampening, which may be explained by an alteration in the corneal structure. There are some reports that show a decrease of CH in diseases that cause alterations in corneal structure, such as keratoconus[19,20] and myopic eyes,[21] in eyes of patients with diabetes mellitus,[22] in post-laser in situ keratomileusis eyes,[23] and in eyes that have undergone penetrating keratoplasty.[24] However, these alterations in corneal structure are also found in some systemic diseases, such as systemic lupus erythematosus,[25] rheumatoid arthritis,[26] Marfan syndrome,[27] and other inflammatory conditions. The corneas of patients with HT may have similar alterations in the corneal microstructure known to occur in these corneal diseases.

An eye with low CH has a lower ability to absorb energy; in the presence of high IOP, the cornea cannot absorb energy, and all the pressure is exerted on the optic nerve and peripapillary tissues.[28] Thus, low CH is associated with high IOP in both glaucoma patients and healthy individuals, and it may be a risk factor for the progression of glaucoma. In our study, we also found that the IOPcc of HT patients was higher compared with the control group. It is known that the IOPcc is not affected by CCT when measured using the ORA, which might provide a better estimate of the real IOP value than GAT measurements do. Routine IOP measurements using GAT may underestimate IOP in HT patients, so this point should be kept in mind when examining eyes with suspicious cupping and borderline IOP.

In this study, we found no statistically significant difference between the HT patients and the control group regarding CRF. In fact, CRF is mainly determined by the elastic properties of the cornea and is a parameter more closely associated with CCT than CH.[29] Because CCT measurements showed no statistical differences between the HT patients and the healthy subjects, it was consistent that CRF did not differ between the 2 groups.

There are some reports investigating the biomechanical properties of the cornea in patients with GD with or without TED. Karabulut et al. evaluated corneal biomechanical properties in patients with TED using the ORA and found significant decreases in CH but no significant differences in CRF and CCT.[13] They also reported higher IOPg and IOPcc levels among TED patients compared with the control group. Moghimi et al. evaluated TED patients and reported the same findings as in the previous study.[14] These findings and our study results suggest that there is a strong relation between the autoimmune thyroid diseases – HT and GD. The etiology of HT and GD involves common pathways in which thyroid-reactive T cells escape tolerance and infiltrate the thyroid, and unique pathways in which these thyroid-reactive T cells either cause thyroid cell death (in HT) or stimulation (in GD).[30] Thus, it is not surprising that both autoimmune thyroid diseases have similar effects on corneal biomechanical properties. Further studies are warranted to define which inflammatory process in the corneal tissue of these patients is responsible for this biomechanical change.

Some limitations of this study should be mentioned. Firstly, since this is a cross-sectional study, a direct cause and effect cannot be determined. Secondly, the exact mechanisms causing abovementioned alterations should be studied in detail with genetic and specular microscopic evaluation as well. Finally, the small sample size restricted our ability to make generalized conclusions.

Conclusions

In conclusion, our data shows that HT affects corneal biomechanical properties by decreasing CH. Thus, IOPcc measured with the ORA should be taken into account when determining the accurate IOP value in patients with HT.

References

1. Jacobson DL, Gange SJ, Rose NR, Graham NM. Epidemiology and estimated population burden of selected autoimmune diseases in the United States. *Clin Immunol Immunopathol*. 1997;84(3):223–243.
2. McLeod DS, Cooper DS. The incidence and prevalence of thyroid autoimmunity. *Endocrine*. 2012;42(2):252–265.
3. Golden SH, Robinson KA, Saldanha I, Anton B, Ladenson PW. Clinical review. Prevalence and incidence of endocrine and metabolic disorders in the United States: A comprehensive review. *J Clin Endocrinol Metab*. 2009;94(6):1853–1878.
4. Vanderpump MP. The epidemiology of thyroid disease. *Br Med Bull*. 2011;99:39–51.
5. Pearce EN, Farwell AP, Braverman LE. Thyroiditis. *N Engl J Med*. 2003;348(26):2646–2655.

6. Jacobson DM. Dysthyroid orbitopathy. *Sem Neurol*. 2000;20(1):43–54.

7. El-Kaissi S, Frauman AG, Wall JR. Thyroid-associated ophthalmopathy: A practical guide to classification, natural history and management. *Intern Med J*. 2004;34(8):482–491.

8. Bartley GB, Fatourechi V, Kadrmas EF, et al. Clinical features of Graves' ophthalmopathy in an incidence cohort. *Am J Ophthalmol*. 1996;121(3):284–290.

9. Garrity JA, Bahn RS. Pathogenesis of Graves ophthalmopathy: Implications for prediction, prevention and treatment. *Am J Ophthalmol*. 2006;142(1):147–153.

10. Grzesiuk W, Szydlarska D, Pragacz A, Bar-Andziak E. Thyroid-associated orbitopathy in patients with Hashimoto's thyroiditis: A case report. *Pol Arch Med Wewn*. 2008;118(5):318–321.

11. Hiraga A, Mimura M, Kamitsukasa I. Isolated inferior rectus muscle myopathy due to Hashimoto's thyroiditis. *Intern Med*. 2008;47(13):1283–1284.

12. Kan E, Kan EK, Ecemis G, Colak R. Presence of thyroid-associated ophthalmopathy in Hashimoto's thyroiditis. *Int J Ophthalmol*. 2014;7(4):644–647.

13. Karabulut GO, Kaynak P, Altan C, et al. Corneal biomechanical properties in thyroid eye disease. *Kaohsiung J Med Sci*. 2014;30(6):299–304.

14. Moghimi S, Safizadeh M, Mazloumi M, Hosseini H, Vahedian Z, Rajabi MT. Evaluation of corneal biomechanical properties in patients with thyroid eye disease using ocular response analyzer. *J Glaucoma*. 2016;25(3):269–273.

15. Konuk O, Aktas Z, Aksoy S, Onol M, Unal M. Hyperthyroidism and severity of orbital disease do not change the central corneal thickness in Graves' ophthalmopathy. *Eur J Ophthalmol*. 2008;18(1):125–127.

16. Villani E, Viola F, Sala R, et al. Corneal involvement in Graves' orbitopathy: An in vivo confocal study. *Invest Ophthalmol Vis Sci*. 2010;51(9):4574–4578.

17. Luce DA. Determining in vivo biomechanical properties of the cornea with an ocular response analyzer. *J Cataract Refract Surg*. 2005;31(1):156–162.

18. Mandalos A, Anastasopoulos E, Makris L, Dervenis N, Kilintzis V, Topouzis F. Inter-examiner reproducibility of ocular response analyzer using the waveform score quality index in healthy subjects. *J Glaucoma*. 2013;22(2):152–155.

19. Shah S, Laiquzzaman M, Bhojwani R, Mantry S, Cunliffe I. Assessment of the biomechanical properties of the cornea with ocular response analyzer in normal and keratoconic eyes. *Invest Ophthalmol Vis Sci*. 2007;48(7):3026–3031.

20. Fontes BM, Junior RA, Jardim D, Velarde GC, Nose W. Ability of corneal biomechanical metrics and anterior segment data in the differentiation of keratoconus and healthy corneas. *Ophthalmology*. 2010;117(4):673–679.

21. Altan C, Demirel B, Azman E, et al. Biomechanical properties of axially myopic cornea. *Eur J Ophthalmol*. 2012;22(Suppl 7):S24–28.

22. Goldich Y, Barkana Y, Gerber Y, et al. Effect of diabetes mellitus on biomechanical parameters of the cornea. *J Cataract Refract Surg*. 2009;35(4):715–719.

23. Ortiz D, Piñero D, Shabayek MH, Arnalich-Montiel F, Alió JL. Corneal biomechanical properties in normal, post-laser in situ keratomileusis, and keratoconic eyes. *J Cataract Refract Surg*. 2007;33(8):1371–1375.

24. Shin JY, Choi JS, Oh JY, Kim MK, Lee JH, Wee WR. Evaluation of corneal biomechanical properties following penetrating keratoplasty using the ocular response analyzer. *Korean J Ophthalmol*. 2010;24(3):139–142.

25. Yazici AT, Kara N, Yüksel K, et al. The biomechanical properties of the cornea in patients with systemic lupus erythematosus. *Eye (Lond)*. 2011;25(8):1005–1009.

26. Can ME, Erten S, Can GD, Cakmak HB, Sarac O, Cagil N. Corneal biomechanical properties in rheumatoid arthritis. *Eye Contact Lens*. 2015;41(6):382–385.

27. Kara N, Bozkurt E, Baz O, et al. Corneal biomechanical properties and intraocular pressure measurement in Marfan patients. *J Cataract Refract Surg*. 2012;38(2):309–314.

28. Congdon NG, Broman MA, Bandeen-Roche K, Grover D, Quigley HA. Central corneal thickness and hysteresis associated with glaucoma damage. *Am J Ophthalmol*. 2006;141(5):868–875.

29. Shah S, Laiquzzaman M, Cunliffe I, Mantry S. The use of the Reichert ocular response analyzer to establish the relationship between ocular hysteresis, corneal resistance factor and central corneal thickness in normal eyes. *Cont Lens Anterior Eye*. 2006;29(5):257–262.

30. Tomer Y. Genetic susceptibility to autoimmune thyroid disease: Past, present and future. *Thyroid*. 2010;20(7):715–725.

The usefulness of SPECT-CT with radioisotope-labeled leukocytes in diagnosing lead-dependent infective endocarditis

Barbara A. Małecka[1,2,A,B,D,F], Andrzej Ząbek[1,B,C,E,F], Maciej Dębski[1,B,E,F], Wojciech Szot[3,4,B,E,F], Katarzyna Holcman[5,B,E,F], Krzysztof Boczar[1,B,E,F], Mateusz Ulman[1,B,E,F], Jacek Lelakowski[1,2,B,E,F], Magdalena Kostkiewicz[2,5,B,E,F]

[1] Department of Electrocardiology, John Paul II Hospital, Kraków, Poland

[2] Institute of Cardiology, Jagiellonian University Medical College, Kraków, Poland

[3] Department of Hygiene and Dietetics, Jagiellonian University Medical College, Kraków, Poland

[4] Nuclear Medicine Department, John Paul II Hospital, Kraków, Poland

[5] Department of Cardiac and Vascular Diseases, John Paul II Hospital, Kraków, Poland

A – research concept and design; B – collection and/or assembly of data; C – data analysis and interpretation;
D – writing the article; E – critical revision of the article; F – final approval of the article

Address for correspondence
Andrzej Ząbek
E-mail: andrzej_j_z@poczta.onet.pl

Abstract

Background. Lead-dependent infective endocarditis (LDIE) is a life-threatening complication of permanent transvenous cardiac pacing. According to the 2015 European Society of Cardiology (ECS) guidelines, the diagnosis of LDIE is based on the modified Duke criteria (MDC), while single-photon emission computed tomography with conventional computed tomography (SPECT-CT) with radioisotope-labeled leukocytes serves as an additional tool in difficult cases. The major challenge is to differentiate between true vegetation and a thrombus.

Objectives. The aim of the study was to evaluate the usefulness of SPECT-CT with radioisotope-labeled leukocytes in diagnosing LDIE in patients with intracardiac masses (ICMs).

Material and methods. The prospective registry included 40 consecutive patients admitted with an ICM on the lead and suspicion of LDIE. The confirmation or rejection of the LDIE diagnosis was made according to an algorithm based on the MDC. The cohort was divided into 2 groups: patients with definite and possible LDIE diagnoses based on the MDC (the LDIE-positive group), and patients with negative LDIE diagnoses according to the MDC (the LDIE-negative group). All patients underwent SPECT-CT with radioisotope-labeled leukocytes. The diagnostic ability of SPECT-CT was compared to the gold standard MDC.

Results. The LDIE-positive group with diagnosis based on the MDC consisted of 19 patients (LDIE definite – 11; LDIE possible – 8). The LDIE diagnosis was rejected on the basis of the MDC in 21 patients. The SPECT-CT results were compared with the MDC results and showed 73.7% sensitivity, 81.0% specificity, 77.5% accuracy, 77.8% positive predictive value (PPV), 77.3% negative predictive value (NPV), likelihood ratio positive (LR+) 3.868, likelihood ratio negative (LR−) 0.325, and moderate agreement ($\kappa = 0.548$, $p < 0.001$). After the exclusion of 5 patients treated with antibiotics at the time of the SPECT-CT, LR+ and LR− improved to 5.250 and 0, respectively, and inter-test agreement amounted to almost perfect concordance ($\kappa = 0.773$, $p < 0.001$).

Conclusions. Single-photon emission computed tomography with conventional CT with radioisotope-labeled leukocytes is a useful, efficient, single-step test for diagnosing LDIE.

Key words: scintigraphy, vegetation, infective endocarditis, cardiac pacing, artificial, radionuclide imaging

Introduction

Lead-dependent infective endocarditis (LDIE) is a life-threatening complication of permanent transvenous cardiac pacing occurring in the right side of the heart. The term was coined to underline the fact that LDIE is a unique disease process and a distinct entity in the wide spectrum of cardiac device-related infective endocarditis (CDRIE), in which inflammation is associated with various types of implantable devices.[1] According to most of the available reports, LDIE is the major risk factor for mortality after transvenous lead extraction (TLE) procedures.[2] The 2009 guidelines of European Society of Cardiology (ESC) concerning the prevention, diagnosis and treatment of infective endocarditis (IE) outlined straightforward criteria (the Duke criteria) that should be met in order to diagnose IE.[3] The major criteria for diagnosing IE include positive blood cultures and echocardiographic findings characteristic of IE, such as vegetation and abscess formation. To identify patients with indwelling endocardial leads, 2 additional major criteria have been introduced: local signs of infection and pulmonary embolism.

Implementing the results of additional imaging investigations of the source of infection – positron emission tomography/computed tomography (PET-CT) and single-photon emission computed tomography with conventional computed tomography (SPECT-CT) with radioisotope-labeled leukocytes – into the ESC guidelines and giving them the importance of major criteria may significantly improve the diagnostic accuracy of the Duke criteria.[4] The role of nuclear medicine, according to the guidelines, is confined to the diagnosis of prosthetic valve endocarditis. The authors of the guidelines mentioned that PET-CT and SPECT-CT have proven their role in the diagnosis of cardiac implantable electronic devices (CIEDs), but the data is not sufficient for them to be included in the diagnostic criteria of the specific topic of IE on pacemaker or defibrillator leads.[4] Notably, in the chapter on diagnosing cardiac device IE, the authors recognize the utility of SPECT-CT and PET-CT scanning as additional tools in difficult cases, such as in patients with suspected LDIE, positive blood cultures and negative echocardiography (Class IIb, level of evidence C).[4] Erba et al. showed that SPECT-CT allowed LDIE to be confirmed or reliably excluded device-associated infections during febrile episodes and sepsis, with 95% negative predictive value (NPV).[5]

The aim of the present study was to show the diagnostic value of SPECT-CT in patients with an intracardiac mass (ICM) suspected of being vegetation, in comparison to the gold standard modified Duke criteria (MDC).

Material and methods

The prospective registry included consecutive patients with ICMs on the lead admitted to a reference university center (Department of Electrocardiology, John Paul II Hospital, Kraków, Poland) from August 2014 to August 2017. The prerequisites for including a patient in the study were: detection of an ICM on echocardiography and provision of informed consent to participate in the study. Confirmation or rejection of an LDIE diagnosis was made according to the algorithm used in our center and based on the MDC, which is considered the gold standard (Fig. 1). Among the patients, there was a variety of clinical presentations and various degrees of clinical IE suspicion (Table 1). A final diagnosis of LDIE according to the MDC was established after collecting all the tests included in the major and minor criteria. All the patients also underwent SPECT-CT scanning.

The cohort was divided into 2 groups: patients with definite and possible LDIE diagnoses based on the MDC (the LDIE-positive group), and patients with negative
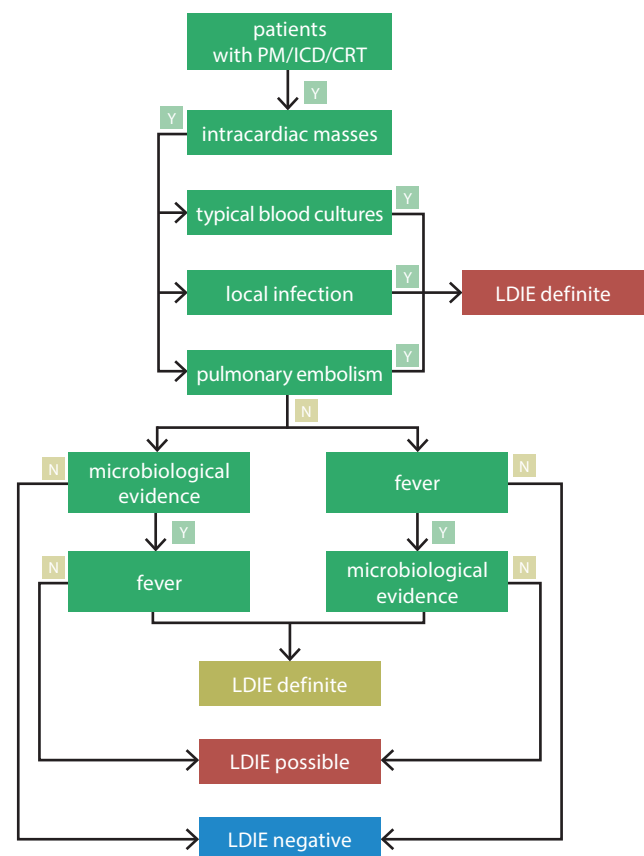
Fig. 1. The diagnostic algorithm for the diagnosis of lead-dependent infective endocarditis (LDIE) based on the modified Duke criteria (MDC). Y – yes, N – no; typical blood cultures: blood cultures for microorganisms consistent with infective endocarditis (IE) from 2 or more separate cultures of blood were treated as major criterion; microbiological evidence: positive blood culture but does not meet major criterion, more than 1 positive blood culture with skin bacteria was treated as a minor criterion, 1 positive blood culture with skin bacteria was treated as sample contamination; local infection: signs of inflammation of the pocket of the cardiac device or pocket skin erosion with purulent drainage; septic pulmonary embolism: clinical, echocardiographic and laboratory features of pulmonary embolism accompanied by evidence of recurrent pulmonary infections

PM – pacemaker; ICD – implantable cardioverter-defibrillator; CRT – cardiac resynchronization therapy.

LDIE diagnoses according to the MDC (the LDIE-negative group). Both groups included patients with positive and negative SPECT-CT results. The diagnostic test evaluated in the present study was SPECT-CT, which was compared with the gold standard MDC.

Approval to conduct the study was obtained from the local ethics committee.

SPECT-CT as a diagnostic modality

In our center, the autologous leukocyte labeling procedure was performed in strict accordance with the Society of Nuclear Medicine Procedure Guidelines.[6] Whole-body scans followed by chest SPECT-CT scans were acquired 6 h and 24 h after the injection of radioisotope-labeled white blood cells (WBCs) with the use of a Symbia T16 SPECT-CT gamma camera system (Siemens AG, Munich, Germany). The first 10 patients underwent SPECT-CT with Scintimun® (Cisbio, Codolet, France) and subsequent patients with ^{99m}Tc-HMPAO (GE Healthcare Ltd., Amersham, UK). The transmission data were reconstructed using filtered back projection to produce cross-sectional images. The resolution of the computed tomography (CT) scan was 2.5 mm, and localization images were produced with a 4.5-mm pixel size, similar to nuclear medicine emission images. The CT scans were reconstructed onto a 256×256 matrix. The SPECT component of the same field of view was acquired using a 128×128 matrix, 360° rotation, 6° angle step, and acquisition time of 25 s per frame. Both attenuation-corrected CT and noncorrected SPECT images were evaluated in the coronal, transaxial and sagittal plane modes. All the studies were evaluated by 2 experienced nuclear medicine specialists. Scintigraphy was considered positive for CDRIE when an area of labeled WBCs uptake superior to the background activity was identified in the involved area and when the signal increased over time (Fig. 2).[7]

Statistical analysis

The statistical analysis was performed using the STATISTICA v. 12.5 data analysis software system (StatSoft Inc., Tulsa, USA). For quantitative variables, minimum, maximum, mean, and standard deviation (SD) values were provided. The results of the tests were expressed as a 2-way contingency table. The assessment of the tests included the following parameters: sensitivity, specificity, positive predictive value (PPV), negative predictive value (NPV), accuracy, likelihood ratio for a positive test result (LR+), and likelihood ratio for a negative test result (LR−).

The interpretation of the likelihood ratios (LRs) was performed according to Attia.[8] A test has real diagnostic utility if the LR is ≥10 or ≤0.1. Values between 5 and 10 and between 0.1 and 0.2 show that a test is moderately useful. An LR between 0.5 and 2 indicates that the test has no diagnostic value.[9] Inter-observer variability was calculated using multi-rater Cohen's kappa (κ) statistics with

Table 1. Indications for echocardiography in consecutive patients with ICM: clinical presentation, diagnosis based on the Duke criteria and the results of SPECT-CT studies

Patient No.	Clinical presentation	Diagnosis of LDIE based on Duke criteria	SPECT-CT heart	SPECT-CT pocket
1.	A	N	N	N
2.	B	D	N	P
3.	C	D	N	N
4.	DT	N	N	N
5.	DT	N	N	N
6.	A	N	N	N
7.	A	Ps	P	N
8.	A	Ps	P	N
9.	B	D	N	N
10.	A	D	P	N
11.	C	D	P	N
12.	A	Ps	P	N
13.	B	D	P	N
14.	A	N	P	P
15.	A	N	P	N
16.	A	N	N	N
17.	C	D	P	N
18.	DT	N	N	N
19.	A	N	N	N
20.	C	D	P	N
21.	E	Ps	N	N
22.	A	N	P	N
23.	A	N	N	N
24.	A	Ps	P	N
25.	A	Ps	P	N
26.	B	D	N	N
27.	DT	N	P	N
28.	A	N	N	N
29.	DT	N	N	N
30.	A	N	N	N
31.	E	Ps	P	N
32.	E	N	N	N
33.	C	D	P	N
34.	A	N	N	N
35.	A	N	N	N
36.	B	D	P	P
37.	DT	N	N	N
38.	E	Ps	P	P
39.	A	N	N	N
40.	A	N	N	N

A – diagnostic work-up of dyspnoea and/or heart failure; B – diagnostic work-up prior to transvenous lead extraction due to pocket infection; C – diagnostic work-up of sepsis; DT – diagnostic work-up prior to transvenous lead extraction due to lead dysfunction/system change/system upgrade; E – diagnostic work-up of fever; N – negative; P – positive; Ps –possible; D – definite; ICM – intracardiac mass; LDIE – lead-dependent infective endocarditis; SPECT-CT – single-photon emission computed tomography with conventional computed tomography.
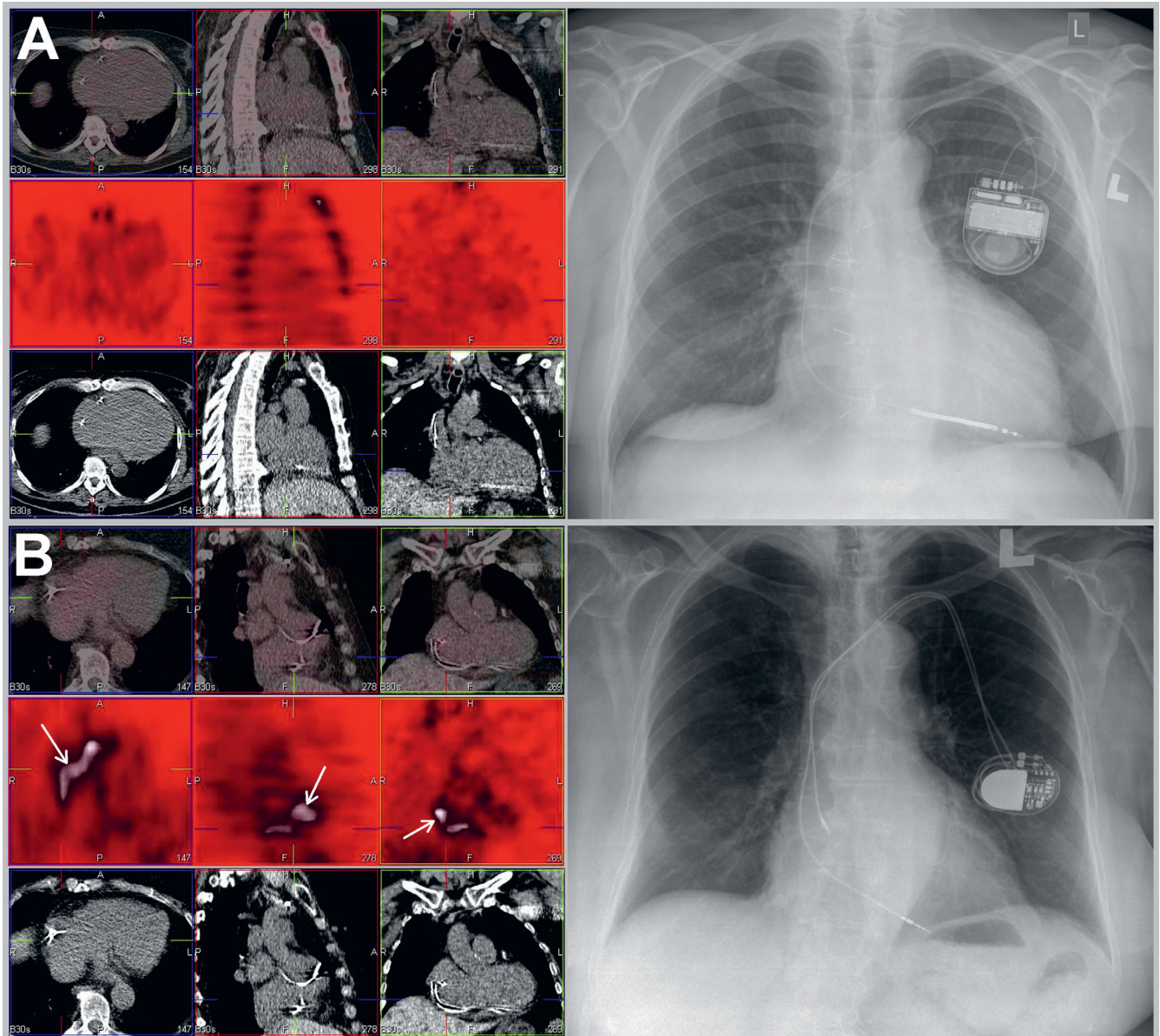
Fig. 2. Single-photon emission computed tomography with conventional computed tomography (SPECT-CT) and chest X-ray in patients with negative and positive SPECT-CT results. A – Single-chamber implantable cardioverter-defibrillators (ICD) system. The SPECT-CT study with the use of ^{99m}Tc-HMPAO-labeled leukocytes on the left side of the picture and chest X-ray picture on the right side. The negative result of the SPECT-CT study is presented in the upper and middle panels of the SPECT-CT figure. B – Dual-chamber pacemaker (DDD) pacing system. SPECT-CT study with the use of ^{99m}Tc-HMPAO-labeled leukocytes on the left side of the picture and chest X-ray picture on the right side. Positive result suggesting infective endocarditis (IE) is presented in the upper and middle panels of the SPECT-CT figure. Focal uptake observed in the right atrium and partially in the right ventricle near the lead (arrows)

a 95% confidence interval (CI). The definitions presented by Landis and Koch were used to evaluate the strength of the rater agreement and were categorized as slight (0–0.20); fair (0.21–0.40); moderate (0.41–0.60); substantial (0.61–0.80); and almost perfect (0.81–1.00).[10] A 2-tailed p-value <0.05 was considered significant.

Results

The study population consisted of 40 patients (7 females and 33 males), mean age 62.0 ±16.5 years (range: 23.8–89.0), with different types of CIEDs and ICMs detected by transthoracic or transesophageal echocardiography (TTE/TEE). The patients were implanted with the following types of CIED: 19 had pacemakers, 12 had implantable cardioverter-defibrillators (ICD), 7 had undergone cardiac resynchronization therapy (CRT), and 2 had pacemakers and ICDs on both sides of the chest. Lead dwell time was 102.1 ±85.5 months (range: 0.6–434.1).

In the LDIE-positive group, there were 19 patients (3 female) with an average age of 72.6 ±8.9 years. Definite LDIE was diagnosed in 11 patients on the basis of at least 2 major criteria fulfilled: along with ICMs there was septic pulmonary embolism in 6 patients and local infection in 5 patients. Two patients with definite LDIE had positive blood cultures

for *Staphylococcus aureus*, thus meeting a major Duke criterion. Possible LDIE was diagnosed in 8 patients in the presence of 1 major and 1 minor criterion (Table 1). The major Duke criterion in each of these patients was an ICM; the minor criteria were fever in 6 patients and positive blood cultures that did not meet the major Duke criterion in 2 patients.

In the LDIE-negative group, there were 21 patients (4 female) with an average age of 57.9 ±21.8 years. When compared with the MDC results, the results obtained by SPECT-CT were true positive (TP) in 14 patients, false negative (FN) in 5, false positive (FP) in 4, and true negative (TN) in 17 patients. The SPECT-CT results were FN in 5 patients in whom antibiotic treatment had been administered before the examination. Based on the number of patients with TP, FN, FP, and TN results, the diagnostic value of SPECT-CT in relation to MDC was calculated (Table 2). Diagnostic test using SPECT-CT showed high sensitivity, specificity and accuracy (73.7%, 81.0% and 77.5%, respectively) and high PPV and NPV (PPV 77.8% and NPV 77.3%). The scintigraphic test can be useful to diagnose or rule out LDIE (LR+ = 3.868, LR− = 0.325). Agreement between the 2 tests was moderate but statistically significant ($\kappa = 0.548$, $p < 0.001$), according to Landis and Koch.[10]

After the exclusion of the 5 patients undergoing antibiotic treatment at the time of the examination, the SPECT-CT test sensitivity, accuracy and NPV significantly increased

Table 2. The diagnostic value of SPECT-CT in relation to MDC

Parameter		Test based on SPECT-CT
Sensitivity	result	73.7%
	95% CI	55.1–86.1%
Specificity	result	81.0%
	95% CI	64.2–92.2%
PPV	result	77.8%
	95% CI	58.2–90.9%
NPV	result	77.3%
	95% CI	61.3–88.0%
ACC	result	77.5%
	95% CI	59.9–89.3%
LR+	result	3.868
	95% CI	1.539–11.065
LR−	result	0.325
	95% CI	0.150–0.699
κ	κ	0.548
	SE	0.133
	95% CI	0.193–0.785
	Z	3.447
	p-value	<0.001

CI – confidence interval; PPV – positive predictive value; NPV – negative predictive value; ACC – accuracy; LR+ – likelihood ratio for a positive test result; LR− – likelihood ratio for a negative test result; MDC – modified Duke criteria; SPECT-CT – single-photon emission computed tomography with conventional computed tomography; κ – multi-rater Cohen's kappa; SE – standard error; Z – z-score.

Table 3. The diagnostic value of SPECT-CT for MDC after exclusion of 5 patients with false negative (FN) results due to ongoing antibiotic treatment at the time of the SPECT-CT

Parameter		Test based on SPECT-CT
Sensitivity	result	100.0%
	95% CI	79.0–100.0%
Specificity	result	81.0%
	95% CI	67.0–81.0%
PPV	result	77.8%
	95% CI	61.5–77.8%
NPV	result	100.0%
	95% CI	82.7–100.0%
ACC	result	88.6%
	95% CI	71.8–88.6%
LR+	result	5.250
	95% CI	2.391–5.250
LR−	result	0.000
	95% CI	0.000-0.313
κ	κ	0.773
	SE	0.107
	95% CI	0.439–0.773
	Z	4.598
	p-value	<0.001

CI – confidence interval; PPV – positive predictive value; NPV – negative predictive value; ACC – accuracy; LR+ – likelihood ratio for a positive test result; LR− – likelihood ratio for a negative test result; MDC – modified Duke criteria; SPECT-CT – single-photon emission computed tomography with conventional computed tomography; κ – multi-rater Cohen's kappa; SE – standard error; Z – z-score.

to 100%, 88.6% and 100%, respectively (Table 3). Furthermore, LR+ amounted to 5.250 and LR− reached 0; agreement between the 2 tests improved to almost perfect concordance ($\kappa = 0.773$, $p < 0.001$).[10]

Discussion

The detection of an ICM in a patient with indwelling endocardial leads requires a complete diagnostic workup to identify or exclude infection of the endocardium. A lack of other symptoms of inflammation leaves clinicians in uncertainty, because LDIE can have an oligosymptomatic course and non-characteristic symptoms.[11] On the other hand, the presence of an implanted lead can promote thrombus formation.[12,13] Therefore, accurate clinical judgment is necessary to detect pulmonary embolism caused by uninfected lead-related thrombi, which should not be considered the major Duke criterion of LDIE.

The available literature supplies vast evidence of the difficulties in real-world clinical practice regarding diagnosing IE in patients with CIEDs using the MDC.

Polewczyk et al., conducting research in a single patient cohort, did not differentiate definite from possible LDIE

in one study, but introduced this division in a subsequent report.[14,15] In the first study, the authors used their own modification of the Duke criteria to allow for a diagnosis of definite LDIE when 1 major and 2 minor criteria were satisfied. In the subsequent study, they used the criteria proposed by the ESC; however, the total number of diagnosed IE cases did not change. Furthermore, the authors did not provide information on the method used to diagnose LDIE in 1/3 of the patients without vegetation in the assessed group of 500 patients; however, they drew significant conclusions about the different mechanisms of LDIE development in these patients.[16]

We presented the diagnostic scheme adopted in our institution to confirm possible and definite LDIE in patients with CIEDs using the MDC. The detection of LDIE based on this interpretation of the Duke criteria, the gold standard of IE diagnosis, allowed us to evaluate the utility of using an accessory imaging modality such as SPECT-CT in the diagnostic workup of LDIE. A high correlation was observed in the results obtained using the 2 tests in the diagnosis of LDIE. In 5 patients with definite LDIE diagnoses who had received antibiotic treatment before admission to our institute, the SPECT-CT result was FN. Similar observations have been reported in the literature. The initiation of antimicrobial treatment before the termination of the diagnostic workup was the probable cause of the FN results of SPECT-CT and PET.[17,18]

The primary difficulty we encountered when attempting to compare our observations with other reports on patients referred for TLE procedures is the lack of consistency in the application of the Duke criteria in real-world clinical practice. In a French study, the authors acknowledged a positive lead culture and permanently positive bacterial culture with pathogens not consistent with IE as the major microbiological Duke criterion, which is discordant with ESC guidelines.[17]

We demonstrated the high sensitivity, specificity and accuracy of SPECT-CT scans in LDIE diagnosis (73.7%, 81.0% and 77.5%, respectively), with high positive and negative predictive values (77.8% and 77.3%, respectively). Our outcomes differed from the results obtained by positron emission tomography (PET) testing in a study by Cautela et al., who reported significantly lower sensitivity and specificity in LDIE detection (30.8% and 62.5%, respectively).[17] The discrepancy in the reported results of diagnostic tests might have been due to the adoption of different criteria to diagnose LDIE. A recent meta-analysis of 6 studies using fluorine-18-fluorodeoxyglucose positron emission tomography/computed tomography (^{18}F-FDG PET-CT) reported a pooled sensitivity of 65% and specificity of 88% for lead-dependent CIED infections, which concurs with our results.[19]

In our cohort, the agreement between SPECT-CT and MDC results according to Landis and Koch was moderate, but statistically significant.[10] Importantly, when analyzing patients who had not been treated with antibiotics before SPECT-CT, the agreement between the 2 tests was almost perfect. The scintigraphic test can be useful to diagnose or rule out LDIE (LR+ = 3.868, LR− = 0.325). The implementation of SPECT-CT in the ESC guidelines has enabled precise diagnoses in difficult cases, such as in patients with isolated ICMs, and helped to avoid the risk of serious complications associated with TLE procedures.

Conducting a single imaging test is an advantage of using SPECT-CT, whereas diagnostic evaluation using the MDC requires multiple blood cultures and TTE/TEE assessments.

One limitation of the present study is the relatively small sample size; however, the results did not differ significantly from other similar reports.[19] The radiotracer used in SPECT-CT was not uniform in the whole cohort: the first 10 patients underwent assessment with Scintimun® and subsequent patients with ^{99m}Tc-HMPAO. These 2 methods have not been compared in the diagnosis of IE, but in the authors' opinion, the use of 2 radiotracers did not add much bias, because only information about positive or negative results was taken into consideration. However, a multicenter phase III clinical trial comparing Scintimun® and ^{99m}Tc-HMPAO in diagnosing peripheral bone infections provided evidence of good agreement between the 2 methods and of the efficacious diagnostic ability of both tracers to differentiate infection from sterile inflammation.[20]

Conclusions

Single-photon emission computed tomography with conventional CT with radioisotope-labeled leukocytes is a useful, efficient, single-step test for LDIE diagnosis with high sensitivity and specificity, and a satisfactory overall predictive value of over 77%.

References

1. Małecka B, Kutarski A. Lead-dependent infective endocarditis: An old problem, a new name. *Cardiol J*. 2010;17(2):205–210.
2. Deckx S, Marynissen T, Rega F, et al. Predictors of 30-day and 1-year mortality after transvenous lead extraction: A single-centre experience. *Europace*. 2014;16(8):1218–1225.
3. Habib G, Hoen B, Tornos P, et al; ESC Committee for Practice Guidelines. Guidelines on the prevention, diagnosis, and treatment of infective endocarditis (new version 2009): The Task Force on the Prevention, Diagnosis and Treatment of Infective Endocarditis of the European Society of Cardiology (ESC). *Eur Heart J*. 2009;30(19):2369–2413.
4. Habib G, Lancellotti P, Antunes MJ, et al; ESC Scientific Document Group. 2015 ESC Guidelines for the management of infective endocarditis. *Eur Heart J*. 2015;36(44):3075–3128.
5. Erba PA, Sollini M, Conti U, et al. Radiolabeled WBC scintigraphy in the diagnostic workup of patients with suspected device-related infections. *JACC Cardiovasc Imaging*. 2013;6(10):1075–1086.
6. Palestro CJ, Brown ML, Forstrom LA, et al. Society of Nuclear Medicine Procedure Guideline for ^{99m}Tc-exametazime (HMPAO)-labeled leukocyte scintigraphy for suspected infection/inflammation. Version 3.0, approved June 2, 2004. http://snmmi.files.cms-plus.com/docs/Leukocyte_v3.pdf. Accessed October 2, 2018.

7. Sarrazin JF, Philippon F, Trottier M, Tessier M. Role of radionuclide imaging for diagnosis of device and prosthetic valve infections. *World J Cardiol*. 2016;8(9):534–546.

8. Attia J. Moving beyond sensitivity and specificity: Using likelihood ratios to help interpret diagnostic tests. *Australian Prescriber*. 2003;26(5):111–113.

9. Jaeschke R, Cook D, Guyatt G. Ocena artykułów na temat testów diagnostycznych. Cz. II – metody określenia przydatności testu. *Med Prakt*. 1998;11:184–191.

10. Landis JR, Koch GG. The measurement of observer agreement for categorical data. *Biometrics*. 1977;33(1):159–174.

11. Małecka B, Ząbek A, Mertyna P, Boczar K, Rydlewska A, Lelakowski J. Infection of permanent pacing system with negative inflammatory markers. *Pol Arch Med Wewn*. 2014;124(5):272–273.

12. Downey BC, Juselius WE, Pandian NG, Estes NA, Link MS. Incidence and significance of pacemaker and implantable cardioverter-defibrillator lead masses discovered during transesophageal echocardiography. *Pacing Clin Electrophysiol*. 2011;34(6):679–683.

13. Lo R, D'Anca M, Cohen T, Kerwin T. Incidence and prognosis of pacemaker lead associated masses: A study of 1,569 transesophageal echocardiograms. *J Invasive Cardiol*. 2006;18(12):599–601.

14. Polewczyk A, Janion M, Podlaski R, Kutarski A. Clinical manifestations of lead-dependent infective endocarditis: Analysis of 414 cases. *Eur J Clin Microbiol Infect Dis*. 2014;33(9):1601–1608.

15. Polewczyk A, Jacheć W, Janion M, Podlaski R, Kutarski A. Lead-dependent infective endocarditis: The role of factors predisposing to its development in an analysis of 414 clinical cases. *Pacing Clin Electrophysiol*. 2015;38(7):846–856.

16. Polewczyk A, Jacheć W, Tomaszewski A, et al. Lead-related infective endocarditis: Factors influencing the formation of large vegetations. *Europace*. 2017;19(6):1022–1030.

17. Cautela J, Alessandrini S, Cammilleri S, et al. Diagnostic yield of FDG positron-emission tomography/computed tomography in patients with CEID infection: A pilot study. *Europace*. 2013;15(2):252–257.

18. Graziosi M, Nanni C, Lorenzini M, et al. Role of ^{18}F-FDG PET/CT in diagnosis of infective endocarditis in patients with an implanted cardiac device: A prospective study. *Eur J Nucl Med Mol Imaging*. 2014;41(8):1617–1623.

19. Juneau D, Golfam M, Hazra S, et al. Positron emission tomography and single-photon emission computed tomography imaging in the diagnosis of cardiac implantable electronic device infection: A systematic review and meta-analysis. *Circ Cardiovasc Imaging*. 2017;10(4). pii: e005772. doi:10.1161/CIRCIMAGING.116.005772.

20. Richter WS, Ivancevic V, Meller J, et al. ^{99m}Tc-besilesomab (Scintimun) in peripheral osteomyelitis: Comparison with ^{99m}Tc-labeled white blood cells. *Eur J Nucl Med Mol Imaging*. 2011;38(5):899–910.

Making HIV clinic appointments for clients with positive HIV results at testing sites can improve referral rates

Bartosz Szetela[1,A–F], Łukasz Łapiński[2,B–F], Jacek Gasiorowski[1,C–F], Brygida Knysz[3,E,F]

[1] Independent Laboratory for Monitoring Infections among Drug Users at the Department of Infectious Diseases, Liver Disease and Acquired Immune Deficiencies, Wroclaw Medical University, Poland

[2] Department of Clinical Pharmacology, Wroclaw Medical University, Poland

[3] Department of Infectious Diseases, Liver Disease and Acquired Immune Deficiencies, Wroclaw Medical University, Poland

A – research concept and design; B – collection and/or assembly of data; C – data analysis and interpretation;
D – writing the article; E – critical revision of the article; F – final approval of the article

Address for correspondence
Bartosz Szetela
E-mail: bartekszetela@poczta.fm

Abstract

Background. The percentage of people living with undiagnosed HIV infection remains very high in Poland and exceeds 50% – one of the highest rates in Europe. At the same time, the number of HIV tests performed by medical doctors per 1,000 inhabitants is the lowest in Europe. Thus, every effort should be made to keep diagnosed patients in care. However, a number of patients are lost to care (LTC), with the percentage depending on the testing modality used (voluntary counseling and testing sites – VCTs, private laboratories, medical clinics, clubs) and communication skills of persons giving the results. Until now, there was only 1 prospective study in Poland that looked into the problem of continuum of care.

Objectives. The objective of the study was to assess VCT clients' willingness to accept help with making the first appointment at a local HIV clinic after receiving positive results and the percentage of patients getting into care at the clinic after referral.

Material and methods. Referral efficacy analysis between 2010 and 2014 was a joint venture between VCT site and the largest HIV clinic in Wrocław. Every patient diagnosed with HIV infection was offered personal help with making the first appointment at the HIV clinic. Later, it was assessed whether the first visit actually took place.

Results. All the patients who collected their positive results came for their first visit at the HIV clinic with a referral rate reaching 100%, falling to 97.1% only in 2013. Most visits took place during 1–2 weeks.

Conclusions. Patients were willing to use counselors' help with making appointments at the HIV clinic, which in turn increased referral rates and numbers of patients retained in care.

Key words: HIV, point of care testing, linkage to care, referral rate, voluntary counseling and testing sites

Introduction

The percentage of people living with undiagnosed HIV infection remains very high in Poland and exceeds 50% – one of the highest rates in Europe.[1] Efforts are undertaken to increase HIV testing and coverage among both medical professionals and patients. However, at the same time, people living with diagnosed HIV infection are lost to care due to psychological trauma and feelings of guilt not alleviated when collecting positive HIV results or at any later occasion.[2] This, in turn, often leads to delayed linkage to care and lost treatment opportunities as well as to continued spread of HIV.[3–8]

As an organization running a voluntary counseling and testing site (VCT) in Wrocław (southwest Poland), we decided to modify the post-test visit for clients obtaining positive results. Commonly, clients who are given positive results are offered counseling and given phone numbers and/or addresses of relevant HIV clinics. It is up to them to make the appointment. As this step may be difficult, the VCT staff decided to offer help with making the necessary appointments already during the post-test visit.

The aim of the study was to observe if such help was accepted and, as a proof-of-concept, if it led to better linkage to care.

Material and methods

Between 2010 and 2014, we followed 14,371 patients at a VCT site for HIV in Wrocław, Poland (Wszystkich Świętych Street), run by "Podwale Siedem" society (Stowarzyszenie Na Rzecz Osób Wykluczonych i Zagrożonych Wykluczeniem Społecznym "Podwale Siedem") – a nongovernmental organization (NGO). The patients lived mostly in Wrocław and in nearby cities and were between 20 and 40 years of age. Two thirds of them decided to take the HIV test due to heterosexual and 1/3 due to homosexual exposures. All 221 patients who received positive results were referred to a co-located HIV clinic for care and treatment. All new patients at the clinic were cross-referenced to the point of origin of their HIV test results, either the local VCT site or a different external site, allowing us to measure the referral rate of the VCT site (Table 1).

For the efficacy assessment, a joint venture was created with the 2nd largest HIV clinic in Poland, which takes care of 1000 HIV-infected patients and is also located in Wrocław. Knowing how cost-ineffective and epidemiologically damaging losing diagnosed patients is already at the stage of designing the VCT site, we addressed this issue. The VCT site was located in the same building as the HIV clinic. However, the VCT site and the clinic are separated and have different entrances. This arrangement was and still is unique for Polish testing sites. Such proximity and full cooperation between these 2 entities was supposed to allow smooth patient referral. After confirming HIV infection, the importance of immediate medical care was explained to each patient, who, with his/her approval, was referred to the HIV clinic. Counselors made appointments according to patients' wishes and psychological support was offered at the clinic as needed. Patients received notes with the date and time of the visit at the clinic.

Apart from HIV laboratory and rapid tests (free of charge), the full spectrum of sexually transmitted infections (STI) tests was offered (syphilis rapid and laboratory tests – free of charge; gonorrhea and chlamydia – partial charge) as well as hepatitis B and C tests (full charge). This was made possible thanks to close cooperation between the NGO and the HIV clinic. Otherwise such a wide range of STI tests would be impossible for any NGO due to strict Polish law (concerning infection control and access to medical procedures).

Descriptive statistics included a number of HIV tests performed in the analyzed period, number of positive results, number of uncollected results, number of referrals, number of actual HIV clinic visits, as well as referral rate, i.e., percentage of HIV-positive patients who came for the first visit after referral (calculated for collected results only and for all positive results).

The data was collected and analyzed with Microsoft Excel 2008 for Mac, v. 12.3.6 (Microsoft Corp., Armonk, USA).

Bioethics Committee opinion was not necessary for this study.

Results

Between 2010 and 2014, 14,371 patients were tested for HIV and received 251 positive results (prevalence: 1.74%). Thirty patients did not collect their positive results.

Table 1. Human immunodeficiency virus (HIV) test results and referral rates at the voluntary counseling and testing site in Wrocław between 2010 and 2014

Year	HIV tests performed	Positive HIV results	Uncollected results	Referrals	Actual HIV clinic visits	Referral rate (collected results only) [%]	Referral rate (all positive results) [%]
2010	2,309	38	4	34	34	100	89.5
2011	2,647	35	6	29	29	100	82.8
2012	2,869	49	7	42	42	100	85.7
2013	3,306	77	8	69	67	97.1	87.0
2014	3,240	52	5	47	47	100	90.4

Out of 221 referrals, we confirmed 219 HIV clinic visits, which represents a 99% referral rate. Specific yearly results are shown in Table 1.

During the 5-year period, among patients who obtained positive results, only 2 refused to make the appointment during the post-test visit. One patient wanted to go to his hometown for further treatment and care, while the other required more time to think about his future. Eventually, the 2nd patient came back to make the appointment on his own.

Most patients came for their visits within 1–2 weeks after diagnosis, although we did not measure this time prospectively. Moreover, each year we managed to diagnose from 1 to 4 acute retroviral infections before seroconversion (1.5–10% of all diagnosed infections), a situation also vital to reduction of HIV spread.[6–7]

Most HIV infections were diagnosed among men who have sex with men (50–65%, depending on the year), the 2nd most common cause being heterosexual transmission (30–35%), with intravenous drug use accounting for not more than 4–8% of newly diagnosed infections.

Discussion

Voluntary counseling and testing site remains one of the most important HIV testing modalities in Poland and should be available for persons taking risky behavior, who are often unwilling to use medical clinics.[9] Negative attitudes toward people reporting risky behavior may be especially harmful and are often seen in medical settings and among medical workers not used to such patients.[10–12] Although different venues have been created to increase HIV testing (VCT centers, medical clinics, checkpoints, club testing, home sampling, home testing), no diagnosed individual should be left without referral to HIV clinics, where proper medical care and treatment can be offered. Proper linkage to care helps to achieve both individual and epidemiological goals of reducing the HIV burden and increasing fund efficacy.

Ankiersztejn-Bartczak et al. in their TAK project, observed a high percentage of HIV-positive VCT clients lost to care (LTC) – 42% in Warszawa, Poland. This happened despite universal adoption of proactive linkage procedures by Polish VCT centers.[13] Such high number of persons LTC necessitates rapid improvement so that neither funds nor lives are lost despite timely diagnosis.

On the other hand, a checkpoint in Barcelona, Spain, achieved a very high referral rate of 90.5% by employing the same technique as we did in this project (making appointments with the client's approval), regardless of the distance of the site from HIV clinics.[14] Torian et al. in New York, USA, have shown that collocation of VCT sites and medical clinics allows referral rates to be increased substantially.[3]

Current HIV epidemiology, especially among men who have sex with men, shows that knowing one's HIV status is not enough to change behavior.[15–18] International and national guidelines for starting HIV therapy almost universally advocate early combined antiretroviral therapy (cART) commencement. Early therapy is said to be beneficial both for patients and for the epidemiological situation (reduction of the population viral load). After recent results of the Strategic Timing of Antiretroviral Treatment (START) trial, early therapy may become even more important for HIV-infected individuals. Hence, both early diagnosis and quick referral and antiretroviral therapy are paramount to reduce HIV spread or even stop the epidemic.

Polish AIDS Scientific Society advocates that all patients receiving positive HIV results should also receive adequate linkage to care. This means either making appointments in HIV clinics with the patient's approval or at least distributing the phone number and address of the nearest clinic. Higher linkage to care can be achieved if the patients are made aware of the importance of early treatment for their own and their relatives' health.

Conclusions

Patients were willing to use counselors' help with making appointments at the HIV clinic, which in turn increased referral rates and numbers of patients retained in care. This may further lead to a higher percentage of patients with undetectable viraemia.

We recommend that more VCT sites be located near HIV clinics or co-located, not only to improve referral rates but also to allow easy access to professional medical knowledge. If such location is impossible, very close ties between VCT centers and medical clinics are necessary. We also advise that the referral rates of the VCT sites be checked regularly to achieve and sustain high efficacy and cost-effectiveness.

This has been a proof-of-concept study, and it does not obviate the need for varied modalities in HIV testing (clinics, VCT centers, checkpoints, clubs) to cater for special needs of different groups of patients and allow easy access to testing.

Limitations

Positive and nonjudgmental counseling attitudes at the analyzed VCT site and patients getting to know the clinic and its surroundings before the first visit may have positively impacted referral rates. This may have been the major confounding factor, even though all counselors at Polish VCT sites are educated centrally and are supposed to work under the same guidelines.

Additionally, almost all counselors were medical doctors or had a medical background, which may have favored medicalization attitudes among staff and confounded the results.

References

1. Hamers FF, Phillips AN. Diagnosed and undiagnosed HIV-infected populations in Europe. *HIV Med*. 2008;9(Suppl 2):6–12.

2. Rogowska-Szadkowska D, Chlabicz S, Gąsiorowski J, Zubkiewicz-Zarębska A, Knysz B. Experience of Polish patients diagnosed with HIV before and after highly active antiretroviral therapy (HAART) availability. *HIV & AIDS Review*. 2013;12(1):9–13.

3. Torian LV, Wiewel EW, Liu KL, Sackoff JE, Frieden TR. Risk factors for delayed initiation of medical care after diagnosis of human immunodeficiency virus. *Arch Intern Med*. 2008;168(11):1181–1187.

4. Eichler MR, Ray SM, del Rio C. The effectiveness of HIV post-test counseling in determining healthcare-seeking behavior. *AIDS*. 2002;16(6):943–945.

5. Samet JM, Freedberg KA, Stein MD, et al. Trillion virion delay: Time from testing positive for HIV to presentation for primary care. *Arch Intern Med*. 1998;158(7):734–740.

6. Cohen MS, Chen YQ, McCauley M, et al; HPTN 052 Study Team. Prevention of HIV-1 infection with early antiretroviral therapy. *N Engl J Med*. 2011;365(6):493–505.

7. Granich RM, Gilks F, Dye C, De Cock KM, Williams BG. Universal voluntary HIV testing with immediate antiretroviral therapy as a strategy for elimination of HIV transmission: A mathematical model. *Lancet*. 2009;373(9657):48–57.

8. Mocroft A, Lundgren JD, Sabin M, et al; Collaboration of Observational HIV Epidemiological Research Europe (COHERE) study in EuroCoord. Risk factors and outcomes for late presentation for HIV-positive persons in Europe: Results from the Collaboration of Observational HIV Epidemiological Research Europe Study (COHERE). *PLOS Med*. 2013;10(9):e1001510. doi:10.1371/journal.pmed.1001510

9. Raport z analiz ankiet wypełnianych w Punktach Konsultacyjno--Diagnostycznych w roku 2010. Krajowe Centrum ds. AIDS, 2011. http://www.aids.gov.pl/badania_spoleczne/254/. Accessed January 15, 2017.

10. Rosińska M, Marzec-Bogusławska A, Janiec J, et al; for the CASCADE Collaboration in EuroCoord. HIV infection among HIV-positive individuals newly diagnosed at voluntary counseling and testing sites in Poland. *AIDS Res Hum Retroviruses*. 2013;29(5):805–813.

11. European Centre for Disease Prevention and Control and European Monitoring Centre for Drugs and Drug Addiction. Prevention and control of infectious diseases among people who inject drugs. Guidance in brief. Stockholm, Sweden: ECDC; 2011. http://www.emcdda.europa.eu/system/files/publications/638/ECDC-EMCDDA_IDU_guidance_-_web_version_328027.pdf. Accessed March 24, 2017.

12. HIV-related stigma: Late testing, late treatment. A cross analysis of findings from the People Living with HIV Stigma Index in Estonia, Moldova, Poland, Turkey, and Ukraine. Global Network of People Living with HIV (GNP+), 2011. http://www.gnpplus.net/images/stories/Rights_and_stigma/2011_HIVStigma_Report_EN.pdf. Accessed January 15, 2017.

13. Ankiersztejn-Bartczak M, Firląg-Burkacka E, Czeszko-Paprocka H, et al. Factors responsible for incomplete linkage to care after HIV diagnosis: Preliminary results from the Test and Keep in Care (TAK) project. *HIV Med*. 2015;16(2):88–94.

14. Meulbroek M, Ditzel E, Saz J, et al. BCN Checkpoint, a community-based centre for men who have sex with men in Barcelona, Catalonia, Spain, shows high efficiency in HIV detection and linkage to care. *HIV Med*. 2013;14(Suppl 3):25–28.

15. Desquilbet L, Deveau C, Goujard C, Hubert JB, Derouineau J, Meyer L; PRIMO Cohort Study Group. Increase in at-risk sexual behavior among HIV-1-infected patients followed in the French PRIMO cohort. *AIDS*. 2002;16(17):2329–2333.

16. Fisher JD, Fisher WA, Cornman DH, Amico RK, Bryan A, Friedland GH. Clinician-delivered intervention during routine clinical care reduces unprotected sexual behavior among HIV-infected patients. *J Acquir Immune Defic Syndr*. 2006;41(1):44–52.

17. Marks G, Crepaz N, Senterfitt JW, Janssen RS. Meta-analysis of high-risk sexual behavior in persons aware and unaware they are infected with HIV in the United States: Implications for HIV prevention programs. *J Acquir Immune Defic Syndr*. 2005;39(4):446–453.

18. Crepaz N, Lyles CM, Wolitski R, et al; HIV/AIDS Prevention Research Synthesis (PRS) Team. Do prevention interventions reduce HIV risk behaviors among people living with HIV? A meta-analytic review of controlled trials. *AIDS*. 2006;20(2):143–157.

Original papers

Preoperative Th1/Th2 and related cytokines: Prediction value in postoperative febrile UTI after ureteroscopy in patients with ureteral calculi

Zhen Li[A], Kang-Er Wang[B,C], Xie-Lai Zhou[C,D], Jin Zhou[D,E], Chun-Hua Ye[F]

Department of Urology, Affiliated Hospital of Hangzhou Normal University, China

A – research concept and design; B – collection and/or assembly of data; C – data analysis and interpretation;
D – writing the article; E – critical revision of the article; F – final approval of the article

Address for correspondence
Chun-Hua Ye
E-mail: Chun_Hua_Ye@163.com

Abstract

Background. The topic of whether preoperative Th1/Th2 cells and their related factors have a predictive value for postoperative febrile urinary tract infection (UTI) in patients with ureteral calculi has not been explored.

Objectives. The objective of this study was to investigate the role of preoperative Th1/Th2 cells and related cytokines in the prediction of postoperative febrile UTI after ureteroscopy in patients with ureteral calculi.

Material and methods. One hundred sixty patients who underwent ureteroscopic pneumatic lithotripsy in the Affiliated Hospital of Hangzhou Normal University (China) were recruited and divided into febrile UTI group (n = 78) and non-UTI group (n = 82). Flow cytometry was used to detect the proportions of Th1 and Th2 cells (Th1% and Th2%). Detection of Th1/Th2 cell-related cytokines was conducted using enzyme-linked immunosorbent assay (ELISA). Quantitative real-time polymerase chain reaction (qRT-PCR) was applied to measure the expression of T-bet and GATA3.

Results. Compared with patients in non-UTI group, those in febrile UTI group had significantly increased proportions of Th2 cells, levels of Th2 cytokines (interleukin (IL)-4, IL-10 and IL-5), and mRNA expression of Th2-associated transcription factor GATA3 (all p < 0.05). In addition, the Th1/Th2 ratio of febrile UTI group was significantly lower than that of non-UTI group (p < 0.001). Receiver operating characteristic (ROC) curve analysis showed that the accuracy rate of Th2%, Th1/Th2 ratio, and IL-4, IL-10 and IL-5 levels for the diagnosis of postoperative febrile UTI in patients with ureteral calculi was 90.63%, 85.00%, 72.50%, 87.50%, and 91.88%, respectively, and their combined diagnostic sensitivity was 97.4% with specificity as high as 100%.

Conclusions. Perioperative Th2 dominance was correlated with the risk of postoperative febrile UTI after ureterscopy in patients with ureteral calculi, which can provide clinical guidance for the development of in-dividualized treatment.

Key words: Th1/Th2, ureteral calculi, febrile urinary tract infection

126

Z. Li, et al. Th1/Th2 in UTI with ureteral calculi

Introduction

Urinary calculus is the most common acute disease in urology surgery, seen in approx. 15% of the population, and is responsible for 20% of cases of urolithiasis.[1,2] Patients with ureteral calculi often develop renal or ureteral colic, leading to severe pain in the waist or midsection accompanied by other symptoms such as nausea, vomiting and hematuria, seriously affecting the quality of life.[3] With the advancement of ureteroscopic technologies, treatments for the removal of ureteral calculi have shown decreased procedural invasiveness with high success rates and limited morbidity.[4] In their paper, de la Rosette et al. analyzed 11,885 ureteral calculi patients treated with ureteroscopy and revealed that the stone-free rate and postoperative complication rate were 85.6% and 3.5%, respectively,[5] suggesting that ureteroscopy can be used in patients with larger and more complicated stones, as well as elderly patients with significant comorbidities.[4] However, the incidence of severe complications is still high after ureteroscopy treatment, including febrile urinary tract infection (UTI). Therefore, it is urgent to explore factors that may affect the postoperative occurrence of febrile UTI to provide a new therapeutic target for the treatment of ureteral calculi.

CD4^{+} T cells can be classified into Th1 and Th2 subsets based on the cytokines secreted in long-term cultured murine cells that mediate immune functions.[6] Recently, many studies have found that Th1 and Th2 cells have different effects on immune responses.[7,8] Specifically, Th1 cells can produce interferon-γ (IFN-γ) and interleukin-2 (IL-2), as well as tumor necrosis factor-α (TNF-α) to regulate cellular immunity; additionally, Th2 cells can promote the differentiation and response of Th1 cells, secrete IL-4, IL-10, and IL-5, and regulate humoral immunity.[9,10] Furthermore, Th1 and Th2 cells cross-inhibit each other and produce different cytokines to maintain the balance of the immune response.[11,12] The occurrence and progression of infectious diseases are closely associated with Th1/Th2 cells and related cytokines. For instance, Kang et al. found that the concentration ratio of Th1/Th2 cytokines in patients co-infected with HIV/HCV was apparently higher than in patients infected only with HCV or without infection, but significantly lower than in patients infected only with HIV.[13] Tang et al. revealed that children with fevers had higher levels of IL-4, IL-6, IL-10, TNF-α, and IFN-γ than healthy controls, and their cytokine levels were also different from those with hemophagocytic lymphohistiocytosis (HLH) or viral infection.[14] Additionally, they demonstrated that the patients with microbiologically documented infection (MDI) had much higher IL-6 levels than HLH patients, and the IFN-γ levels were only slightly increased in MDI patients. In the intestinal mucosa of patients with post-infectious irritable bowel syndrome, the IFN-γ levels were upregulated, while IL-10 levels were downregulated, suggesting that infection may break the balance between Th1 and Th2 cells.[15] Meanwhile, it was reported that serum

Th1/Th2 cytokines may be conducive to the prediction of prognosis and selection of target therapies for patients with Kawasaki disease.[16] These studies indicated that a Th1/Th2 imbalance exists in many infectious diseases and affects the outcome and prognosis of diseases. However, it has not been explored whether preoperative Th1/Th2 cells and their related factors have predictive value for postoperative febrile UTI in patients with ureteral calculi.

Therefore, 160 cases were recruited in this study before receiving ureteroscopic pneumatic lithotripsy; after treatment, the patients were divided into 2 groups depending on the presence of postoperative febrile UTI: UTI group (n = 78) and non-UTI group (n = 82). Flow cytometry was used to measure the proportions of Th1 and Th2 cells. Enzyme-linked immunosorbent assay (ELISA) was utilized to detect the levels of Th1/Th2-related cytokines. The expression levels of Th1/Th2-related transcription factors T-bet and GATA3 were determined using quantitative real-time polymerase chain reaction (qRT-PCR). This data was used to analyze the value of preoperative Th1/Th2 cells and related cytokines in the prediction of postoperative febrile UTI in patients with ureteral calculi.

Material and methods

Ethics statement

This study was approved by the Ethics Committee of the Affiliated Hospital of Hangzhou Normal University (China) and was conducted in strict accordance with the Declaration of Helsinki.[17] Additionally, informed consent was obtained from each participant prior to the study.

Subjects

From December 2009 to December 2016, 160 patients with ureteral stones diagnosed by kidney-ureter-bladder (KUB) X-ray, intravenous urography (IVP), color Doppler ultrasound, computed tomography (CT), and magnetic resonance (MR) urography at the Affiliated Hospital of Hangzhou Normal University were recruited as subjects of this study. After receiving ureteroscopic pneumatic lithotripsy, 160 patients were divided into 2 groups based on the presence of postoperative febrile UTI at any point postoperatively during the follow-up. Among them, 78 patients had postoperative febrile UTI (UTI group), including 49 men and 29 women, whose age range was 16–90 years (mean age 55.14 ±21.90 years); the other 82 patients who did not have postoperative febrile UTI (non-UTI group) comprised of 55 men and 27 women with an age range of 17–88 years (mean age 52.51 ±20.97 years). Postoperative febrile UTI was defined as a body temperature higher than 38°C.[18] The inclusion criteria were as follows: all patients had undergone ureteroscopic pneumatic lithotripsy; all patients had received prophylactic antibiotics according to physicians' discretion, consisting of second generation

cephalosporin (7 days) and metronidazole (5 days) intravenously; all patients had no chills, shivers, fever, or any acute infection history such as urinary irritation symptoms approx. 2 weeks before the operation; each case was confirmed with sufficient clinical examinations. The exclusion criteria were as follows: patients with a history of immune system diseases such as diabetes, Crohn's disease, systemic lupus erythematosus, rheumatoid arthritis, and rheumatoid disease; patients with other immune diseases, including severe liver and kidney diseases, cardiovascular and cerebrovascular diseases and severe infections; patients with a malignant tumor; patients with a recent history of using immune agent use; and pregnant and lactating women. Blood samples from patients were drawn in the morning before ureteroscopic pneumatic lithotripsy.

Ureteroscopic pneumatic lithotripsy

Patients were placed in the lithotomy position for epidural block anesthesia. The ureteroscope (DUR-D Gyrus ACMI, Southborough, USA) was inserted into the ureter from the external ureteral orifice of the patients. During the process, an F4 safety guide wire was slowly inserted from the diseased ureter, and a hydraulic pump was used to expand the ureteral orifice. The ureteroscope was gradually pushed to reach the stones. The size, movement and incarceration of the stones were observed to confirm the feasibility of the operation. Next, the ureteroscope was removed, and the probe for ureteroscopic pneumatic lithotripsy was inserted from the ureteral passage to smash the stones. Stones with a small diameter were discharged with urine, and those with a larger diameter (>3 mm) were removed with a stone basket or stone forceps. It was very important to avoid injury of the ureteral mucosa during the stone removal procedure. The large stones from patients with inflammatory polyps were sent to the pathology department for further examination. In all cases, the procedures were carried out by 2 experienced urologists. All the patients were followed up utilizing outpatient assessments and telephone contact within a 1-month period.

Measurement of indexes

In the cases of multiple stones, the stone size was calculated by the total diameter of the stone cluster. The criterion of being stone-free was no obvious stones or stones less than 2 mm in diameter detected using X-ray or ultrasound examination at 1 month after ureteroscopy. Additionally, pyuria indicated 10 or more white blood cells per high-power field (HPF).

Flow cytometry

Approximately 200 μL of peripheral blood was added into RPMI 1640 medium (200 μL). Next, 19 μL of 1 μg/mL phorbol 12-myristate 13-acetate (PMA) solution, 6 μL

of 50 μg/mL lincomycin solution and 6 μL of monensin solution were added subsequently to a uniform level to culture for 5 h at 37°C. Later, 100 μL of the incubated cell suspension was added into a flow cytometer, and CD4-FITC and CD8-APC monoclonal antibodies were added for 15 min under dark–light reaction at room temperature. Next, the cells were washed twice with phosphate-buffered saline (PBS), and then, 100 μL of membrane breaking agent was added for 15 min at room temperature. The cells were then washed twice again with PBS before adding IFN-γ-PE-CY5 and IL-4-PE monoclonal antibodies for 20 min at room temperature under dark–light reaction. The cells were resuspended with 300 μL of PBS after washing twice with PBS. Next, FACS CANTO II flow cytometry was used to detect the proportions of Th1 and Th2 cells and the levels of $CD4^+$ and $CD8^+$ T cells.

ELISA

Serum separated from 2 mL of venous blood was examined using ELISA. The contents of IL-2, IL-4, IL-5, IL-10, IFN-γ, and TNF-α were determined in strict accordance with the instructions for each ELISA kit (Shanghai Westang Biotechnology Co., Ltd., Shanghai, China).

qRT-PCR

Total RNA from PBMCs was extracted strictly following the manufacturer's instructions (RNeasy mini kit; Qiagen, Tokyo, Japan). cDNA synthesis was conducted using the T-Primed First-Strand Kit for qRT-PCR (Amersham Biosciences United Kingdom, Little Chalfont, UK). Additionally, the expression levels were determined with qRT-PCR using the Light Cycler-Fast Start DNA Master SYBR Green I kit (Roche Diagnostics, Mannheim, Germany). Based on the gene sequences published in the GenBank database, the primers were designed using the Primer v. 5.0 software and were synthesized by Shanghai Sangon Biotechnology Co. Ltd. (Shanghai, China; Table 1). The qRT-PCR conditions were as follows: denaturation at 95°C for 10 min, then 45 cycles of denaturation at 95°C for 10 s, annealing for 10 s (at 58°C for T-bet and 60°C for GATA3), and extension at 72°C for 7 s. The internal reference gene *GAPDH* was also treated under the aforementioned conditions, except that its extension was at 72°C for 8 s. The ratio of the gene expression levels was calculated using the $2^{-\Delta\Delta Ct}$ method.

Table 1. Primer sequences for qRT-PCR

Gene	Primer	Sequences
GATA3	forward	5′-CTGGCCACAGTTGTTTCATG-3′
	reverse	5′-GCAACTGGTGAACGGTAACA-3′
T-bet	forward	5′-GTCAATTCCTTGGGGGAGAT-3′
	reverse	5′-TCATGCTGACTGCTCGAAAC-3′
GAPDH	forward	5′-ACCCAGAAGACTGTGGATGG-3′
	reverse	5′-TTCTAGACGGCAGGTCAGGT-3′

128

Z. Li, et al. Th1/Th2 in UTI with ureteral calculi

Statistical methods

All statistical data was analyzed using SPSS v. 22.0 software (IBM Corp., Armonk, USA). The measurement data was presented as means ± standard deviation (±SD). The Kolmogorov–Smirnov test was used to analyze the normal distribution, and the measurement data consistent with a normal distribution was analyzed using a Student's t-test. Enumeration data was analyzed using a χ^2 test. The results of clinical experiments were plotted on a receiver operating characteristic (ROC) curve, and the area under the curve and 95% confidence intervals (95% CIs) were calculated to predict febrile UTI after ureteroscopic pneumatic lithotripsy. The value of p < 0.05 was regarded as significantly different.

Results

Comparison of the characteristics and surgical outcomes between the 2 groups

As shown in Table 2, no differences were found in the age, sex, BMI index, pyuria, preoperative ureteral stent, and levels of C-reactive protein (CRP) and procalcitonin (PCT), mean time from the first visit to surgery and operation time (all p > 0.05). In addition, the 2 groups of patients showed no obvious differences in the number of stones, stone size, operative time, and number of residual stones (all p > 0.05).

Table 2. The characteristics and surgical outcomes in non-UTI group and UTI group

Parameters	Number of patients	non-UTI (n = 82)	UTI (n = 78)	p-value
Age [years] <65 ≥65	103 57	56 26	47 31	0.324

Gender
  male
  female
	104
	56
		55
		27
			49
			29
				0.621

Body mass index <30 ≥30	142 18	75 7	67 11	0.321
Mean time from diagnosis to treatment [days]	160	20.00 ±5.02	21.05 ±2.98	0.131

CRP [mg/L]
  <6
  6~18
  >18
	74
	29
	57
		40
		15
		27
			34
			14
			30
				0.749

PCT [ng/mL]
  >0.1
  ≤0.1
	46
	114
		26
		56
			20
			58
				0.485

Stone history
  no
  yes
	92
	68
		45
		37
			47
			31
				0.525

Pyuria
  no
  yes
	76
	83
		41
		41
			35
			42
				0.039

Preoperative ureteral stent
  no
  yes
	98
	62
		53
		29
			45
			33
				0.418

Number of stones
  single
  multiple
	93
	67
		51
		31
			42
			36
				0.337

Stone size [mm] <20 ≥20	98 62	56 26	42 36	0.075
Operative time [min] <15 ≥15	91 69	49 33	42 36	0.524

Residual stones
  no
  yes
	137
	23
		73
		9
			64
			14
				0.262

UTI – urinary tract infection.

Comparison of the peripheral blood T-cell subsets and Th1/Th2 ratio between the 2 groups

As shown in Table 3, no significant difference was found between the 2 groups of patients in terms of the white blood cell and lymphocyte distribution (both p > 0.05). Compared with patients in the non-UTI group, those in the febrile UTI group showed increased proportions of Th2 cells (Th2%) in peripheral blood (3.43 ±1.02 vs 1.63 ±0.44, t = 14.620; p < 0.001) and a decreased Th1/Th2 ratio (7.21 ±2.98 vs 14.94 ±6.91, t = 9.106; p < 0.001), but their proportions of Th1 cells (Th1%) showed no significant difference (22.01 ±5.75 vs 22.35 ±4.87; p = 0.224) (Fig. 1).

Expression of Th1/Th2-related cytokines and associated transcription factors in the 2 groups

As shown in Fig. 2, compared with patients in the non-UTI group, patients in the febrile UTI group showed no difference in the levels of Th1 cytokines (IL-2, IFN-γ and TNF-α) in the peripheral blood (all p > 0.05), but their Th2 cytokines were remarkably upregulated (IL-4: 4.37 ±0.92 vs 3.61 ±0.47; IL-10: 3.53 ±0.75 vs 2.43 ±0.35; IL-5: 4.76 ±0.41 vs 3.04 ±0.19 (all p < 0.05). Additionally, the mRNA expression of T-bet, as a Th1-associated transcription factor, in febrile UTI patients was not different from that in the non-UTI group (p > 0.05), but the mRNA expression of GATA3, namely, a Th2-associated transcription factor, was markedly upregulated in patients in the febrile UTI group (p < 0.05; Fig. 3).
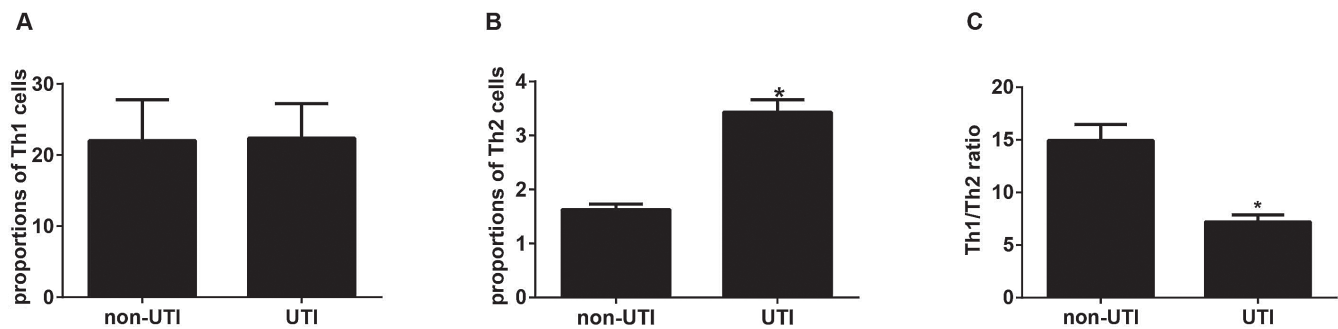

Fig. 1. Proportions of Th1 cells (A) and Th2 cells (B), as well as the Th1/Th2 ratio (C), in the non-UTI group and UTI group
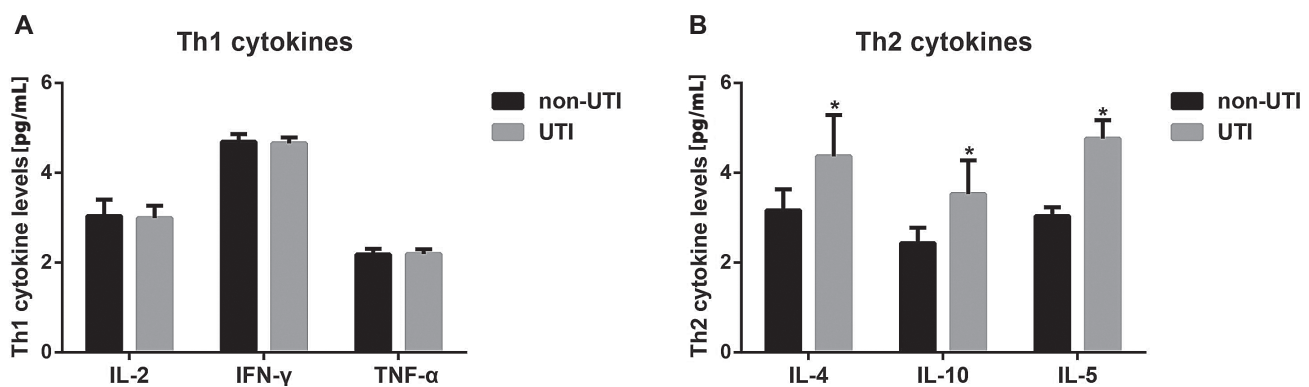
* p < 0.05 compared with patients in the non-UTI group

Fig. 2. Levels of Th1/Th2-related cytokines in each group detected using ELISA

A – Th1-related cytokines; B – Th2-related cytokines; * p < 0.05 compared with patients in the non-UTI group.

Table 3. White blood cell and lymphocyte distribution in non-UTI group and UTI group

Subpopulations	non-UTI (n = 82)	UTI (n = 78)	Student's t-test	p-value
Leukocytes [count/L]	5,626 ±1,378	5,401 ±879	1.224	0.223
Lymphocytes [count/L]	1,683 ±601	1,481 ±452	1.801	0.074
CD4+ T-lymphocytes [%]	46.92 ±3.05	47.07 ±3.59	0.285	0.776
CD8+ T-lymphocytes [%]	24.15 ±2.99	25.04 ±3.04	1.867	0.064
CD4/CD8 ratio	1.97 ±0.26	1.91 ±0.31	1.329	0.186

UTI – urinary tract infection.
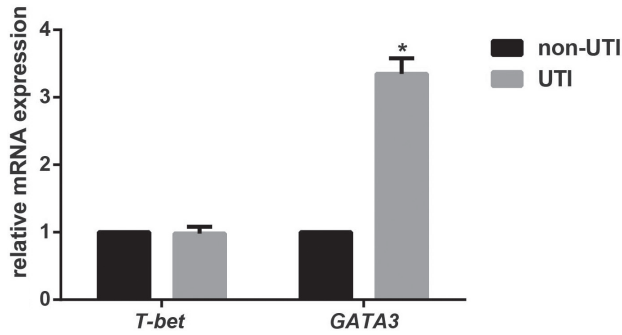
130

Z. Li, et al. Th1/Th2 in UTI with ureteral calculi

Fig. 3. mRNA expression of Th1/Th2-associated transcription factor T-bet and GATA3 in the non-UTI group and UTI group, as detected using qRT-PCR

* p < 0.05 compared with patients in the non-UTI group.

The predictive value of Th1/Th2 cells and related cytokines for the diagnosis of postoperative febrile UTI in patients with ureteral calculi

Receiver operating characteristic curve analysis was conducted for indexes that were significantly different between the 2 groups, and the results are shown in Fig. 4 and Table 4. The sensitivity values of Th2%, the Th1/Th2 ratio, IL-4, IL-10 and IL-5 for the diagnosis of postoperative febrile UTI in patients with ureteral calculi were 87.18%, 82.05%, 71.79%, 76.92%, and 87.18%, respectively. The specificity values were 93.90%, 87.80%, 73.17%, 97.56%,

Table 4. ROC curve analysis of the value of Th2%, Th1/Th2 ratio, IL-4, IL-10, and IL-5 in predicting postoperative febrile UTI in patients with ureteral calculi

Th1/Th2 cells and related cytokines	Cut-off	AUC	95% CI	Sensitivity [%]	Specificity [%]	PPV [%]	NPV [%]	Accuracy [%]
Th2%	2.275	0.956	0.926~0.986	87.18	93.90	93.15	88.51	90.63
Th1/Th2 ratio	8.742	0.897	0.849~0.944	82.05	87.80	86.49	83.72	85.00
IL-4	3.868	0.773	0.698~0.848	71.79	73.17	71.79	73.17	72.50
IL-10	3.024	0.915	0.869~0.961	76.92	97.56	96.77	81.63	87.50
IL-5	3.381	0.943	0.904~0.982	87.18	96.34	95.77	88.76	91.88

AUC – area under the ROC curve; CI – confidence interval; PPV – positive predictive value; NPV – negative predictive value.
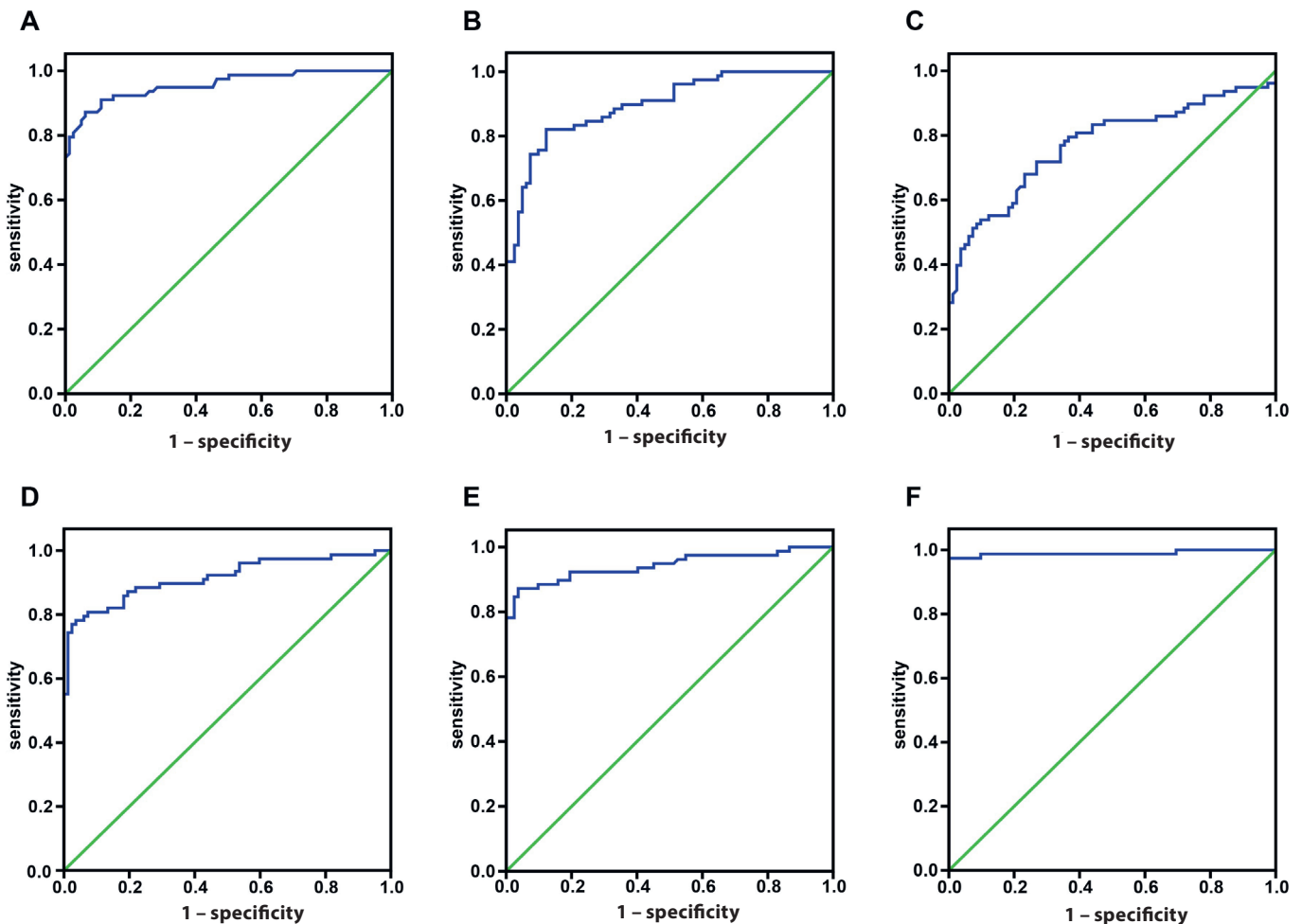

Fig. 4. ROC curve analysis of the value of Th2% (A), Th1/Th2 ratio (B), IL-4 (C), IL-10 (D), IL-5 (E), and combined indexes (F) for the diagnosis of postoperative febrile UTI in patients with ureteral calculi

and 96.34%, respectively. The accuracy values were 90.63%, 85.00%, 72.50%, 87.50%, and 91.88%, respectively. In addition, the sensitivity of the combined diagnosis was 97.4% with specificity as high as 100%.

Discussion

The most important finding of this study is that patients with postoperative febrile UTI showed a significantly elevated proportion of Th2 cells without an obvious change in the number of Th1 cells, thus resulting in the reduction of their Th1/Th2 ratio. Under normal circumstances, Th1 and Th2 cells interact and restrict each other to maintain the balance of the immune responses.[19] When infection occurs, the imbalanced differentiation of Th1 and Th2 cells leads to an abnormal Th1/Th2 ratio.[20] It has also been reported that infected and non-infected patients showed no notable difference in the proportion of Th1 cells, but the former showed an appreciably higher proportion of Th2 cells, and, thus, a remarkably lower Th1/Th2 ratio than the latter[21]; these previous findings are consistent with our findings and can be explained as postoperative infectious complications being associated with the imbalance of Th1/Th2, particularly inadequate Th2 responses. Additionally, several studies have shown that the Th2 dominance in the Th1/Th2 balance in the human immune system renders patients more susceptible to infections by viruses, protozoa, and intracellular bacteria.[22,23] However, interestingly, Tatsumi et al. revealed that preoperative Th2 cells are suppressed in infected patients but not in non-infected patients.[24] On the other hand, Ishikawa et al. reported that no significant difference was observed in the preoperative Th1/Th2 ratio between patients with postoperative complications and those without postoperative complications.[25] One explanation for the discrepancy in our results may be the difference in background disease.

Cytokines have been recognized as key factors in determining host resistance to infectious pathogens. Specifically, the balance of Th1/Th2 cytokines in hosts is closely related to the prognosis and outcome of infections induced by intracellular microbes.[26,27] Additionally, the hallmark cytokines of Th1 cells, including IFN-γ and lymphotoxin, can activate microbicidal activity, as well as cytokine production in macrophages.[28] IFN-γ signals can also activate a downstream transcription factor, T-bet, to upregulate the expression of genes specific to Th1 cells.[29] By contrast, IL-4 can enhance the expression level of GATA3, a transcription factor critical for both IL-4 production and Th2 cell differentiation.[30] To further explore the significance of the Th1/Th2 balance, we used ELISA to determine the expression levels of Th1/Th2 cytokines and applied qRT-PCR to detect the mRNA expression of T-bet and GATA3. We found that patients with postoperative febrile UTI had significantly higher levels of Th2-related cytokines (IL-4, IL-10 and IL-5) and GATA3 than those

without postoperative febrile UTI, but no difference was found in the level of Th1-related cytokines (IFN-γ, IL-2 and TNF-α) and T-bet. These results further confirmed that the preoperative dominance of Th2 cells in the Th1/Th2 balance may exert a large impact on the occurrence and development of postoperative infection. These findings suggest that the failure of Th2 cells to regulate the Th1 responses or promote the production of antibodies can profoundly affect the host immunity against postoperative infection.

Another important finding of our study was that the preoperative Th2%, Th1/Th2 ratio, and IL-4, IL-10 and IL-5 values were predictive in postoperative febrile UTI in patients with ureteral calculi with accuracies of 90.63%, 85.00%, 72.50%, 87.50%, and 91.88%, respectively; the sensitivity of the combined diagnosis was 97.4% with a specificity as high as 100%. In addition, Tang et al. revealed that the sensitivity and specificity of severe infection prediction were 62.0% and 85.0%, respectively, when the cut-off value of IL-10 was set at 42.0 pg/mL.[14] Additionally, the IL-5 levels were higher than the calculated cut-off value (11 pg/mL) in 22/37 of patients with perennial allergic rhinitis and 4/20 in the non-atopic healthy controls.[31] Given the above-mentioned results, we may conclude that the preoperative Th2%, Th1/Th2 ratio and cytokine levels can be used as effective reference indicators for the diagnosis of postoperative febrile UTI in patients with ureteral calculi.

Nevertheless, this study had also some limitations. For instance, the stones in the UTI group were larger than those in the non-UTI group because no statistical difference was revealed between them. Moreover, the stone size could be the risk factor of febrile UTI after ureteroscopy in patients with ureteral calculi.[32] Additionally, we included patients with pyuria and/or those who used a preoperative ureteral stent, which could be a sign of active inflammation. Thus, to eliminate the effects of other risk factors in the future, we should further expand the sample size, consider more clinical indexes and exclude patients with possible inflammation.

Overall, preoperative Th2 dominance was correlated with postoperative febrile UTI in patients with ureteral calculi. In addition, the preoperative values of the Th2%, Th1/Th2 ratio, IL-4, IL-10 and IL-5 were good predictive indexes in postoperative febrile UTI in patients with ureteral calculi. These results provide further information that may direct future treatments based on the Th1/Th2 concept focusing on decreasing the risk of postoperative infection.

References

1. Cheng Y, Liu GL. Current state and advance of flexible ureteroscope in the treatment of upper urinary calculi. *J Mod Urol.* 2014;5:285–288.
2. Cavildak IK, Nalbant I, Tuygun C, et al. Comparison of flexible ureterorenoscopy and laparoscopic ureterolithotomy methods for proximal ureteric stones greater than 10 mm. *Urol J.* 2016;13(1): 2484–2489.
3. Korkes F, Gomes SA, Heilberg IP. Diagnosis and treatment of ureteral calculi. *J Bras Nefrol.* 2009;31:55–61.

4. El-Qadhi M. Outcome of ureteroscopy for the management of distal ureteric calculi: 5-years' experience. *Afr J Urol*. 2015;21(1):67–71.

5. de la Rosette J, Denstedt J, Geavlete P, et al; CROES URS Study Group. The clinical research office of the endourological society ureteroscopy global study: Indications, complications, and outcomes in 11,885 patients. *J Endourol*. 2014;28(2):131–139.

6. Krowka JF, Singh B, Fotedar A, Mosmann T, Giedlin MA, Pilarski LM. A requirement for physical linkage between determinants recognized by helper molecules and cytotoxic T cell precursors in the induction of cytotoxic T cell responses. *J Immunol*. 1986;136(10):3561–3566.

7. Feng Y, Tian J, Xie HQ, et al. Effects of acute low-dose exposure to the chlorinated flame retardant dechlorane 602 and Th1 and Th2 immune responses in adult male mice. *Environ Health Perspect*. 2016; 124(9):1406–1413.

8. Ebrahimian M, Hashemi M, Maleki M, et al. Induction of a balanced Th1/Th2 immune responses by co-delivery of PLGA/ovalbumin nanospheres and CpG ODNs/PEI-SWCNT nanoparticles as TLR9 agonist in BALB/c mice. *Int J Pharm*. 2016;515(1–2):708–720.

9. Miyake K, Akahoshi M, Nakashima H. Th subset balance in lupus nephritis. *J Biomed Biotechnol*. 2011;2011:1–7.

10. Yuan D, Yuan Q, Cui Q, et al. Vaccine adjuvant ginsenoside Rg 1 enhances immune responses against hepatitis B surface antigen in mice. *Can J Physiol Pharm*. 2016;94(6):676–681.

11. Behfarjam F, Sanati MH, Nasseri Moghaddam S, Ataei M, Nikfam S, Jadali Z. Role of Th1/Th2 cells and related cytokines in autoimmune hepatitis. *Turk J Gastroenterol*. 2017;28(2):110–114.

12. Wintrob ZA, Hammel JP, Nimako GK, et al. TH1 and TH2 cytokines dataset in insulin users with diabetes mellitus and newly diagnosed breast cancer. *Data Brief*. 2017;11:331–348.

13. Kang W, Li Y, Zhuang Y, Zhao K, Huang D, Sun Y. Dynamic analysis of Th1/Th2 cytokine concentration during antiretroviral therapy of HIV-1/HCV co-infected patients. *BMC Infect Dis*. 2012;12:102.

14. Tang Y, Liao C, Xu X, et al. Evaluation of Th1/Th2 cytokines as a rapid diagnostic tool for severe infection in paediatric haematology/oncology patients by the use of cytometric bead array technology. *Clin Microbiol Infect*. 2011;17(11):1666–1673.

15. Chen J, Zhang Y, Deng Z. Imbalanced shift of cytokine expression between T helper 1 and T helper 2 (Th1/Th2) in intestinal mucosa of patients with post-infectious irritable bowel syndrome. *BMC Gastroenterol*. 2012;12:91.

16. Wang Y, Wang W, Gong F, et al. Evaluation of intravenous immunoglobulin resistance and coronary artery lesions in relation to Th1/Th2 cytokine profiles in patients with Kawasaki disease. *Arthritis Rheum*. 2013;65(3):805–814.

17. Bădărău DO. Declaration of Helsinki. *Phys Ther*. 2013;45:1418–1419.

18. Mitsuzuka K, Nakano O, Takahashi N, Satoh M. Identification of factors associated with postoperative febrile urinary tract infection after ureteroscopy for urinary stones. *Urolithiasis*. 2016;44(3):257–262.

19. Yoon SJ, Kim SJ, Lee SM. Overexpression of HO-1 contributes to sepsis-induced immunosuppression by modulating the Th1/Th2 balance and regulatory T-cell function. *J Infect Dis*. 2017;215(10):1608–1618.

20. Rubbo PA, Tuaillon E, Bollore K, et al. The potential impact of CD4^{+} T cell activation and enhanced Th1/Th2 cytokine ratio on HIV-1 secretion in the lungs of individuals with advanced AIDS and active pulmonary infection. *Clin Immunol*. 2011;139(2):142–154.

21. Matsuda A, Furukawa K, Suzuki H, et al. Does impaired TH1/TH2 balance cause postoperative infectious complications in colorectal cancer surgery? *J Surg Res*. 2007;139(1):15–21.

22. Del Prete G, Maggi E, Romagnani S. Human Th1 and Th2 cells: Functional properties, mechanisms of regulation, and role in disease. *Lab Invest*. 1994;70(3):299–306.

23. Romagnani S. The Th1/Th2 paradigm. *Immunol Today*. 1997;18(6):263.

24. Tatsumi H, Ura H, Ikeda S, et al. Surgical influence on TH1/TH2 balance and monocyte surface antigen expression and its relation to infectious complications. *World J Surg*. 2003;27(5):522–528.

25. Ishikawa M, Nishioka M, Hanaki N, et al. Hepatic resection leads to predominance of the T helper-2 lymphocyte phenotype. *Hepatol Res*. 2004;30:96–103.

26. de Sá KS, Santana BB, de Souza Ferreira TC, et al. IL28B gene polymorphisms and Th1/Th2 cytokine levels might be associated with HTLV-associated arthropathy. *Cytokine*. 2016;77:79–87.

27. Koguchi Y, Kawakami K. Cryptococcal infection and Th1-Th2 cytokine balance. *Int Rev Immunol*. 2002;21(4–5):423–438.

28. Suzuki D, Furukawa K, Kimura F, et al. Effects of perioperative immunonutrition on cell-mediated immunity, T helper type 1 (Th1)/Th2 differentiation, and Th17 response after pancreaticoduodenectomy. *Surgery*. 2010;148(3):573–581.

29. Nosko A, Kluger MA, Diefenhardt P, et al. T-Bet enhances regulatory T cell fitness and directs control of th1 responses in crescentic GN. *J Am Soc Nephrol*. 2017;28(1):185–196.

30. Hercor M, Anciaux M, Denanglaire S, Debuisson D, Leo O, Andris F. Antigen-presenting cell-derived IL-6 restricts the expression of GATA3 and IL-4 by follicular helper T cells. *J Leukoc Biol*. 2017;101(1):5–14.

31. Hafez SF, Sallam MM, Ibraheem SA. Local expression of IL-4 and IL-5 in perennial allergic rhinitis and their modulation by topical corticosteroid therapy. *Egypt J Immunol*. 2004;11(1):111–121.

32. Kato Y, Koseki T, Mastsutani R, et al. MP33-01 risk factors for febrile urinary tract infection after ureteroscopic stone removal. *J Urol*. 2016; 195(4):e436–e436.

Mortality predictor pattern in hemodialysis and peritoneal dialysis in diabetic patients

Marian Klinger[A–F], Katarzyna Madziarska[A–F]

Department of Nephrology and Transplantation Medicine, Wroclaw Medical University, Poland

A – research concept and design; B – collection and/or assembly of data; C – data analysis and interpretation;
D – writing the article; E – critical revision of the article; F – final approval of the article

Address for correspondence
Katarzyna Madziarska
E-mail: kmadziarska@wp.pl

Abstract

An excessive mortality in dialysis programs is the result of cardiovascular injuries and immune deficiency caused by uremic toxins. The vulnerability of dialysis patients is still increasing due to the growing number of diabetics, elderly and patients with a history of cardiovascular disease. Peritoneal dialysis (PD) and hemodialysis (HD) offer similar effectiveness during the first 2 years of the treatment. However, the survival advantage of HD subsequently appears. The problem of the factors responsible for the mortality during long-term PD and HD treatment was analyzed in our recently published investigation. A lower death risk for PD patients during the first several months was lessened over time, and, therefore, no survival advantage of PD was noticeable by the completion of the 2-year period. A sign of the diminishing benefit of PD was a high rate of modality switch – 57%, contrasting with 6% switched in the HD group. Longer observations confirmed that the extension of the treatment period above 2 years with HD was associated with improved survival among subgroups with cardiovascular disease and diabetes. A very relevant problem is the timely transfer of PD patients to the HD program, when an adequate nutritional intake cannot be ascertained and a decline of serum albumin level is observed. The aim of this overview was to compare the factors affecting the survival of diabetic patients in HD and PD patients.

Key words: hemodialysis, elderly, mortality, peritoneal dialysis, diabetics

Introduction

The mortality in dialysis patients exceeds very significantly the rate observed in the general population, even exceeding the figures occurring in neoplastic disease. In addition to specific cardiovascular harm and immune deficiency caused by uremic toxicity, the pessimistic prognosis in the dialysis program is connected with the current clinical characteristics of dialysis patients, i.e., growing participation of the elderly carrying the frailty phenotype and a pronounced increase of type 2 diabetes. These features are evidenced by 46% rate of the 5-year survival in non-diabetic dialysis patients and barely 30% in type 2 diabetics.[1] The aim of this overview was to compare the factors affecting the survival of diabetic patients in hemodialysis (HD) and peritoneal dialysis (PD) patients.

Mortality comparison of the peritoneal dialysis and hemodialysis diabetic patients

In indirect comparisons using data from the Canada-USA Peritoneal Dialysis Study Group (CANUSA) study, encompassing PD and Regional Kidney Disease Program in Minneapolis for HD incident patients, the lack of disparity in the survival between both dialysis modalities was shown during the first 2 treatment years. It was also demonstrated that the same factors, i.e., lowering serum albumin level, older age, diabetes presence, and smaller dialysis dose measured by Kt/V negatively affected the outcome.[2]

In a large American cohort of incident dialysis patients (22360 HD and 1358 PD) undergoing dialysis treatment, examined on day 90 and followed for 24 months, no survival difference appeared between PD and HD patients after adjustment for diabetes mellitus, age, sex, and race.[3] A lower death risk for PD patients during the first several months was lessened over time, and, therefore, no survival advantage of PD was noticeable by the completion of the 2-year period. A sign of the diminishing benefit of PD over time was a high rate of modality switch – 57%, contrasting with 6% switched in the HD group. The problem of the effectiveness of PD treatment, diminishing with the elapsed time in comparison with HD, was depicted clearly by recent observations of the Korean group (Lee et al.).[4] They noticed in the prospective observations of the cohort of 1,000 dialysis patients that during 11 months, the risk of the PD technique failure was 10-fold higher than that of HD.

Longer observations by Weinhandl et al. confirmed that with the extension of the treatment period above 2 years, HD was associated with improved survival among subgroups with cardiovascular disease and diabetes.[5] These results support the conclusions of the earlier Netherlands Cooperative Study on the Adequacy of Dialysis, in which no statistically significant differences in adjusted mortality rates between HD and PD patients were observed during the first 2 years of dialysis.[6] However, in the years thereafter (months 24 to 36), increases in mortality rates for PD patients and resulting decreases in a relative risk of death in favor of HD were noticed.

Collectively, this observational data indicates that PD and HD can be regarded as complementary modalities for incident end-stage kidney disease patients, bringing a comparable outcome during the first 2 years of treatment, but after that offering a consistent survival benefit associated with the HD therapy. The improvement accompanying long-term treatment with HD is particularly noticeable in high-risk groups: the elderly, patients with a cardiovascular disease history and diabetics. Such findings open the question of timely PD patient transfer to HD, when the threats of an ominous outcome appear during PD program. This issue will be discussed in the next part of the article, which is based on our study results.

Different mortality predictor pattern in hemodialysis and peritoneal dialysis diabetic patients in 4-year prospective observation

The problem of the factors responsible for the mortality during long-term PD and HD treatment was analyzed in our recently published investigation.[7] It encompassed 61 prevalent diabetic subjects, treated with maintenance HD (35 persons) and PD (26 persons). The particular features of the cohort were as follows: longevity of dialysis therapy (median period: 17 months), retained urine excretion (median value: 500 mL/day) and elevated cardiovascular risk. All diabetic individuals included in the study group were older than 40 years. They carried Mönckeberg medial calcific arteriosclerosis on the forearm (proved by X-ray). Twenty-six subjects (43%) were older than 70 years. The cohort was prospectively followed for 4 years. Twenty-one individuals (12 treated by HD (34.3%) and 9 (34.6%) in the PD program) from the original set survived the entire 4-year follow-up. The survivors on HD were marked by lower interleukin (IL)-6 level (p = 0.04), higher albumin concentration (p = 0.03) and increased cholesterol concentration (p = 0.004). The only distinction in the PD program was the younger age of the survivors (p = 0.05). The younger age of PD survivors was also reflected in comparison with HD survivors (58.2 ±10.5 years vs 69.8 ±8.4 years; p = 0.017), even though at the study onset, HD and PD patients were of similar age. In addition, PD survivors displayed a significantly lower albumin concentration than HD survivors (3.4 ±0.5 g/dL vs 4.0 ±0.5 g/dL; p = 0.012). Cardiovascular diseases were the most common cause of mortality – 18 patients (45% of all deaths – 7 PD/11 HD), followed by infection – 12 patients (30% – 6 PD/6 HD), malignancy – 5 patients (12.5% – 1 PD/4 HD) and

Table 1. Cox's proportional hazard regression model. Dependent variable: survival time since the beginning of investigation

Variable	Parameter estimate	Wald test	p-value	HR	HR 95% lower	HR 95% upper
Serum albumin [g/dL]	−0.588	3.962	0.047*	0.556	0.311	0.991
HD patients (n = 35)						
Cholesterol [mmol/L]	−0.597	8.15	0.004*	0.551	0.365	0.829
PD patients (n = 26)						
Age [years]	0.050	3.93	0.047*	1.051	1.001	1.104

All patients (n = 61); HR – hazard ratio; HD – hemodialysis; PD – peritoneal dialysis; * statistical significance.

others reasons – 5 patients (12.5% – 3 PD/2 HD). Cox's proportional hazard regression analysis (Table 1) exhibited in respect to the entire diabetic study group that the lowering of serum albumin is the only variable with a significant negative impact on 4-year survival (p = 0.047).

This data is in agreement with long-term observations published by Browne et al.[8] They showed that the patients who had died during 10 years of the dialysis program were marked by significantly lower albumin concentration at the start of the renal replacement therapy.

In creating a division for dialysis modality, the significant mortality predictor in HD patients was low cholesterol concentration (p = 0.004) and only older age (p = 0.047) in PD patients. There was a different tendency in the serum albumin behavior in the PD and HD programs during the 4-year follow-up. In the PD group, a significant decrease of albumin concentration was observed, but no changes occurred under HD treatment. This data indicates that the majority of diabetics in the PD program are not capable of restituting the peritoneal albumin loss, amounting to 6–8 g per day.

Summary: When peritoneal dialysis diabetic patient should be transferred to the hemodialysis program?

The key issue in approaching maintenance dialysis patients is the effective prevention of protein energy waste.[9,10] Peritoneal dialysis patients require protein intake >1.2 g/kg/day with energy providing 30–35 kcal/kg/day. When an inadequate nutritional intake is noticed in PD patients, the dialysis dose should be increased, using 2.5 L exchanges for average-sized patients and 3.5 L exchanges for larger patients. An oral protein supplement can be also introduced. The lack of improvement during the subsequent 3-month observation with progressive serum albumin decline should be recognized as a warning signal, urging to shift from PD to HD modality. Particular attention should be given to high-risk patients: elderly, diabetics and with a cardiovascular disease history.

References

1. Stel VS, van de Luijtgaarden MW, Wanner C, Jager KJ; on behalf of the European Renal Registry Investigators. The 2008 ERA-EDTA Registry Annual Report-a précis. *NDT Plus* 2011;4(1):1–13.
2. Keshaviah P, Collins AJ, Ma JZ, Churchill DN, Thorpe KE. Survival comparison between hemodialysis and peritoneal dialysis based on matched doses of delivered therapy. *J Am Soc Nephrol.* 2002;13(Suppl 1):S48–S52.
3. Lukowsky LR, Mehrotra R, Kheifets L, Arah OA, Nissenson AR, Kalantar-Zadeh K. Comparing mortality of peritoneal and hemodialysis patients in the first 2 years of dialysis therapy: A marginal structural model analysis. *Clin J Am Soc Nephrol.* 2013;8(4):619–628.
4. Lee J-H, Park S-H, Lim J-H, et al. Impact of dialysis modality on technique survival in end-stage renal disease patients. *Korean J Intern Med.* 2016;31(1):106–115.
5. Weinhandl ED, Foley RN, Gilbertson DT, Arneson TJ, Snyder JJ, Collins AJ. Propensity-matched mortality comparison of incident hemodialysis and peritoneal dialysis patients. *J Am Soc Nephrol.* 2010;21(3):499–506.
6. Termorshuizen F, Korevaar JC, Dekker FW, van Manen JG, Boeschoten EW, Krediet RT; Netherlands Cooperative Study on the Adequacy of Dialysis Study Group. Hemodialysis and peritoneal dialysis: Comparison of adjusted mortality rates according to the duration of dialysis: Analysis of The Netherlands Cooperative Study on the Adequacy of Dialysis 2. *J Am Soc Nephrol.* 2003;14(11):2851–2860.
7. Madziarska K, Weyde W, Penar J, et al. Different mortality predictor pattern in hemodialysis and peritoneal dialysis diabetic patients in 4-year prospective observation. *Postepy Hig Med Dosw (Online).* 2013;67:1076–1082.
8. Browne OT, Allgar V, Bhandari S. Analysis of factors predicting mortality of new patients commencing renal replacement therapy: 10 years of follow-up. *BMC Nephrology.* 2014;20:15–20.
9. Han SH, Han DS. Nutrition in patients on peritoneal dialysis. *Nat Rev Nephrol.*2012;8(3):163–175.
10. Ikizler TA, Cano NJ, Franch H, et al.; International Society of Renal Nutrition and Metabolism. Prevention and treatment of protein energy wasting in chronic kidney disease patients: A consensus statement by the International Society of Renal Nutrition and Metabolism. *Kidney Int.* 2013;84(6):1096–1107.

Academic chemistry and related fields in Wrocław: Density-equalizing mapping studies over the past decades

David A. Groneberg

Institute of Occupational Medicine, Social Medicine and Environmental Medicine, Goethe University Frankfurt, Frankfurt am Main, Germany

A – research concept and design; B – collection and/or assembly of data; C – data analysis and interpretation;
D – writing the article; E – critical revision of the article; F – final approval of the article

Address for correspondence
David A. Groneberg
E-mail: arbsozmed@uni-frankfurt.de

Abstract

Chemistry and related areas of science have a strong background in Wrocław with 3 Nobel laureates.

The aim of this study was to assess the evolution of scientific excellence and productivity after the Second World War, when Polish scientists rebuilt academic life in these important areas.

The present approach used the established platform of the New Quality and Quantity Indicators in Science (NewQIS) project and density-equalizing mapping calculations.

In total, 15,267 original research articles related to chemistry published by Wrocław scientists were identified in the Web of Science between 1972 and 2016. They were cited 170,606 times. The highest citation numbers were reached in the years 2001 and 2004. In total, 4,362 research collaborations were performed with 83 different countries, leading to a percentage of 28.6%. Wrocław chemistry institutions established a vast international network with the USA (688 articles), France (658 articles) and Germany (679 articles) as their main partner countries. Besides chemistry, the main research fields are biochemistry and molecular biology, as well as physics, with 2,177 and 2,007 articles, respectively.

This study visualized the great success and virtue by which Polish scientists rebuilt a scientific community in the area of chemistry in Wrocław after the Second World War. Wrocław is now a key Central European player in chemistry and related areas, which serves as a nodal point between Eastern and Western countries.

Key words: scientometrics, chemistry, Wrocław, density-equalizing maps

138

D. Groneberg. Density-equalizing map of Wrocław research

Introduction

Chemistry and related areas of science has represented the cornerstone of the academic life in Wrocław for centuries. Here, 3 Nobel laureates in chemistry lived, studied or worked. Eduard Buchner (1860–1917) was awarded the Nobel Prize in chemistry in 1907. He is also called the father of biochemistry in a test tube and the father of experimental molecular bioscience.[1,2] Fritz Haber (1868–1934) was awarded the Nobel Prize in 1918 for his studies on the fixation of nitrogen from the air. Haber was the first scientist to introduce poison gas to warfare. As stated by his nephew Fritz Stern and others, Haber's life encompassed triumph and tragedy.[3–5] Lastly, Friedrich Bergius (1884–1949) was awarded the Nobel Prize in 1931 for his contributions to the invention and development of chemical high-pressure methods. This fruitful academic life was destroyed by Nazi Germany. The former University of Wrocław ceased to exist in 1945. In the Nazi period, more than 250 doctorate degrees of the scientists in Wrocław were nullified. Directly after the war, thanks to the scientists from the University of Lviv, a new Polish state university was established.[6,7] Today, research related to academic chemistry is conducted at the University of Wroclaw, sister universities such as Wroclaw University of Science and Technology, Wroclaw Medical University or Wrocław University of Environmental and Life Sciences, and other research institutions.

While there are numerous excellent historical articles about the development of Wrocław academic chemistry after 1945, a concise scientometric study that addresses the evolution of postwar chemical research activities is still missing. Therefore, the aim of the present study was to assess the scientific evolution, using the New Quality and Quantity Indicators in Science (NewQIS) methodology.[8,9]

Material and methods

New Quality and Quantity Indicators in Science platform

The NewQIS studies were established in 2008 and 2009 at the Charité – Universitätsmedizin Berlin, Germany, by an interdisciplinary team, consisting of computational science, economy, engineering, and medical experts.[8,9] Since then, more than 50 studies have used this methodology, which combines advanced visualization techniques with scientometric approaches.[10–14] One key technology are the density-equalizing mapping procedures (DEMP) developed by Gastner and Newman.[15] Recently, the platform has been used to assess various areas of science in Wrocław.[16]

Search strategy

The present study is part of the NewQIS-Wrocław project of NewQIS. Data was retrieved from the Web of Science database as carried out in former NewQIS studies: "Wroclaw" was entered as the target parameter in the address field.[17] As the next step, the search was restricted to publication type "articles" in order to focus solely on original research. Then, the data set was scanned for research categories that are linked only to the fields of chemistry. The search was carried out on August 26, 2016.

Density-equalizing mapping

In 2004, Gastner and Newman published an algorithm for density-equalizing mapping.[15] This approach was used in the present study and DEMP was integrated as described in previous NewQIS studies, with the territories of the countries being re-distributed according to the chosen variable, e.g., the number of joint research articles with Wrocław institutions.[18–24]

International collaborations

International research collaborations in the field of chemistry were analyzed in order to depict a sketch of the global research network that has been built by Wrocław scientists over the past decades. All affiliations of foreign scientists who jointly published original research contributions together with the scientists from Wrocław were analyzed as previously described.[25,26] Bilateral collaborations between Poland and another country were defined as at least 1 author originating from Wrocław affiliations and at least 1 other co-author originating from an affiliation outside of Poland. After the total numbers were assessed, a special matrix with all networking countries was computed to visualize scientific networking activities.

Results

Wrocław research activity

In total, a number of 15,267 original articles were identified from 1972 to 2016 in chemistry and related fields (Fig. 1). Regression analysis demonstrated a significant increase in research activity (correlation coefficient (r^2) = 0.9237) with a maximum yearly output of 727 articles in 2014. Density-equalizing mapping of Wrocław chemistry research output with the cooperating foreign scientists led to a research architecture depicted in Fig. 1, with Poland in the center, accompanied by strong partners, including the USA, France and Germany. When the numbers of institutions were analyzed, more than 300 institutions were devoted to research in the areas of chemistry in Poland, followed by more than 200 different American institutions and more than 150 French and German institutions (Fig. 2A,B).
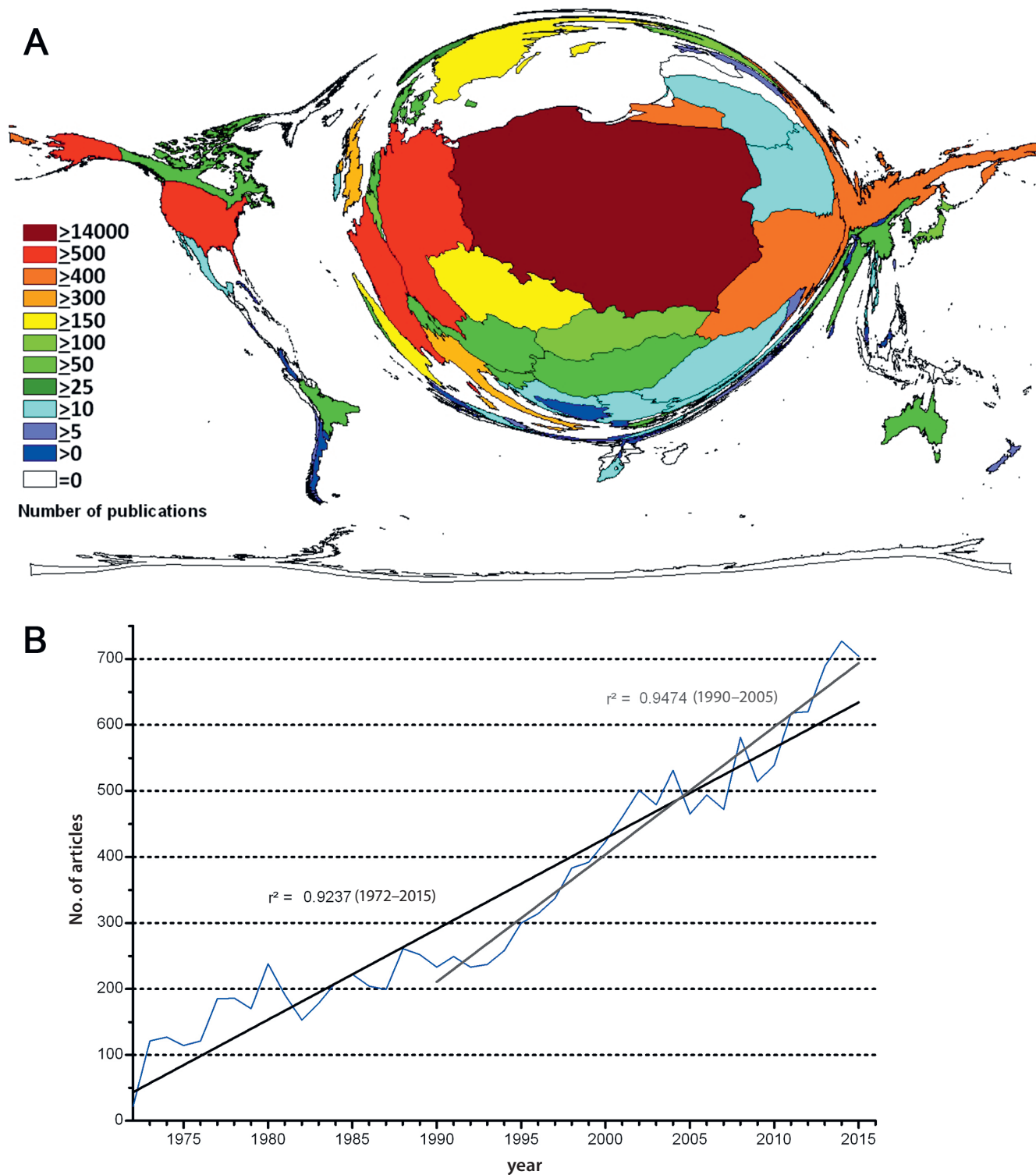
A

Number of publications

≥14000
≥500
≥400
≥300
≥150
≥100
≥50
≥25
≥10
≥5
>0
=0

B

r² = 0.9474 (1990–2005)

r² = 0.9237 (1972–2015)

Fig. 1. Publication output

A – density-equalizing map projection of the number of articles per country; B – number of articles per year.

Network analysis of Wrocław chemical research in cooperation with other countries

In the next step, the proportion of cooperation research was analyzed and a total of 4,362 research collaborations were found. These collaborations of Wrocław scientists encompassed a total of 83 different countries, leading to a percentage of 28.6% of all research activities. When the international research collaborations were further analyzed, 3,246 were found to be bilateral between one of Wrocław institutions and a foreign institution. There were also 888 collaborations between Wrocław and 2 other countries, and 175 with 3 other countries. The analysis
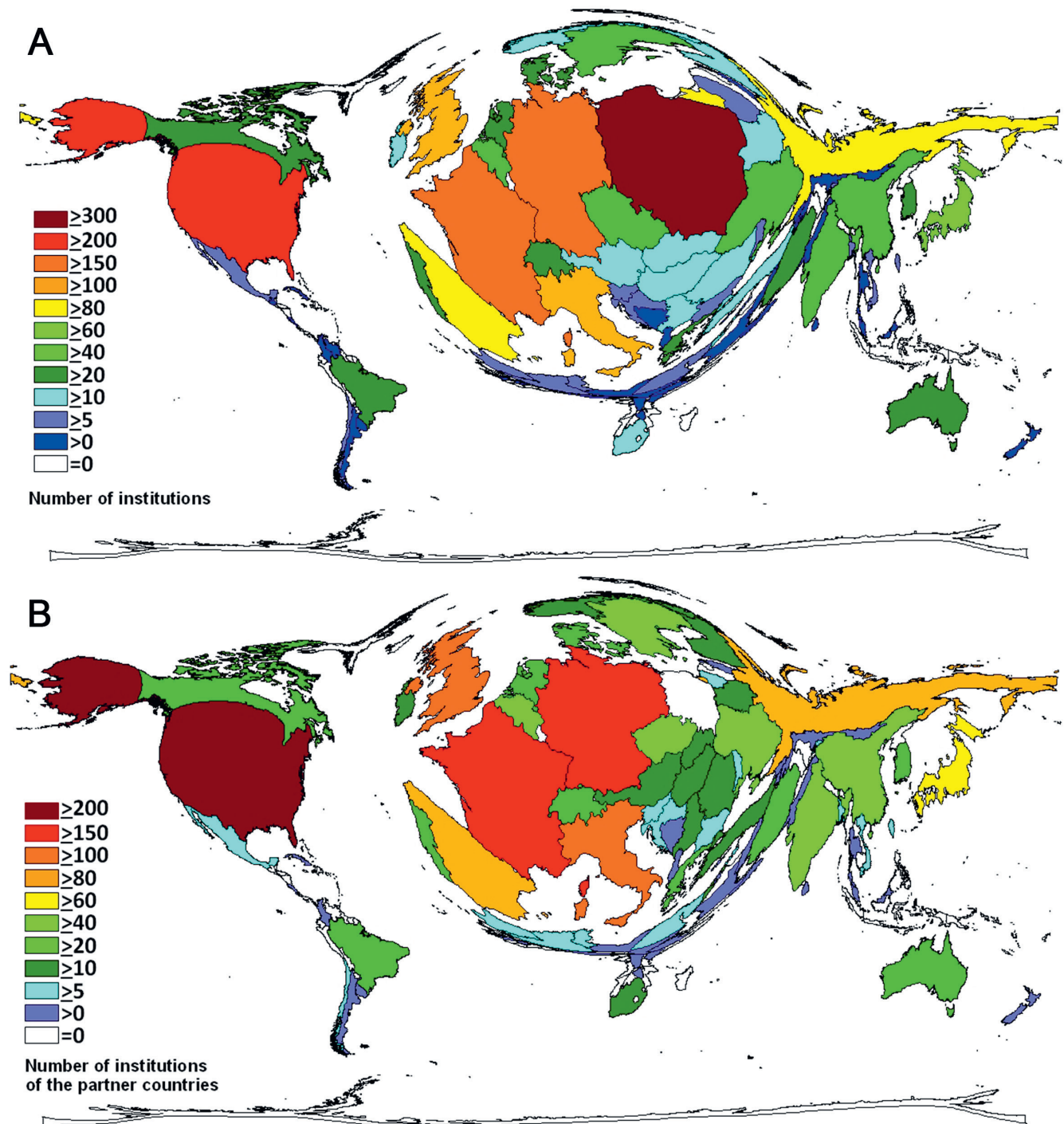
Fig. 2. Number of institutions

A – all countries; B – cooperation countries.

of time evolution demonstrates that there has been an increase in international research collaborations since 1972. Especially after 1990 there is a strong increase in these numbers with the year 2015 exhibiting a record number of 254 collaborations.

Network analysis diagrams were then used to visualize the global Wrocław research network with contributions from the USA (688 articles), France (658 articles) and Germany (679 articles). One can also observe strong bonds with Russia (409 articles) and Ukraine (406 articles),

followed by Italy (373 articles) and the UK (322 articles). Network diagrams also illustrated frequent collaborations with Sweden (152 articles) and Spain (161 articles) (Fig. 3A,B).

Semi-qualitative indicators: citations and Hirsch index

Surrogate parameters of quality were based on citation analysis and the semi-qualitative markers of total
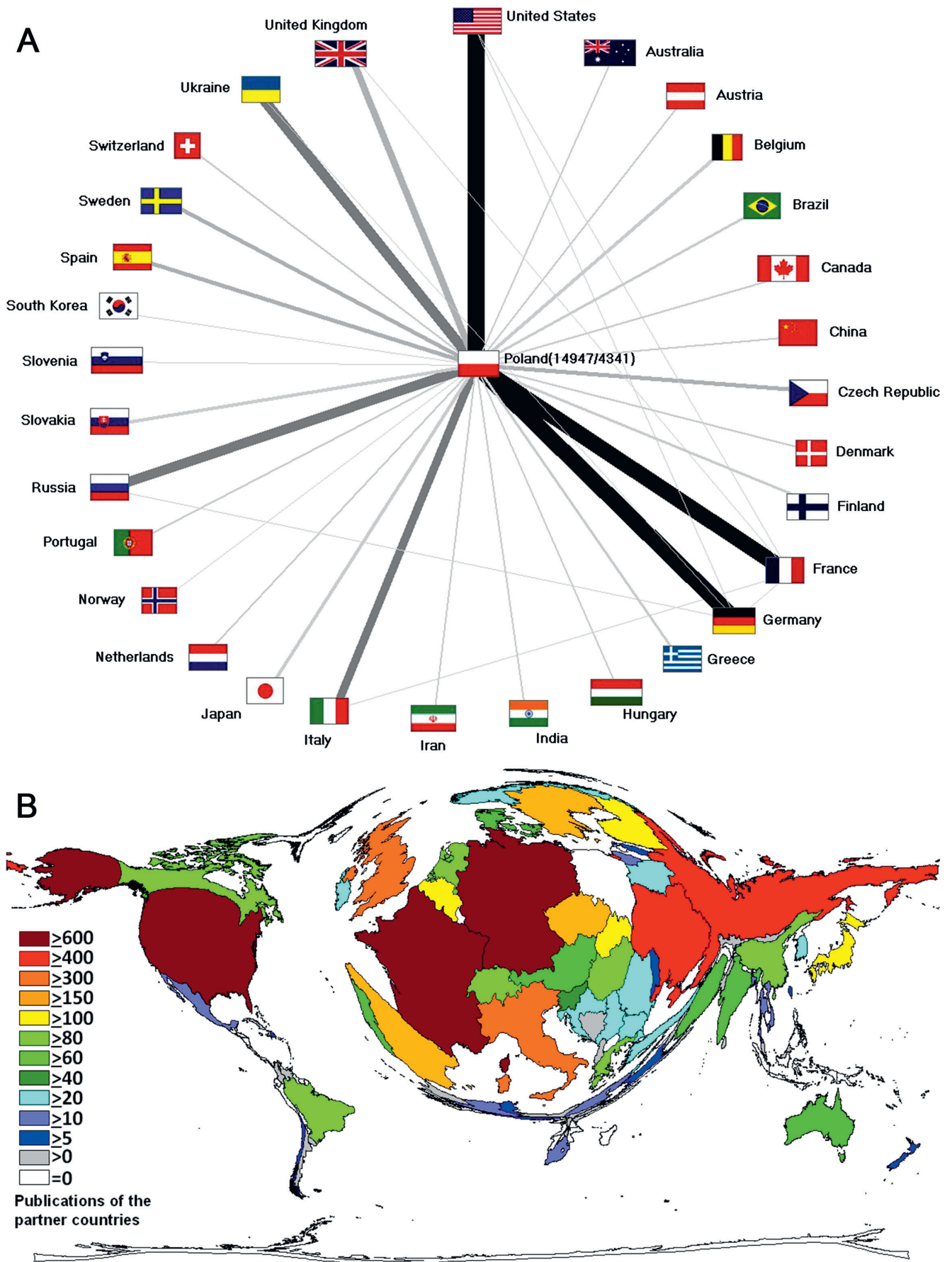
Fig. 3. International collaborations

A – international network; B – density-equalizing map of the number of articles per partner country.
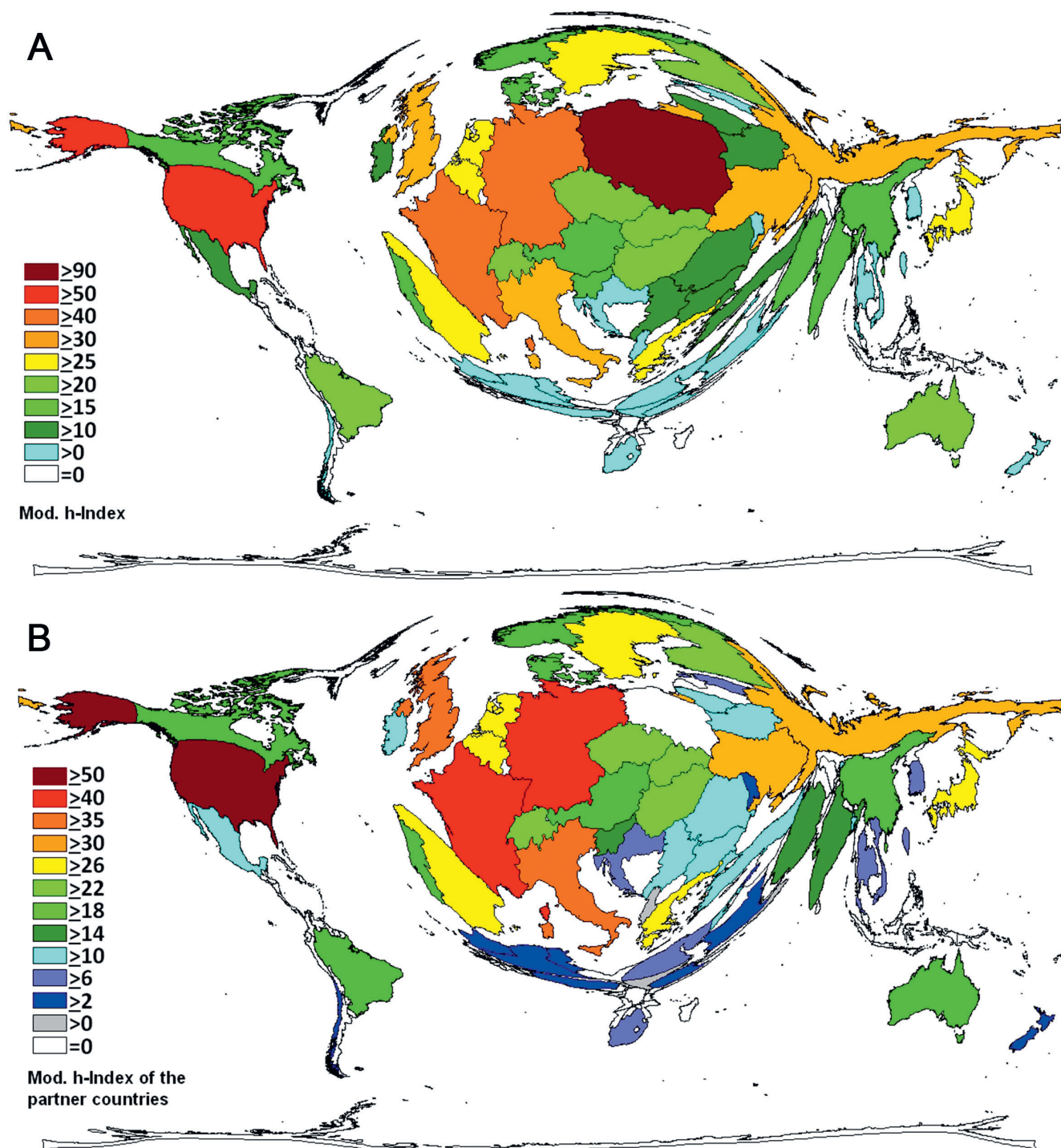
A

B

Fig. 4. Density-equalizing maps of the country-specific (modified) Hirsch index (h-index)

A – all countries; B – partner countries.

citations, Hirsch index (h-index) and citation rate per article were calculated. In total, the 15,267 original articles from Wrocław were cited 170,606 times (Fig. 4). The articles with cooperating American institutions were cited 16,304 times. Maxima were observed for the articles from the years 2001 (8,568 citations) and 2004 (9,438 citations). The increase from 1972 to 2007 was significant with $r^2 = 0.8455$. Density-equalizing mapping for h-indices

illustrated h-indices for Poland (h-index = 96), followed by those for the USA (h-index = 56), France (h-index = 45) and Germany (h-index = 44) (Fig. 4).

Research areas

Among different fields of science related to chemistry, the subject area "chemistry" dominated by far with 11,516
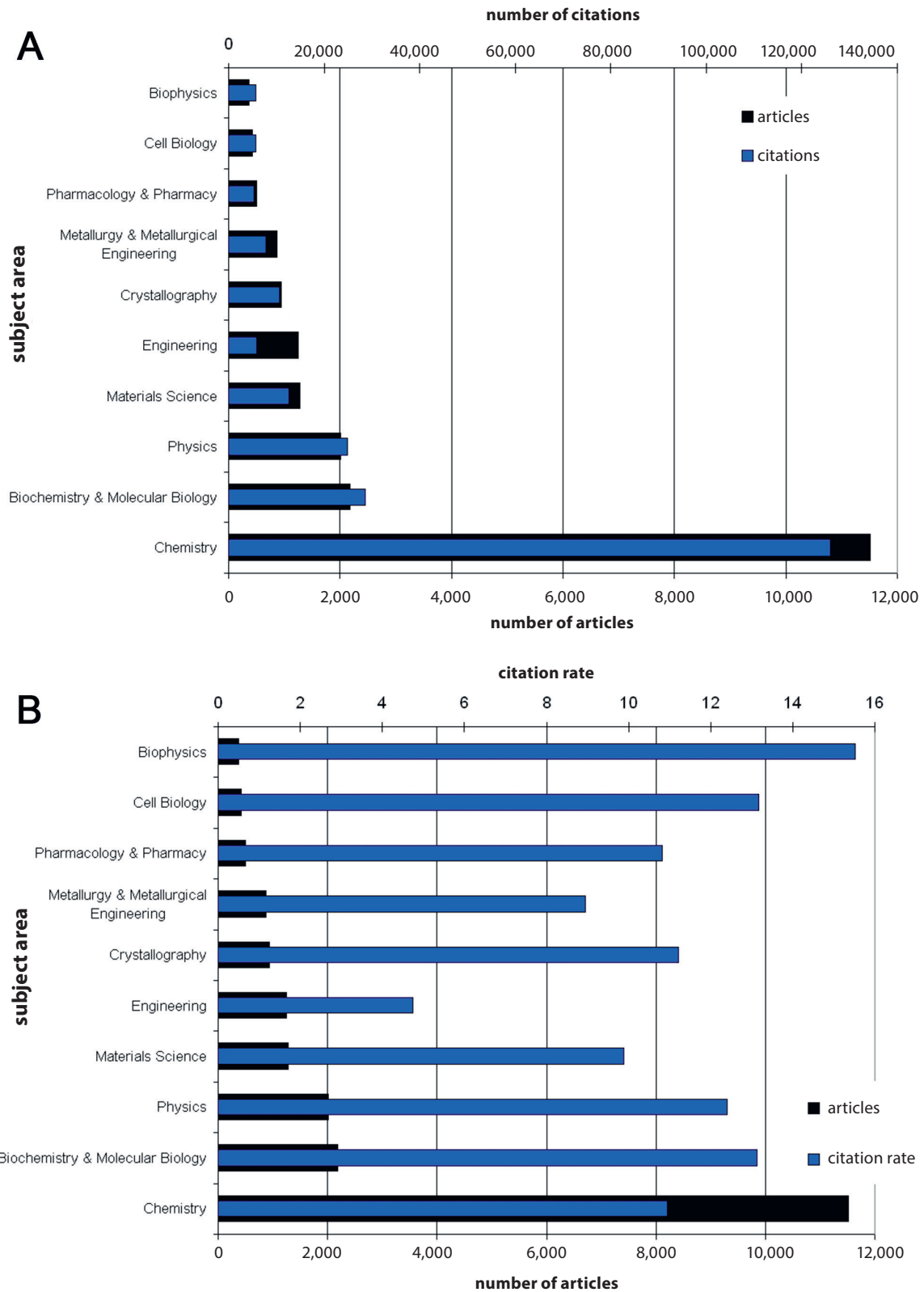
Fig. 5. Research areas

A – number of articles and citations of the most assigned subject areas; B – number of articles and citation rate of the most assigned subject areas.

articles. It was followed by the field of "biochemistry & molecular biology" and the field of "physics" with 2,177 and 2,007 articles, respectively (Fig. 5A). The analysis of citation trends in the different research areas revealed a relative homologous citation rate (cr): cr = 10.94 for "chemistry"; cr = 13.12 for "biochemistry & molecular biology"; and cr = 12.40 for "physics". The highest cr of the most assigned subject areas was noted for the articles published in the
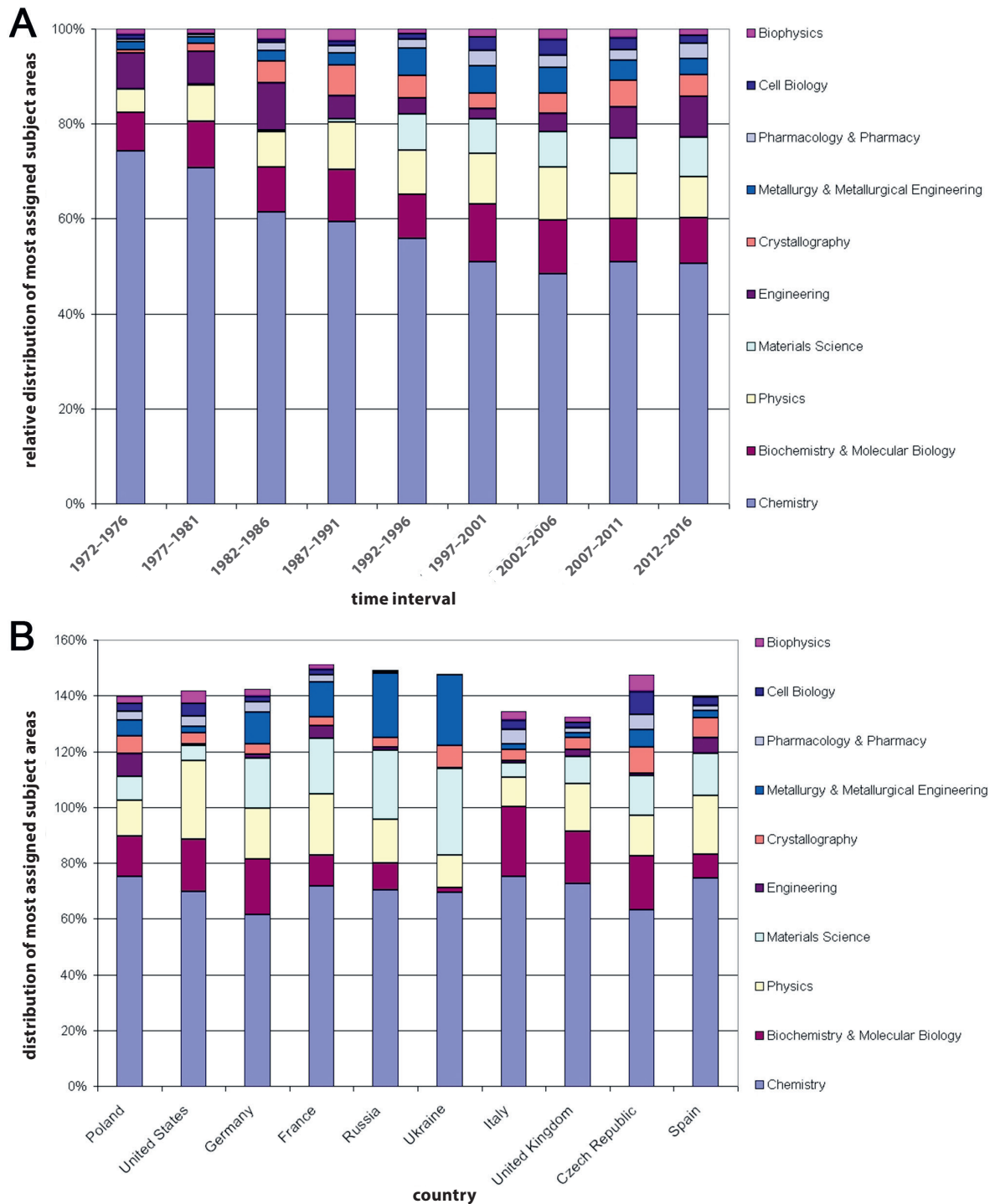
Fig. 6. Proportions of the most assigned subject areas

A – relative distribution in 5-year intervals (1972–2016); B – distribution of the countries publishing the most.

field of "biophysics" with cr = 15.52, whereas the lowest cr was found for the articles which were related to "engineering" (cr = 4.74) (Fig. 5B).

When the relative proportion of subject areas was assessed, a clear dominance of the area „chemistry" was present, beginning with more than 74% of all articles in the period 1972–1976 to about 50% currently, in the period 2012–2016 (Fig. 6A).

When the subject nature of the international collaborations was analyzed for the top cooperating countries, it became evident that "chemistry" dominated all collaborations with the proportion of over 60%. However, some countries have special subject area links to Wrocław scientists, i.e., "metallurgy & metallurgical engineering" is related to research collaborations of Wrocław scientists with Russia and Ukraine (Fig. 6B).

Discussion

A large number of excellent articles have described the historical background of Wrocław academic life over the past centuries,with a special focus on the time after 1945, when primarily the scientists from the Jan Kazimierz University of Lviv established new universities in Wrocław.[27–31] Basing on these historical facts, the present study incorporates scientometric approaches, together with novel visualization techniques, in order to illustrate the evaluation of chemistry and related areas in Wrocław. Scientometrics is a field of science, also termed as meta-science, that was propagated by key researchers such as Garfield or de Solla Price decades ago in world-renowned journals such as "Science" or "Nature".[32–36] The present approach uses established scientometric instruments such as the citation indexing,the Web of Science databank or Hirsch indices to illustrate the scientific advances in Wrocław chemistry research in the postwar time, reaching to the end of 2016.[37–39] It does not stop here, but extends the approach, using a combination with the so-called density-equalizing mapping visualization technique, which was established by Gastner and Newman in 2004 in the "Proceedings of the National Academy of Sciences of the USA" and incorporated to NewQIS in 2009.[8,15]

The density-equalizing maps related to Wrocław research in the areas of chemistry, including biochemistry and molecular biology, point to a strong development of these areas of science after the war. This is paralleled by a similar increase in other biomedical areas as shown recently.[16] Thus, the heritage of 3 Nobel Prize laureates in chemistry, linked to Wrocław, has been transformed into a vivid scientific community in the field of chemistry, although Nazi Germany completely destroyed academic life in Wrocław. This reconstructive work has its foundation on the shoulders of a few scientists who came from Lviv, i.e., professors Bogusława Jeżowska-Trzebiatowska, Wanda L. Mejbaum-Katzenellebogen, Henryk Kuczyński, and Lucjan Sobczyk. They lost their home universities and were thrown many years back in their scientific work due to the Second World War and repressions by Nazi Germany, but managed to rebuild their own scientific capabilities in Wrocław. Their former students now represent the diverse faculties in Wrocław universities and research institutions, and authored more than 15,000 original articles in the period 1972–2016. Within this vast amount of scientific works, also 4,362 international research collaborations with a total of 83 different countries were published by Wrocław scientists. This is nearly 1/3 of all Wrocław chemistry-related publications, symbolizing that Wrocław scientists function as ambassadors of Poland to the world. Especially after 1990 there has been an increase in international collaborations with western countries such as the USA or France. This shows how important the new political area was for the fields of science with Wrocław scientists being able again to carry out any scientific cooperation – not limited to communist countries, but directed toward the scientific background of the collaborating institutions.

The analysis of research areas demonstrated that research in Wrocław is not narrow-focused, but open to all aspects of chemistry. With the core chemistry areas in the center, areas such as biochemistry also gained more and more attention. From a historical perspective, this is extremely fortunate, since the Wrocław 1907 Nobel laureate Eduard Buchner (1860–1917) is also known as the father of biochemistry in a test tube or the father of experimental molecular bioscience – this legacy was continued at the Polish state university of Wrocław half a century later by professors such as Wanda Mejbaum-Katzenellenbogen, who published articles on biochemistry between the 1940s and the end of the 1980s. With regard to the prominent role of Mejbaum-Katzenellenbogen and other female scientists from Wrocław, it is enticing to speculate that Wrocław scientific community can be characterized as more gender-balanced than other scientometric communities. This needs to be studied in further projects with a focus on gender issues.

To conclude, this study is the first combined density-equalizing and scientometric analysis that visualizes the great success of Polish scientists who rebuilt academic life in the area of chemistry after the Second World War. With the heritage of 3 Nobel Prizes for chemistry and the scientific field completely destroyed by Nazi Germany, they succeeded and regained scientific power in the following 50 years. The chemistry research of Wrocław is again a leading Central European player with a fruitful international network to both Western and Eastern countries.

References

1. Jaenicke L. Centenary of the award of a Nobel prize to Eduard Buchner, the father of biochemistry in a test tube and thus of experimental molecular bioscience. *Angew Chem Int Ed Engl*. 2007;46(36): 6776–6782.
2. Kisielow P. Proceedings of the conference "Lymphocyte development, tolerance and autoimmunity: Solved and open questions", held at the Ludwik Hirszfeld Institute of Immunology and Experimental Therapy, Polish Academy of Sciences, on May 12, 2011 (Wrocław, Poland): Lymphocyte development, tolerance and auto-immunity: A personal perspective. *Arch Immunol Ther Exp (Warsz)*. 2011;59(5):327–330.
3. Dunikowska M, Turko L. Fritz Haber: The damned scientist. *Angew Chem Int Ed Engl*. 2011;50(43):10050–10062.
4. Manchester KL. Man of destiny: The life and work of Fritz Haber. *Endeavour*. 2002;26(2):64–69.
5. Stern F. Fritz Haber: Flawed greatness of person and country. *Angew Chem Int Ed Engl*. 2012;51(1):50–56.
6. Ogorzalek A. Embryology at the Universities of Lviv and Wrocław. *Int J Dev Biol*. 2008;52(2–3):135–139.
7. Kierzek A, Kuciel-Lewandowska J, Paprocka-Borowicz M, Pozowski A. Professor Ludwik Hirszfeld in his relations with students and junior researchers. *Adv Clin Exp Med*. 2013;22(6):909–914.
8. Groneberg-Kloft B, Quarcoo D, Scutaru C. Quality and quantity indices in science: Use of visualization tools. *EMBO Rep*. 2009;10(8): 800–803.
9. Groneberg-Kloft B, Fischer TC, Quarcoo D, Scutaru C. New quality and quantity indices in science (NewQIS): The study protocol of an international project. *J Occup Med Toxicol*. 2009;4:16.

10. Kusma B, Scutaru C, Quarcoo D, Welte T, Fischer TC, Groneberg-Kloft B. Tobacco control: Visualisation of research activity using density-equalizing mapping and scientometric benchmarking procedures. *Int J Environ Res Public Health*. 2009;6(6):1856–1869.

11. Bundschuh M, Groneberg DA, Klingelhofer D, Gerber A. Yellow fever disease: Density-equalizing mapping and gender analysis of international research output. *Parasit Vectors*. 2013;6:331.

12. Healy NA, Glynn RW, Scutaru C, Groneberg D, Kerin MJ, Sweeney KJ. The h-index and the identification of global benchmarks for breast cancer research output. *Breast Cancer Res Treat*. 2011;127(3):845–851.

13. Geaney F, Scutaru C, Kelly C, Glynn RW, Perry IJ. Type 2 diabetes research yield, 1951–2012: Bibliometrics analysis and density-equalizing mapping. *PLoS ONE*. 2015;10(7):e0133009.

14. Gotting M, Schwarzer M, Gerber A, Klingelhofer D, Groneberg DA. Pulmonary hypertension: Scientometric analysis and density-equalizing mapping. *PLoS ONE*. 2017;12(1):e0169238.

15. Gastner MT, Newman ME. Diffusion-based method for producing density-equalizing maps. *Proc Natl Acad Sci U S A*. 2004;101(20):7499–7504.

16. Groneberg DA. Biomedical research in Wroclaw: A combined density-equalizing mapping and scientometric analysis. *Arch Immunol Ther Exp (Warsz)*. 2018;66(1):1–9.

17. Bruggmann D, Maule LS, Klingelhofer D, et al. World-wide architecture of osteoporosis research: Density-equalizing mapping studies and gender analysis. *Climacteric*. 2016;19(5):463–470.

18. Schoffel N, Gfroerer S, Rolle U, Bendels MH, Klingelhofer D, Groneberg-Kloft B. Hirschsprung disease: Critical evaluation of the global research architecture employing scientometrics and density-equalizing mapping. *Eur J Pediatr Surg*. 2017;27(2):185–191.

19. Bruggmann D, Wagner C, Klingelhofer D, et al. Maternal depression research: Socioeconomic analysis and density-equalizing mapping of the global research architecture. *Arch Womens Ment Health*. 2017;20(1):25–37.

20. Schoffel N, Krempel M, Bundschuh M, Bendels MH, Bruggmann D, Groneberg DA. Pancreatic cancer: Critical examination of the global research architecture and recent scientific developments. *Pancreas*. 2016;45(10):1378–1385.

21. Bruggmann D, Pulch K, Klingelhofer D, Pearce CL, Groneberg DA. Ovarian cancer: Density-equalizing mapping of the global research architecture. *Int J Health Geogr*. 2017;16(1):3.

22. Bruggmann D, Lohlein LK, Louwen F, et al. Caesarean section: A density-equalizing mapping study to depict its global research architecture. *Int J Environ Res Public Health*. 2015;12(11):14690–14708.

23. Groneberg DA, Rahimian S, Bundschuh M, Schwarzer M, Gerber A, Kloft B. Telemedicine: A scientometric and density-equalizing analysis. *J Occup Med Toxicol*. 2015;10:38.

24. Bruggmann D, Handl V, Klingelhofer D, Jaque J, Groneberg DA. Congenital toxoplasmosis: An in-depth density-equalizing mapping analysis to explore its global research architecture. *Parasit Vector*. 2015;8:646.

25. Carl J, Schwarzer M, Klingelhoefer D, Ohlendorf D, Groneberg DA. Curare – a curative poison: A scientometric analysis. *PLoS ONE*. 2014; 9(11):e112026.

26. Groneberg DA, Weber E, Gerber A, Fischer A, Klingelhofer D, Brueggmann D. Density-equalizing mapping of the global tuberculosis research architecture. *Tuberculosis (Edinb)*. 2015;95(4):515–522.

27. Zajaczkowski T. History of medicine, surgery and urology in Breslau/Wroclaw. *Ann Acad Med Stetin*. 2014;60(2):113–126.

28. Kustrzycki WA. J. Mikulicz-Radecki, K. H. Bauer, and W. Bross: Three great surgeons, three different epochs, one clinic in Wroclaw. *Thorac Cardiovasc Surg*. 2013;61(6):464–469.

29. Kacała RR, Woźniak S, Porwolik M, et al. Remembrance of professor Tadeusz Marciniak: Lviv tradition in Wroclaw. *Adv Clin Exp Med*. 2015;24(1):173–178.

30. Zarsky V. Jan Evangelista Purkyne/Purkinje (1787–1869) and the establishment of cellular physiology: Wroclaw/Breslau as a central European cradle for a new science. *Protoplasma*. 2012;249(4):1173–1179.

31. Wojtkiewicz-Rok W. The effect of Lviv medical tradition on development of medical sciences in postwar Wroclaw [in Polish]. *Wiad Lek*. 2002;55(5-6):354–359.

32. Schoenbach UH, Garfield E. Citation indexes for science. *Science*. 1956;123(3185):61–62.

33. de Solla Price DJ. *Little Science, Big Science*. New York, NY: Columbia University Press; 1963.

34. Garfield E. Science citation index: A new dimension in indexing. *Science*. 1964;144(3619):649–654.

35. Garfield E. Information retrieval. *Science*. 1967;156(780):1398–1401.

36. Garfield E. Significant journals of science. *Nature*. 1976;264(5587): 609–615.

37. Garfield E. Citation indexes for science: A new dimension in documentation through association of ideas. *Science*. 1955;122(3159): 108–111.

38. Sevinc A. Web of science: A unique method of cited reference searching. *J Natl Med Assoc*. 2004;96(7):980–983.

39. Hirsch JE. An index to quantify an individual's scientific research output. *Proc Natl Acad Sci U S A*. 2005;102(46):16569–16572.